

Alma Mater Studiorum – Università di Bologna

**DOTTORATO DI RICERCA IN
Scienze Chimiche**

Ciclo XXIII

Settore/i scientifico-disciplinare/i di afferenza: CHIM/06

**SYNTHESIS AND APPLICATION OF NEW ION-TAGGED LIGANDS AND
ORGANOCATALYSTS**

Presentata da: Michel Chiarucci

Coordinatore Dottorato

Prof. Giuliano Longoni

Relatore

Prof. Marco Lombardo

Esame finale anno 2011

SUMMARY

SUMMARY	2
ABSTRACT	4
CHAPTER 1: INTRODUCTION	5
1.1. Multiphasic homogeneous catalysis	5
1.2. Ion-tagged catalysts and “electrosteric” activation	8
1.3. Ion-tagged organometallic catalysts	10
1.3.1. Catalytic hydrogenation of olefins.....	11
1.3.2. Catalytic hydroformylation of olefins.....	15
1.3.3. Ring closing metathesis (RCM).....	21
1.3.4. Olefins epoxidation.....	26
1.3.5. Olefins polymerization.....	27
1.3.6. Pd cross coupling (CC).....	28
1.3.7. Tsuji-Trost allylation.....	38
1.3.8. Copper catalyzed reactions.....	39
1.3.9. Asymmetric transfer hydrogenation of ketones.....	41
1.3.10. Catalytic asymmetric addition of nucleophiles to aldehydes.....	43
1.4. Ion-tagged organocatalysts	45
1.4.1. Ion-tagged Brønsted acids.....	46
1.4.2. Asymmetric cross aldol condensation.....	46
1.4.3. Asymmetric Michael addition.....	51
1.4.4. Morita – Baylis – Hillman (MBH) reaction.....	58
1.4.5. Asymmetric reduction of ketones.....	59
1.4.6. Alcohols oxidation.....	59
Bibliography	62
CHAPTER 2: RESULTS AND DISCUSSION	64
2.1. Enantioselective addition of ZnEt₂ to aldehydes in ILs catalyzed by a recyclable ion-tagged diphenylprolinol	64
2.1.1. Reaction overview.....	64
2.1.2. Discussion.....	66
2.1.3. Conclusion.....	73
2.1.4. Experimental section.....	74

Bibliography.....	81
2.2. A recyclable triethylammonium ion-tagged diphenylphosphine palladium complex for the Suzuki–Miyaura reaction in ionic liquids.	82
2.2.1. Reaction overview.....	82
2.2.2. Discussion.....	84
2.2.3. Synthesis of tetracene derivatives by Suzuki-Miyaura coupling in ionic liquids.....	92
2.2.4. Conclusions.....	96
2.2.5. Experimental section.....	97
Bibliography.....	108
2.3. Ion-Tagged Imidazolidinone for the Enantioselective Organocatalytic Diels-Alder Reaction	109
2.3.1. Reaction overview.....	109
2.3.2. Discussion.....	112
2.5.3. Conclusions.....	118
2.3.4. Experimental section.....	119
Bibliography.....	126
2.4. Highly Efficient Ion-Tagged Catalyst for the Enantioselective Michael Addition of Aldehydes to Nitroalkenes	128
2.4.1. Reaction overview.....	128
2.4.2. Discussion.....	131
2.4.3. Conclusion.....	139
2.4.4. Experimental section.....	140
<i>FINAL REMARKS</i>	<i>150</i>
<i>ABBREVIATIONS</i>	<i>151</i>

ABSTRACT

We report in this work the synthesis and application of some ion-tagged catalysts in organometallic catalysis and organocatalysis. With the installation of an ionic group on the backbone of a known catalyst, two main effects are generally obtained. i) a modification of the solubility of the catalyst: if judicious choice of the ion pair is made, the ion-tag can confer to the catalyst a solubility profile suitable for catalyst recycling. ii) the ionic group can play a non-innocent role in the process considered: if stabilizing interaction between the ionic group and the developing charges in the transition state are established, the reaction can speed up. These characteristics make ion-tagged catalysts an attractive solution to develop catalytic systems combining high reactivity and selectivity with easy product isolation and catalyst recycling.

Here we report the use of ion-tagged diphenylprolinol as a Zn ligand. The chiral ligand grafted onto an ionic liquid (IL) was recycled 10 times with no loss of reactivity and selectivity when it was employed in the first example of enantioselective addition of ZnEt_2 to aldehydes in ILs. An ammonium-tagged phosphine displayed the capability to stabilize Pd catalysts for the Suzuki reaction in ILs. Thanks to the thermoregulated nature of the solvent pair $[\text{bmpy}][\text{NTf}_2]/\text{H}_2\text{O}$ and to the high affinity of the ion-tagged catalyst for the IL, the ionic phase was recycled 6 times with no detectable loss of activity and very low Pd leaching in the organic phase. This catalytic system was also employed for the functionalization in mild conditions of the challenging substrate 5,11-dibromotetracene, obtaining diaryl derivatives, which are compounds with interesting optoelectronic properties.

In the field of organocatalysis, we prepared two ion-tagged derivatives of the well known McMillan imidazolidinone. The results of the asymmetric Diels-Alder (DA) reaction between *trans*-cinnamaldehyde and cyclopentadiene, catalyzed by the two ionic organocatalysts, exhibited great dependence on the position and nature of the ionic group. When an imidazolium ion was installed far away from the reactive centre, the ionic group did not influence the reaction outcome, while a detrimental effect on reactivity and selectivity was observed when a sterically demanding triphenylphosphonium ion was installed close to the reactive amine. Finally, when *O*-TMS diphenylprolinol was tagged with an imidazolium ion, exploiting a silyl ether linker, an efficient catalyst for the asymmetric addition of aldehydes to nitroolefins was achieved. The catalyst displayed enhanced reactivity and the same high level of selectivity of the untagged parent catalyst and it could be employed in a wide range of reaction conditions, including use of water as solvent.

CHAPTER 1: INTRODUCTION

1.1. Multiphasic homogeneous catalysis.

A catalyst can be defined as a species which increases the rate of a chemical reaction without being consumed in the process.¹ The rate enhancement is due to the opening of a new and faster reaction pathway with a lower activation energy. If suitable conditions occur, the lowest energy pathway will be preferred, thus, besides rate enhancement, catalyzed reaction can lead to improved selectivity in terms of chemoselectivity, regioselectivity, diastereoselectivity or enantioselectivity, when chiral catalysts are employed. Higher selectivity and use of sub-stoichiometric amount of reagents means that for a given process less waste are produced and less reactants are consumed. For this reason one of the twelve principles of “Green Chemistry”, listed by Anastas and Werner, states that: “Catalytic reagents (as selective as possible) are superior to stoichiometric reagents”.^{2,3}

Catalysts are commonly classified as homogeneous or heterogeneous. In the homogeneous catalysis the catalyst and the substrate are in the same phase, commonly they are both dissolved in a suitable solvent where the reaction takes place. In the heterogeneous catalysis the substrate and the catalyst reside in different phases; typical examples involve solid catalysts and liquid or gaseous reactants. Heterogeneous catalysts often exhibit lower reactivity and selectivity compared to their homogeneous analogues but, on the other hand, they enable an easier product isolation and they normally can be recovered and reused for several reaction cycles or employed in flow processes.

Because of the key role played by catalysis in the development of new and more sustainable processes, the searching for new and more efficient catalytic transformations is a task of great interest. Many efforts have been committed, indeed, to the design of novel catalytic transformations and to the improvement of efficiency of known processes. In this contest many studies focused on the immobilization of homogeneous catalysts on several supports in the attempt to build up catalytic systems merging the best of both homogeneous and heterogeneous catalysis: high reactivity and selectivity, easy product isolation and catalyst recyclability.^{4,5} Immobilization of homogeneous catalyst on insoluble supports like inorganic solids or highly cross-linked polymers by the means of different binding mechanism (covalent or ionic bonding, physical entrapment, adsorption) allows continuous flow operation, catalyst recovering by simple filtration and easy product isolation, but they suffer typical drawbacks of heterogeneous catalysts.

Liquid-liquid multiphase homogeneous catalysis has emerged in recent years as a promising solution to this problem. The key strategy to this approach is the immobilization of the homogeneous catalyst onto a liquid phase in which the reaction takes place in homogeneous fashion but, at the end of the reaction, the catalyst and the product are separated into two mutually

immiscible phases in which they possess high and complementary partition coefficients, thus both the catalyst and the product are easily recovered with minimal or no cross-contamination (fig.1).⁶

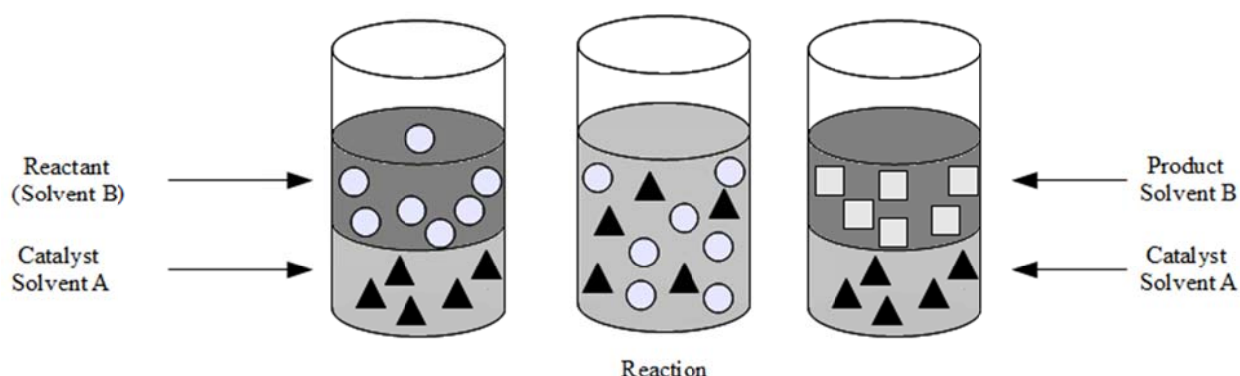


Fig. 1: Schematic representation of a liquid-liquid biphasic homogeneous catalytic process.

To address successfully this goal the solvent pair forming the catalytic system must be carefully chosen. Besides of classic organic solvents an ever larger collection of so-called unconventional media has emerged as suitable candidates for catalyst immobilization: water, supercritical fluids, fluorinated solvents and ionic liquids found wide application as catalyst immobilizing liquid phases. Water is certainly the most appealing solvent because it is cheap, readily available, environmentally friendly, non-toxic, non-flammable and it exhibits unique chemical and physical properties. However many organic compounds are only sparingly soluble in water and many reactions are incompatible with aqueous environment.⁷

The most employed supercritical fluid is supercritical CO₂ (scCO₂) which is non-toxic, non-flammable, inexpensive, relatively inert towards reactive compounds and readily separable from products upon depressurization, but scCO₂ is apolar and generally only suitable for compounds of low polarity in catalytic processes.⁸

Fluorinated solvents possess unusual physicochemical properties, such as low dielectric constants, high chemical and thermal stability, and low toxicity. They commonly exhibit temperature-dependent miscibility with organic solvents. Usually they are immiscible at low temperature, but miscible at elevated temperature, thus allowing for homogeneous catalysis at high temperature and easy catalyst-product separation at ambient condition.⁹

Ionic liquids (ILs) are salts with low melting points, they are typically constituted by ammonium or phosphonium cations and halogenated anions (fig.2).

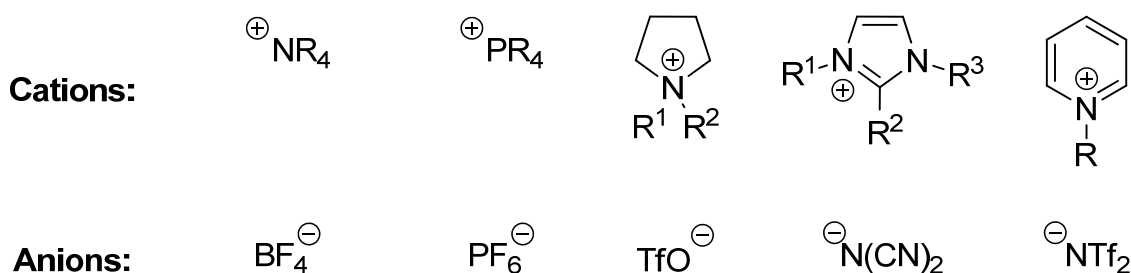


Fig. 2: Cations and anions commonly employed for the preparation of ILs (Tf = CF_3SO_2^-).

ILs display physicochemical properties, like low melting point, negligible vapor pressure, low flammability, tunable polarity and miscibility with other organic or inorganic compounds, that are appealing to catalysis and separation processes. Catalysts can be immobilized onto the ionic phase where the reaction takes place and the product is subsequently extracted with non-polar solvent or scCO_2 , so that ionic phase containing the catalyst can be recovered.¹⁰

In order to improve the efficiency of the catalyst separation step, its solubility in the immobilizing phase should be maximized. A common strategy to trap the catalyst in the supporting liquid phase is to install a tag on the catalyst backbone. The tag works as an element of molecular recognition providing high affinity for the chosen solvent.¹¹ A schematic representation of a tagged catalyst is showed in fig.3.



Fig. 3: Schematic representation of a tagged catalyst.

Obviously the chemical nature of the tag strongly depends on the solvent of choice. For example, soluble polymers are suitable supports to anchor homogeneous catalyst. After the reaction is complete, the polymer-anchored catalyst is separated from the reaction mixture and recovered, commonly by the addition of an anti-solvent followed by filtration. In particular polyethylene glycol (PEG) chains can be covalently attached to the catalyst skeleton to provide species soluble in polar solvent, like water, liquid PEG and polar organic solvents, where the reaction runs homogeneously. At the end of the reaction the polymer-bound catalyst is often recovered after diethyl ether addition.^{12,13} Perfluorinated alkyl tags enhance catalyst solubility in perfluorinated solvents for fluorine – organic biphasic systems.^{9,14} Finally installing an ion group onto the catalyst backbone normally provides a more hydrophilic catalyst whose solubility in water or ILs depends on the hydrophilicity of the catalyst backbone and the counter ion. This solubility profile enables the application of different strategies for catalyst recycling: water and ILs can be used as supporting phases for the ion-tagged catalyst and the catalyst containing aqueous or ionic phases can be

recovered at the end of the reaction, after product extraction or distillation. Organic solvents can be used as well, in this case the catalyst is recovered after addition of a non-polar solvent which dissolve the product and induces catalyst precipitation.

Development and application of ion-tagged ligands and organocatalysts, to set up efficient and recyclable catalytic systems, is the main topic of this work. In the following sections deeper description of structure and role of the ion-tag and examples of catalytic application reported in literature will be examined.^{15,16,17,18,19,20}

1.2. Ion-tagged catalysts and “electrosteric” activation.

Ion tagged catalysts differs from the general scheme reported in fig.3 for the presence of a counter ion, commonly the anion, given that it is usually the cation to be covalently bounded to the catalytic centre (fig.4).

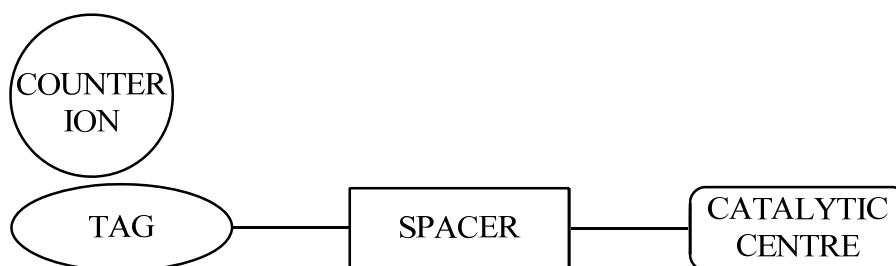


Fig. 4: General structure of an ion-tagged catalyst.

The presence of the counter ion is of great importance to determine the solubility profile of the catalyst. Because of their ionic character, ion-tagged catalysts are usually insoluble in non-polar, organic solvents, such as hexane or diethyl ether. They are usually soluble in polar, organic solvents, like acetonitrile, dimethylformamide, methanol, and in halogenated solvents, like chloroform or dichloromethane.¹⁵ The solubility in water, which is a key parameter for catalyst recovery when aqueous work-up is required, depends on the nature of the tag: hydrophobicity can be achieved using cations bearing long alkyl chains or using hydrophobic counter ions, like PF_6^- or NTf_2^- . Cations and anions commonly employed are borrowed from the chemistry of ILs, thus ammonium and phosphonium ions are the most common choice for the cation, while inorganic, halogenated anions are often chosen as counter ions (fig.2). Among the ammonium ions, imidazolium and pyridinium are the most widely used, because of their stability in many chemical transformations. The nature of the spacer is fundamental in determining the catalyst behavior as well. First of all the linker must be stable in the reaction conditions, moreover spacer length and flexibility should be wisely designed to achieve the best catalytic performance. The use of an ion-tag as a catalyst recovery strategy (fig.5) displays several attractive advantages: the careful choice

of the cation and anion structure enables fine tuning of the solubility, so that immobilization on the supporting phase can be optimized, and catalyst leaching reduced. In addition, ion-tags have better loading capacity compared to polymeric supports and they can be employed with common organic solvents, water and ILs (which are commonly addressed as benign solvents from an environmental point of view), whereas perfluorinated solvents are required with perfluoroalkyl-tagged catalysts.²¹

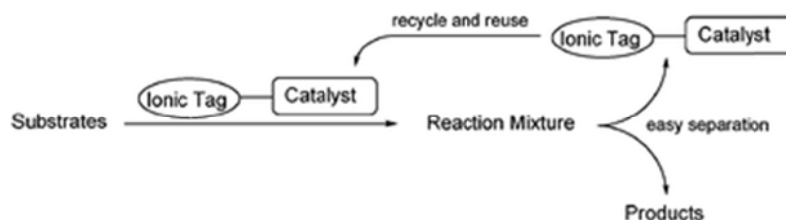


Fig. 5: Catalyst recovery strategy using an ion-tagged catalyst.

Finally, due to the presence of a charged group, the ion-tag can have a non-innocent role in the reaction and some ion-tagged catalysts displayed improved catalytic performance compared to their analogous untagged counterparts, when similar experimental conditions were applied. We were deeply interested in this aspect of ion-tagged catalysts chemistry, which usually deserves less attention compared to their use for catalyst immobilization. Experimental evidences emerged in our laboratory, along with examples reported in literature, where the reaction rate enhancement could be ascribed to the ion-tag, prompted us to speculate that the ionic group could stabilize the transition state, lowering the activation energy for the process.²² We posited as work hypothesis that, if the tag ion pair can approach charges that develop along the reaction coordinate with minimal distortion of bond angles and distances, it can lower the free-energy barrier by complementing charge separation in the dipolar transition state. As a consequence, the catalyst loading can be reduced compared to the reference homogeneous catalyst. In a similar manner to that in which organocatalysis mechanistically mimics enzymes with small organic molecules, the electrostatic stabilization of a transition state by an ion tag could be considered a simplified version of the electrostatic activation of enzymatic reactions, due to protein cationic and anionic residues oriented towards the charges of a dipolar transition state. Moreover the presence of the ion pair also determines new steric interactions. Since the overall effect is the resultant of electrostatic and steric interactions, we define it either as “electrosteric stabilization” of the transition state by the ionic tag, or “electrosteric activation” of the catalytic process (fig.6). The term “electrosteric stabilization” is commonly used in colloid and nanoparticle chemistry to define their stabilization towards aggregation by polyelectrolytes or quaternary ammonium salts through combined electrostatic and steric effects.

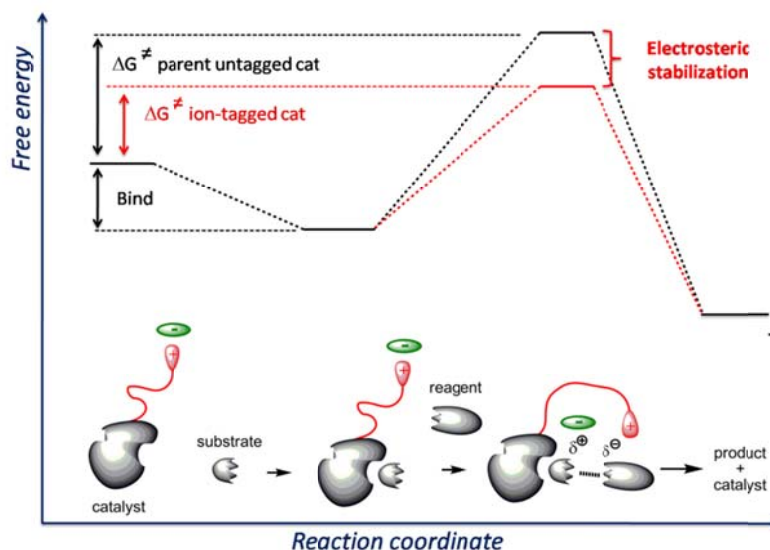


Fig. 6: Schematic representation of the transition state “electrosteric stabilization” performed by an ion-tagged catalyst.

Provided that interactions between the ionic group and the transition state take place, it is conceivable that the stereochemical outcome of the reaction could be affected as well. Indeed, if parallel reaction pathways leading to stereoisomeric products are accessible electrosteric interactions may affect competitive transition states to a different extent. However, predicting the effect of the ion-tag on reactivity and selectivity, is an extremely challenging issue, since it depends on several factors: the ion covalently bounded to the catalyst, the nature of the potentially exchangeable counter ion, the length and flexibility of the spacer, which must ensure the best charge approach with minimal strain energy. In addition, also the interaction of the solvent with the polar transition state and the ionic group should be taken into account, particularly when polar and highly structured solvents, like water and ILs, are employed.²² The number and complexity of these factors are in fact the major limitation to the rational design of new ion-tagged catalysts.

1.3. Ion-tagged organometallic catalysts

ILs turned out to be suitable solvents for many transition-metal catalyzed transformations, due to their capability to dissolve and stabilize many organometallic complexes. Nevertheless non-ionic catalysts often suffer from catalyst leaching and poor recyclability. Ion-tagged ligands provide an attractive solution for increasing catalyst stability and recyclability and to prevent catalyst leaching and consequent product contamination. Literature examples of reactions catalyzed by ion-tagged organometallic complexes are reported in the next paragraphs.

1.3.1. Catalytic hydrogenation of olefins.

Asymmetric alkene hydrogenation is a powerful tool in organic chemistry to prepare enantiopure compounds with excellent atom economy. The catalysts applied in this transformation are generally based on Rh (I) and chiral phosphines, which are extremely expensive, therefore a reusable catalytic system is highly desirable for this transformation. Generally olefins bearing a metal coordinating group are required to achieve products with high enantiomeric excess (ee): methyl α -acetamidoacrylate (**1**), methyl α -acetamido cinnamate (**2**) and dimethyl itaconate (**3**) are the most common substrates to evaluate the catalytic system performances (fig.7).²³

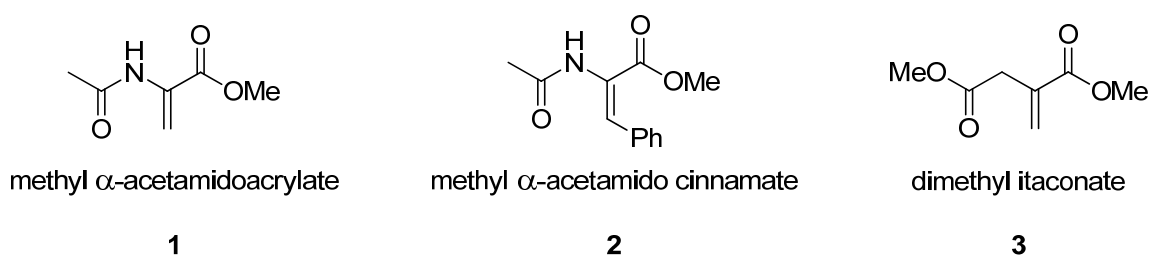
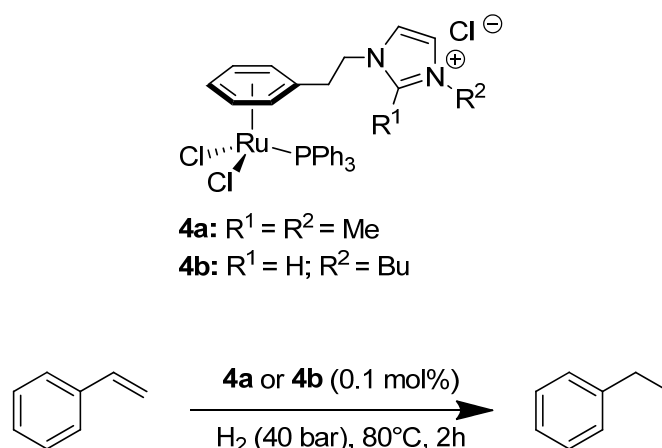


Fig. 7: Commonly employed substrates in asymmetric catalytic hydrogenation.

Although Rh is the metal of choice for this transformation other transition-metals may be utilized. Dyson *et al.* reported that Ru complexes **4a** and **4b**, bearing a phenyl ionic ligand, acted as catalysts for styrene hydrogenation, either in water or in the IL [C₂pic][NTf₂] (N-ethyl-3-methylpicolinium bis(trifluoromethane)sulfonimide) (fig.8).

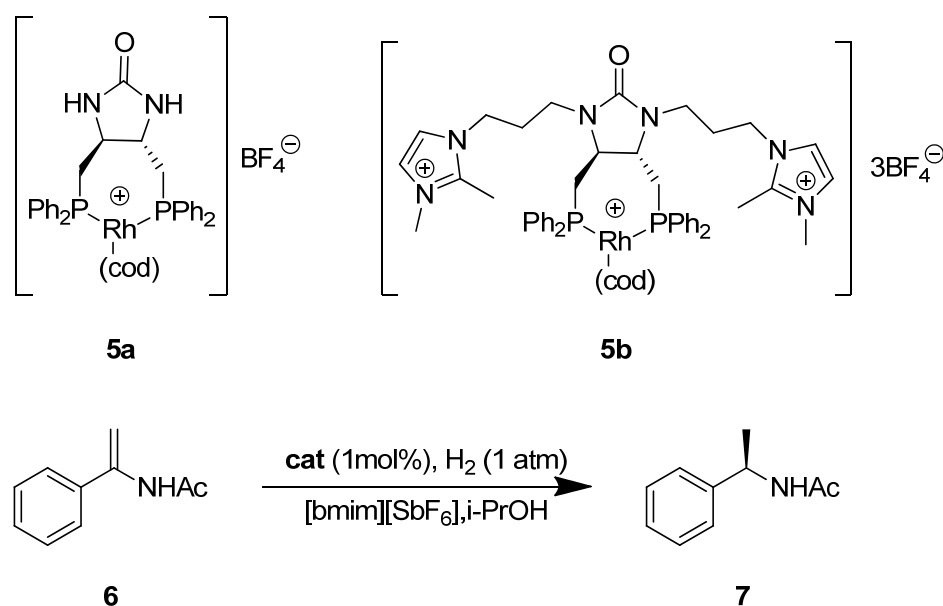


Entry	Catalyst	Run 1 (%)	Run 3 (%)	Run 3 (%)
1	4a – H ₂ O	>99	97	97
2	4b – H ₂ O	98	85	75
3	4b – [C ₂ pic][NTf ₂]	11	10.5	14

Fig. 8: Catalytic hydrogenation of styrene with ion-tagged Ru complexes.

In water **4a** and **4b** showed good activity (Entry 1-2), while compound **4b**, when immobilized in [C₂pic][NTf₂], afforded markedly lower reaction rates (Entry 3). However immobilization of the catalysts in water resulted in slight leaching into the organic phase, whereas in the ionic liquid-organic system no leaching was observed and greater stability of the catalyst in the IL was demonstrated by experimental observation (in the course of the catalytic runs the color of the aqueous solution changed from orange to brown-purple, whereas the IL solution remained orange) and NMR studies.²⁴

Chiral ion-tagged diphosphine ligand for Rh catalyzed asymmetric hydrogenation of enamide **6** was reported by Lee and co-workers (fig.9).



Entry	Cat	Run	Time (h)	Conv.(%)	ee (%)
1	5b (1 mol%)	1	1	100	97.0
2	5b (1 mol%)	2	1	100	96.6
3	5b (1 mol%)	3	1	100	96.2
4	5b (1 mol%)	4	1	82	95.4
5	5b (1 mol%)	4	8	100	95.4
6	5a (1 mol%)	1	1	100	95.8
7	5a (1 mol%)	2	1	100	95.1
8	5a (1 mol%)	3	1	78	94.2
9	5a (1 mol%)	4	1	51	91.4
10	5a (1 mol%)	4	12	85	88.0
11	5a (0.5 mol%)	1	1	100	95.6

Fig. 9: Asymmetric enamide hydrogenation catalyzed by ion-tagged Rh complex.

The reactivity of catalyst **5b**, bearing two imidazolium moieties, was compared to the untagged analogous **5a**, in the biphasic system [bmim][SbF₆] / i-PrOH ([bmim][SbF₆] = 1-Butyl-3-methylimidazolium hexafluoroantimonate). As expected, the IL grafted Rh-complex **5b** was successfully immobilized in the IL, which could be reused three times without any loss of catalytic efficiency (Entries 1 - 3). In the fourth run, the catalytic activity was slightly decreased (Entry 4), but the reaction was completed when the reaction time was prolonged to 8 hours, with almost no loss in enantioselectivity (Entry 5). On the other hand, the catalytic efficiency of complex **5a** dropped significantly after two runs (Entries 6-8). After the fourth cycle (Entry 9) the reactions did not complete even with prolonged reaction time (entry 10). Moreover in the i-PrOH layer, separated from the first run with **5b**, no Rh and phosphorus were detected, whereas leaching of Rh and phosphorus was observed when the reaction was carried out with **5a**. However, catalyst leaching was not the only reason for the decreased catalytic activity of **5a**, since complete conversion of the reaction could be achieved in the presence of only 0.5 mol% of catalyst (entry 11). Therefore the imidazolium moieties on the ligand backbone not only prevented catalyst leaching from the IL layer but also increased the catalyst stability.²⁵

Josiphos ligands were tagged with an imidazolium ion *via* an amide linker and used as Rh ligands for asymmetric hydrogenation of **1** and **3** in the biphasic system [bmim][BF₄] / MTBE (fig.10).

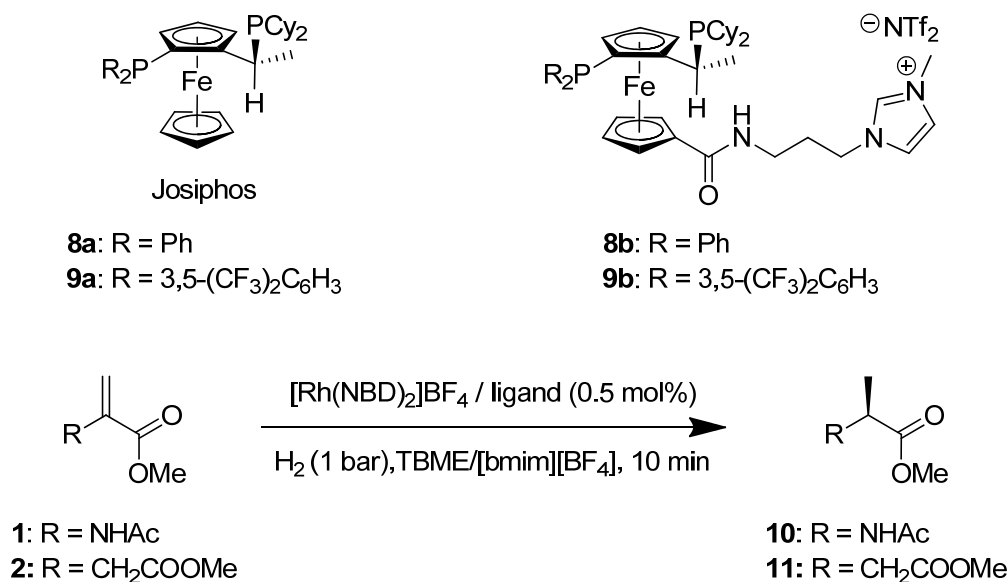
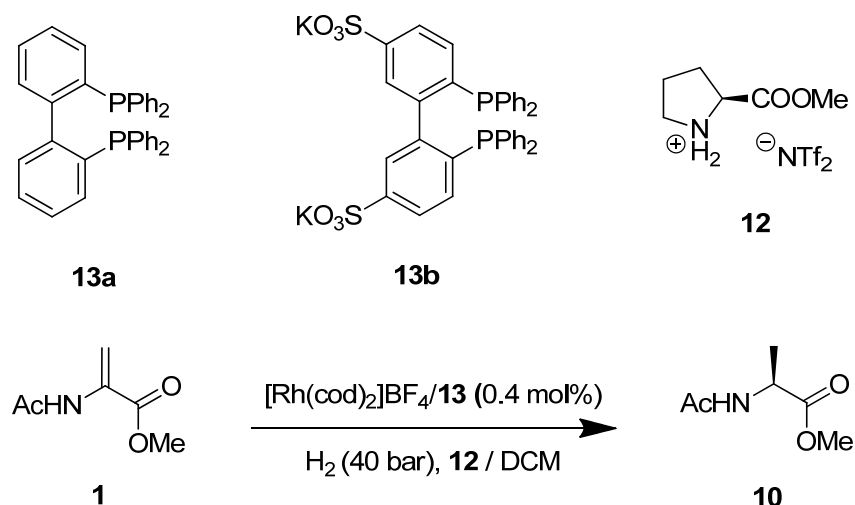


Fig. 10: Asymmetric olefins hydrogenation with ionic Josiphos-type ligands.

The ion tagged ligands displayed selectivity and reactivity similar to the untagged analogous both in organic solvent and biphasic system, but again ion tagged catalysts **8b** and **9b** exhibited greater recyclability and stability in the ionic phase and catalyst leaching was prevented: with **9b** hydrogenation of **1** could be carried out with only 15 % of TOF decreasing after 8 reactions runs.²⁶

Asymmetric hydrogenation of **1** with *tropos* ionic diphosphine in a chiral IL was reported by Leitner and co-workers (fig.11).



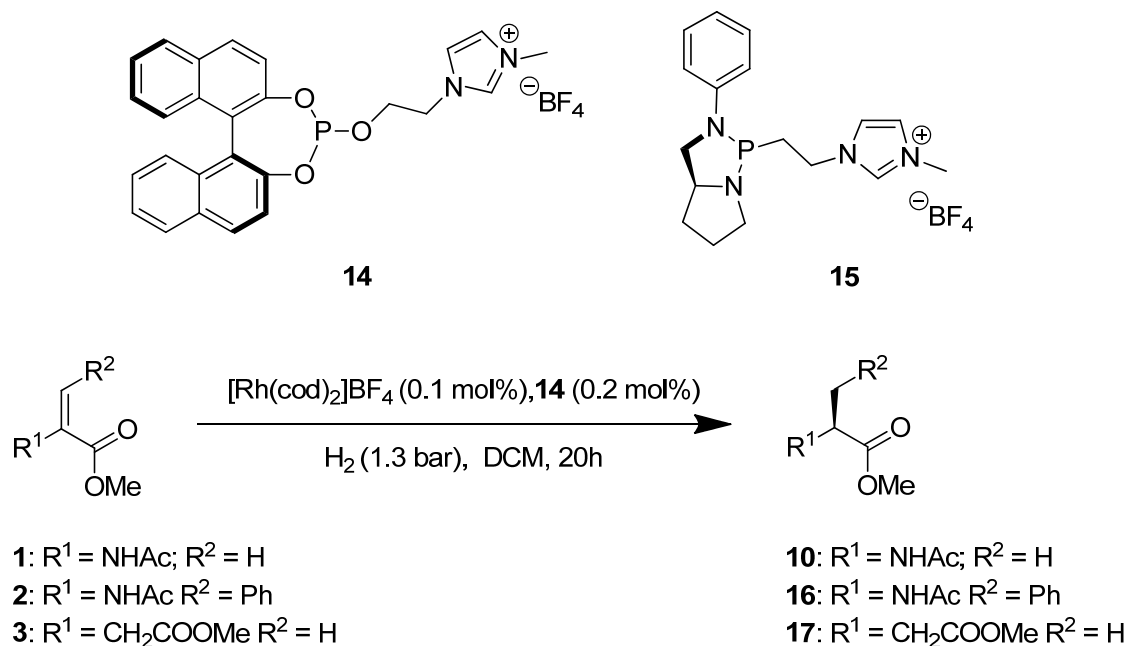
Entry	Ligand	Additive	ee (%)
1	13a	-	28 (<i>S</i>)
2	13b	-	49 (<i>S</i>)
3	13b	TEA (20 eq.)	69 (<i>S</i>)

Fig. 11: Asymmetric hydrogenation of enamide catalyzed by a Rh - *tropos* ionic ligand complex in a chiral IL.

Tropos ligands don't bear a permanent chiral information, since, in contrast with binaphthyl ligands, they don't possess a "locked" structure because, due to the lack of substituents in the 6,6' position, free rotation around the single bond connecting the two phenyl ring is allowed. However, if an external chiral bias is present, one of the two enantiomeric conformation may become favoured. In the example reported the chiral information was held by the chiral IL liquid **12**. The ionic biphenyl ligand **13b** showed clearly greater enantioselectivity compared to the non-ionic analogous **13a** in the condition reported (Entry 1-2). Addition of TEA (TEA = NEt₃) further improved the enantioselectivity (Entry 3). The catalytic system could be recycled, but depletion of reactivity and selectivity appeared in the 3rd run.²⁷ Although the exact mechanism leading to the chiral induction was not completely cleared, further studies, conducted by the same group on a similar reaction, suggested that the role of the chiral IL might be to effectively block the catalytic cycle for one of the two enantiomers of the catalyst (chiral poisoning).²⁸

The ion-tagged phosphite **14** and the diamidophosphite **15** were synthesized by Reetz group and tested as monodentate Rh ligands for asymmetric hydrogenation of substrates **1,2** and **3** in organic solvent and ILs (fig.12). **14**-Rh complex acted as an efficient catalyst for this transformation yielding, with all the substrates, products with complete conversion and elevated ee (Entry 1,3,4).

The Rh complex with **14** could be reused with no loss of reactivity and selectivity when hydrogenation of **1** was carried out in DCM (Entry 1,2).²⁹



Entry	Substrate	Conversion (%)	ee (%)
1	1 (1 st run)	100	94 (<i>S</i>)
2	1 (2 nd run)	100	94 (<i>S</i>)
3	2	100	93 (<i>R</i>)
4	3	100	96 (<i>R</i>)

Fig. 12: Asymmetric hydrogenation of olefins with ionic phosphite – Rh complex.

1.3.2. Catalytic hydroformylation of olefins.

The hydroformylation reaction constitutes one of the most successful organometallic reactions in organic synthesis history. In this transformation an alkene is reacted with molecular hydrogen and carbon monoxide (synthesis gas or syngas) to obtain an aldehyde with high atom economy (fig.13).²³

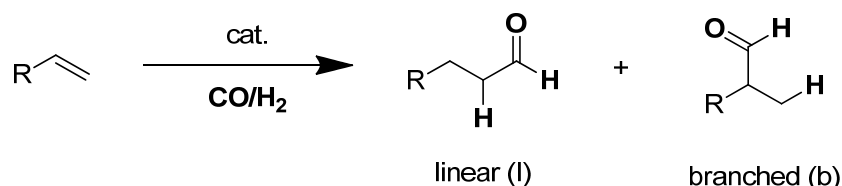


Fig. 13: General scheme for catalytic hydroformylation of olefins.

The most common catalysts for this transformation are complex of Rh bearing phosphine ligands. The major issues to address in this reaction, besides the activity of the catalytic system, are the

regioselectivity (l/b ratio) and the effective separation and recovery of the catalytic system. The last point deserve particular attention due to the outstanding importance of this reaction from an industrial point of view. Hydroformylation is indeed an important process in the bulk chemicals industry producing more than 6 M tons of aldehydes and alcohols per annum for the manufacture of soaps, detergents, and plasticizers.³⁰ In the Ruhrchemie/Rhône-Poulenc process,³¹ for the large scale production of short chain aldehydes, the hydroformylation is carried out in a biphasic aqueous system where the Rh catalyst is immobilized in the aqueous phase using the hydrosoluble ionic ligand **18** (fig.14). Unfortunately this strategy fails for olefins with longer chains, due to their very low solubility in water. Many examples of recoverable catalytic systems based on ion-tagged ligands are present in literature. Several research groups exploited ionic ligands derived from sulfonated PPh₃ (fig.14) as Rh ligands in various biphasic systems.

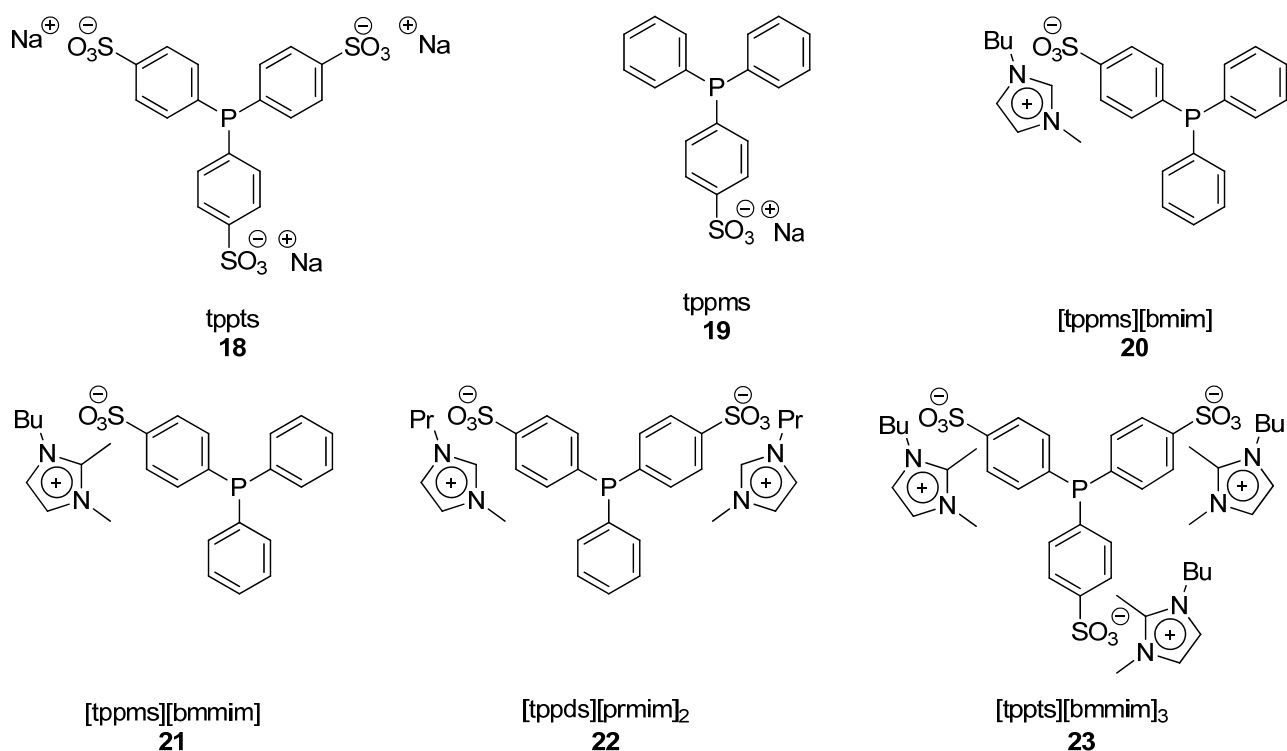
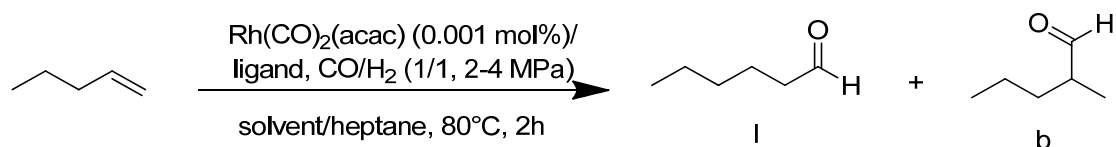


Fig. 14: Sulfonated phosphines for Rh catalyzed hydroformylation.

The first report about the use of sulfonated phosphines in ILs was made by Chauvin's group. **18** and **19** acted as Rh ligands in the hydroformylation of 1-pentene in imidazolium ILs (Tab.1) with lower yield and reactivity compared with untagged PPh₃ (Entry 1). However the use of sulfonated phosphines prevented the leaching of Rh and phosphorous into the organic phase, still maintaining acceptable values of TOF and similar regioselectivity (Entry 2,3).³² The use of imidazolium counter ions for the sulfonated phosphines led to better solubility of the complex in the ionic media, improving the catalyst performance. [tppms][bmim] (**20**) and [tppms][bmmim] (**21**) were employed as Rh ligand for hydroformylation of 1-octene in IL / scCO₂.



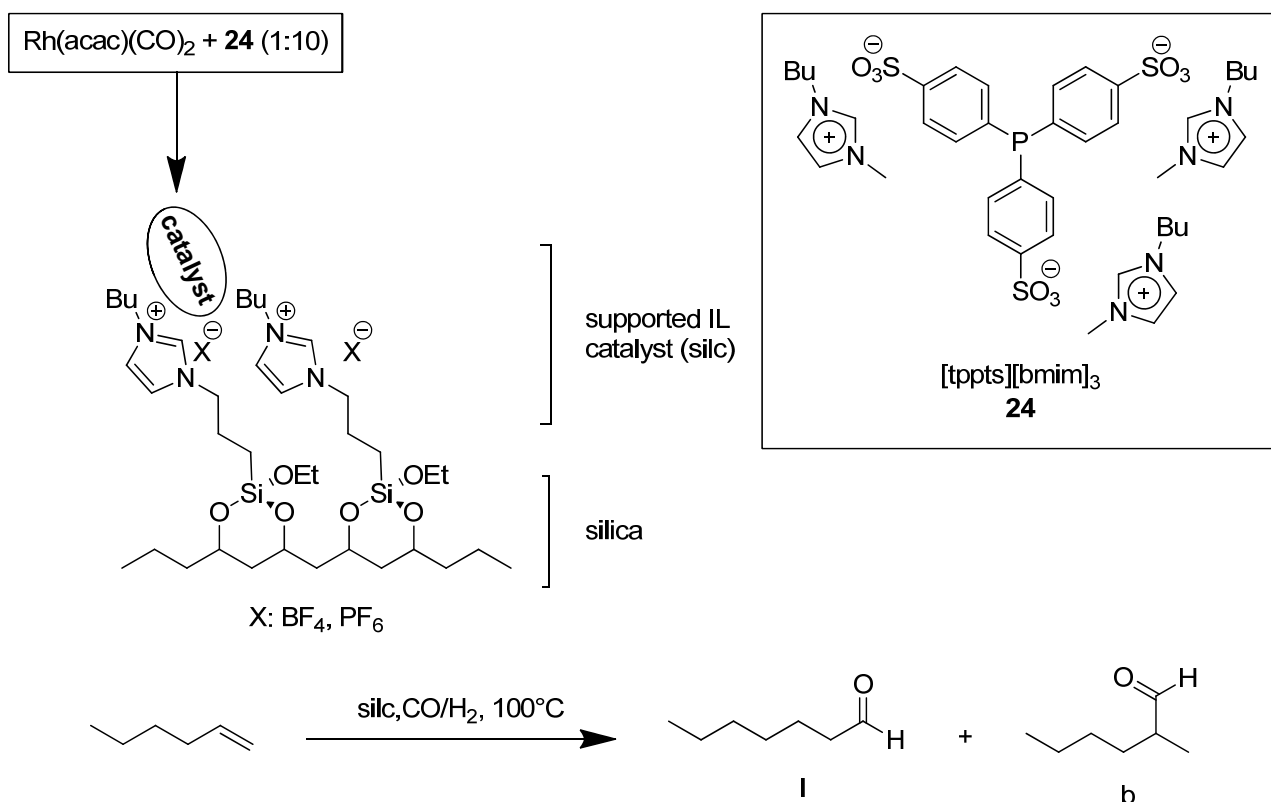
Entry	Solvent	Ligand	Rh/P	Yield (%)	l/b	TOF (h ⁻¹)
1	[bmim][PF ₆]	PPh ₃	0.106	99	3	333
2	[bmim][PF ₆]	tppms (19)	0.106	16	3.9	59
3	[emim][BF ₄]	tppts (18)	0.33	33	2.8	103

Tab. 1: Hydroformylation of 1-pentene in ILs with sulfonated phosphines.

The system turned out to be moderately reactive and highly recyclable: up to 9 reaction runs could be made with only a small loss of reactivity, whereas regioselectivity remained unchanged and no Rh leaching into the product phase was detected. Moreover a Rh complex with [tppts][primim]₂ (**22**), grafted on an imidazolium based IL, after careful optimization of the reaction parameters, was employed in continuous-flow system for hydroformylation of long chain olefins. The catalyst displayed high reactivity and stability, working for several days with a very low Rh leaching in the product phase.³⁰

Rh - [tppts][bmmim]₃ (**23**) complex was immobilized in different imidazolium based ILs to explore biphasic hydroformylation of 1-hexene. The catalytic system exhibited reactivity of about an order of magnitude (based on the TOF) lower than the common employed catalyst Rh/PPh₃, as expected because of the lower solubility of the apolar olefin in the ionic phase. Nevertheless the system still displayed acceptable reactivity and selectivity, and the ionic phase could be recycled up to 10 times with only a small drop in the catalyst performance. The Rh leaching in the organic phase was found to be depending on the aldehyde.³³ An interesting system to support the ionic Rh complex was reported by Mehnert and co-workers. An imidazolium moiety was covalently attached to silica gel, creating an IL layer which covered the silica surface. The catalyst was prepared by mixing Rh(acac)(CO)₂ and ligand **24** in CH₃CN (fig.15) and adding this solution to the surface modified silica. After solvent evaporation the supported IL catalyst (sile) was collected as a solid which was tested in hydroformylation of 1-hexene. The advantage of this strategy was that the reaction took place in a homogeneous fashion in the ionic layers, but the solid sile could be easily separated from the product. Sile based catalyst exhibited lower reactivity and similar selectivity, compared to the homogeneous system (Entry 5), either using [bmim][BF₄] or [bmim][PF₆] (Entry 1,2). On the other hand they showed higher TOF compared to the “classic” biphasic system IL / organic solvent (Entry 3,4), probably due to the higher substrate concentration in the ionic layer when sile was employed. Catalyst leaching in the organic phase depended both on the aldehyde concentration and

on the IL support: since [bmim][BF₄] was more soluble in the organic phase, its use resulted in higher metal and phosphorus leaching.³⁴



Entry	Catalyst	Solvent	Time (min)	Yield (%)	I/b	TOF (h ⁻¹)
1	silc	[bmim][BF ₄]	300	33	2.4	65
2	silc	[bmim][PF ₆]	270	46	2.4	60
3	biphasic	[bmim][BF ₄]	230	58	2.2	23
4	biphasic	[bmim][PF ₆]	180	70	2.5	22
5	homog/PPh ₃	Toluene	120	95	2.6	400

Fig. 15: Olefins hydroformylation catalyzed by Rh-silc.

Besides sulfonation, other strategies were developed for the synthesis of ion-tagged phosphine ligands. Olivier-Bourbigou's group compared the catalytic behavior of some ionic phosphines and phosphites bearing various ionic groups (fig.16). Ligands **25** and **26**, all based on PPh₃ structure, displayed a similar performance when combined with Rh(acac)(CO)₂ in [bmim][BF₄] for the hydroformylation of 1-hexene. **25a** and **25b**, bearing a guanidinium ion, showed greater selectivity for the linear aldehyde compared to **26** (Entry 1-3), whereas ligand **26**, tagged with a pyridinium moiety, exhibited a slightly higher reactivity (Entry 3). The ionic phosphite **27** turned out to be the more efficient ligand (entry 4). In this case the ionic phase could also be recycled for 3 times with

only a small loss of reactivity (Entry 4-6), demonstrating the stability of the ligand, in contrast with aqueous biphasic system, where phosphite ligands decompose by hydrolysis.³⁵

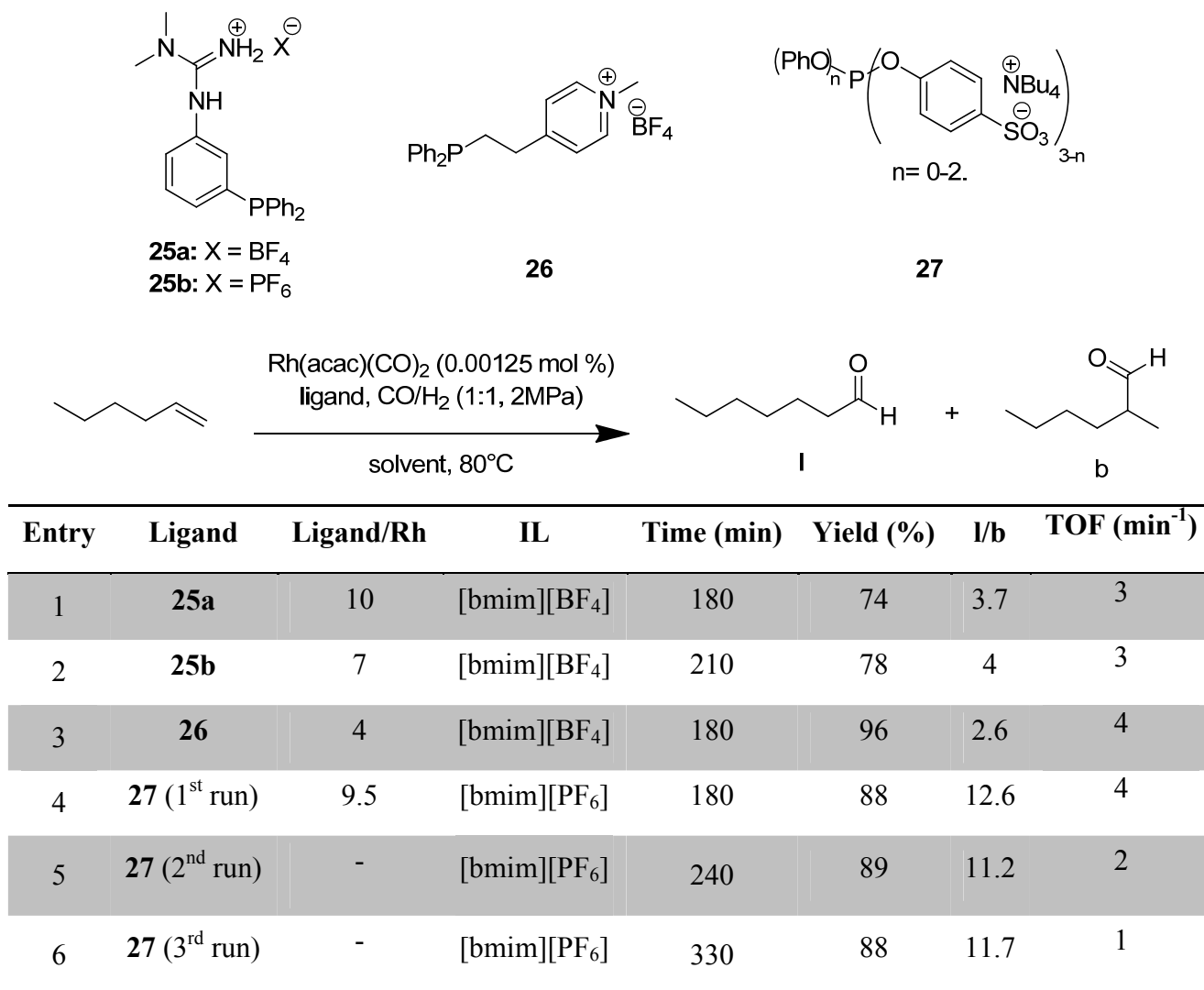


Fig. 16: Olefines hydroformylation catalyzed by various Rh – ionic phosphine complexes.

Imidazolium tagged phosphines was reported by Wasserscheid *et al.* Ligand **28** (fig.17) was prepared by addition of phenylphosphine to 1-vinylimidazole. When hydroformylation of 1-octene was carried out in [bmim][PF₆] no leaching of Rh in the organic phase was detected.³⁶

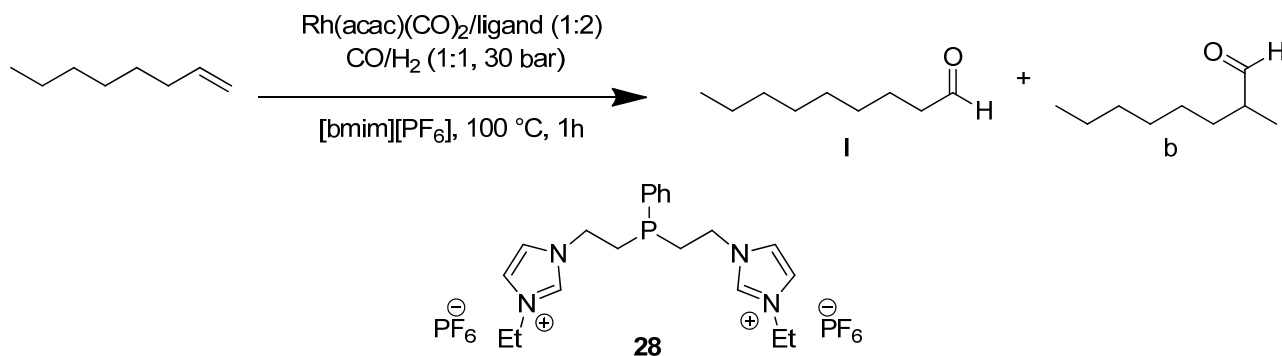
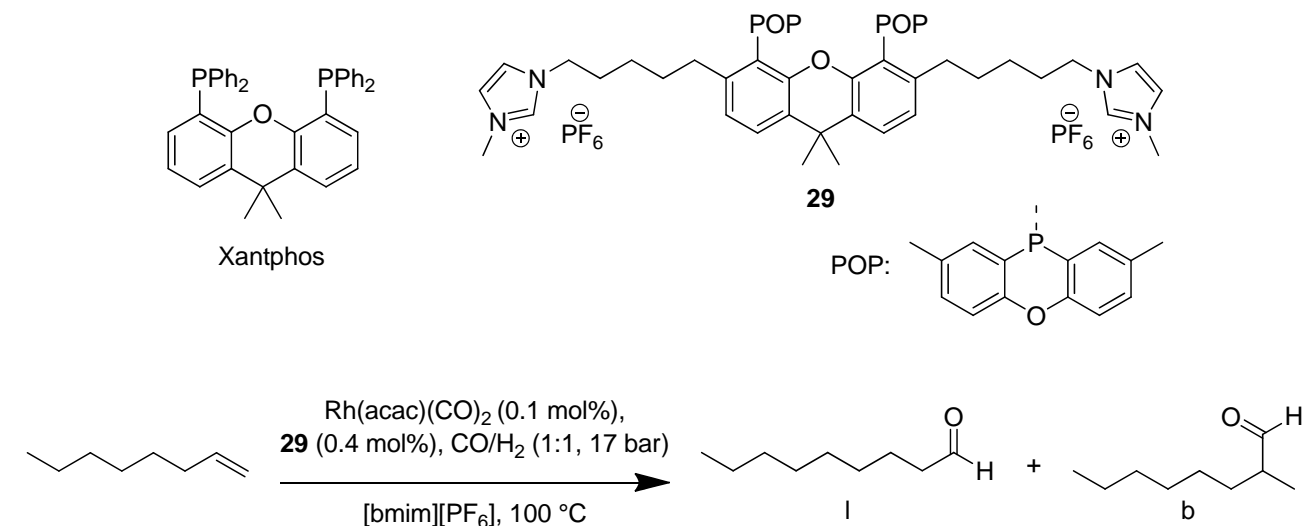


Fig. 17: Imidazolium-tagged phosphine ligand for Rh catalyzed hydroformylation.

The Xantphos-type ligand **29** (fig.18), bearing two ionic moieties, displayed high reactivity and selectivity and outstanding stability when immobilized in [bmim][PF₆]. Catalyst could be recycled for 7 times (Entry 1-7) with no loss in activity, yielding the linear aldehyde with high selectivity. No depletion in the catalytic activity was observed even after storing the catalyst solution under air atmosphere for 14 days.³⁷



Cycle	Aldehyde % ^a	I/b ^a	TOF (h ⁻¹) ^a
1	86.2	44	65
2	89.8	49	88
3	90.1	44	93
4	90.3	44	112
5	88.1	38	107
6 ^b	85.0	49	318
7 ^b	80.8	55	305

(a) Calculated at 30 % of conversion
 (b) pH₂ = 40 bar, pCO = 6 bar.

Fig. 18: Rh catalyzed hydroformylation with Xantphos-type ionic ligand.

Ligand **30a** (fig.19) was based on PPh₃ with the phenyl rings bearing an amidine moiety. Amidine group was capable to react with CO₂, forming an ionic group which made the ligand **30b** soluble in water. The reaction with CO₂ is reversible, and bubbling N₂ into the reaction mixture the toluene soluble, non-ionic ligand **30a** was re-formed. This switchable ionic ligand was employed for the hydroformylation of olefins in the biphasic system toluene-water. The system displayed outstanding reactivity (TOF of about 10000 h⁻¹) and catalyst recycle was possible for at least 3 times (Entry 1-

3). The reaction took place in the organic phase, where the olefin is highly soluble, in an efficient way and at the end of the reaction the ionic catalyst **30b** migrated efficiently in the aqueous phase, when CO₂ was bubbled into the reaction mixture. After the organic phase containing the product was separated, a fresh 1-octene solution in toluene was added. Bubbling N₂ the species **30a** was formed again and it moved into the organic phase where the reaction started again.³⁸

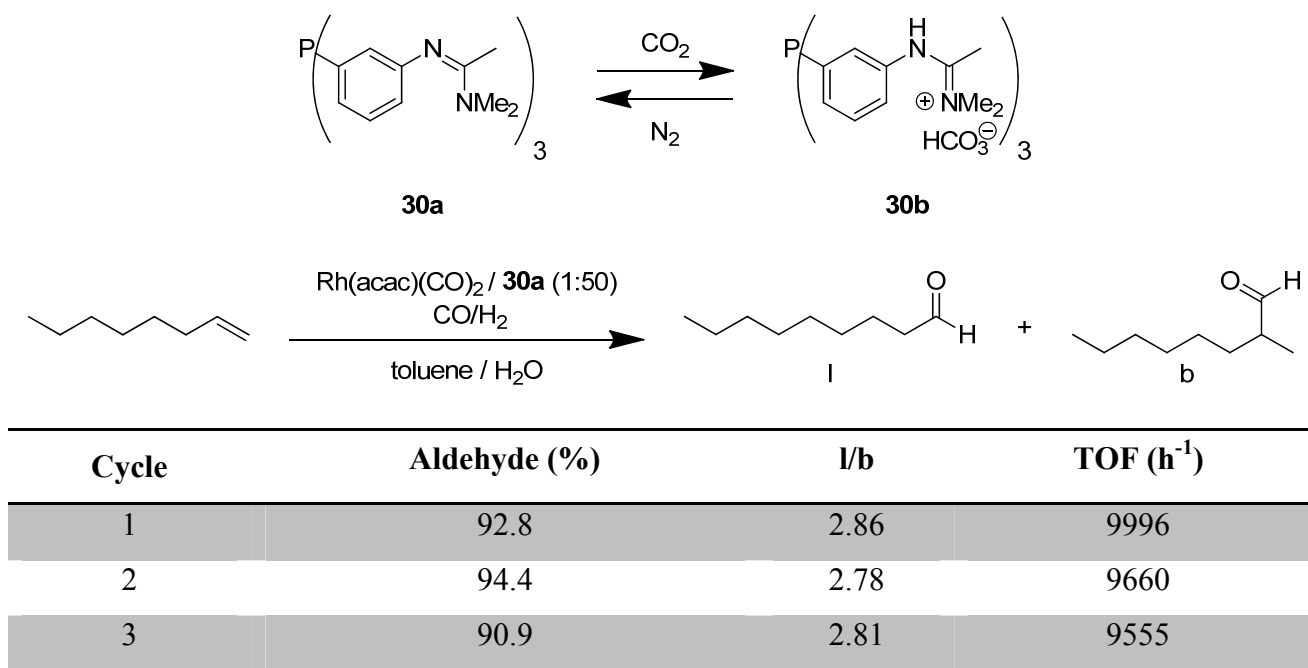


Fig. 19: Rh catalyzed hydroformylation of 1-octene with switchable ionic ligand.

1.3.3. Ring closing metathesis (RCM).

Olefin metathesis is an outstanding methodology for C=C bond formation because of the mild reaction conditions, functional group tolerance, high activity, stable precatalysts and easily available alkenes as starting materials. Grubbs' Ru catalyst and analogues (fig.20) effectively catalyzed olefin metathesis in ILs, but the catalytic activity vanished quickly in subsequent recycling runs due to catalytic systems decomposition or to catalyst leaching into the organic phase during product extraction procedures.¹⁵ In order to overcome this difficult several ion-tagged ligands were designed. Catalysts **31-33** (fig.20) presented several attractive points to install the ionic tag and, although the phenyl ring was the most common choice, the isopropoxy group and the phosphine moiety were exploited as well.

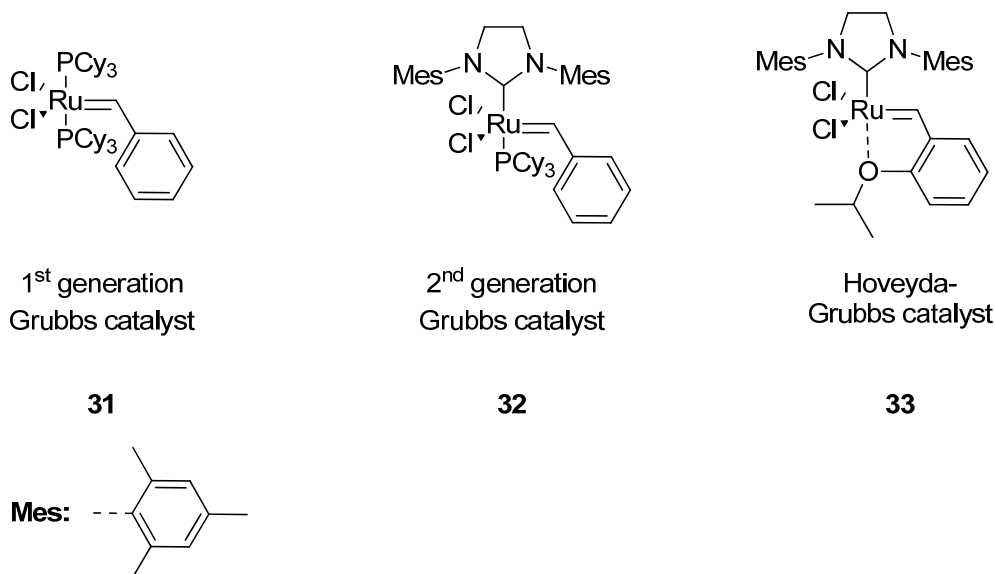


Fig. 20: Ru catalysts commonly employed in olefin metathesis.

Guillemin³⁹ and Yao⁴⁰ designed independently almost the same imidazolium tagged catalysts based on Hoveyda-Grubbs 1st generation catalyst (**34** and **35** fig.21)

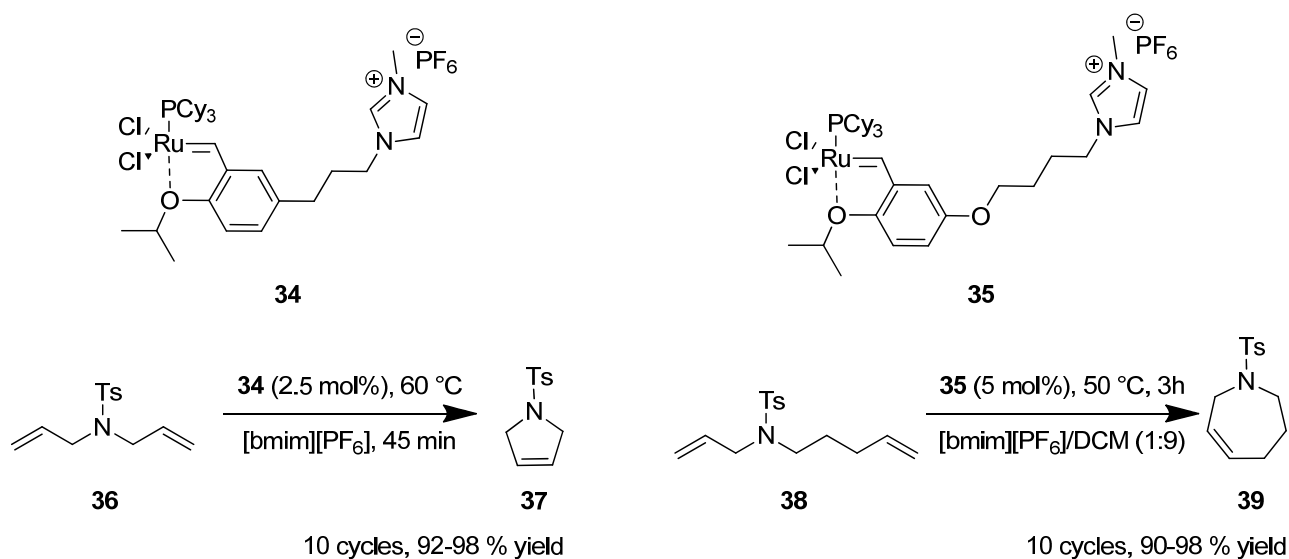


Fig. 21: RCM catalyzed by imidazolium tagged 1st generation Grubbs-Hoveyda catalysts.

The only difference between catalyst **34** and **35** was the spacer. In **34** a three carbon alkyl chain joined the ionic group to the catalyst, while in **35** a four carbon chain linked the imidazolium group to the phenyl ring *via* a phenol ether bond. The catalytic performance of the two catalysts was similar. When **34** and **35** were grafted onto IL [bmim][PF₆] both of them could be recycled for 10 times with almost no loss of activity, when the RCM of allyl amines **36** and **38** were carried out (fig.21). The same group reported successively the corresponding 2nd generation catalysts **40** and **41** (fig.22),^{41,42} which presented, compared to the 1st generation analogues, an higher activity and a

wider scope, allowing to perform RCM of more challenging substrates, like steric hindered olefins and olefins containing heteroatoms.

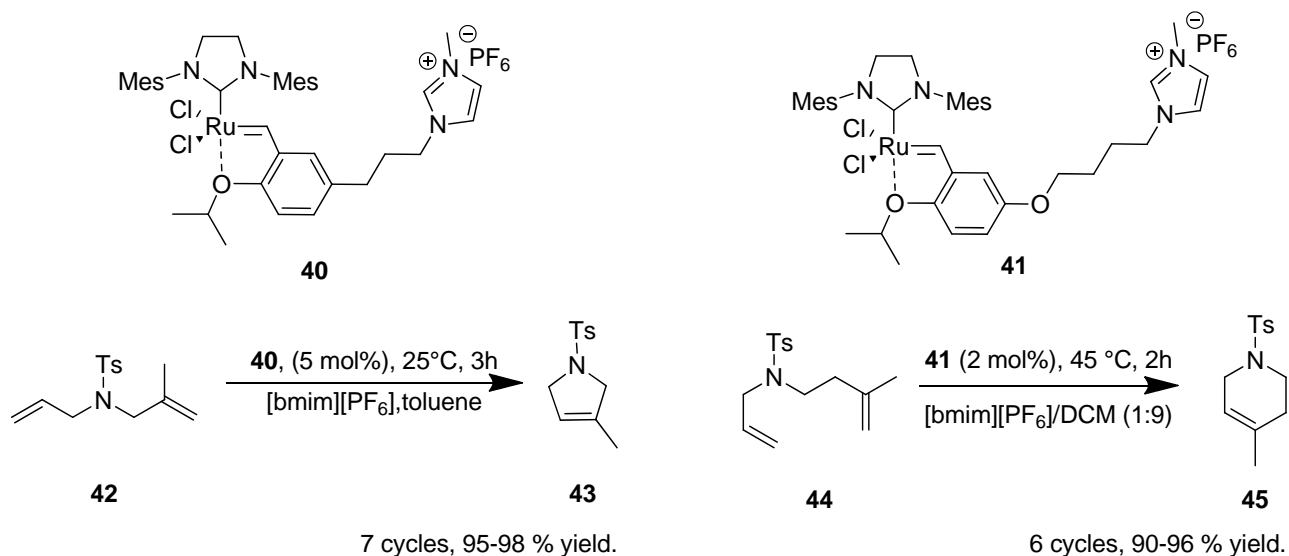


Fig. 22: RCM catalyzed by imidazolium tagged 2nd generation Grubbs-Hoveyda catalysts.

Again, the two catalyst displayed a similar behavior, acting as efficient catalysts for the RCM of a wide range of olefins. For example, trisubstituted olefins **43** and **45** could be synthesized in mild condition with high yield, recycling the catalyst for 7 and 6 times respectively (fig.22).

Due to its acidic proton imidazolium ion without substituents in the position 2 can interact with metals, forming NHC-metal complexes. In order to avoid this phenomena imidazolium ion can be replaced by pyridinium. Pyridinium tagged 2nd generation Hoveyda-Grubbs Ru catalysts **46-48** were reported by Grela and co-workers (fig.23).^{43,44}

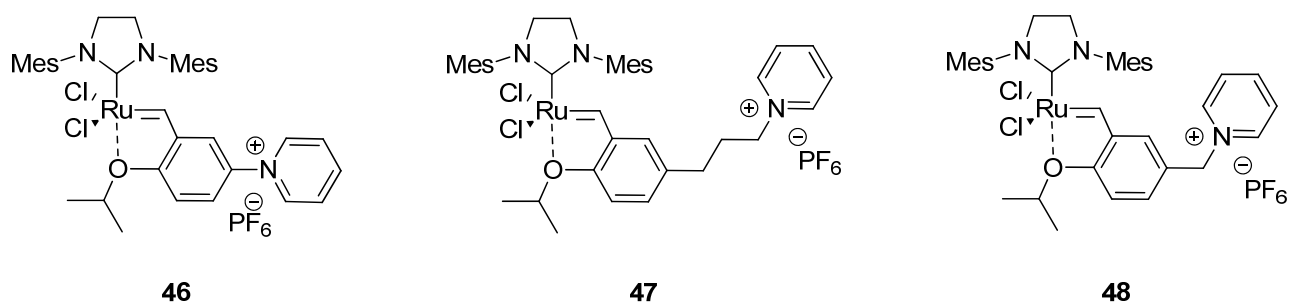


Fig. 23: Pyridinium tagged 2nd generation Hoveyda-Grubbs catalysts.

It was worth noting how the length of the spacers was important to determine the catalytic performance. It was known that electron withdrawing groups (EWG) on the phenyl ring increased the reactivity of the catalyst, weakening the Ru-O bond. Therefore the catalyst **46**, bearing the EWG pyridinium, was expected to be more reactive. Indeed it turned out to be more reactive than ionic catalysts **40** and **48** and even than non-ionic catalyst **33**, as shown in fig. 24, where the kinetics for RCM of diethyl 2-allyl-2-(2-methylallyl)malonate (**49**), with various Ru catalysts, is reported.

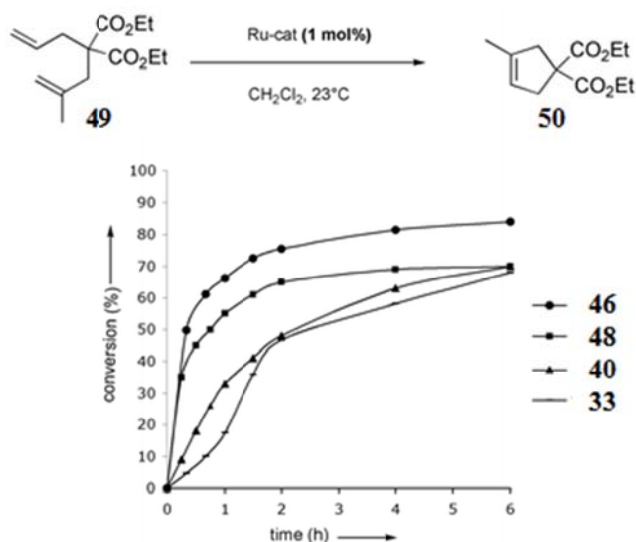


Fig. 24: Compared reactivity of some Ru catalysts.

During the reaction the bond between the ion-tagged ligand and the Ru atom is cleaved, delivering a 14-electron Ru complex that resides preferentially in the organic phase. Once the substrate has been consumed, the catalytically active complex returns to the IL phase by reattachment to the ion-tagged ligand, preventing catalyst leaching. Due to the greater difficulty in forming the metal-ligand bond in catalyst **46**, probably the “release and return” mechanism didn’t work properly and the catalyst couldn’t be recycled efficiently. The fact that poor recyclability was due to the spacer length and not to the pyridinium ion was confirmed by **47**, which exhibited recyclability similar to the imidazolium-tagged analogous **40** (fig.25).

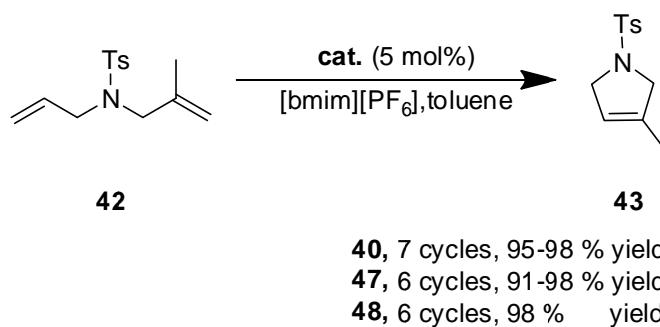


Fig. 25: Compared recyclability of various ion tagged catalysts.

In order to combine the high reactivity of **46** and recyclability of **47**, catalyst **48** was synthesized using a methylene as spacer. As expected **48** was easily recycled (fig.25) and it turned out to be almost as reactive as **46**, especially at the beginning of the reaction (fig.24). Finally is interesting to note that the pyridinium group in **46** and **48** was not installed by usual pyridine alkylation, but using Zincke reaction,⁴⁵ which transforms a primary amine into a pyridinium ion, as schematically depicted in fig.26.

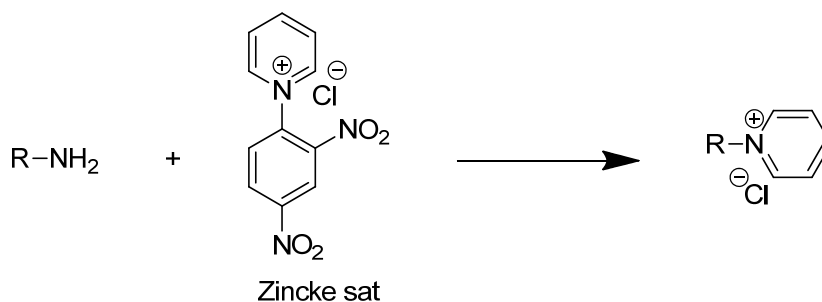


Fig. 26: Schematic representation of Zincke reaction.

The isopropoxy group was exploited as an attachment point for the ion-tag as well. Ligands **51-54** (fig.27) bore the ionic-tag attached either to the isopropoxy group or to the free *ortho* position next to it.^{46,47} As expected, factors weakening the Ru-O bond increased catalyst activity and had detrimental effect on catalyst recyclability. Thus **51** turned out to be more active than **52**, due the steric hindrance of the *ortho* substituent, and **54** proved to be more active than **53**, due to the nearer ionic EWG. However only **53b** demonstrated appreciable recyclability (fig.27)

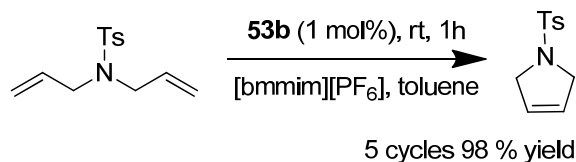
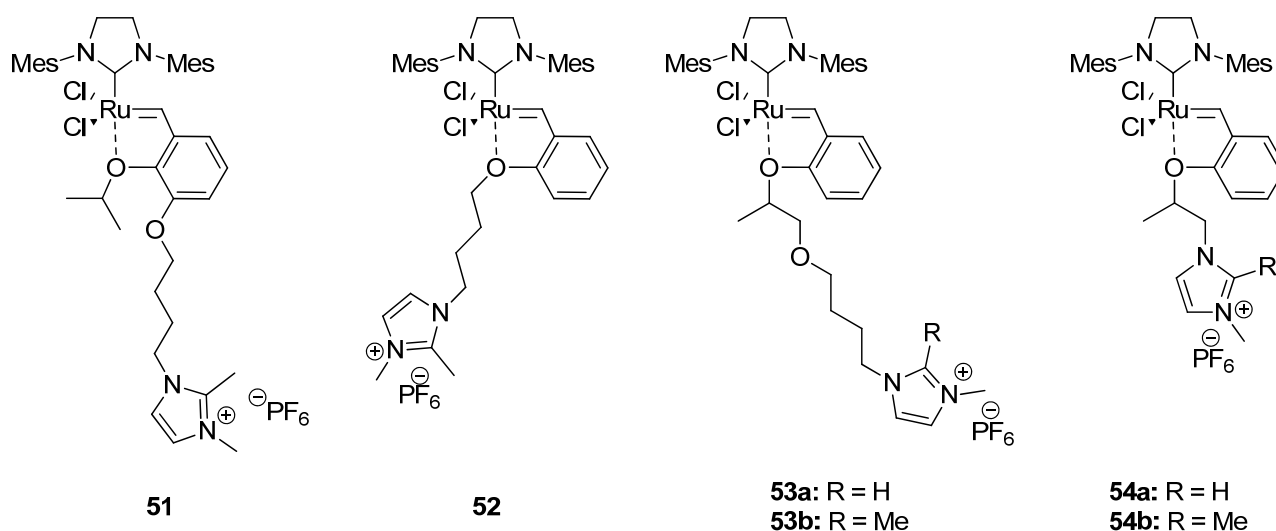


Fig. 27: Hoveyda-Grubbs catalysts tagged exploiting the isopropoxy moiety.

Interestingly 2nd generation Grubbs catalyst was tagged using an ionic phosphine prepared by radical addition of phosphines to vinyl or allyl imidazolium (fig.28). **55** exhibited the usual high activity and wide scope of 2nd generation Grubbs catalysts and it showed also remarkable recyclability with very low Ru leaching, when the RCM of 1,7-octadiene was performed in [bmim][PF₆] / toluene (fig.28).

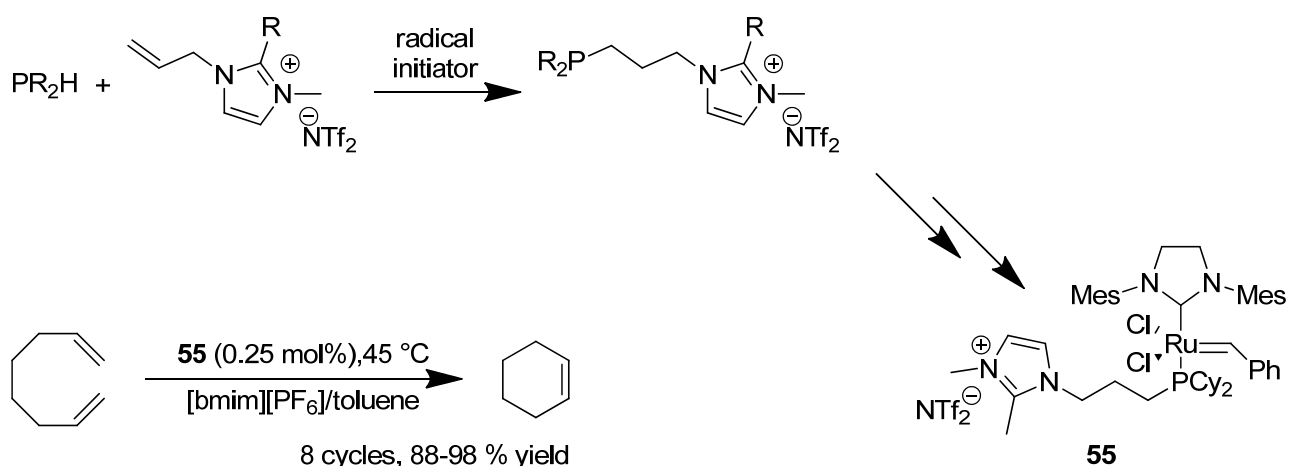


Fig. 28: RCM catalyzed by 2nd generation Grubb catalyst tagged with an ionic phosphine.

1.3.4. Olefins epoxidation.

Epoxidation is a powerful means for olefins functionalization. Ion-tagged metalloporphyrins **56** and **57**, grafted on ILs, acted as recyclable catalysts for the epoxidation of styrene (fig.29). When **56**, a Fe(III)-porphyrin bearing four phenyl sulfonated groups, were immobilized on [bmim][Br], epoxidation of styrene with H₂O₂ could be carried out with good selectivity towards the formation of the styrene oxide, recycling the ionic phase up to 5 times with almost no loss of reactivity (fig 29).⁴⁸

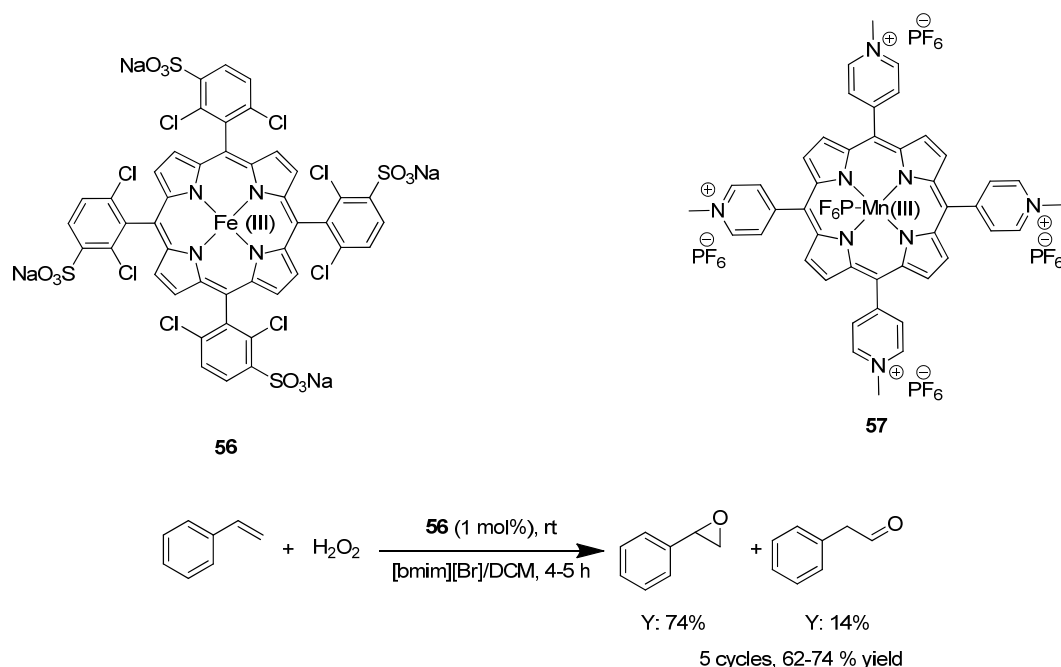
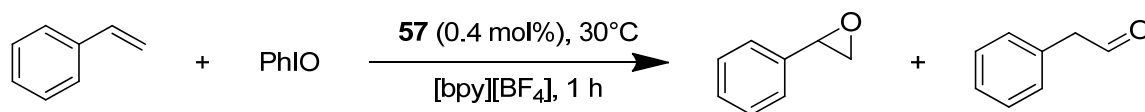


Fig. 29: Styrene epoxidation catalyzed by ion-tagged metalloporphyrins.

When Mn(III)-porphyrin **57**, tagged with four pyridinium ion, was employed in the same transformation in [bpy][BF₄], with iodosyl benzene as stoichiometric oxidant, the catalyst exhibited

good activity and the ionic phase could be reused five times with a little loss of activity, but complete inversion of the chemoselectivity from styrene oxide to phenylacetaldehyde was observed through the five runs (tab.2).⁴⁹



Run	Conversion	Styrene oxide (%)	Phenylacetaldehyde (%)
1	96	90	10
2	92	90	10
3	87	60	40
4	79	17	82
5	71	0	99

Tab. 2: Epoxidation of styrene with ion tagged Mn(III)-porphyrin **57**.

A Mn(III)–Schiff base complex with an imidazolium tag was employed as an efficient and recyclable catalyst for chalcone epoxidation with MCPBA/NMO. Complex **58** turned out to be an efficient catalyst affording the corresponding epoxide with excellent yields under mild conditions. Moreover **58** was recovered and recycled for at least five runs without any loss of activity (fig.30).⁵⁰

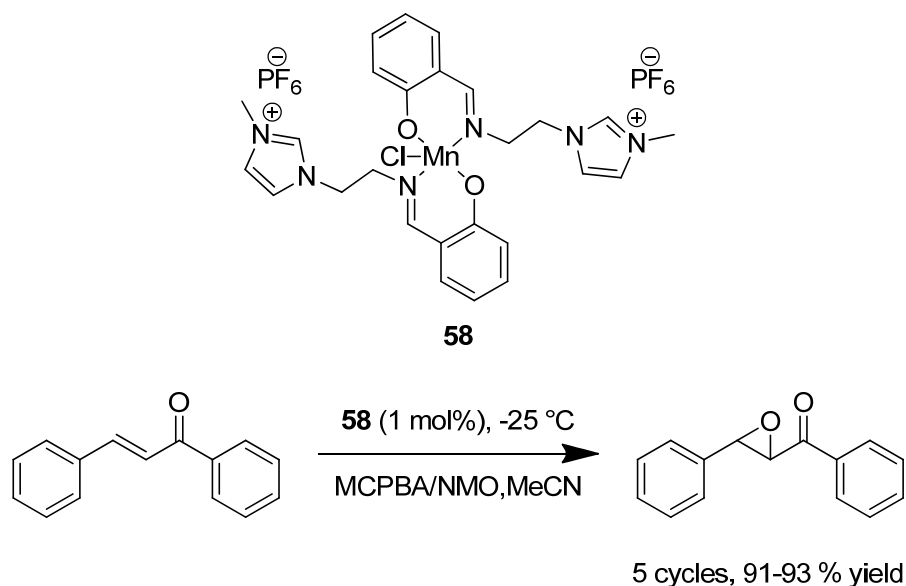


Fig. 30: Chalcone epoxidation with ion-tagged Mn(III)-Schiff base complex.

1.3.5. Olefins polymerization.

The use of ion-tagged ligands for transition-metal catalyzed polymerization can be an usual means to achieve easy catalyst – product separation, avoiding product contamination. An imidazolium

tagged tri-amino ligand for CuBr (**58**) served as a catalyst for radical polymerization of methyl methacrylate (MMA) (fig.31).

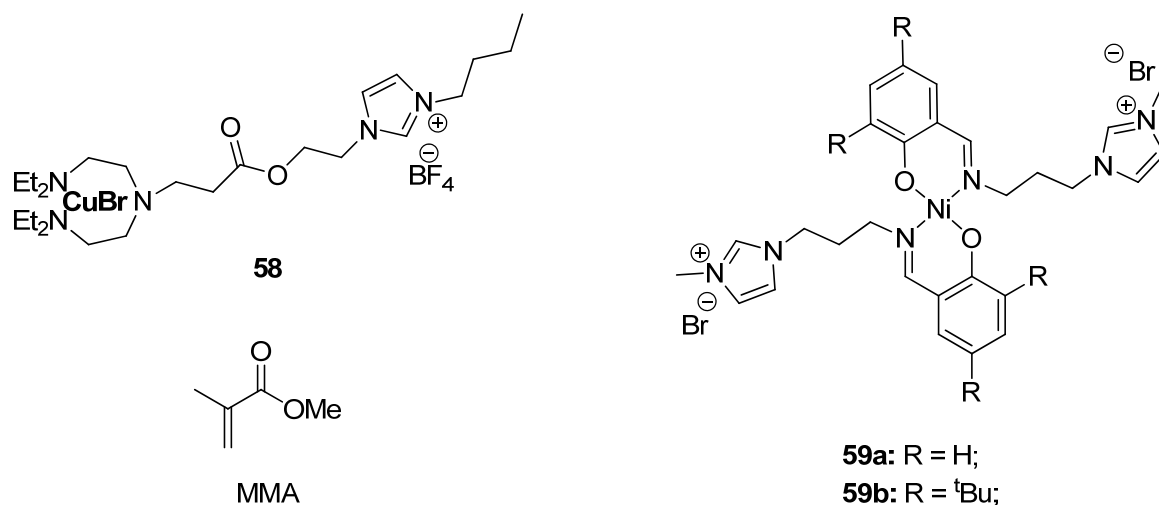


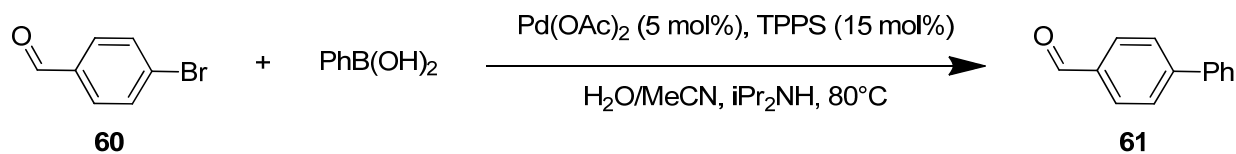
Fig. 31: Ion-tagged catalyst for olefins polymerization.

58 was insoluble in the mixture of MMA and toluene but could be easily dispersed in the reaction media. The polymerization of MMA at 60 °C was well controlled, producing polymers with low polydispersity. The catalyst was easily isolated from the polymer solution and after regeneration it exhibited similar or even higher activity and improved control when used in the 2nd run. The residual catalyst concentrations in the polymers were in the range 50-100 ppm and the addition of a small amount of silica gel to the polymer solution could further reduce the residual catalyst concentration.⁵¹ The ion-tagged Ni complex **59** (fig.31) acted as an efficient catalyst for ethylene oligomerization in a biphasic system formed by a chloroaluminate IL and an organic solvent. The ionic phase could be recycled at least three times without any change neither in the catalyst activity nor in the product composition.⁵²

1.3.6. Pd cross coupling (CC).

Pd cross coupling (CC) is the most important reaction to form new sp² C-C bond. Although ligand free protocols have been developed the use of ligands for Pd usually ensures better catalyst stability, leading to higher TON for the catalytic system. Phosphines are the most commonly employed ligands, although a number of other ligands have been reported. Even several ion-tagged ligands have been designed for this transformation, with the aim to develop catalytic systems displaying high reactivity, stability, recyclability and easy product isolation. Ionic phosphine tppts (**18**) was used as hydrosoluble Pd ligand in Suzuki CC (tab.3). The catalyst exhibited good activity: complete conversion of the aryl bromide was obtained at 80°C in one hour (Entry 1) and TON up to 6400 were reported when reactions with low Pd loading were carried out. The catalyst could be recycled

up to 5 times, but longer reaction time were required due to a small decrease in the catalyst activity (Entry 1-5).⁵³



Run	Time (h)	Yield (%)
1	1	97
2	4	98
3	5	97
4	6.5	95
5	7.2	87

Tab. 3: Suzuki CC catalyzed by Pd – TPPTS.

The same year, water-soluble aliphatic phosphines **62** and **63** (fig.32) were proposed as the first ligands that allowed Suzuki CC to be performed at room temperature, in aqueous solvent and in high efficiency, with average TOF of 184000 h⁻¹.

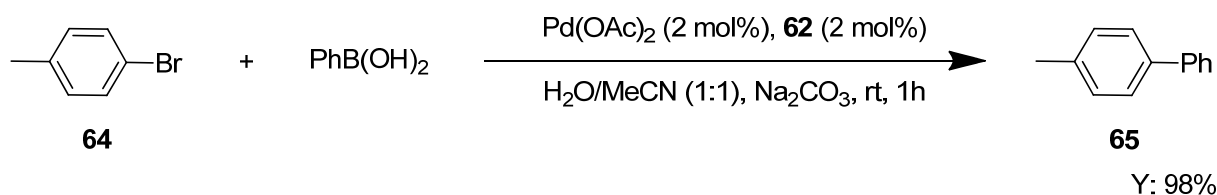


Fig. 32: Suzuki CC catalyzed by Pd with sterically demanding, water-soluble alkylphosphines.

Under the same conditions reported for **62**, P^tBu₃ was virtually inactive. On reducing the ligand/Pd(OAc)₂ ratio to 1:1, **65** was obtained in 98% in 1 h at room temperature (fig.32). Such a remarkable rate enhancement with respect to P^tBu₃ could be an example of electrosteric activation. However, no testing of possible catalyst recycling was reported.⁵⁴

The dendritic hexaionic phosphine **67**, which was obtained by multiple alkylation of **66**, turned out to be an efficient Pd ligand for Suzuki CC (fig.33).⁵⁵

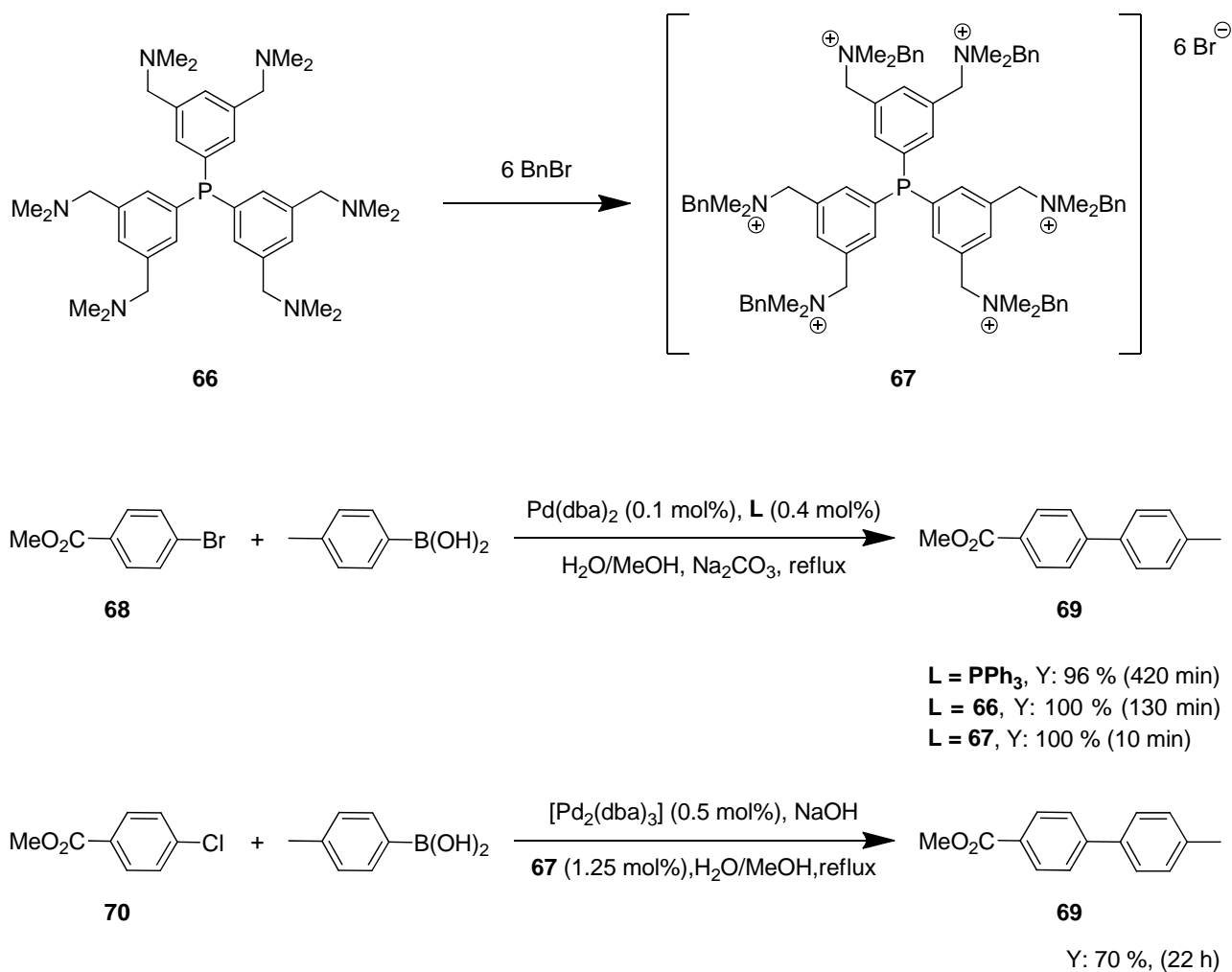


Fig. 33: Suzuki CC catalyzed by Pd – dendritic phosphine **67**.

67 combined a triarylphosphine core with a shell of six ammonium groups. When the model reaction was catalyzed by Pd(dba)₂ in the presence of PPh₃, **66** or **67**, the role of the multiple ionic tag in speeding up the overall catalytic process was apparent. Product **69** was obtained in 100 % yield in considerable lower time when **67** was used as Pd ligand (fig.33). The noticeable higher reactivity of **67** allowed authors to decrease the Pd loading up to 0.01 mol %, still obtaining **69** in 99% yield in 60 min. Moreover even aryl chlorides could be coupled at a low Pd loading, although a consistent increase of the reaction time was necessary (fig.33). The high activity of ligand **67** was ascribed to the formation of a coordinatively unsaturated Pd-phosphine complex. Indeed, despite their triarylphosphine based structure, **67** behaved as a very bulky phosphine, leading to preferential formation of mono-coordinated Pd complexes, which are known to be more active in CC reactions. This behavior was explained with the presence of six permanent cationic charges in the backbone of the ligand, resulting in a significant interligand coulombic repulsion, which made multiple coordination around the Pd atom unfavorable.⁵⁶

Imidazolium tagged phosphine **72**, prepared by metalation of [bmim][PF₆] followed by reaction with Ph₂PCl, acted as an active ligand for Negishi coupling. For example compound **75** was obtained in 90 % yield at room temperature (fig.34) when **72** was used as ligand with Pd(dba)₂ in an IL / organic solvent mixture (fig.34). Attempts to reuse the Pd catalytic system showed a significant decrease in yield after the 3rd cycle.⁵⁷

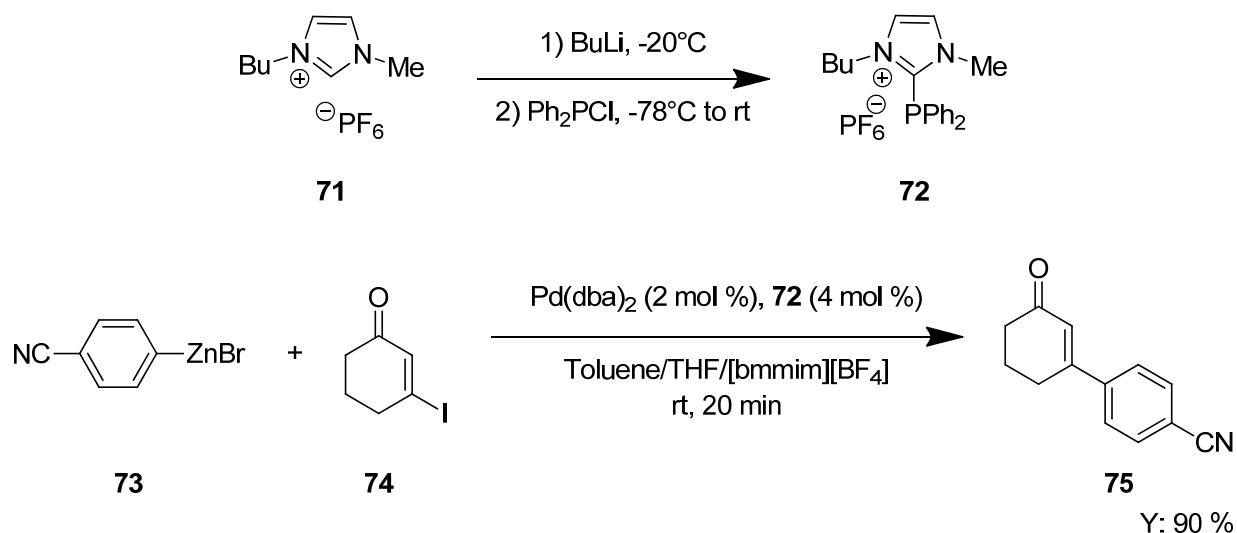


Fig. 34: Negishi CC catalyzed by Pd – imidazolium tagged phosphine **72**.

Besides phosphines many N-donor species were employed as ligands in Pd CC reactions. Dyson and co-workers reported the use of nitrile functionalized ILs which served both as Pd ligands and as solvents in the Suzuki and Stille CC (fig.35). The catalyst was moderately reactive but it exhibited elevated recyclability: the ionic phase could be reused up to nine times both in Suzuki and Stille CC, with no detectable loss of activity and very low level of Pd leaching in the organic phase (< 5 ppm in the Suzuki reaction). Reaction outcomes were not affected by the nature of the Pd catalyst, whereas the use of a nitrile functionalized IL was fundamental for successful catalyst recycling. Pd nanoparticles (NPs), which probably were the active catalytic species, were isolated after the CC reactions. The key role played by the nitrile functionalized IL in the catalyst recycling was probably due to its stabilizing effect on the NPs, preventing aggregation and subsequent deactivation of the catalyst (fig.36).⁵⁸

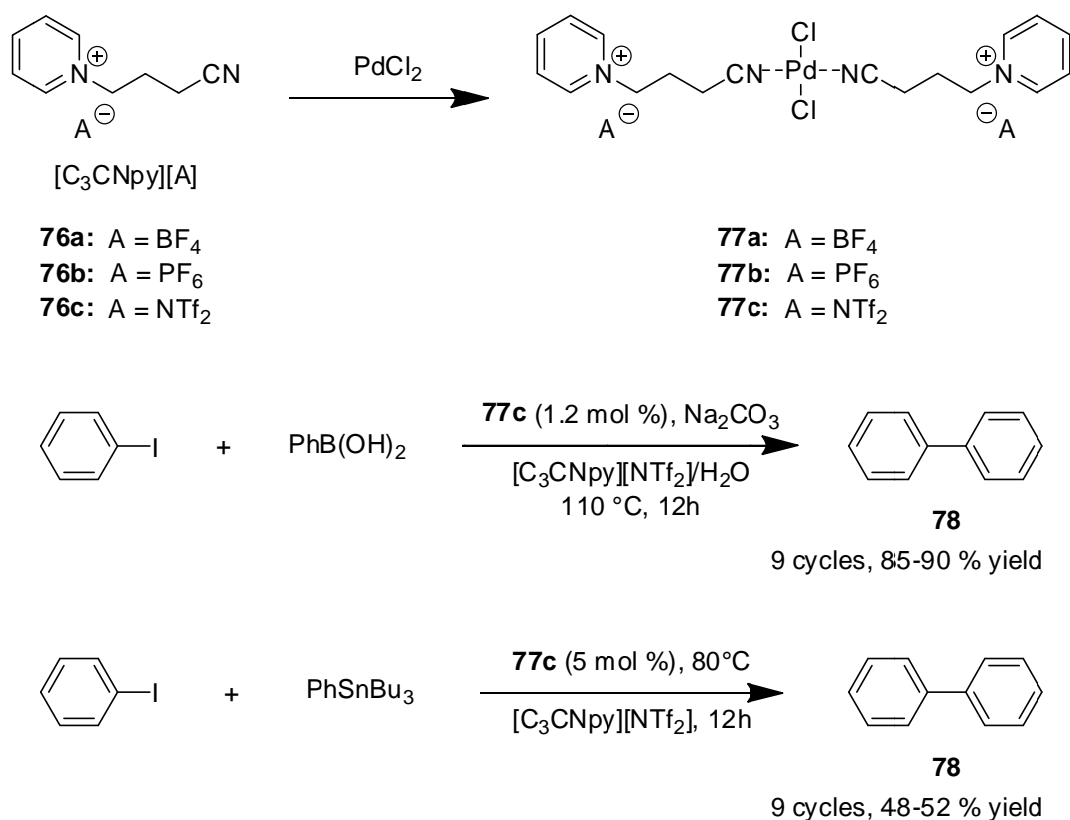


Fig. 35: Suzuki and Stille CC catalyzed by Pd- $[C_3CNpy][NTf_2]$ complex.

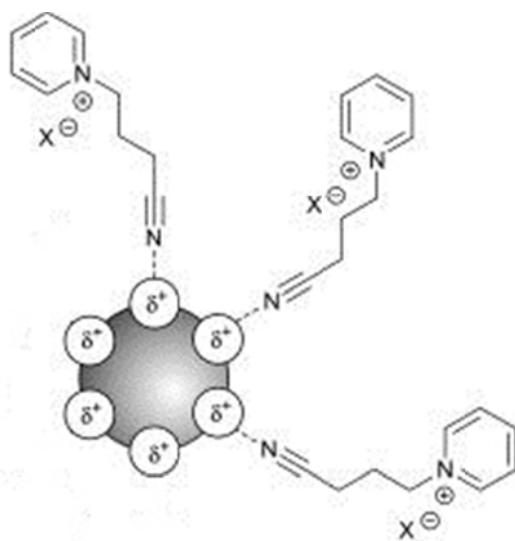


Fig. 36: Schematic representation of the stabilizing effect of nitrile functionalized IL **76** on Pd NPs.

Ionic compound **81** derived from 2,2'-biimidazole **79** served as Pd ligand and IL for the Heck reaction. The synthesis of Pd complex **82** was carried out as shown in fig.37. In basic aqueous environment alkylation of **79** took place at rt, yielding **80** in 88 % yield. When **80** was further alkylated with BuI at $100^\circ C$ only one of the two nitrogen atom was alkylated. After anion exchange with KPF_6 the IL **81** was obtained in overall 95 % yield. When **81** was reacted with $PdCl_2$ the complex **82** was formed *via* coordination of the non-alkylated nitrogen to the metal (fig.37).

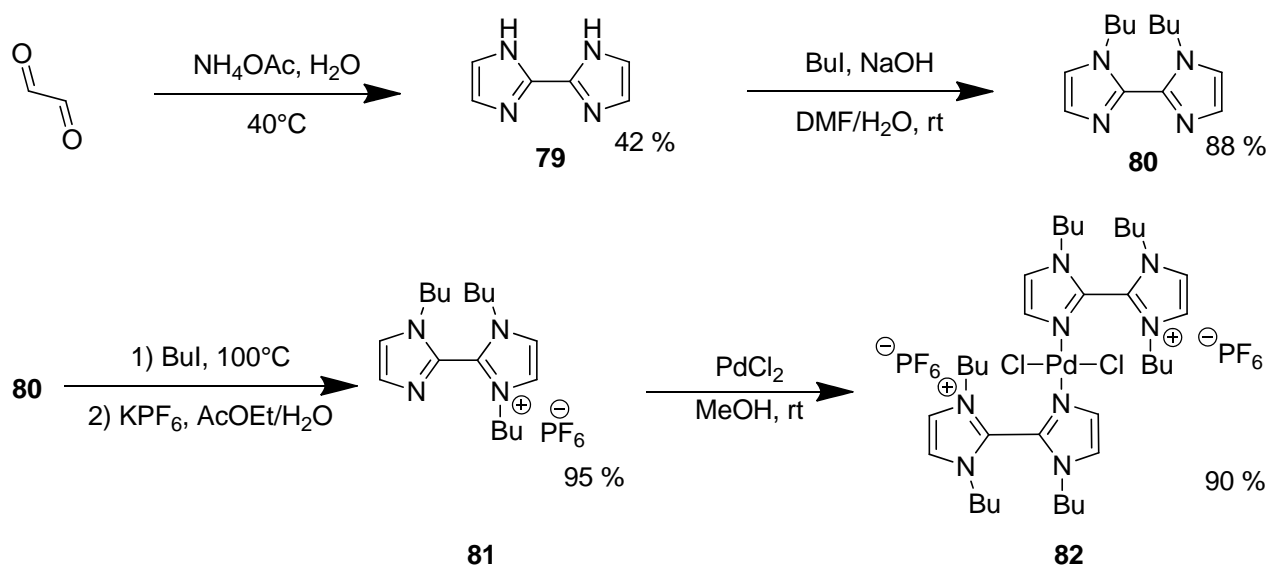
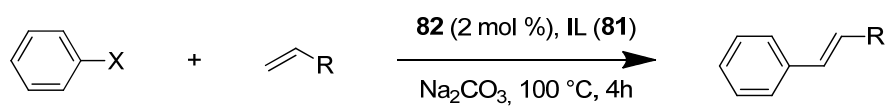


Fig. 37: Synthesis of imidazolium tagged imidazolyl - Pd complex **82**.



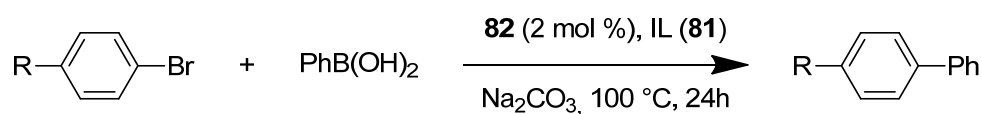
Run	X	R	Yield (%)
1	I	CO ₂ Me	92
2	I	CO ₂ Me	90
3	I	CO ₂ Me	94
4	I	CO ₂ Me	91
5	I	CO ₂ Me	91
6	Cl	CO ₂ Me	70
7	Cl	CO ₂ Me	78
8	Cl	CO ₂ Me	75
9	Cl	Ph	86
10	Cl	Ph	81
11	Cl	Ph	83

Tab. 4: Recycling of catalyst **82** for Heck CC carried out in IL **81**.

This imidazolium tagged Pd complex turned out to be an active and recyclable catalyst for Heck CC between aryl halides and electron poor olefins in IL **81** (tab.4).

The ionic phase could be recycled five times for the reaction between iodobenzene and methyl acrylate (Entry 1-5). Further, the recovered ionic phase was employed to catalyze the Heck CC between chlorobenzene and methyl acrylate (three cycles, entry 6-8) and finally the CC between chlorobenzene and styrene (3 cycles, entry 9-11).⁵⁹

The same system acted as an efficient and highly recyclable catalyst even in the Suzuki CC: the ionic phase was used 15 times with five different aryl bromide without any detectable loss of activity (tab.5).⁶⁰



Entry	Run	R	Yield (%)
1	1 st	H	83
2	2 nd	H	84
3	3 rd	H	80
4	1 st	F	86
5	2 nd	F	86
6	3 rd	F	85
7	1 st	CF ₃	85
8	2 nd	CF ₃	90
9	3 rd	CF ₃	88
10	1 st	NO ₂	86
11	2 nd	NO ₂	86
12	3 rd	NO ₂	90
13	1 st	Me	85
14	2 nd	Me	80
15	3 rd	Me	82

Tab. 5: Recycling of catalyst **82** in the Suzuki CC carried out in IL **81**.

Using a similar synthetic strategies IL **83** and the corresponding Pd complex **84** were prepared and their activity and recyclability in the Heck CC was evaluated. The ionic phase could be reused ten times without any loss of activity, even if non-coordinating IL **85** was utilized as solvent (fig.38).⁶¹

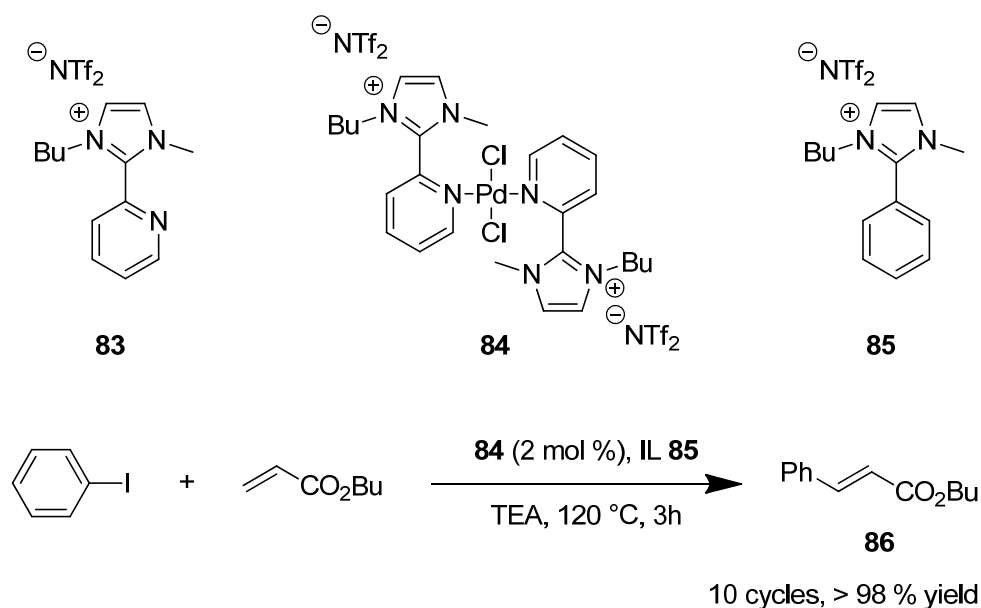


Fig. 38: Heck CC catalyzed by imidazolium tagged pyridyl – Pd catalyst **84**.

Following the same principle which led to the design of ligands **81** and **83**, constituted by an imidazolium group linked to a moiety capable of metal coordination, pyrazolyl functionalized imidazolium salts and their corresponding Pd complex **86** and **87** were synthesized (fig. 39).

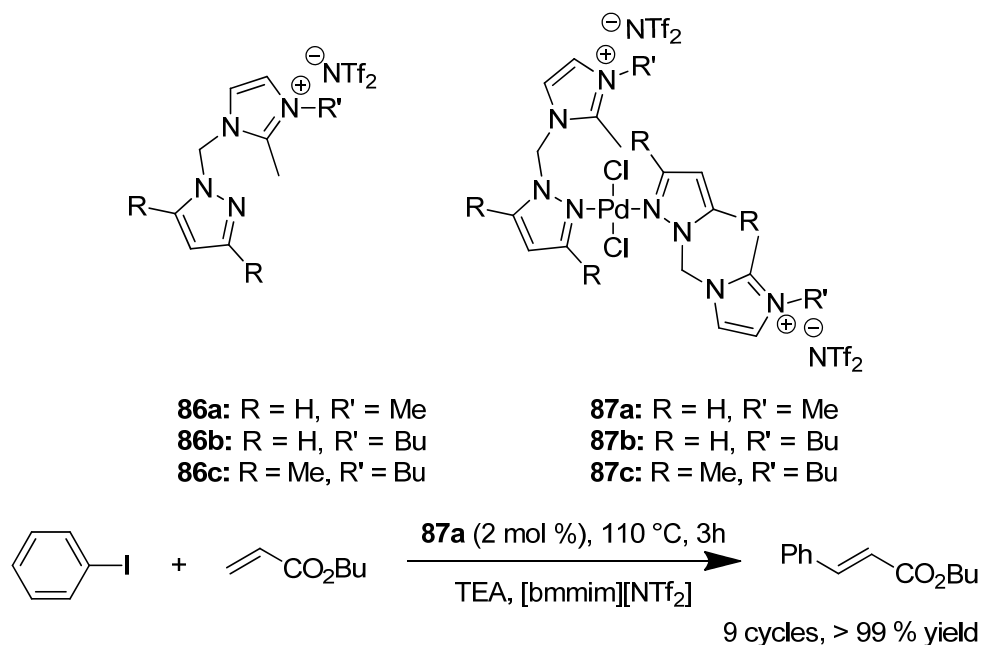
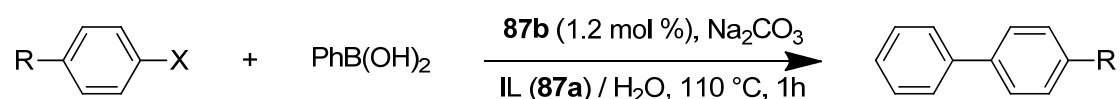


Fig. 39: Heck CC catalyzed by imidazolium tagged pyrazolyl – Pd catalyst **87a**.

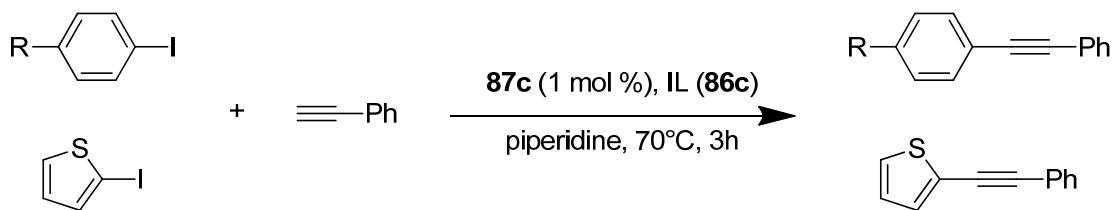
87 turned out to be an efficient catalyst for several CC reactions. Heck CC between iodobenzene and butyl acrylate was carried out in [bmmim][NTf₂] with catalyst **87a**, obtaining product in quantitative yield for 9 consecutive runs (fig.39). When **87b** was grafted in the corresponding IL **86b**, the system displayed outstanding recyclability in the Suzuki CC. The ionic phase was recycled 14 times with seven different aryl halide showing no loss of activity (tab.6).



Run	R	X	Yield % (time)
1	H	Br	76 (1 h)
2	H	Br	91 (15 h)
3	MeO	Br	53 (1 h)
4	MeO	Br	82 (15 h)
5	MeCO	Br	10 (1 h)
6	MeCO	Br	31 (15 h)
7	MeCO	Cl	91 (1 h)
8	MeCO	Cl	93 (3 h)
9	F	Br	92 (1 h)
10	F	Br	90 (3 h)
11	CF ₃	Br	91 (1h)
12	CF ₃	Br	95 (3h)
13	NO ₂	Br	89 (1 h)
14	NO ₂	Br	91 (3 h)

Tab. 6: Suzuki CC catalyzed by imidazolium tagged pyrazolyl – Pd catalyst **87b**.

Finally catalyst **87c** immobilized in the IL **86a** was reported to work as a recyclable catalytic system for Sonogashira CC between various aryl iodide and phenylacetylene. The ionic phase could be recycled six times without any detectable loss of activity, using a different aryl halide in each run (tab.7).⁶² The imidazolium tagged diol **88** was used as Pd ligand in the Heck CC of various aryl halide and acrylates. Low catalyst loading was required and the catalytic system was effectively recycled ten times (fig.40).⁶³



Run	R	Yield (%)
1	H	93
2	Me	91
3	MeO	94
4	F	95
5	NO ₂	91
6	2-iodothiophene	87

Tab. 7: Sonogashira CC catalyzed by imidazolium tagged pyrazolyl – Pd catalyst **87c**.

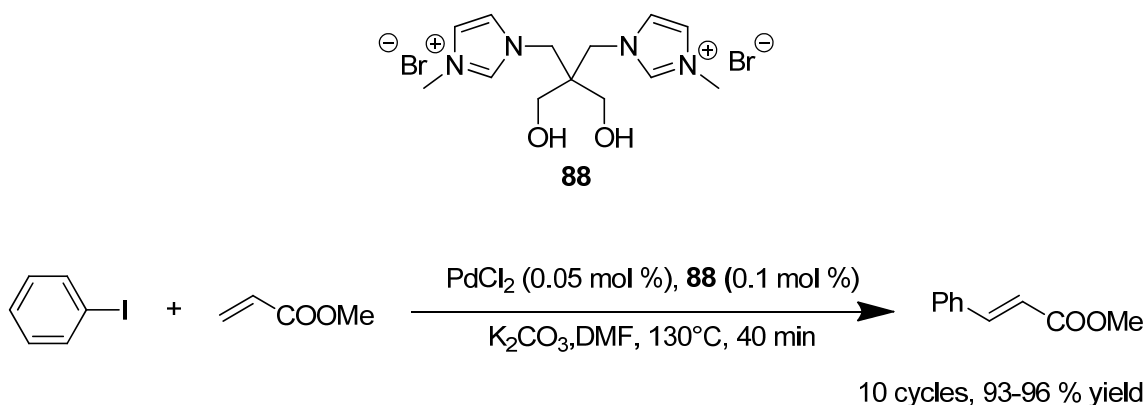


Fig. 40: Heck CC catalyzed by imidazolium tagged diol **88**–Pd complex.

π -acidic alkenes are useful ligand for Pd, but a drawback in their use is that often they share the same polarity of the desired product, thus difficulties in product purification may occur. To overcome this problem ion-tagged olefins derived from chalcone and benzylacetone were prepared (fig.41). Usefulness of ligand **89** and **90** was demonstrated in the first example of Pd catalyzed Hiyama CC in IL ([C₅mpy][NTf₂] = 1-methyl-1-pentylpyrrolidinium bistriflimide). Yields up to 99 % were obtained for the coupling product of cyclohexenyl ethyl carbonate with aryl siloxanes (fig.41). Thanks to the ionic nature of the ligand product isolation was easy and no contamination occurred. However catalyst recycling resulted impossible.⁶⁴

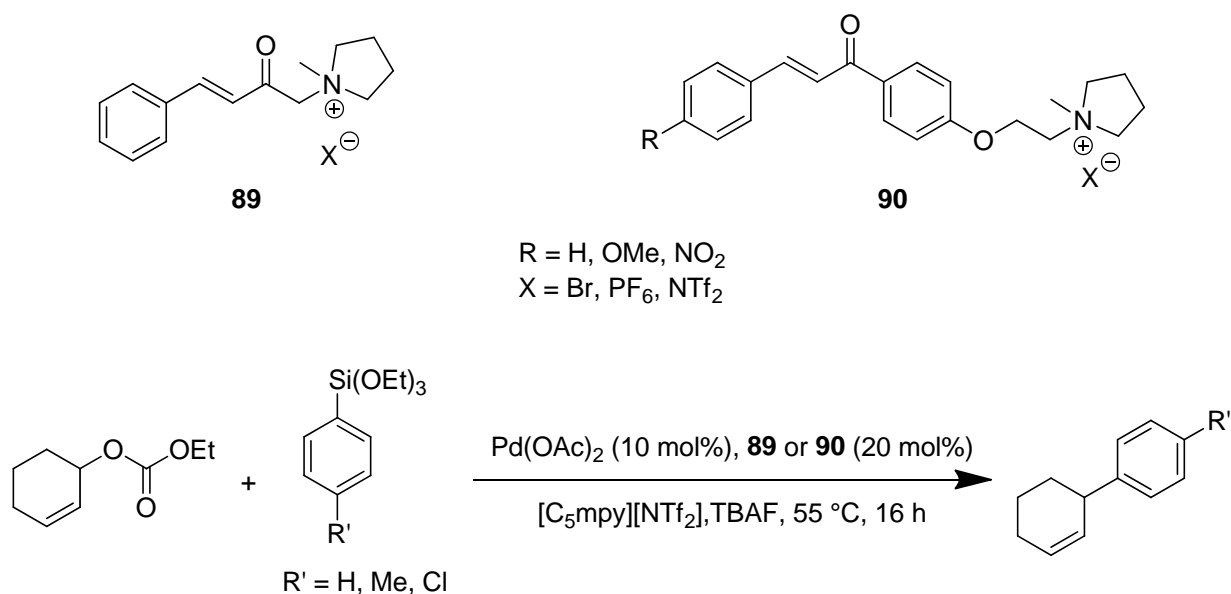


Fig. 41: Hiyama CC catalyzed by pyrrolidinium tagged, π -acid olefin – Pd catalysts **89** and **90**.

1.3.7. Tsuji-Trost allylation.

The Tsuji-Trost reaction is the allylation of various nucleophiles with activated allylic compound, generally catalyzed by Pd. This is an important tool to form new C-C, C-N, C-O and C-S bond in a selective way. tppts (**18**) was used as Pd ligand in a system formed by water and $[\text{emim}][\text{BF}_4]$ under microwaves (MW) irradiation. The system resulted suitable to catalyze the reaction of allyl acetates with various sulfur, nitrogen and carbon nucleophiles, in high yield and with short reaction times. The catalyst could be recycled ten times without any decrease in the catalytic activity when reaction of cinnamyl acetate with sodium benzenesulfinate was chosen as benchmark reaction (Fig.42).⁶⁵

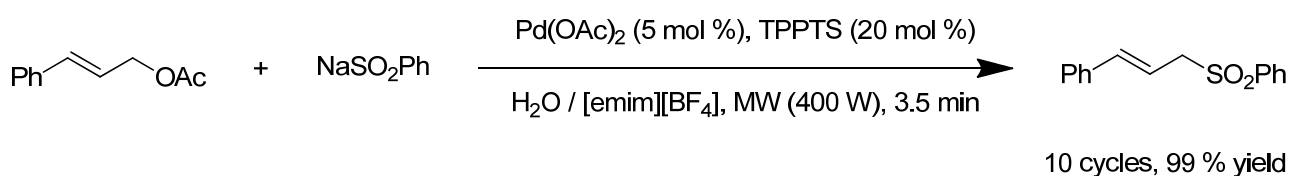


Fig. 42: Tsuji-Trost allylation catalyzed by Pd-tppts.

When chiral ligands for Pd are employed the reaction can be performed in an enantioselective fashion. Ion tagged ligand **14** and **15** served as efficient ligands for asymmetric allylation of various nucleophiles. In particular alkylation and sulfonation of allyl acetate **91** took place with ee up to 93 and 99 % respectively (fig.43).⁶⁶

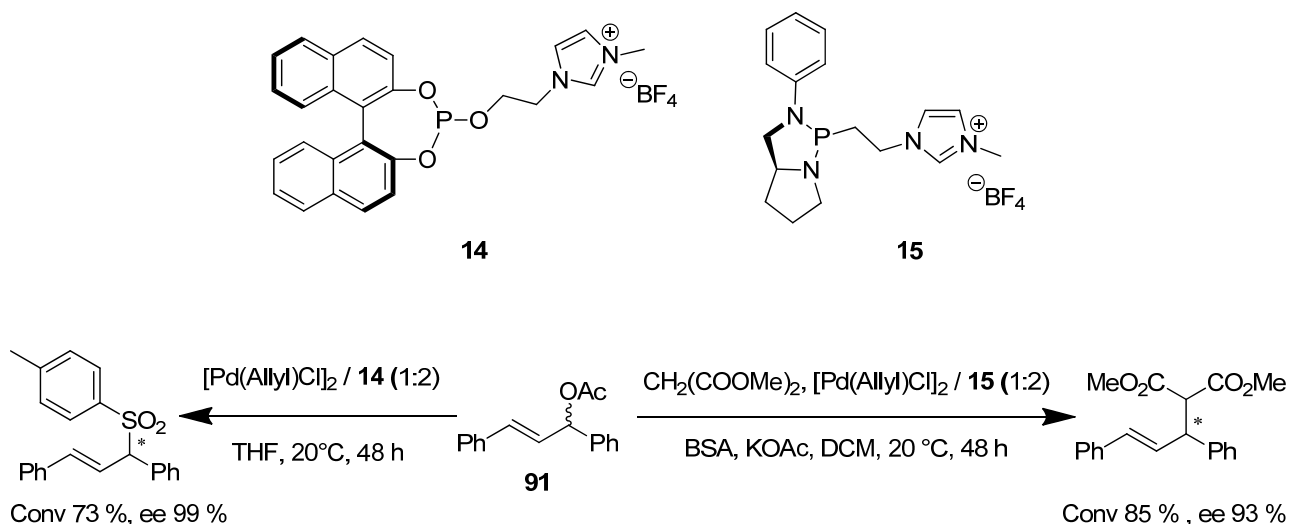


Fig. 43: Asymmetric Tsuji-Trost allylation catalyzed by chiral imidazolium tagged ligand – Pd complexes.

1.3.8. Copper catalyzed reactions.

Copper has found many application in catalysis as it can work as a Lewis acid, as a catalyst for redox reactions or even as a catalysis in CC-type reaction. Nevertheless Cu catalysts exhibit less efficient performance compared to Pd in this latter transformation, so that harsher condition and even stoichiometric amount of Cu are usually required. IL **92**, prepared from 2,2'-bipyridine, was used both as Cu ligand and solvent in the coupling reaction of aryl iodides and perfluoroalkyl iodides, in rather mild condition for this type of reaction (fig.44). IL **92** was reused for five times after easy product isolation by extraction followed by Cu removal by filtration.⁶⁷

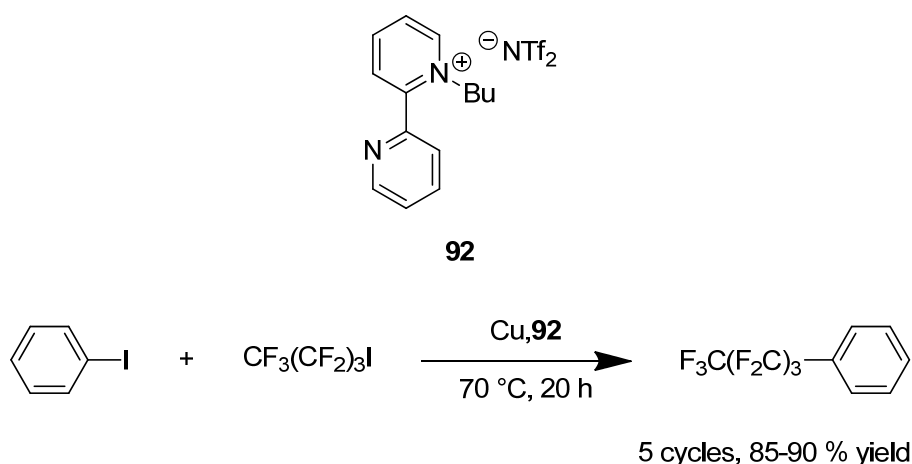


Fig. 44: Copper-catalyzed perfluoroalkylation in IL **92**.

Bis(oxazolines) (BOXs) have proven remarkably effective ligands for stereocontrol in a variety of enantioselective, metal-catalyzed reactions and have been established as among the most versatile ligands in homogenous asymmetric catalysis. Cu-BOX ligand have found application in several

asymmetric catalytic transformation. Doeherty and co-workers reported the preparation of imidazolium tagged BOX **97a** and **97b**, according to the synthetic route reported below (fig.45).

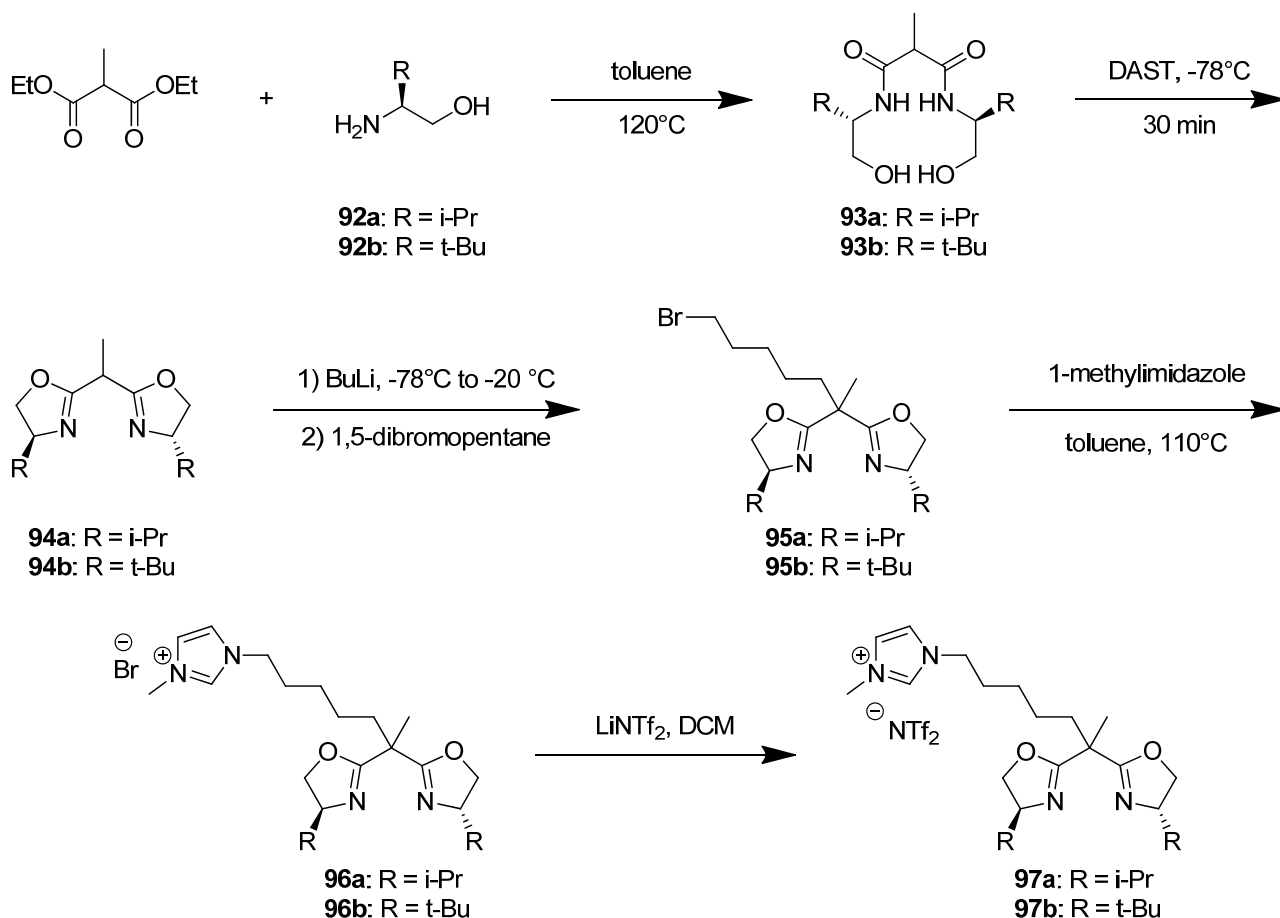


Fig. 45: Synthesis of ion-tagged BOXs ligands **97a** and **97b**.

Condensation of diethyl methylmalonate with (S)-valinol (**92a**) or (S)-tert-leucinol (**92b**) afforded the bis(hydroxyamides) **93a,b**, which were converted into the desired BOX **94a,b** via a DAST-mediated cyclization. Deprotonation of **94a,b** followed by alkylation with an excess of 1,5-dibromopentane gave the bromopentyl-substituted BOX **95a,b**. Treatment of **95a,b** with 1-methylimidazole followed by anion exchange afforded the imidazolium tagged ligands **97a,b**. The chiral ligands **97** have been used in the Cu(II) Lewis acid catalyzed Diels–Alder reaction of N-acryloyl oxazolidinones (**98**) with cyclopentadiene in either DCM or in the IL [emim][NTf₂]. The reaction was faster in the IL, with even in higher ee compared to DCM. Moreover the ion-tagged catalyst could be recycled ten times without any loss in activity or enantioselectivity (fig.46).⁶⁸ Ion-tagged BOX ligand **97b** was also used in the asymmetric Mukaiyama aldol reaction between methyl pyruvate and 1-methoxy-1-trimethylsilyloxypropene under homogeneous and heterogeneous conditions (fig.46). In the homogeneous system, although high activity and excellent product enantioselectivity were produced, lower chemoselectivity was observed, due to the formation of a by-product, deriving from hydrolysis and self condensation of the silyl enol ether in the IL.

Supporting the catalyst on silica and using an IL–Et₂O system, completely suppressed the formation of this by-product without reducing the enantioselectivity. In this condition the catalytic system was recycled up to five times with comparable activities (fig.46).⁶⁹

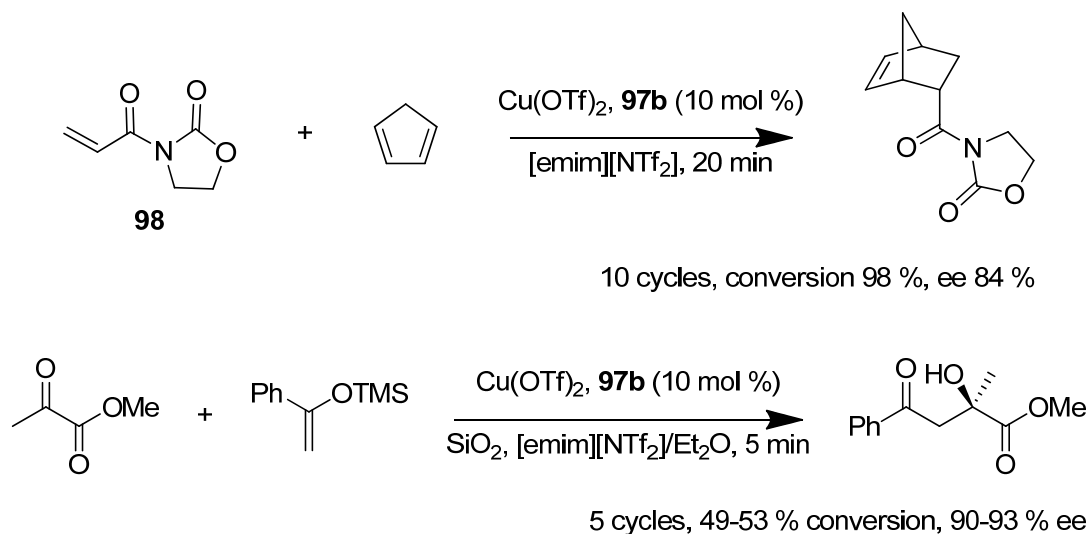


Fig. 46: Diels-Alder and Mukaiyama aldol reaction catalyzed by Cu-ion tagged BOX **97b**.

An imidazolium tagged bipyridyl ligand (**99**) was used in Cu catalyzed alcohol oxidation in IL [bmim][PF₆]. The reaction took place in mild condition and the ionic phase could be reused five times without any significant loss of activity (fig.47).⁷⁰

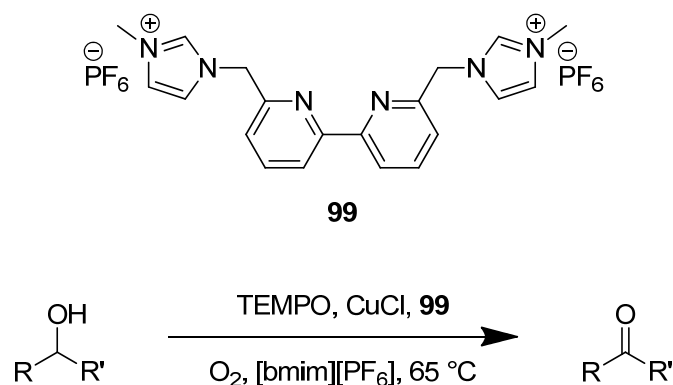


Fig. 47: Alcohol oxidation catalyzed by Cu- ion-tagged bipyridyl ligand.

1.3.9. Asymmetric transfer hydrogenation of ketones.

Catalytic asymmetric transfer hydrogenation is an useful tool to obtain optically active secondary alcohols from carbonyl compounds and is an interesting alternative to hydrogenation with molecular hydrogen. The hydrogen donors most commonly used for ketones are 2-propanol (generally used with a base) and formic acid (generally used as an azeotrope with triethylamine).

Ru-arene complex bearing a chiral amino alcohol or a chiral diamine ligand (**100a** and **101a**) are often employed as catalysts in this reaction (fig.48).

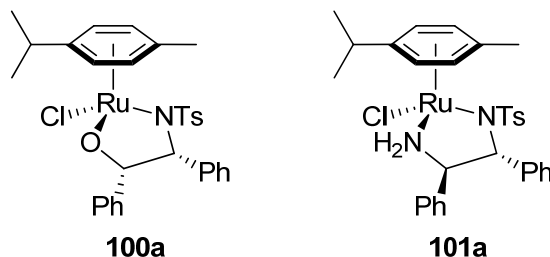


Fig. 48: Neutral Ru complexes for transfer hydrogenation of ketones.

Different strategies to install an ion-tag onto the backbone of these complexes were developed. Dyson and co-workers introduced an imidazolium ion onto the η^6 -arene ligand, preparing the ion-tagged catalysts **100b** and **101b** (fig.49). The performance of the catalysts strongly depended on the reaction conditions. When *i*-PrOH – KOH system was utilized as hydrogen source unsatisfactory catalytic performance was obtained using both **100b** and **101b**. When the *i*-PrOH – KOH system was replaced by HCOOH – TEA azeotrope only **101b** resulted active, yielding 1-phenylethanol with ee of 99 %, like the analogous untagged catalyst **101a**. Unfortunately, when recycling of **101b** was attempted, the yield dropped from 99 % to 52 % in four cycles, although the ee remained unchanged (fig.49). Loss of activity was probably due to the enhanced water solubility of the ionic complex, which led to catalyst leaching in the aqueous phase during the work-up.⁷¹

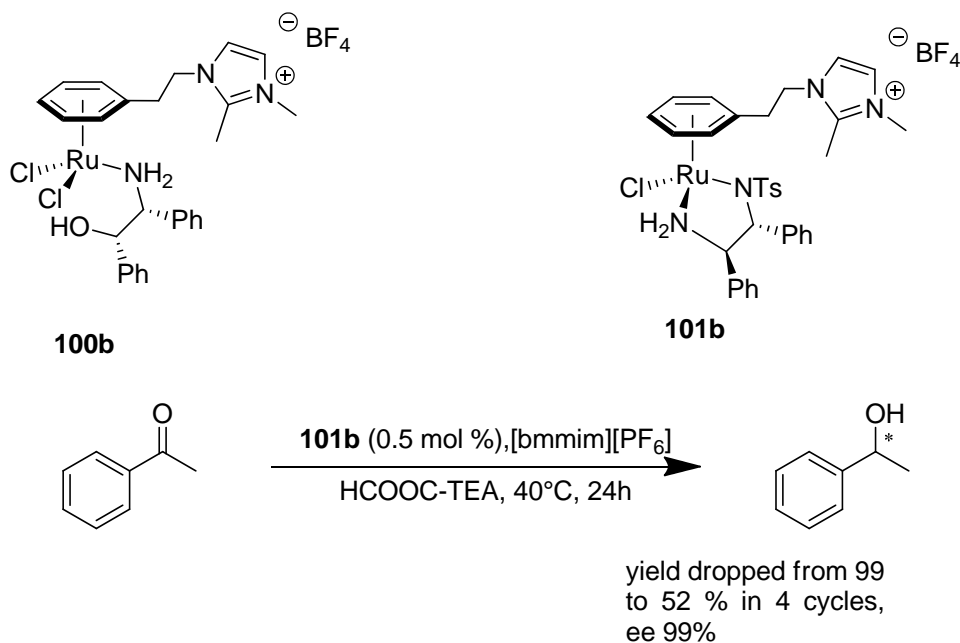


Fig. 49: Ion-tagged Ru catalysts for transfer hydrogenation of ketones.

Installation of the ionic tag onto the diamine backbone *via* a sulfonamide bond, resulted in a more recyclable catalyst (**101c**). When reduction of acetophenone was carried out in [bmim][PF₆] the

ionic phase containing the Ru catalyst could be recycled up to four times without significant loss of activity or enantioselectivity (fig.50).⁷²

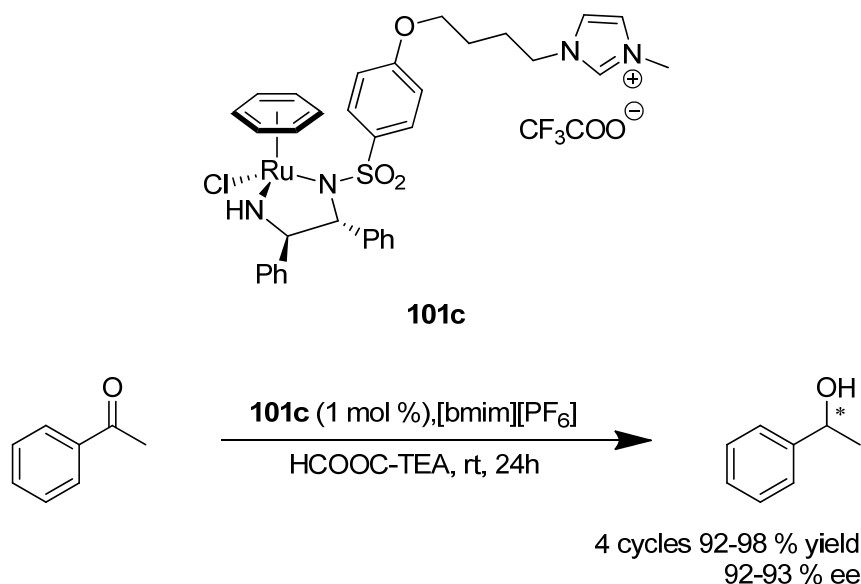


Fig. 50: Ion-tagged Ru catalyst **101c** for transfer hydrogenation of ketones.

1.3.10. Catalytic asymmetric addition of nucleophiles to aldehydes.

The addition of nucleophiles to carbonyl compounds, catalyzed by Lewis acid metals bearing a chiral ligand, is an useful means to obtain chiral enriched alcohols, often accompanied by the formation of a new C-C bond. Garcia and co-workers designed vanadyl – Salen complexes tailored for immobilization onto various supports, like silica, activated carbon, carbon nanotube, ILs. The ion-tagged complex (**103**) demonstrated to be the most active when the cyanosilylation of aldehydes was carried out in [bmim][PF₆]. Unfortunately the ee for the product was substantially lower compared to the parent non-tagged catalyst (**102**) (fig.51). The ion tagged ligand was prepared exploiting the reaction between thiols and terminal alkenes, so that a thioether linker joined the imidazolium ion to the catalyst core. The lower enantioselectivity of **103** was attributed to possible interactions between the chloride counter ion and the vanadium.⁷³

ZnEt₂ addition to aldehydes catalyzed by Ti(Oi-Pr)₄ is a prominent reaction to form new C-C bond in an enantioselective fashion. Several ligands, mainly amino alcohols and diols, have been exploited for this transformation. Moreau's group reported three ion-tagged ligands based on D-canphor-10-sulfonyl chloride (**104**), which were tested as chiral ligands in the addition of ZnEt₂ to benzaldehyde (fig.52). The ionic catalyst system showed catalytic properties similar to those of related non-ionic counterparts, in terms of activity and enantioselectivity. Ionic ligand **105b**, bearing an isborneol moiety, yielded the product with the highest ee. Interestingly, the ionic

ligands could easily be recycled and reused four times without loss of activity or selectivity (fig.52).⁷⁴

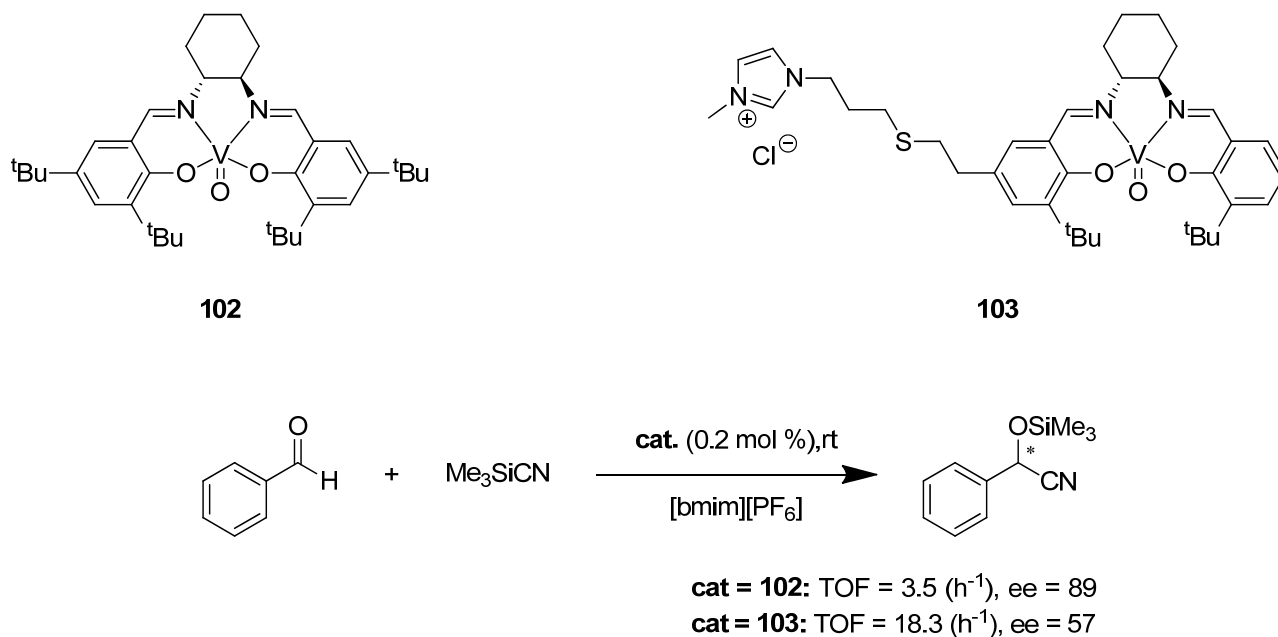


Fig. 51: Aldehyde cyanosilylation catalyzed by ion-tagged vanadyl – Salen complex.

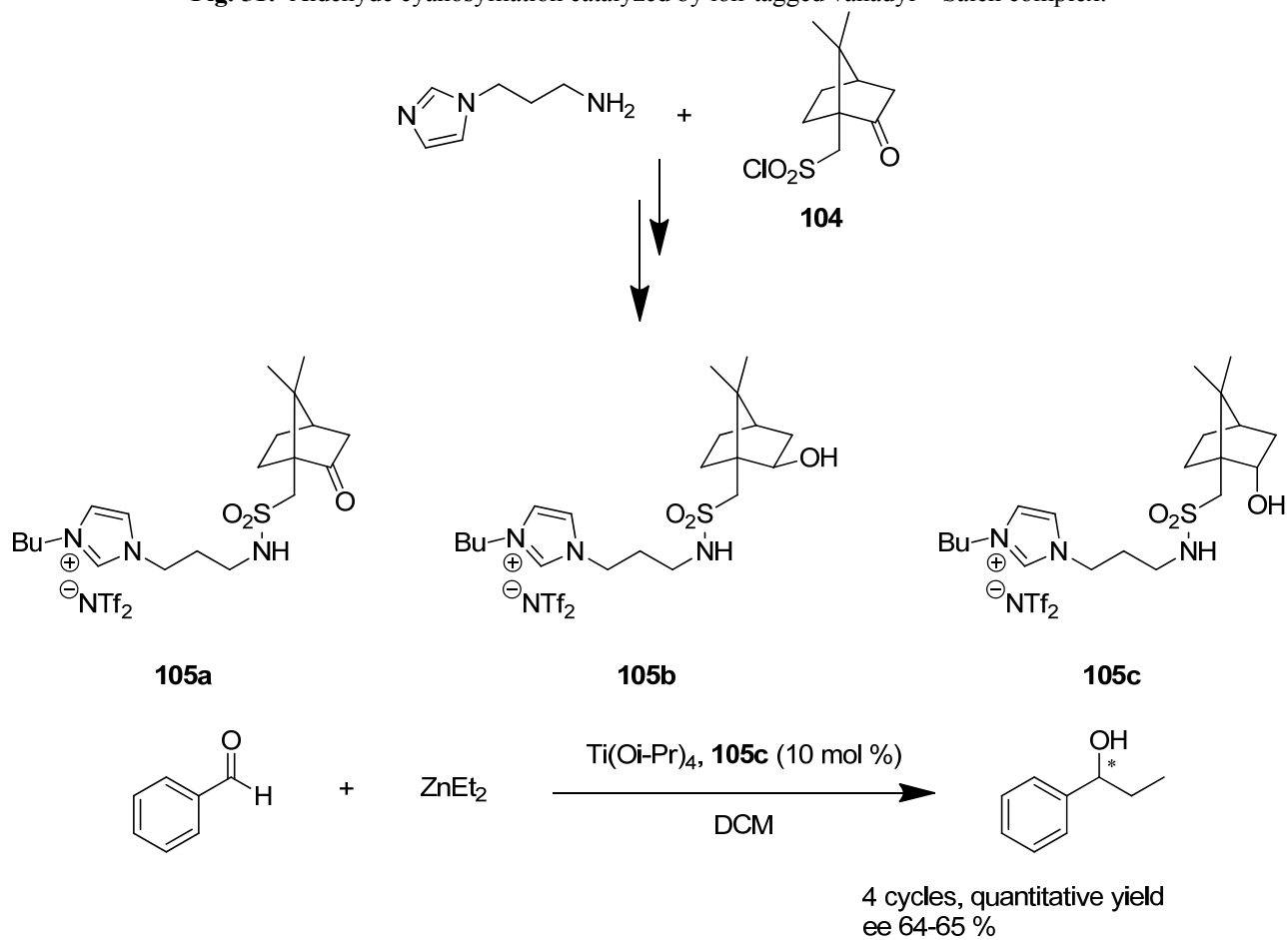


Fig. 52: ZnEt₂ addition to benzaldehyde catalyzed by ion-tagged camphorsulfonamide –Ti(Oi-Pr)₄.

The same group synthesized an ion-tagged BINOL ligand (**106**) which was employed in the same reaction. Again the catalytic system displayed a behavior similar to the non-tagged catalyst. **106** was recovered by filtration, after reaction work-up, almost quantitatively and it could be reused four times without any loss of catalytic activity or enantioselectivity (fig.53).⁷⁵

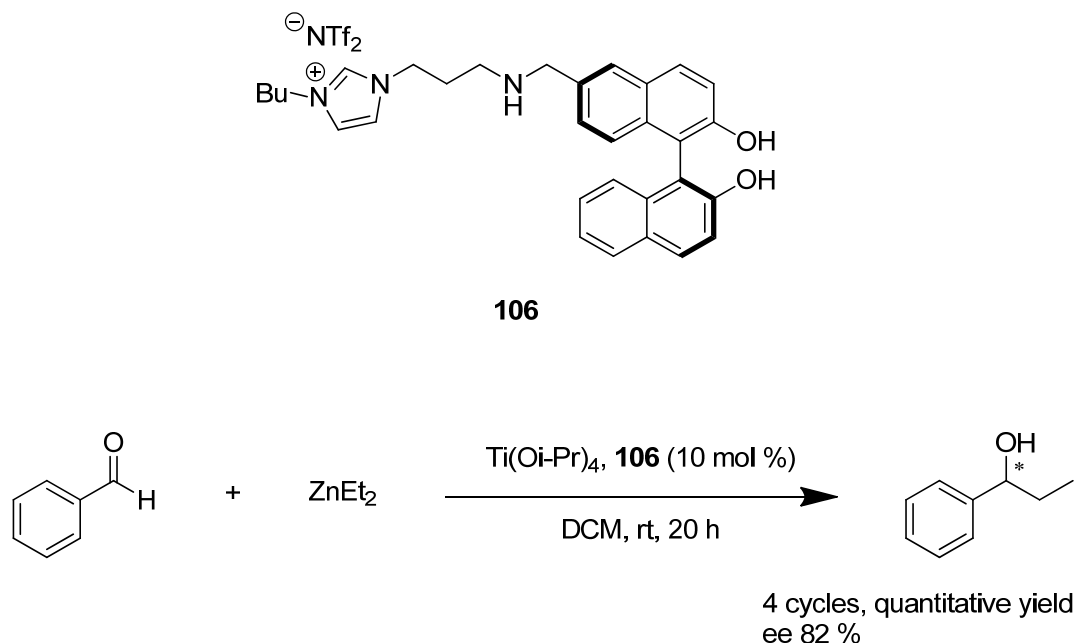


Fig. 53: ZnEt₂ addition to benzaldehyde catalyzed by ion-tagged BINOL –Ti(Oi-Pr)₄.

1.4. Ion-tagged organocatalysts.

Organocatalysis has emerged as a powerful methodology for the catalytic synthesis of enantiomeric pure organic compounds under mild reaction conditions and has become an area of extreme importance in recent years. The use of proline and its derivatives as organocatalysts for asymmetric organic reactions, such as Michael additions, aldol condensations and Mannich reactions, have played an essential role in this area and they have resulted in a very elegant and effective method to form C-C bonds. On the other hand, these organocatalysts still have some drawbacks in that high catalyst loading, 10–30 mol % is typically required, which raises the cost and limits their application. Furthermore, these reactions are usually carried out in high polar solvents, like DMF or DMSO, making the purification even more tedious.²¹ Ion-tagged organocatalysts proved often to be more active catalysts and allowed the use of different solvents, like water and ILs, which made product isolation easier. Some literature example of reactions catalyzed by ion-tagged organocatalysts in various reaction media are reported below.

1.4.1. Ion-tagged Brønsted acids.

One of the earliest examples of ion-tagged organocatalysts was reported by Davis's group who prepared two ion-tagged sulfonic acids, which acted either as catalysts or solvent for some Brønsted acid catalyzed reaction, like Fischer esterification, pinacol rearrangement and alcohol dehydrodimerization (fig.54). Due to their ionic nature acids **107a,b** didn't fume and enabled easy catalyst separation from the reaction mixture. Moreover **107b** was recycled five times with almost no loss of reactivity in the reaction of formation of AcOEt from AcOH and EtOH.⁷⁶

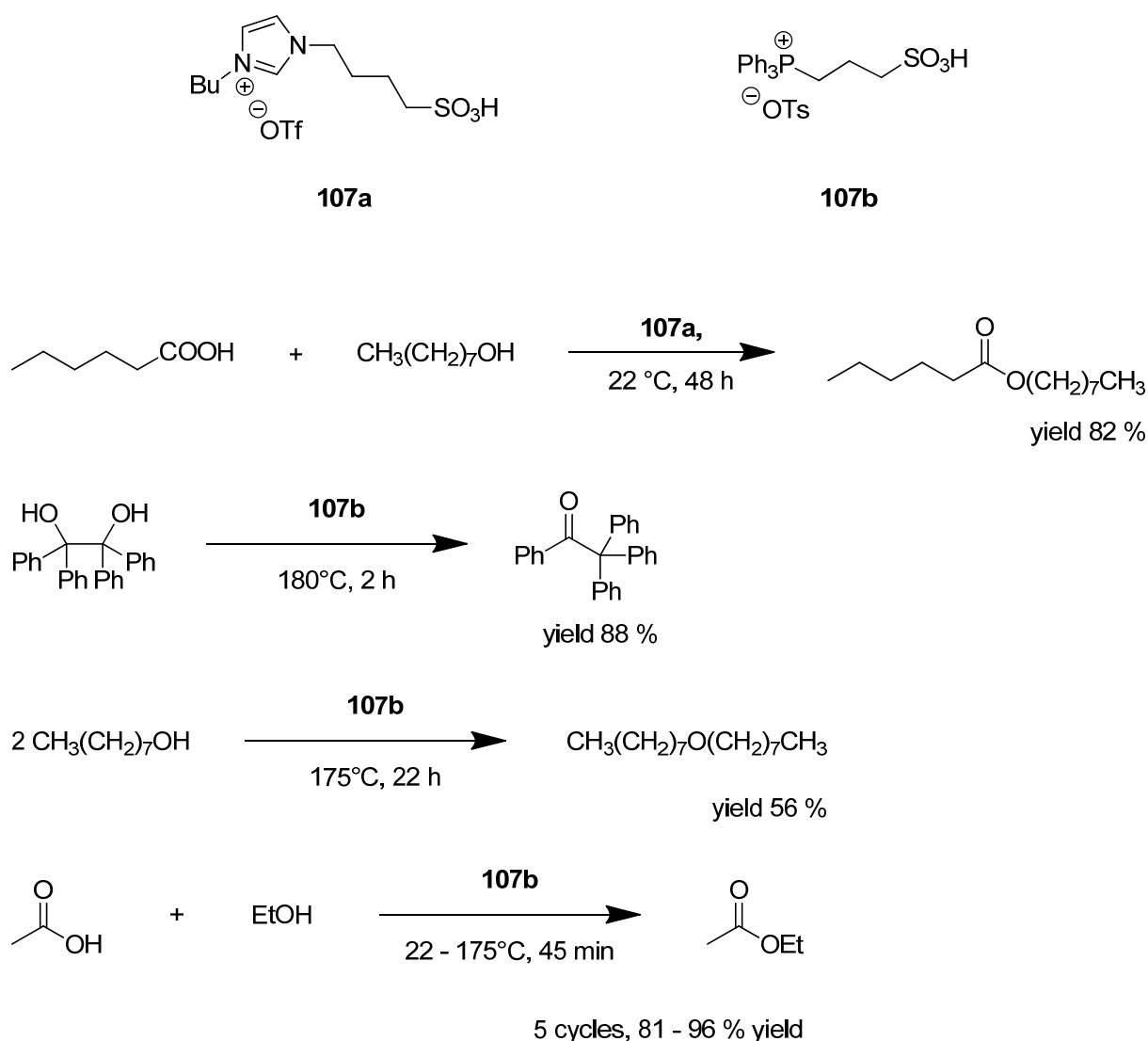


Fig. 54: Reactions catalyzed by ion-tagged Brønsted acids.

1.4.2. Asymmetric cross aldol condensation.

The asymmetric aldol condensation catalyzed by proline, *via* enamine formation, is a prominent organocatalyzed transformation. In the classic protocol the reaction was carried out in DMSO with 30 mol % of proline (fig.55).⁷⁷ In spite of the availability and cheapness of proline the high catalyst

loading and the difficulties in product isolation and catalyst recycling, due to the use of DMSO, led to extensive search for new and more efficient catalysts.

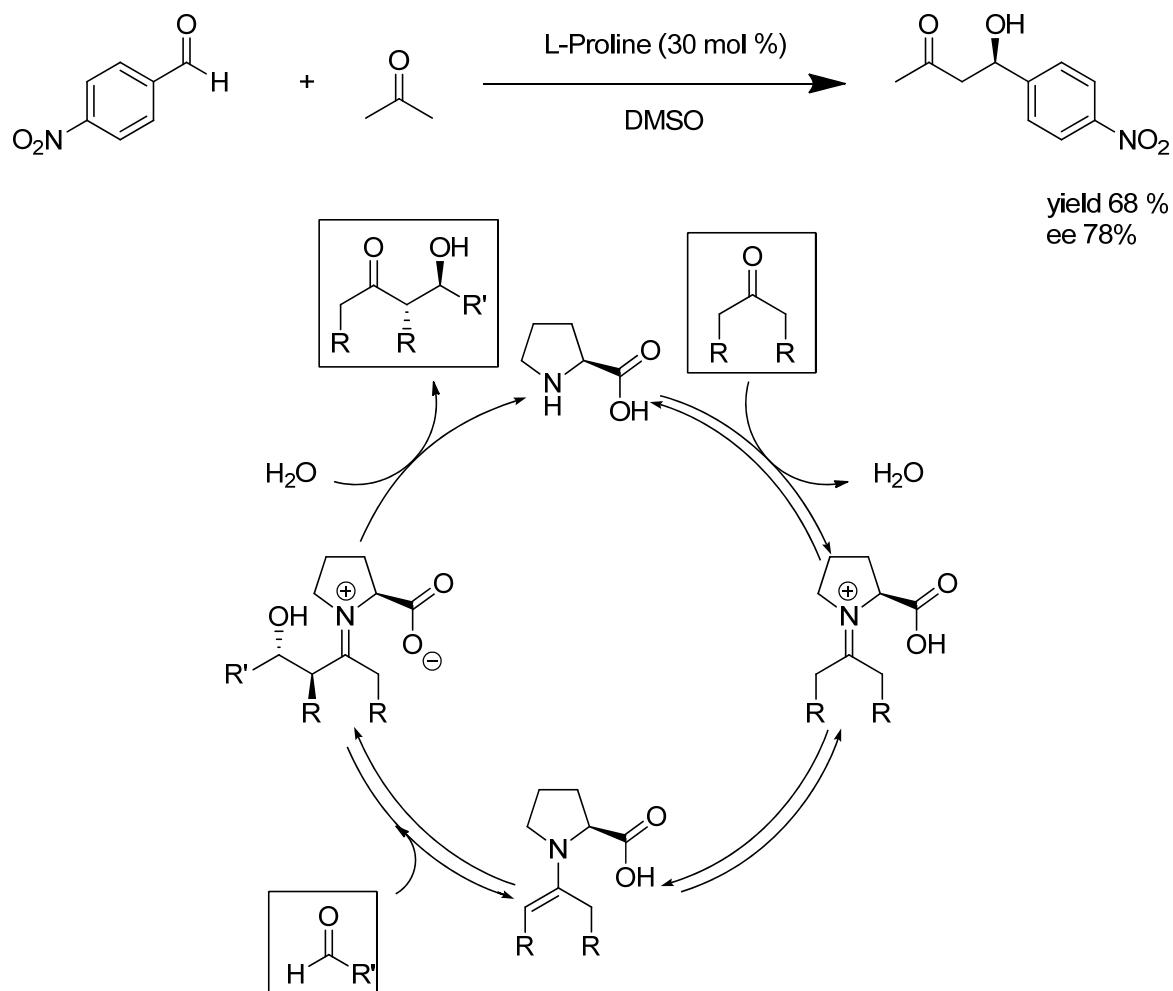


Fig. 55: Mechanism of the cross aldol condensation catalyzed by L-proline.

A number of ion-tagged prolines were designed. Fine tuning of the catalyst structure, along with judicious choice of the reactions conditions, led to the development of catalytic systems displaying higher efficiency compared to the original protocol. Miao and co-workers synthesized an imidazolium-tagged proline (**108**) starting from L-*trans*-4-hydroxyproline which displayed comparable enantioselectivity in DMSO, compared to proline, but better enantioselectivity in neat acetone (fig.56). The catalyst was recycled 4 times with no loss of reactivity and selectivity. From kinetic NMR studies emerged that the reaction with **108** was faster than the reaction catalyzed by proline, suggesting a possible activating role of the ionic group.⁷⁸

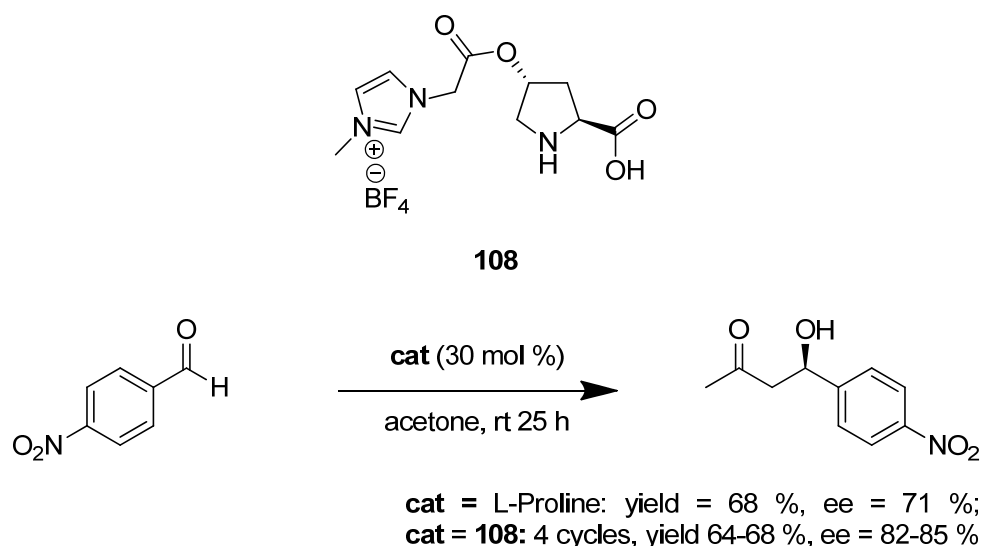


Fig. 56: Asymmetric cross aldol condensation catalyzed by ion-tagged proline **108**.

Trombini and Lombardo's group carried out extensive investigation on the asymmetric aldol condensation catalyzed by ion-tagged prolines. Organocatalysts **109** and **110**, similar to Miao's catalyst, were employed for aldol reaction in ILs. The careful choice of the reaction conditions allowed to lower the catalyst loading up to 5 mol %, when the common benchmark reaction between p-nitrobenzaldehyde and acetone was carried in the IL [bmim][NTf₂] (fig.57). The ionic phase could be recycled, but a drop in activity was observed in the 3rd cycle.⁷⁹

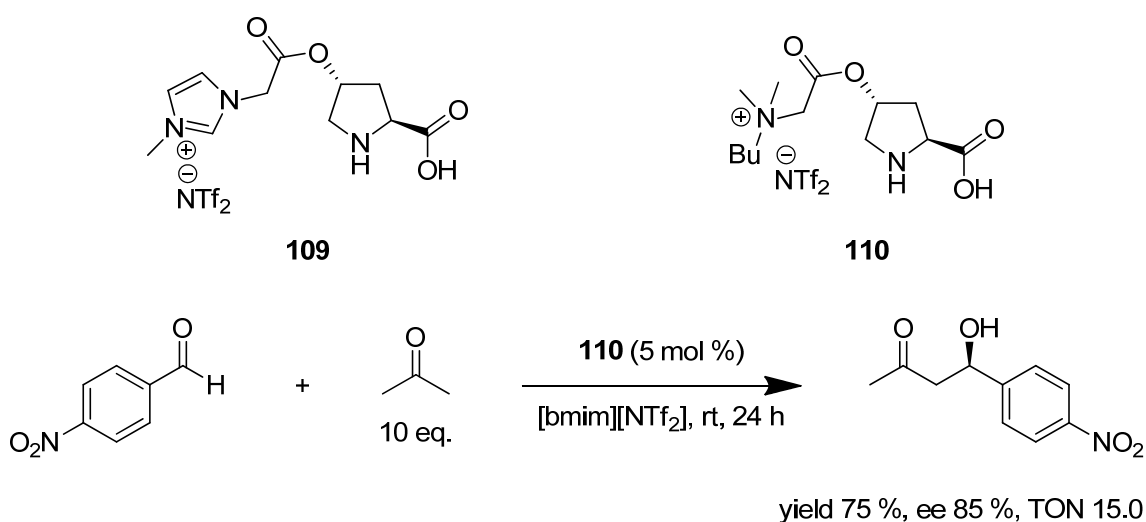


Fig. 57: Asymmetric cross aldol condensation catalyzed by ion-tagged proline **110** in ILs.

The presence of water in the reaction mixture resulted a key parameter for the aldol reaction outcome, mainly because water affect the rate of formation and hydrolysis of the enamine and can even suppress some parasitic pathway leading to catalyst consumption. For these reasons, biphasic protocols involving water and the donor ketone as the organic phase have found wide application. Amphiphilic ion-tagged prolines demonstrated to be performing catalysts for the asymmetric aldol

condensation of cyclic ketones under biphasic conditions. Organocatalyst **111**, bearing an imidazolium ion with a long alkyl chain, catalyzed the reaction between cyclohexanone and aromatic aldehyde **113** with good selectivity. The catalyst was recycled five times with no loss of activity and selectivity.⁸⁰ The hydrosoluble catalyst **112**, bearing an imidazolium tag with an hydrophilic trihydroxy silyl group and a lipophilic counter ion NTf₂, acted as an efficient and selective catalyst in the aldol reaction between p-nitrobenzaldehyde and cyclohexanone under biphasic condition. The product was obtained with high diastereo and enantioselectivity and the catalyst was recycled 3 times with no loss of activity or selectivity (fig.58).⁸¹

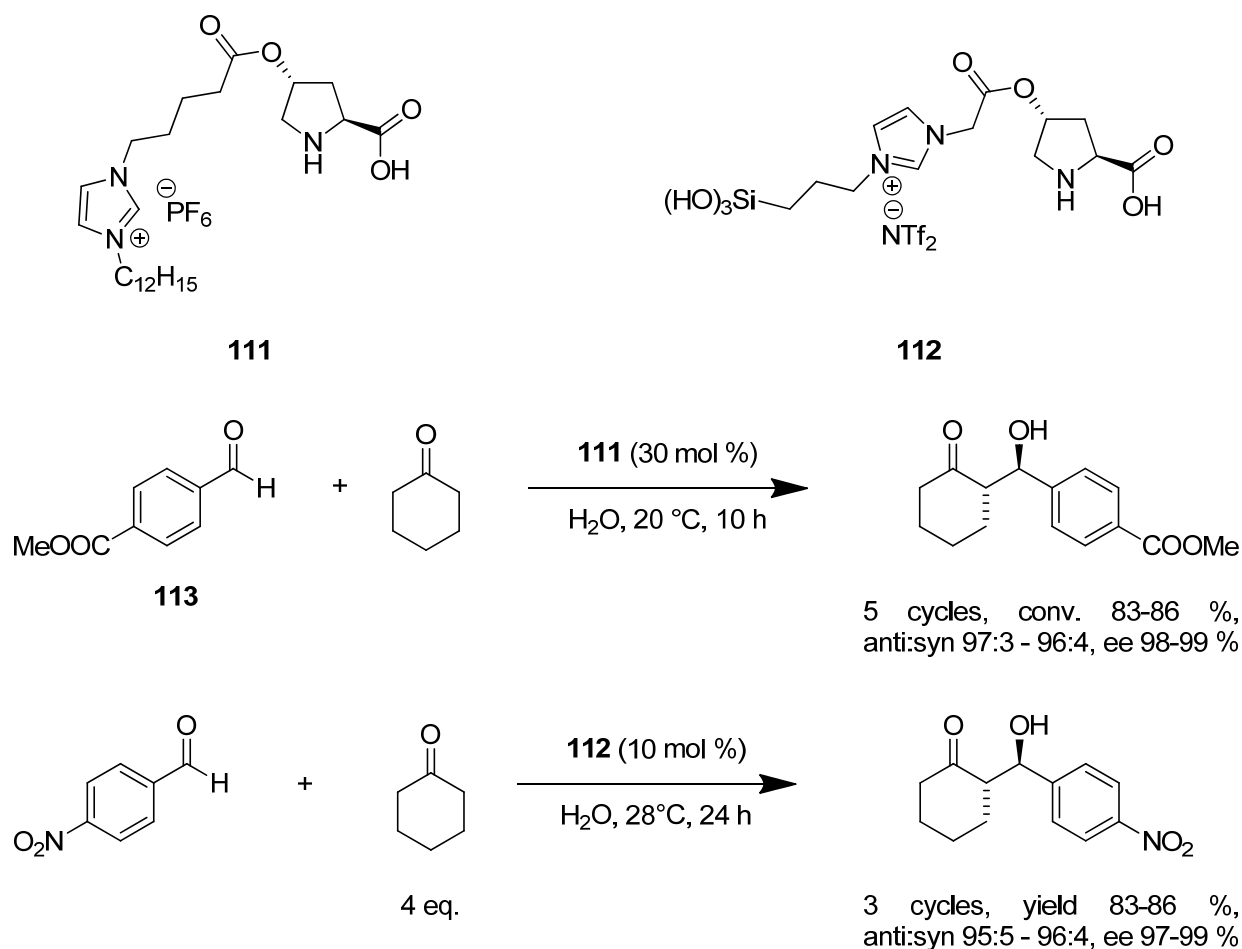


Fig. 58: Asymmetric cross aldol condensation under biphasic condition catalyzed by ion-tagged prolines.

Organocatalyst **114** was different from **109** only for the *cis* configuration of the substituents on the pyrrolidine ring. This catalyst turned out to be particularly efficient when the reaction between aromatic aldehydes and cyclic ketones took place in presence of a stoichiometric amount of water. The aldol reaction between cyclohexanone and p-nitrobenzaldehyde using 1.2 equivalents of water and 5 mol % of **114** was complete in just 20 minutes, with good diastereoselectivity and complete enantiocontrol (fig.59). Moreover, with more reactive aldehydes, the catalyst loading could be further lowered. The reaction between pentafluorobenzaldehyde and cyclohexanone was carried out

in 24 hours with only 0.1 mol % of catalyst, with almost complete selectivity (anti:syn 99:1, ee > 99%) and 93 % yield (fig.59). The *cis* configuration of the substituents in the catalyst placed the ionic group closer to the reactive centre, therefore the enhancement of reactivity of **114** was ascribed to electrosteric activation.⁸²

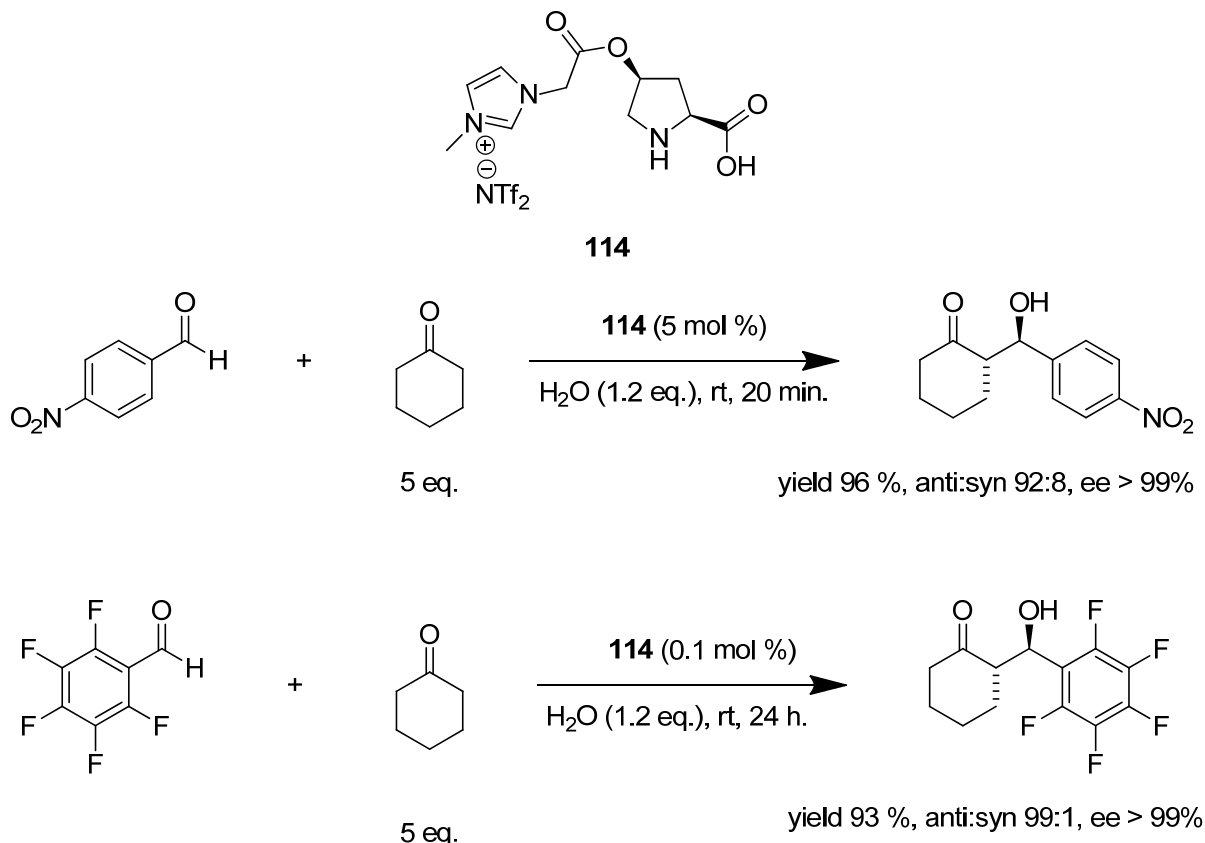
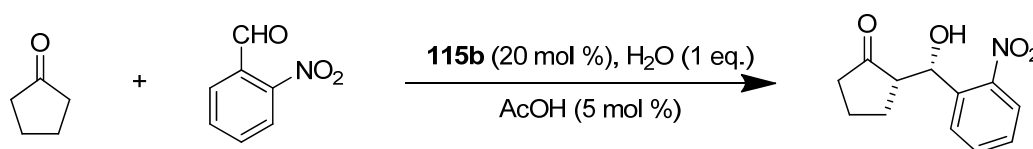
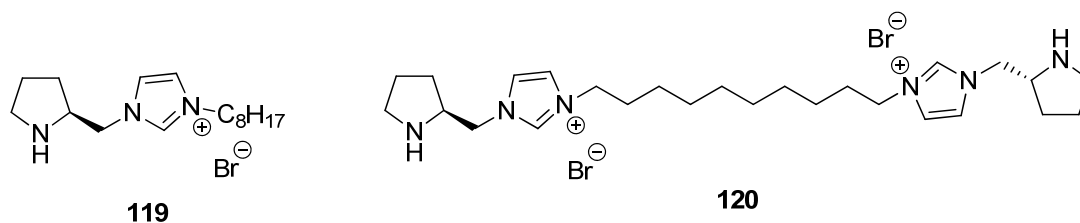
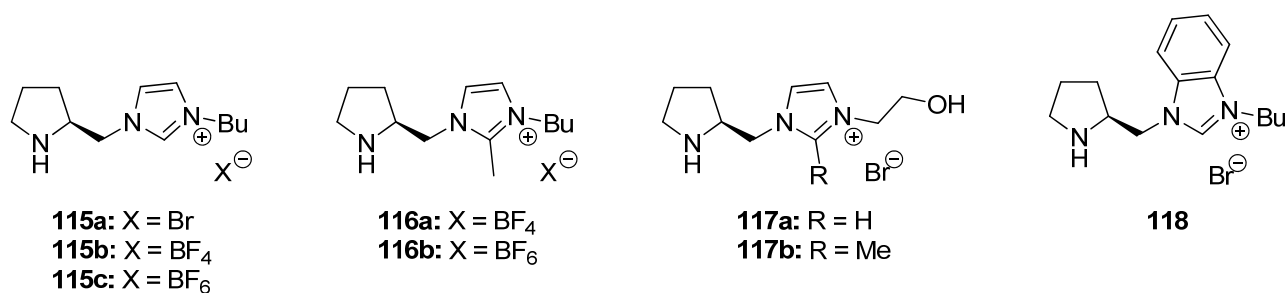


Fig. 59: Asymmetric cross aldol condensation with stoichiometric amount of water catalyzed by ion-tagged proline **114**.

Ion-tagged pyrrolidine were reported to catalyze the aldol reaction in presence of water and acetic acid as additive, but absence of the carboxylic group in the catalyst backbone led to poor enantioselectivity (about 30 % for the minor diastereoisomer). Among the organocatalysts reported, bearing various imidazolium tags and different counterions (**115** – **120**, fig.60) **115b** displayed the best catalytic performance. The catalyst was even recycled six times in the reaction between cyclopentanone and *o*-nitrobenzaldehyde, although with some loss of reactivity and diastereoselectivity, (fig.60).⁸³

Protonated arginine (Arg) was also reported to catalyze the aldol reaction between *p*-nitrobenzaldehyde and cyclohexanone with moderate diastereoselectivity and enantioselectivity. The best result was obtained when the reaction was carried out in the IL [bmpy][OTf]. The ionic phase was recycled three times with only a slightly decrease in the reactivity, but no loss of selectivity (fig.61).⁸⁴



Run	Time (h)	<i>syn/anti</i>	Yield (%)	<i>ee_{syn}</i> (%)	<i>ee_{anti}</i> (%)
1	2	4.8/1	92	11	26
2	4	4.5/1	92	11	28
3	7	4.7/1	94	9	36
4	12	4.0/1	89	<5	33
5	11	2.4/1	96	<5	37
6	17	2.1/1	90	7	35

Fig. 60: Asymmetric cross aldol condensation catalyzed by ion-tagged pyrrolidine.

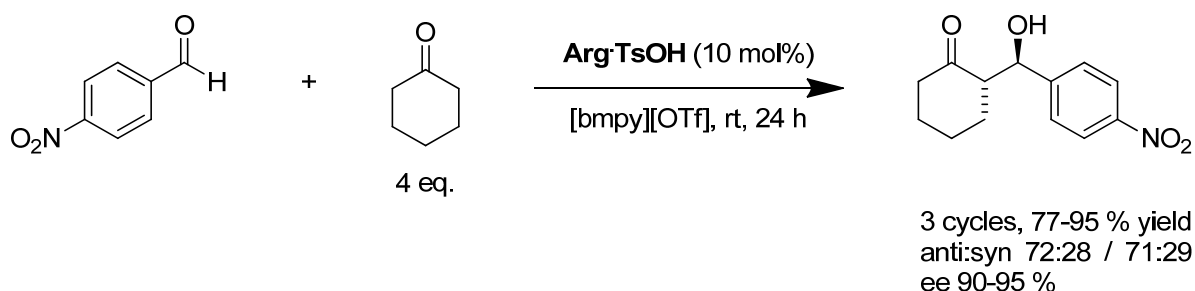


Fig. 61: Asymmetric cross aldol condensation catalyzed by ion-tagged arginine.

1.4.3. Asymmetric Michael addition.

The 1,4-addition of carbon nucleophiles to activated electron poor olefins (i.e. nitroalkenes) is an important reaction to form new C-C bond in an enantioselective way. When the nucleophiles is a

carbonyl compound, secondary amines, mainly pyrrolidine, can catalyze this transformation *via* enamine formation (fig.62)

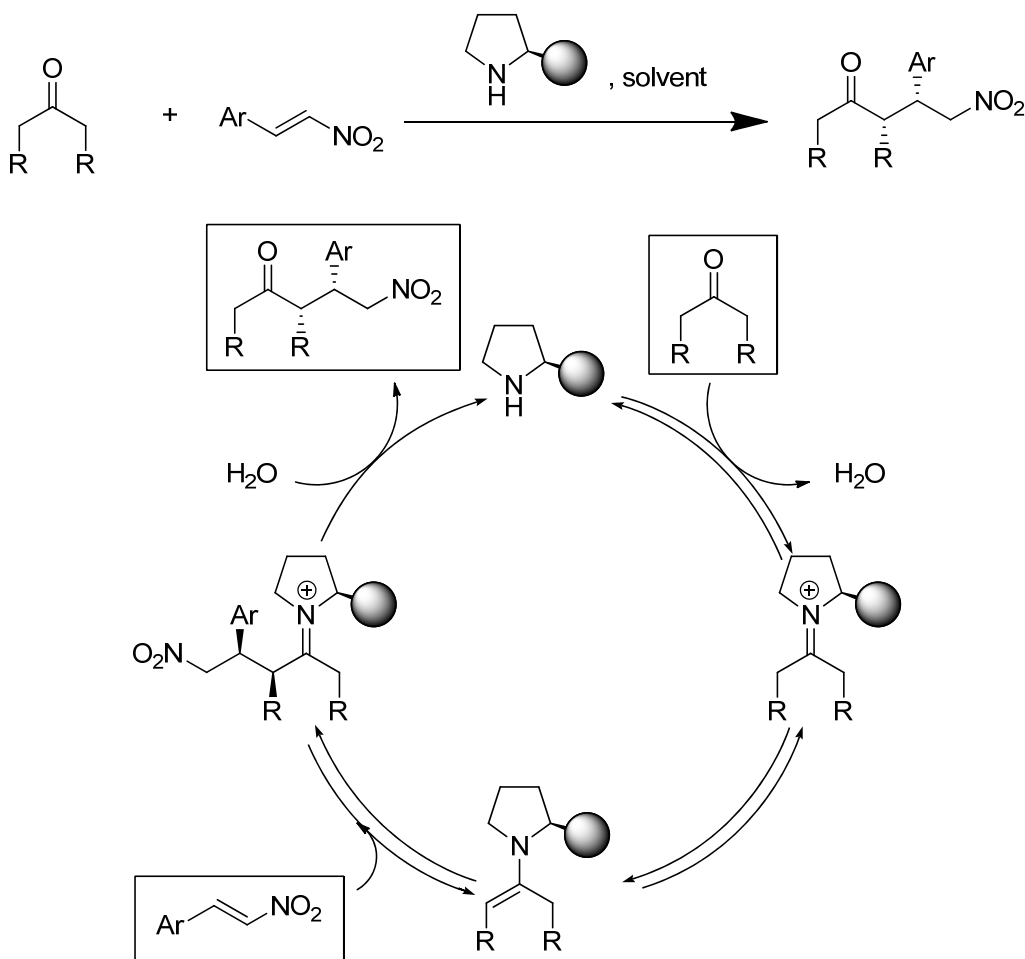


Fig. 62: Mechanism for the organocatalyzed Michael addition of ketones to nitroalkenes.

A number of ion-tagged pyrrolidines were synthesized to accomplish this transformation in various reaction media, mainly ILs, water or neat conditions. Imidazolium tagged pyrrolidine **121** catalyzed the addition of ketones and aldehydes to nitroolefins in the IL [bmim][PF₆]. The reaction proceeded with good yield and selectivity and the ionic phase could be recycled 3 times with no loss of activity and selectivity (fig.63).⁸⁵ Better results were achieved with a similar catalyst when the reaction was carried out in neat conditions, with TFA as additive. The series of imidazolium tagged organocatalyst **115-117** were tested in the addition of cyclohexanone to nitrostyrene (fig. 64). The reaction outcome was sensitive to the nature of the ionic tag. Substitution on the 2' position of the imidazolium ring (**116**), as well as the presence of the hydroxyl group on the catalyst skeleton (**117**) had detrimental effect on the reactivity. The presence of the ionic tag resulted in a better catalytic performance compared to the corresponding non-ionic organocatalyst (Entry 1). Also the counterion affected the catalyst activity and selectivity (Entry 2-4).

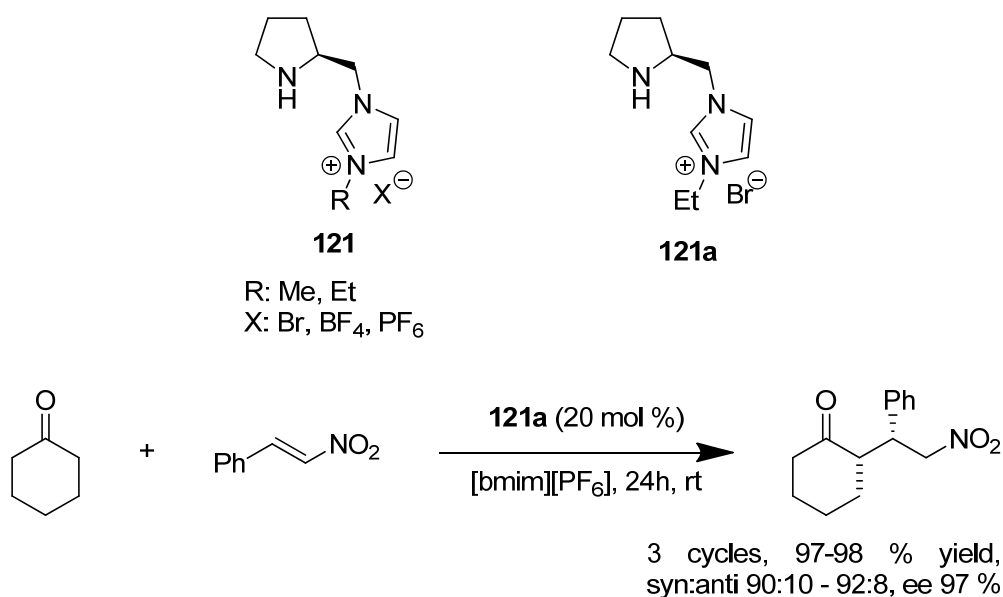
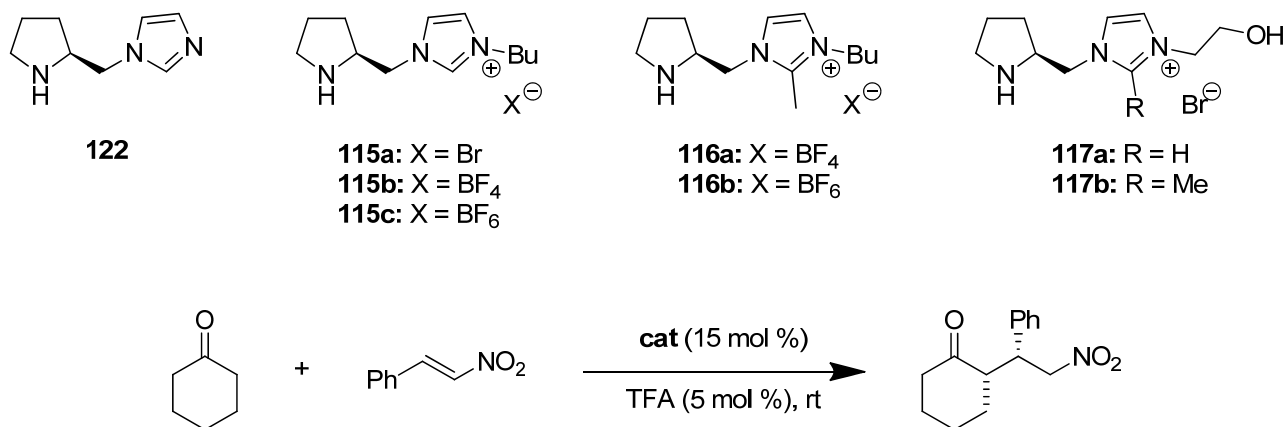


Fig. 63: Addition of ketone to nitroolefins catalyzed by ion-tagged pyrrolidine **121a** in ILs.

Among the catalysts screened, **115b** afforded the best catalytic performance in the addition of different ketones and aldehydes to various nitroolefins. The best results were achieved in the reaction with cyclohexanone and nitrostyrene, which, after 8 hours, gave the product in quantitative yield and with excellent selectivity (Entry 3). The catalytic system could be recycled, albeit drops in reactivity and selectivity were observed.⁸⁶



Entry	cat.	Time (h)	Yield (%)	syn:anti	ee (%)
1	122	18	97	97:3	91
2	115a	10	99	99:1	98
3	115b	8	100	99:1	99
4	115c	12	86	99:1	87

Fig. 64: Addition of ketones to nitroolefins catalyzed by ion-tagged pyrrolidine in neat conditions.

Pyridinium-tagged pyrrolidines were also investigated as organocatalysts for Michael addition. Organocatalyst **124** with various anions were utilized in the addition of ketone to nitroolefins in neat condition. The best counterions turned to be the BF_4 and, like is common for this reaction, cyclohexanone gave the best results in terms of selectivity. The reaction between cyclohexanone and nitrostyrene proceeded with excellent selectivity at 4°C and the catalyst was reused three times without any loss of activity or selectivity.⁸⁷

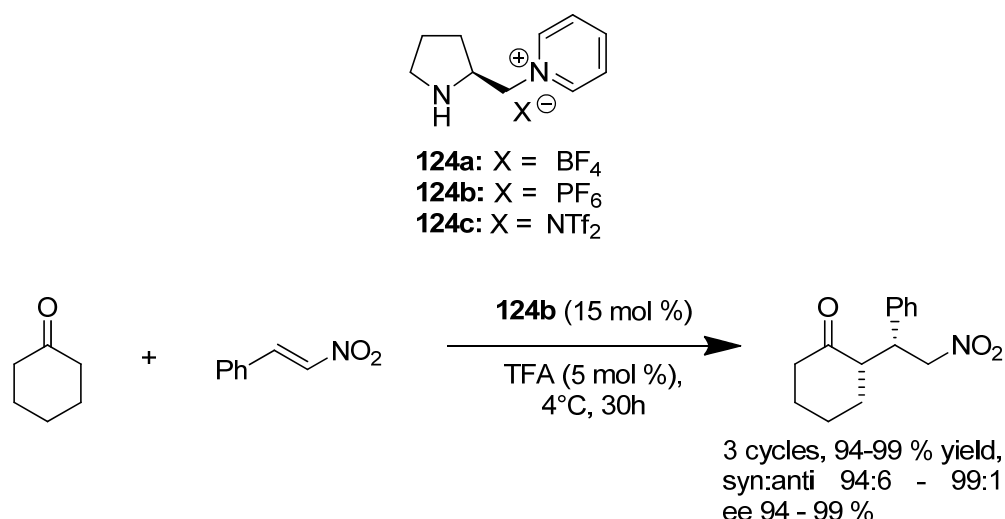


Fig. 65: Addition of ketones to nitroolefins catalyzed by pyridinium-tagged pyrrolidine in neat conditions.

A series of pyridine-tagged pyrrolidines were tested in several solvents and the IL $[\text{bmim}][\text{BF}_4]$, in combination with the isoquinolinic-tagged catalyst **125a**, demonstrated to be the best solvent for this transformation. When the reaction between cyclohexanone and nitrostyrene was carried out in $[\text{bmim}][\text{BF}_4]$ the ionic phase could be recycled five times without any loss of activity or selectivity (fig.66).⁸⁸

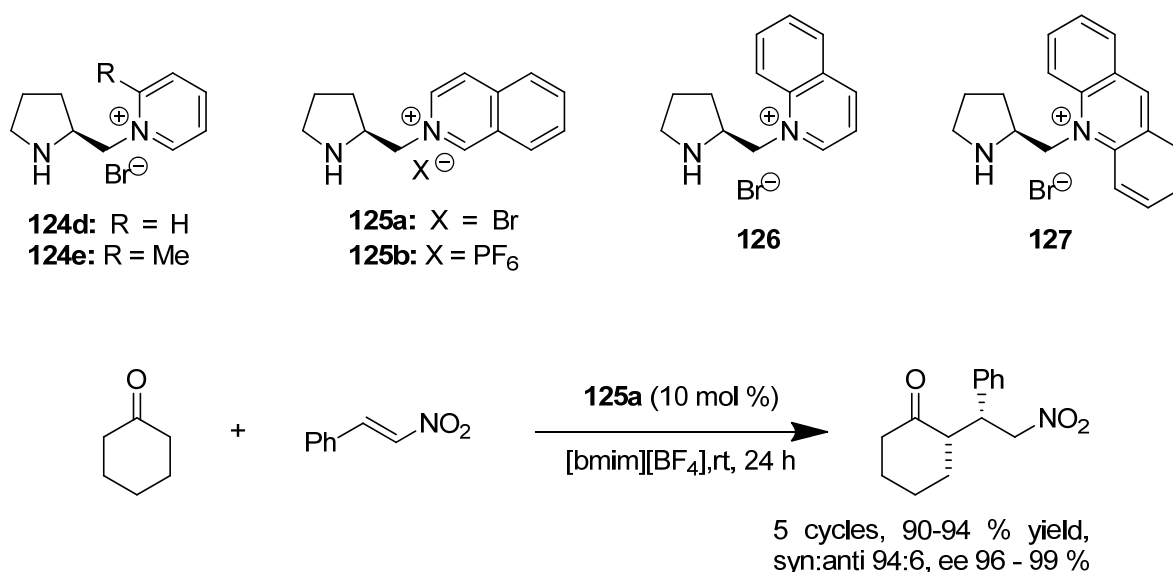


Fig. 66: Addition of ketones to nitroolefins catalyzed by pyridinium-tagged pyrrolidine in ILs.

Ion-tagged catalyst **118** was used in the desymmetrization of 4-substituted cyclohexanones using salicylic acid as additive. The product, containing 3 stereocenters, was obtained with good diastereo and enantioselectivity (fig.67). The catalyst could be recycled by the reactivity dropped after the 2nd run.⁸⁹

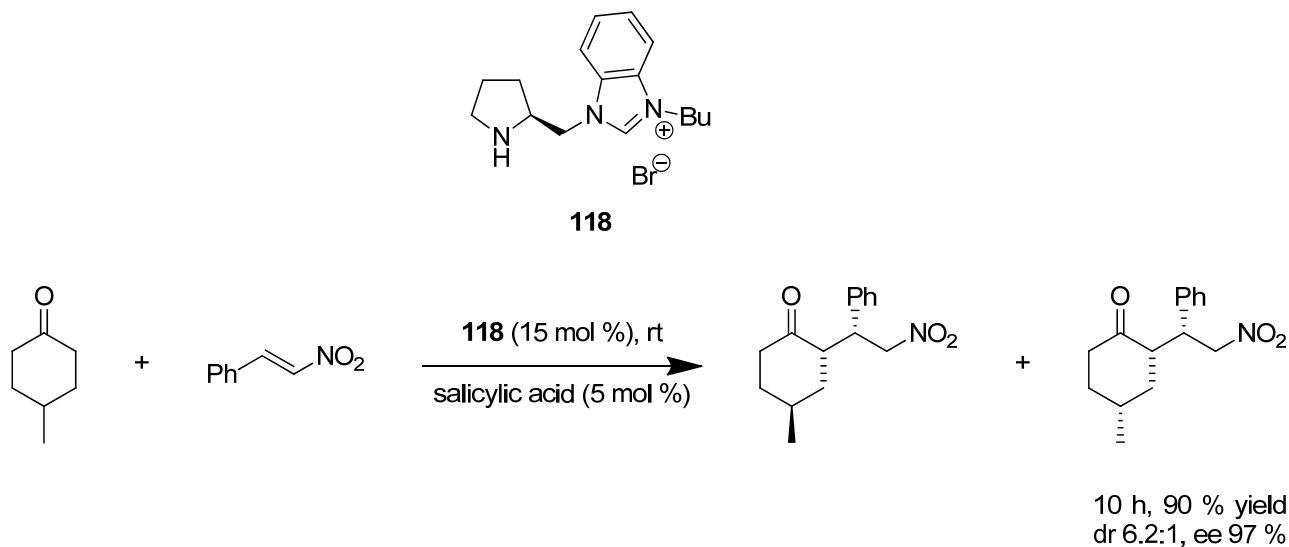


Fig. 67: Desymmetrization of 4-substituted cyclohexanones.

When the bromide ion in catalyst **118** was replaced by a surfactant, the Michael addition of cyclohexanone to nitrostyrene could be accomplished in water with good reactivity and selectivity (fig.68).⁹⁰

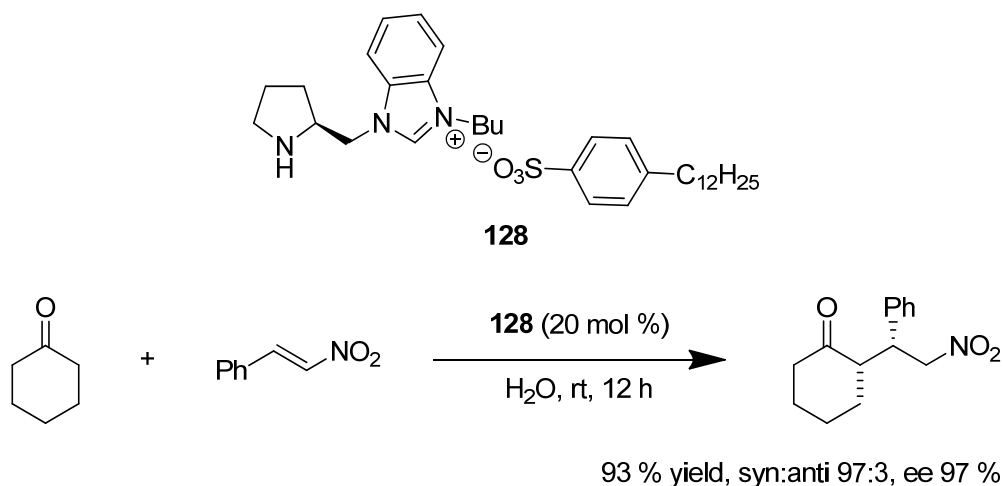


Fig. 68: Addition of ketones to nitroolefins catalyzed by surfactant-type ion-tagged organocatalyst in water.

Two pyrrolidine ion-tagged organocatalysts were synthesized exploiting the chemistry of the triazole ring, which can be efficiently built by the Cu-catalyzed 1,3-dipolar cycloaddition of azides with alkynes. In the catalyst **129a** the triazole ring was directly alkylated and the organocatalyst was employed in the addition of various aldehydes and ketones to nitroolefins in the presence of TFA as

additive. When the reaction between cyclohexanone and nitrostyrene was carried out in the optimized conditions the catalyst was recycled three times with only a small drop in reactivity and selectivity (fig.69).⁹¹

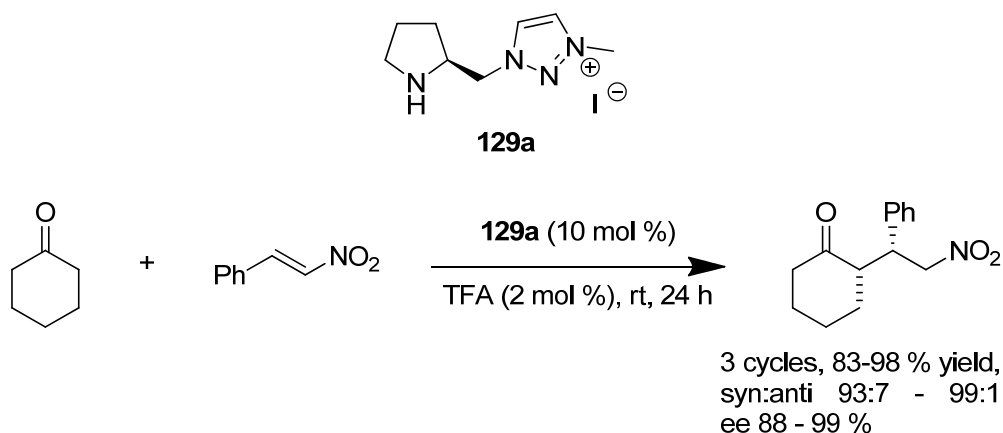


Fig. 69: Addition of ketones to nitroolefins catalyzed by triazolium-tagged pyrrolidine.

In the catalyst **129b** the triazolium ring was instead used as a linker between the pyrrolidine ring and the imidazolium tag. **129b** was recycled four times with no loss of activity or selectivity when the addition of cyclohexanone to nitrostyrene was carried out with TFA as additive (fig.70).⁹²

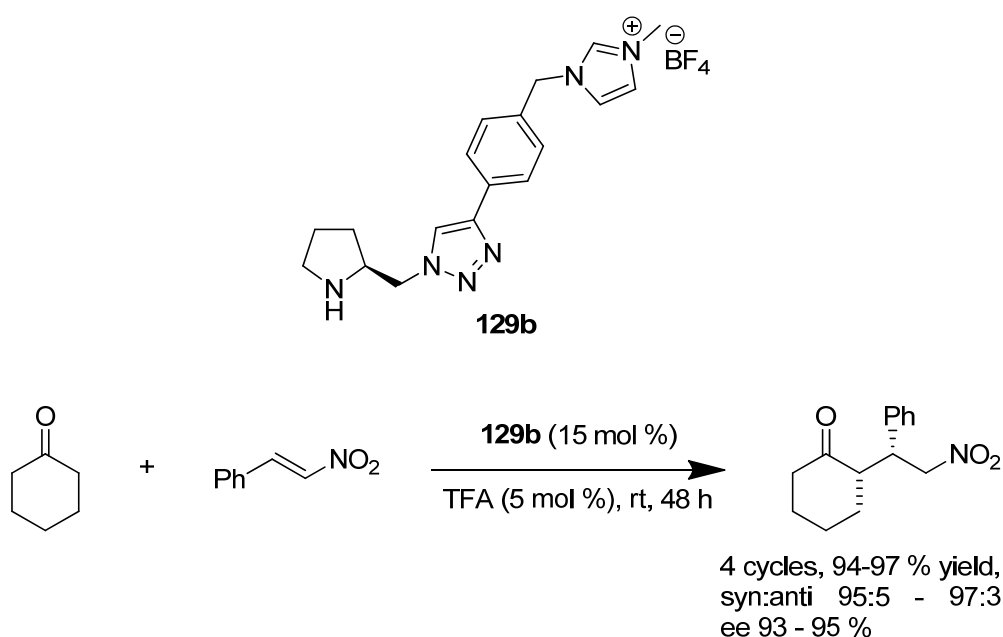


Fig. 70: Addition of ketones to nitroolefins catalyzed by ion-tagged pyrrolidine.

The series of imidazolium tagged pyrrolidine organocatalyst **130a-c** were tested in the Michael addition of aldehydes and ketones to nitroolefins. A sulfonamide bond was exploited to connect the ion tag to the pyrrolidine ring using spacers of different length. The reactivity of the catalytic system increased greatly from **130a** to **130b** and even more using **130c**. This behavior was probably due to the important role played by the acidic N-H bond of the sulfonamide. When the ionic group

was closer to the sulfonamide stronger H-bond were formed and the reactivity increased sensitively. When catalyst **130a** was employed reaction between aldehydes and nitrostyrene gave good yields only after 6 days, with **130b** reaction time could be lowered to 2 days, but only sluggish reaction was observed when ketones were employed as nucleophiles. On the other hand using **130c** reaction between cyclohexanone and nitrostyrene took place in 12 hours and the catalyst was also recycled four times with only a small drop in reactivity (fig.71).^{93,94,95}

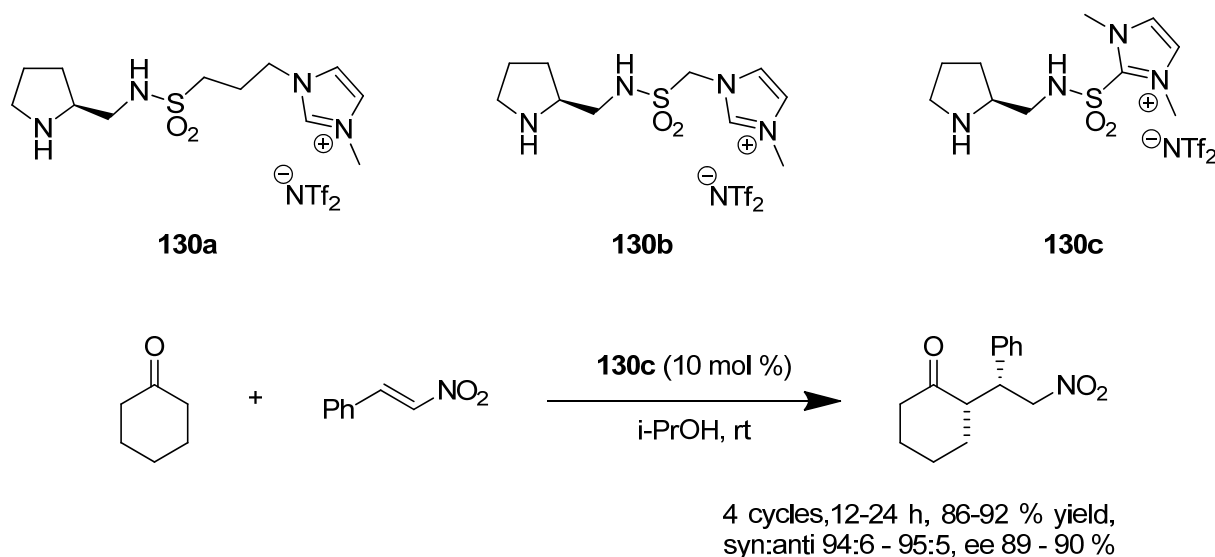


Fig. 71: Addition of ketones to nitroolefins catalyzed by ion-tagged pyrrolidine.

Finally a pyrrolidinyli-thioimidazolium catalyst (**131**) was employed to catalyze the Michael addition of ketones to nitroolefins using PEG-800 as solvent. The PEG chain length and the counterion played a key role for the efficiency of the catalytic system. This was due to the formation of an inclusion complex PEG-cation which improved the catalytic performance. The catalyst was recycled up to seven times with only a small loss of activity (fig.72).⁹⁶

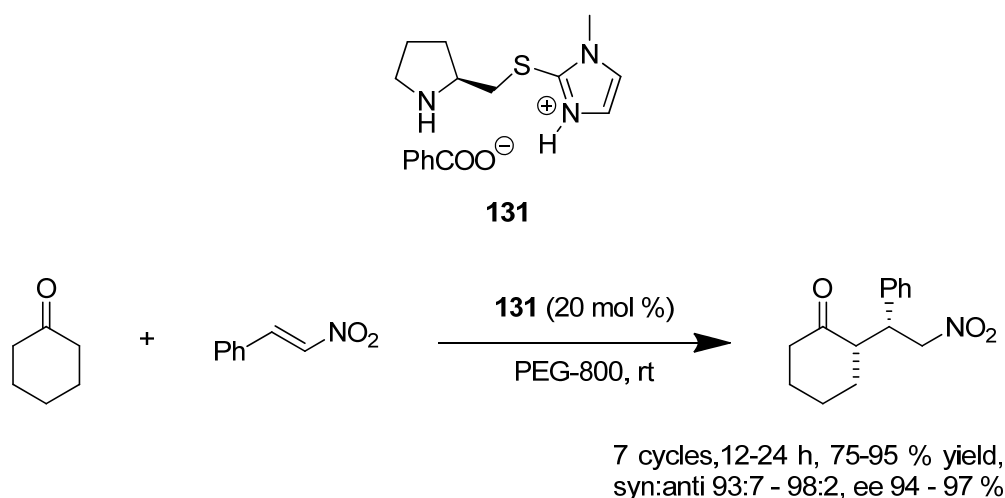


Fig. 72: Addition of ketones to nitroolefins catalyzed by ion-tagged pyrrolidine in liquid PEG.

1.4.4. Morita – Baylis – Hillman (MBH) reaction.

The MBH is an interesting C-C bond forming reaction which usually proceeds in mild condition and with elevated atom economy. Phosphines or tertiary amine nucleophilic catalysis and protic solvents are usually required to speed up the reaction. An imidazolium tagged quinuclidine was synthesized by reductive amination of quinuclidone (**132**, fig.73). When the reaction of p-chlorobenzaldehyde with methyl acrylate was carried out in various conditions, using **132** as catalyst, methanol emerged as the best solvent for this reaction. **132** was recycled six times with only a marginal decrease in the activity, and the scope of the reaction was extended to other activate olefins, like acrylonitrile and cyclic enones, and various aromatic aldehydes.⁹⁷

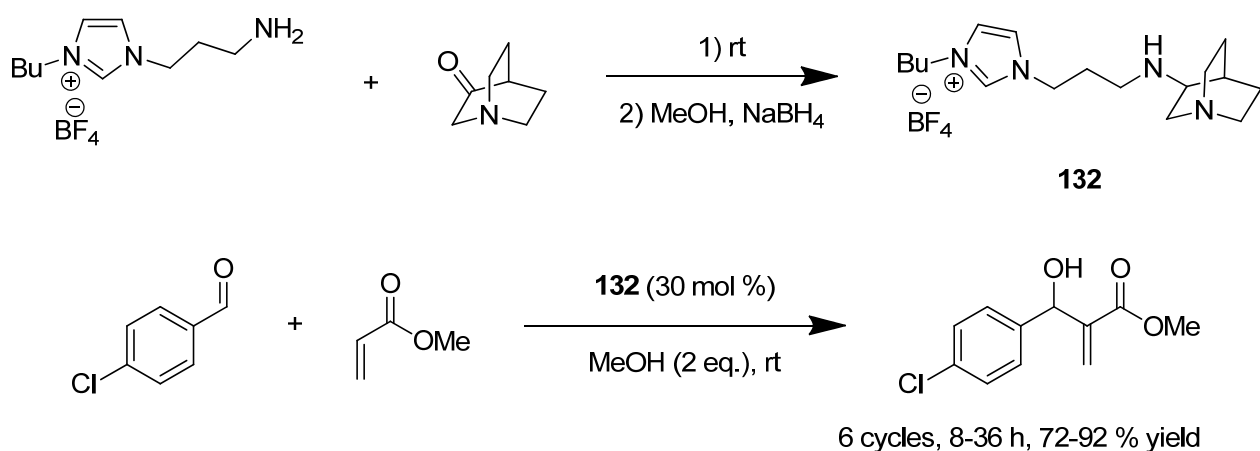


Fig. 73: MBH reaction catalyzed by ion-tagged quinuclidine.

An improvement in the catalyst activity was observed installing an hydroxyl group onto the catalyst backbone (**133**). Reaction rate enhancement was probably observed because, the hydroxyl group in proximity of the active site, accelerated the reaction via hydrogen-bonding activation and/or assisting intra-molecular proton transfer. The catalyst was easily recycled six times without any significant loss in activity when the MBH of p-chlorobenzaldehyde with methyl acrylate was carried out in neat conditions (fig.74).⁹⁸

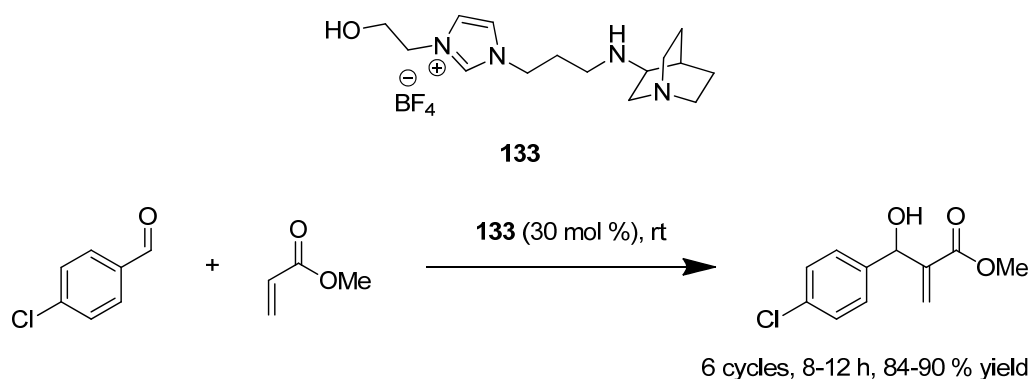


Fig. 74: MBH reaction catalyzed by ion-tagged quinuclidine bearing a hydroxyl group.

1.4.5 Asymmetric reduction of ketones.

Liang and co-workers reported a diphenylprolinol tagged *via* a sulfonamide bond (**134**), for the asymmetric reduction of ketones with borane. The reduction took place in refluxing toluene with good yields and enantioselectivity depending on the nature of the substrate (ees up to 96 % were obtained with *ortho*-substituted aromatic ketones). The catalyst could be recycled after aqueous work-up for at least three times, without any loss of activity or selectivity (fig.75).

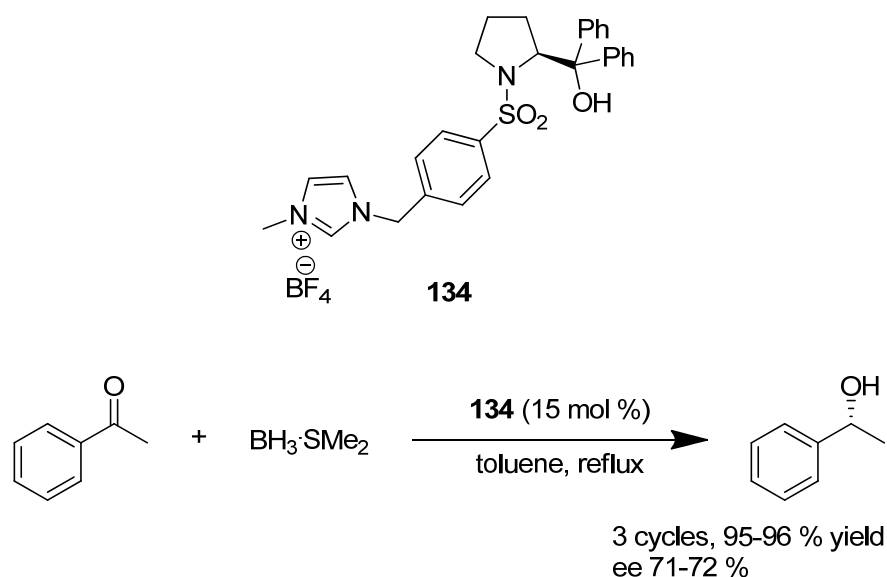


Fig. 75: Asymmetric ketone reduction with ion-tagged diphenylprolinol sulfonamide.

1.4.6. Alcohols oxidation.

Primary and secondary alcohols oxidation to carbonyl compounds can be accomplished efficiently and selectively using 2,2,6,6-tetramethylpiperidine-1-oxyl (TEMPO) together with a terminal oxidant (often bleach). A common problem arising for this oxidation process is the separation of the product from TEMPO. Several ion-tagged TEMPO were proposed to solve this problem. Imidazolium tagged TEMPO **135a** was used for the oxidation of various primary and secondary alcohols in the IL $[\text{bmim}][\text{PF}_6]$, using NaClO as terminal oxidant. The ionic phase containing the catalyst was easily separated from the catalyst and reused at least three times without any loss of activity (fig.76).⁹⁹ Three different ion-tagged TEMPO were reported by Bao and co-workers. The catalysts displayed similar reactivity in the oxidation of various primary and secondary alcohols. It was worth noting the use of the ion-tagged iodophenyl diacetate **138** as stoichiometric oxidant. This allowed the authors to set up a low waste protocol, where both the catalyst TEMPO and the stoichiometric oxidant **138** could be recycled. When *p*-methoxybenzyl alcohol was oxidized to the

corresponding aldehyde the catalytic system was recycled five times with no loss of activity (fig.77).¹⁰⁰

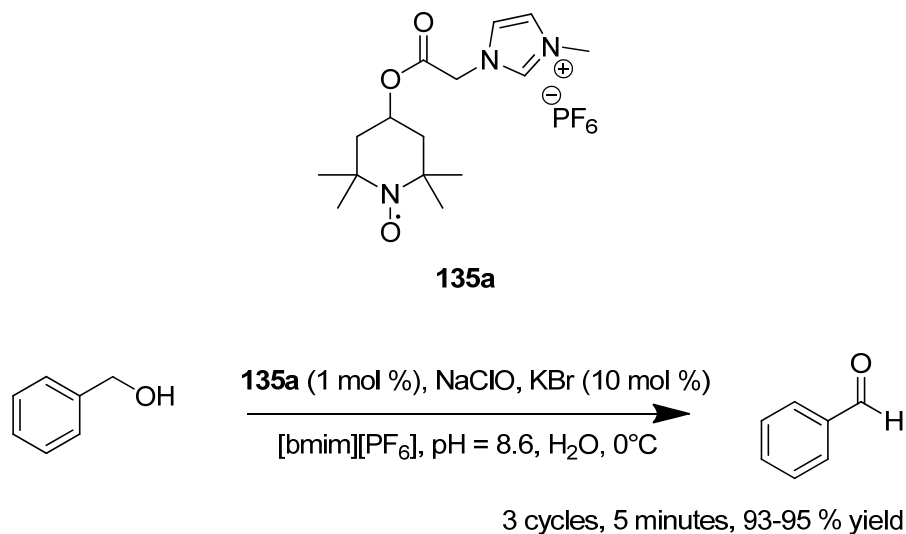


Fig. 76: Alcohol oxidation mediated by ion-tagged TEMPO in ILs.

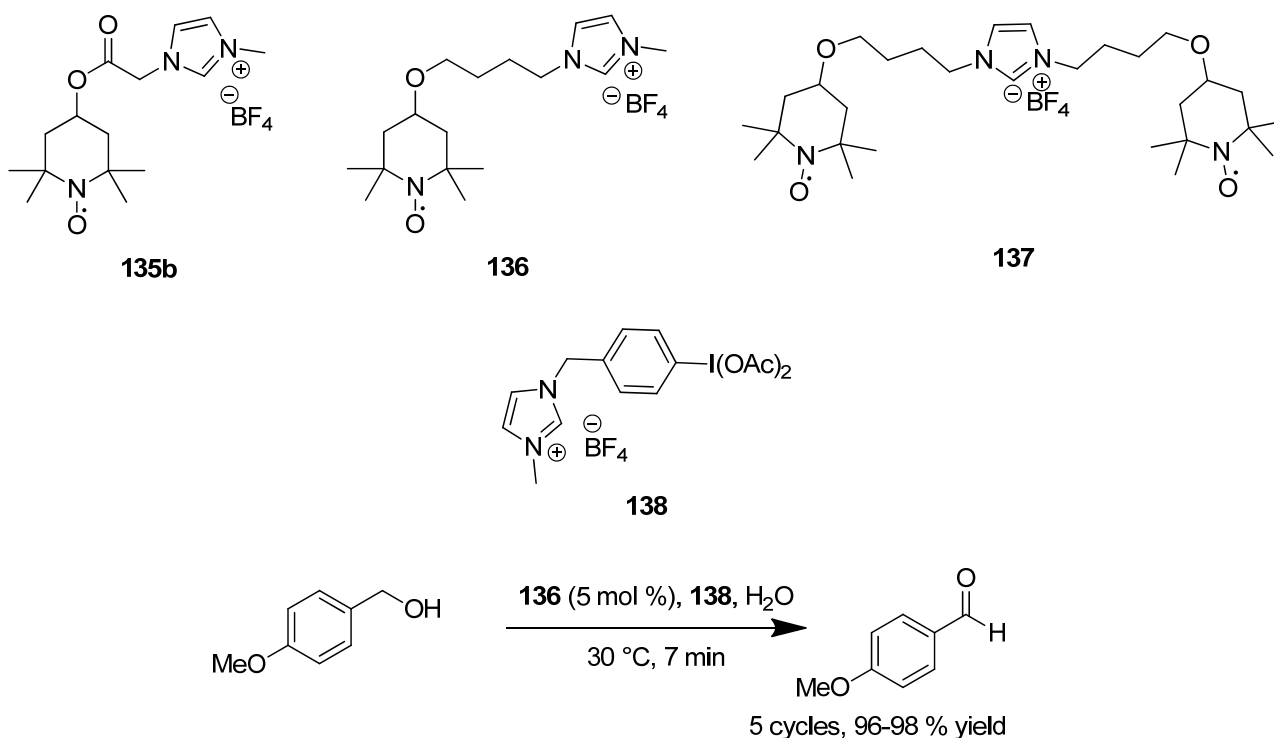
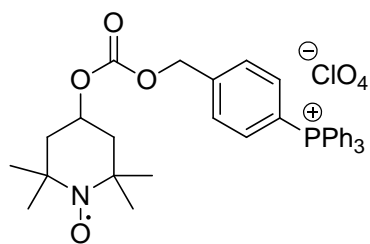


Fig. 77: Alcohol oxidation mediated by ion-tagged TEMPO and ion-tagged iodophenyl diacetate in water.

Finally a phosphonium tagged TEMPO was employed for the oxidation of various alcohols in the biphasic system DCM / water. When the oxidation of 3-phenyl-1-propanol was carried out the catalyst was easily recycled for at least four times without any loss of activity (fig.78).¹⁰¹



139

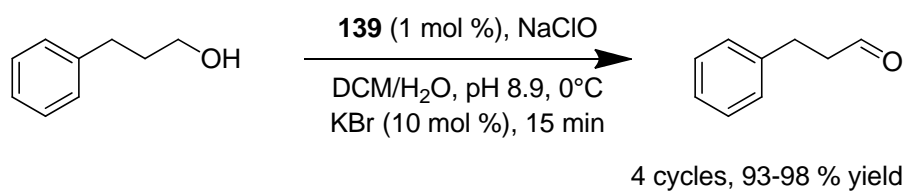


Fig. 78: Alcohol oxidation mediated by ion-tagged TEMPO in water / DCM biphasic system.

Bibliography

- (1) Rothenberg, G. *Catalysis. Concept and Green Applications*, Wiley-VCH, Weinheim, **2008**.
- (2) Anastas, P. T.; Warner, J. *Green Chemistry. Theory and Practice*, Oxford University Press, **2000**.
- (3) Anastas, P. T.; Kirchhoff, M. M. *Acc. Chem. Res.* **2002**, *35*, 686-694.
- (4) *Chem. Rev.* **2009**, *109*, 257-838. Special Issue on Facilitated Synthesis.
- (5) *Adv. Synth. Cat.* **2006**, *348*, 1317-1771. Special Issue on Multiphase Catalysis, Green Solvents and Immobilization.
- (6) Lombardo, M.; Quintavalla, A.; Chiarucci, M.; Trombini, C. *Synlett.* **2010**, 1746-1765.
- (7) Shaughnessy, K. H. *Chem. Rev.* **2009**, *109*, 643-710
- (8) Cole-Hamilton, D. J. *Adv. Synth. Cat.* **2006**, *348*, 1341-1351.
- (9) Zhang, W. *Green Chemistry.* **2009**, *11*, 911-920.
- (10) Liu, S.; Xiao, J. *J. Mol. Cat. A.* **2007**, *270*, 1-43
- (11) Lombardo, M.; Quintavalla, A.; Chiarucci, M.; Trombini, C. *Synlett.* **2010**, 1746-1765.
- (12) Dickerson, T. J.; Reed, N. N.; Janda, K. D. *Chem. Rev.* **2002**, *102*, 3325-3344.
- (13) Bergbreiter, D. E. *Chem. Rev.* **2002**, *102*, 3345-3384.
- (14) Baker, R.T.; Tumas W. *Science* **1999**, *284*, 1477.
- (15) Huo, C.; Chan, T. H. *Chem. Soc. Rev.* **2010**, *39*, 2977-3006.
- (16) Luo, S.; Zhang, L.; Cheng, J.-P. *Chem. Asian J.* **2009**, *4*, 1184-1195.
- (17) Domínguez de María, P. *Angew. Chem. Int. ed.* **2008**, *47*, 6960-6968.
- (18) Sebesta, R. *Green Chemistry.* **2008**, 484-496.
- (19) Liu, S.; Xiao, J. *J. Mol. Cat. A.* **2007**, *270*, 1-43.
- (20) Lee, S. *Chem. Comm.* **2006**, 1049-1063
- (21) Ni, B.; Headley, A. D. *Chem. Eur. J.* **2010**, *16*, 4426-4436.
- (22) Lombardo, M.; Trombini, C. *ChemCatChem.* **2010**, *2*, 135-145.
- (23) Trindade, A. F.; Gois, P. M. P.; Afonso, C. A. M. *Chem. Rev.* **2009**, *109*, 418-514.
- (24) Geldbach, T. J.; Scopelliti, R.; Dyson, P. J. *Organometallics.* **2006**, *25*, 733-742.
- (25) Lee, S.-gi; Zhang, J.; Piao, Y.; Yoon, H.; Song, E.; Choi, H. *Chem. Comm.* **2003**, 2624-2625.
- (26) Feng, X.; Pugin, B.; Küsters, E.; Sedelmeier, G.; Blaser, H.-U. *Adv. Synth. Cat.* **2007**, *349*, 1803-1807.
- (27) Schmitkamp, M.; Chen, D.; Leitner, W.; Klankermayer, J.; Franciò, G. *Chem. Comm.* **2007**, 4012-4014.
- (28) Chen, D.; Schmitkamp, M.; Franciò, G.; Klankermayer, J.; Leitner, W. *Angew. Chem. Int. ed.* **2008**, *47*, 7339-7341.
- (29) Gavrilov, K. N.; Lyubimov, S. E.; Bondarev, O. G.; Maksimova, M. G.; Zheglov, S. V.; Petrovskii, P. V.; Davankov, V. A.; Reetz, M. T. *Adv. Synth. Cat.* **2007**, *349*, 609-616.
- (30) Webb, P. B.; Sellin, M. F.; Kunene, T. E.; Williamson, S.; Slawin, A. M. Z.; Cole-Hamilton, D. J. *J. Am. Chem. Soc.* **2003**, *125*, 15577-15588.
- (31) E. G. Kuntz, *Fr. Pat.* **1975**, 2314910.
- (32) Chauvin, Y.; Mussmann, L.; Olivier, H. *Angew. Chem. Int. ed.* **1996**, *34*, 2698-2700.
- (33) Mehnert, C. P.; Cook, R. A.; Dispenziere, N. C.; Mozeleski, E. J. *Polyhedron.* **2004**, *23*, 2679-2688.
- (34) Mehnert, C. P.; Cook, R. A.; Dispenziere, N. C.; Afeworki, M. *J. Am. Chem. Soc.* **2002**, *124*, 12932-12933.
- (35) Favre, F.; Olivier-Bourbigou, H.; Commereuc, D.; Saussine, L. *Chem. Comm.* **2001**, *2*, 1360-1361.
- (36) Kottsieper, K. W.; Stelzer, O.; Wasserscheid, P. *J. Mol. Cat. A.* **2001**, *175*, 285-288.
- (37) Bronger, R. P. J.; Silva, S. M.; Kamer, C. J.; Van Leeuwen, P. W. N. M. *Chem. Comm.* **2002**, 3044-3045.
- (38) Desset, S. L.; Cole-Hamilton, D. J. *Angew. Chem. Int. ed.* **2009**, *48*, 1472-1474.
- (39) Audic, N.; Clavier, H.; Mauduit, M.; Guillemin, J.-C. *J. Am. Chem. Soc.* **2003**, *125*, 9248-9249.
- (40) Yao, Q.; Zhang, Y. *Angew. Chem. Int. Ed.* **2003**, *42*, 3395-3398.
- (41) Clavier, H.; Audic, N.; Guillemin, J.; Mauduit, M. *J. Organomet. Chem.* **2005**, *690*, 3585-3599.
- (42) Yao, Q.; Sheets, M. *J. Organomet. Chem.* **2005**, *690*, 3577-3584.
- (43) Rix, D.; Clavier, H.; Coutard, Y.; Gulajski, L.; Grela, K.; Mauduit, M. *J. Organomet. Chem.* **2006**, *691*, 5397-5405.
- (44) Rix, D.; Caïjo, F.; Laurent, I.; Gulajski, L.; Grela, K.; Mauduit, M. *Chem. Comm.* **2007**, 3771-3773.
- (45) Zincke, T.H.; Heuser, G.; Möller, W.; *Ann. Chim.* **1904**, 333 296;
- (46) Thurier, C.; Fischmeister, C.; Bruneau, C.; Olivier-Bourbigou, H.; Dixneuf, P. H. *J. Mol. Cat. A.* **2007**, *268*, 127-133.
- (47) Chen, S.-W.; Kim, J. H.; Ryu, K. Y.; Lee, W.-W.; Hong, J.; Lee, S.-gi *Tetrahedron.* **2009**, *65*, 3397-3403.
- (48) Srinivas, K. A.; Kumar, A.; Chauhan, S. M. S. *Chem. Comm.* **2002**, 2456-2457.
- (49) Liu, Y.; Zhang, H.-J.; Lu, Y.; Cai, Y.-Q.; Liu, X.-L. *Green Chem.* **2007**, *9*, 1114-1119.
- (50) Peng, Y.; Cai, Y.; Song, G.; Chen, J. *Synlett.* **2005**, 2147-2150.
- (51) Ding, S.; Radosz, M.; Shen, Y. *Macromolecules.* **2005**, *38*, 5921-5928.
- (52) Song, K.-M.; Gao, H.-Y.; Liu, F.-S.; Pan, J.; Guo, L.-H.; Zai, S.-B.; Wu, Q. *Catal. Lett.* **2009**, *131*, 566-573.
- (53) Dupuis, C.; Adiey, K.; Charrault, L.; Michelet, V. *Tetrahedron Lett.* **2001**, *42*, 6523-6526.

- (54) Shaughnessy, K. H.; Booth, R. S. *Org. Lett.* **2001**, *3*, 2757-2759.
- (55) Snelders, D. J. M.; Kreiter, R.; Firet, J. J.; Koten, G. van; Klein Gebbink, R. J. M. *Adv. Synth. Cat.* **2008**, *350*, 262-266.
- (56) Snelders, D. J. M.; Koten, G. van; Klein Gebbink, R. J. M. *J. Am. Chem. Soc.* **2009**, *131*, 11407-11416.
- (57) Sirieix, J.; Oßberger, M.; Betzemeier, B.; Knochel, P. *Synlett.* **2000**, *2000*, 1613-1615.
- (58) Zhao, D.; Fei, Z.; Geldbach, T. J.; Scopelliti, R.; Dyson, P. J. *J. Am. Chem. Soc.* **2004**, *126*, 15876-15882.
- (59) Xiao, J.-C.; Twamley, B.; Shreeve, J. M. *Org. Lett.* **2004**, *6*, 3845-3847.
- (60) Xiao, J.-C.; Shreeve, J. M. *J. Org. Chem.* **2005**, *70*, 3072-3078.
- (61) Wang, R.; Xiao, J.-C.; Twamley, B.; Shreeve, J. M. *Org. Biomol. Chem.* **2007**, *5*, 671-678.
- (62) Wang, R.; Piekarski, M. M.; Shreeve, J. M. *Org. Biomol. Chem.* **2006**, *4*, 1878-1886.
- (63) Cai, Y. Q.; Lu, Y.; Liu, Y.; Gao, G. H. *Catal. Lett.* **2007**, *119*, 154-158.
- (64) Bäuerlein, P. S.; Fairlamb, I. J. S.; Jarvis, A. G.; Lee, A. F.; Müller, C.; Slattery, J. M.; Thatcher, R. J.; Vogt, D.; Whitwood, A. C. *Chem. Comm.* **2009**, 5734-7536.
- (65) Liao, M.-chun; Duan, X.-hua; Liang, Y.-min *Tetrahedron Lett.* **2005**, *46*, 3469-3472.
- (66) Gavrilov, K. N.; Lyubimov, S. E.; Bondarev, O. G.; Maksimova, M. G.; Zheglov, S. V.; Petrovskii, P. V.; Davankov, V. A.; Reetz, M. T. *Adv. Synth. Cat.* **2007**, *349*, 609-616.
- (67) Xiao, J.-C.; Ye, C.; Shreeve, J. M. *Org. Lett.* **2005**, *7*, 1963-1965.
- (68) Doherty, S.; Goodrich, P.; Hardacre, C.; Knight, J. G.; Nguyen, M. T.; Pârvulescu, V. I.; Paun, C. *Adv. Synth. Cat.* **2007**, *349*, 951-963.
- (69) Doherty, S.; Goodrich, P.; Hardacre, C.; Pârvulescu, V.; Paun, C. *Adv. Synth. Cat.* **2008**, *350*, 295-302.
- (70) Wu, X.-E.; Ma, L.; Ding, M.-X.; Gao, L.-X. *Chem. Lett.* **2005**, *34*, 312-313.
- (71) Geldbach, T. J.; Dyson, P. J. *J. Am. Chem. Soc.* **2004**, *126*, 8114-8115.
- (72) Kawasaki, I.; Tsunoda, K.; Tsuji, T.; Yamaguchi, T.; Shibuta, H.; Uchida, N.; Yamashita, M.; Ohta, S. *Chem. Comm.* **2005**, *2*, 2134-2136.
- (73) Baleizao, C.; Gigante, B.; Garcia, H.; Corma, A. *Tetrahedron.* **2004**, *60*, 10461-10468.
- (74) Gadenne, B.; Hesemann, P.; Moreau, J. J. E. *Tetrahedron Lett.* **2004**, *45*, 8157-8160.
- (75) Gadenne, B.; Hesemann, P.; Moreau, J. *Tetrahedron Asymmetry.* **2005**, *16*, 2001-2006.
- (76) Cole, A. C.; Jensen, J. L.; Ntai, I.; Tran, K. L. T.; Weaver, K. J.; Forbes, D. C.; Davis, J. H. *J. Am. Chem. Soc.* **2002**, *124*, 5962-5963.
- (77) List, B.; Lerner, R. A.; Barbas III, C. F. *J. Am. Chem. Soc.* **2000**, *122*, 2395-2396.
- (78) Miao, W.; Chan, T. H. *Adv. Synth. Cat.* **2006**, *348*, 1711-1718.
- (79) Lombardo, M.; Pasi, F.; Easwar, S.; Trombini, C. *Adv. Synth. Cat.* **2007**, *349*, 2061-2065.
- (80) Siyutkin, D. E.; Kucherenko, A. S.; Struchkova, M. I.; Zlotin, S. G. *Tetrahedron Lett.* **2008**, *49*, 1212-1216.
- (81) Lombardo, M.; Easwar, S.; De Marco, A.; Pasi, F.; Trombini, C. *Org. Biomol. Chem.* **2008**, *6*, 4224-4229.
- (82) Lombardo, M.; Easwar, S.; Pasi, F.; Trombini, C. *Adv. Synth. Cat.* **2009**, *351*, 276-282.
- (83) Luo, S.; Mi, X.; Zhang, L.; Liu, S.; Xu, H.; Cheng, J.-P. *Tetrahedron.* **2007**, *63*, 1923-1930.
- (84) Lombardo, M.; Easwar, S.; Pasi, F.; Trombini, C.; Dhavale, D. D. *Tetrahedron.* **2008**, *64*, 9203-9207.
- (85) Xu, D.; Luo, S.; Yue, H.; Wang, L.; Liu, Y.; Xu, Z. *Synlett.* **2006**, *2006*, 2569-2572.
- (86) Luo, S.; Mi, X.; Zhang, L.; Liu, S.; Xu, H.; Cheng, J.-P. *Angew. Chem. Int. ed.* **2006**, *45*, 3093-3097.
- (87) Ni, B.; Zhang, Q.; Headley, A. D. *Tetrahedron Lett.* **2008**, *49*, 1249-1252.
- (88) Xu, D.-Q.; Wang, B.-T.; Luo, S.-P.; Yue, H.-D.; Wang, L.-P.; Xu, Z.-Y. *Tetrahedron Asymmetry.* **2007**, *18*, 1788-1794.
- (89) Luo, S.; Zhang, L.; Mi, X.; Qiao, Y.; Cheng, J. P. *J. Org. Chem.* **2007**, *72*, 9350-9352.
- (90) Luo, S.; Mi, X.; Liu, S.; Xu, H.; Cheng, J.-P. *Chem. Comm.* **2006**, 3687-3689.
- (91) Yacob, Z.; Shah, J.; Leistner, J.; Liebscher, J. *Synlett.* **2008**, *2008*, 2342-2344.
- (92) Wu, L.-Y.; Yan, Z.-Y.; Xie, Y.-X.; Niu, Y.-N.; Liang, Y.-M. *Tetrahedron Asymmetry.* **2007**, *18*, 2086-2090.
- (93) Ni, B.; Zhang, Q.; Headley, A. D. *Green Chem.* **2007**, *9*, 737-739.
- (94) Zhang, Q.; Ni, B.; Headley, A. D. *Tetrahedron.* **2008**, *64*, 5091-5097.
- (95) Ni, B.; Zhang, Q.; Dhungana, K.; Headley, A. D. *Org. Lett.* **2009**, *11*, 1037-1040.
- (96) Xu, D. Q.; Luo, S. P.; Wang, Y. F.; Xia, A. B.; Yue, H. D.; Wang, L. P.; Xu, Z. Y. *Chem. Comm.* **2007**, 4393-4395.
- (97) Mi, X.; Luo, S.; Cheng, J. P. *J. Org. Chem.* **2005**, *70*, 2338-2341.
- (98) Mi, X.; Luo, S.; Xu, H.; Zhang, L.; Cheng, J.-P. *Tetrahedron.* **2006**, *62*, 2537-2544.
- (99) Wu, X.-E.; Ma, L.; Ding, M.-X.; Gao, L.-X. *Synlett.* **2005**, 607-610.
- (100) Qian, W.; Jin, E.; Bao, W.; Zhang, Y. *Tetrahedron.* **2006**, *62*, 556-562.
- (101) Roy, M.-N.; Poupon, J.-C.; Charette, A. B. *J. Org. Chem.* **2009**, *74*, 8510-8515.

CHAPTER 2: RESULTS AND DISCUSSION

2.1. Enantioselective addition of ZnEt_2 to aldehydes in ILs catalyzed by a recyclable ion-tagged diphenylprolinol.¹

2.1.1. Reaction overview.

The addition of dialkyl zinc (ZnR_2) to carbonyl compounds is a very well studied process and it is often chosen as a benchmark reaction for testing the catalytic performance of new chiral ligands. In absence of a ligand the addition of ZnR_2 to aldehydes or ketones is negligible at room temperature. Indeed a ligand, activates the zinc reagent by coordination and, if chiral, can promote the enantioselective addition to carbonyl compounds. It was demonstrated that, after coordination, the linear ZnR_2 adopts a tetrahedral-type structure, the Zn-C bond is weakened and, subsequently, the nucleophilicity of the zinc species increases (fig.1).²

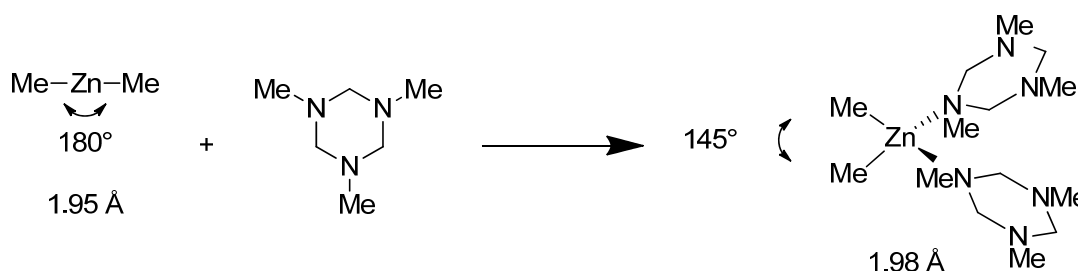


Fig. 1: Effect of ligand coordination on the ZnR_2 species.

Among the number of ligands employed, amino-alcohols, diamines and diols found extensive application.^{3,4} The first example of asymmetric addition of ZnEt_2 to benzaldehyde was reported by Ognuni and Omi using (*S*)-leucinol as chiral ligand (fig.2).⁵

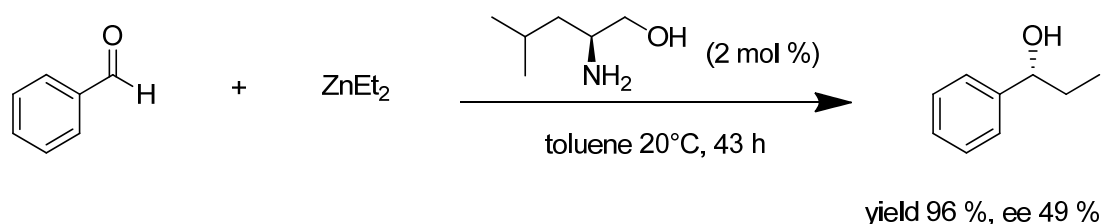


Fig. 2: First example of asymmetric addition of ZnEt_2 to benzaldehyde.

The first addition displaying high level of enantioselectivity was reported by Noyori and co-workers using the (-)-3-*exo*-(dimethylamino)isoborneol, (-)-DAIB, as chiral ligand (fig.3).⁶

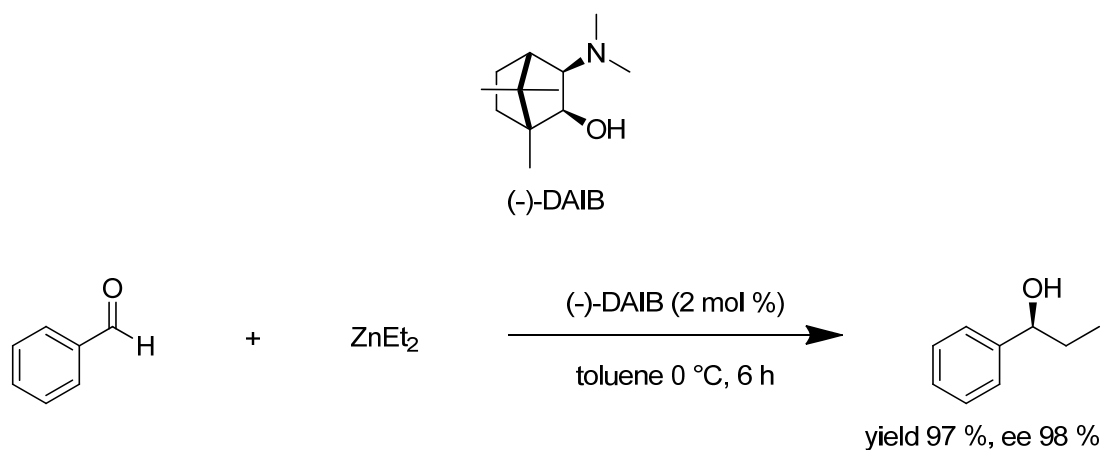


Fig. 3: First example of highly enantioselective addition of ZnEt_2 to benzaldehyde using (-)-DAIB chiral ligand.

Noyori's group also elucidated the mechanism for this reaction (fig.4). The ZnR_2 species, together with the amino-alcohol ligand, formed in the solution several aggregates. In particular when ZnR_2 and ligand were mixed in a 1:1 ratio, no aldehyde alkylation occurred, but a dimeric species were formed which acted as catalyst precursor (**1**). The alkylation proceeds via a dinuclear zinc species containing the DAIB auxiliary, an aldehyde ligand, and three alkyl groups, where it was the bridging alkyl group, rather than the terminal alkyls, that migrates from zinc to the aldehyde (**2**). The alkyl transfer turned out to be the rate determining step for the catalytic cycle.⁷

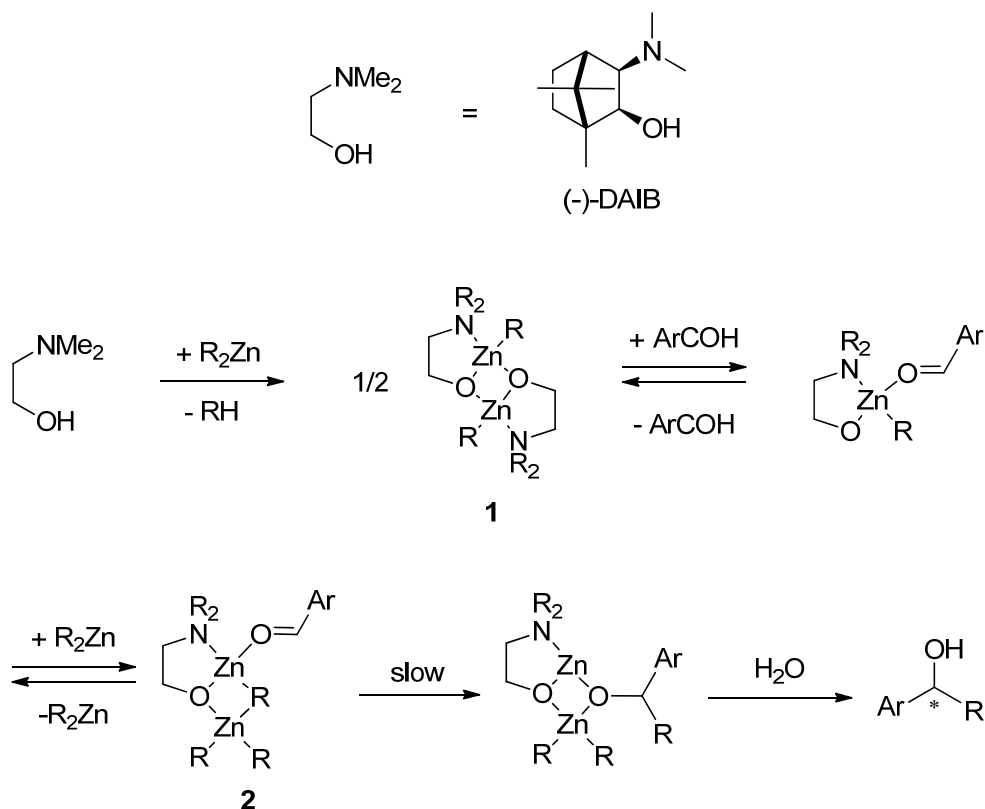


Fig. 4: Simplified version of the mechanism for the ZnR_2 addition to aldehydes, reported by Noyori's group.

The formation of dimeric species in solution led to a strong non-linear effect, since the heterochiral dimer (**3**) was more stable and virtually unreactive, whereas the homochiral dimer (**4a,b**) promptly dissociate to form the active species in presence of excess of ZnR_2 or aldehyde (fig.5).^{7,8}

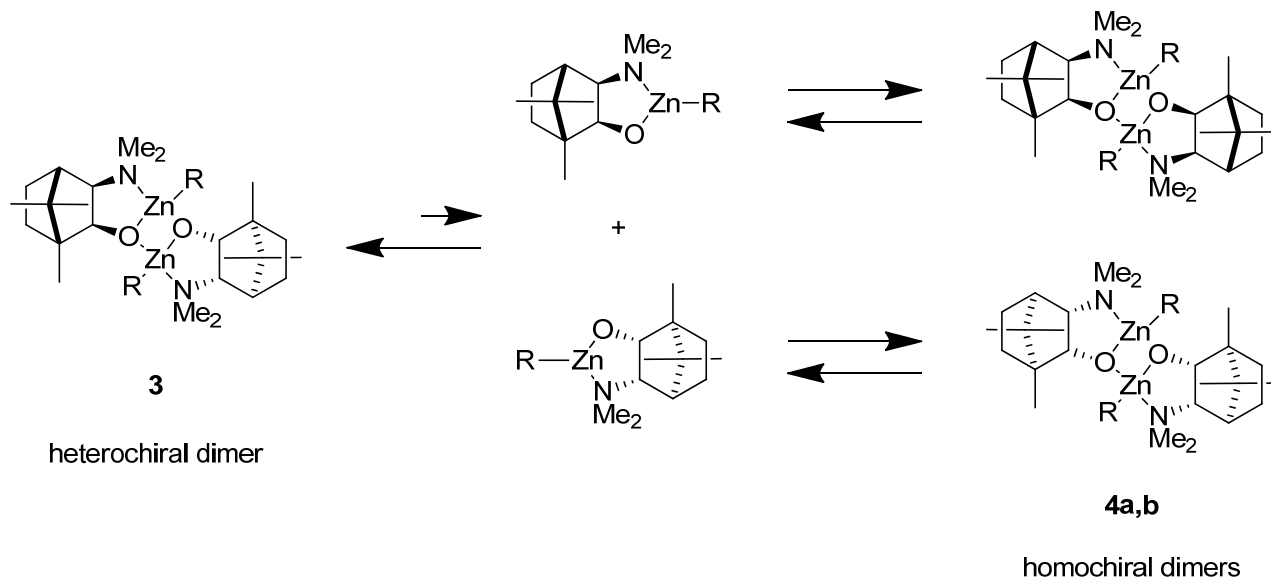


Fig.5: Dimeric species formed in solution with non-enantiopure ligands.

2.1.2 Discussion.

In 2004 Chang and co-workers reported the addition of pure $ZnEt_2$ to various aldehyde in the IL $[bpy][BF_4]$. In contrast with organic solvents, the reaction proceeded quickly and cleanly without the need of any ligand or Lewis acid to activate the addition (fig.6).⁹

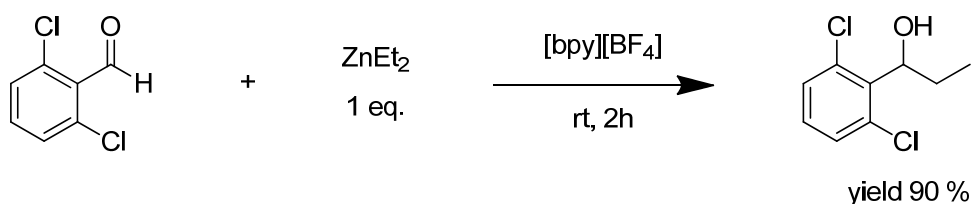


Fig. 6: Addition of $ZnEt_2$ to aldehydes in the IL $[bpy][BF_4]$.

However, when we sought to alkylate benzaldehyde in $[bpy][BF_4]$ using a commercial solution of diethylzinc in *n*-hexane, the reaction was so sluggish that only a negligible amount of alkylation product was recovered after 12h at 20 °C. This observation attracted our attention, since it inspired us to exploit ligand accelerated catalysis (LAC)¹⁰ and to put into play the ionic-tagging strategy to design a recyclable catalysts soluble in ILs. Although ion-tagged catalyst for this reaction had already been reported by Moreau and co-workers (see paragraph 1.3.10.), stoichiometric amount of $Ti(i-PrO)_4$ were required to activate the addition and no IL were tested as solvent. Thus we selected,

from among the plethora of chiral ligands available in the literature, enantiopure *N*-methyl-diphenylprolinol (DPP, **5**) as the reference structure from which to develop new ion-tagged ligands. DPP represented an attractive option, since optically pure DPP is commercially available or can be easily prepared in multigram scale starting from simple L-proline (fig.7).¹¹

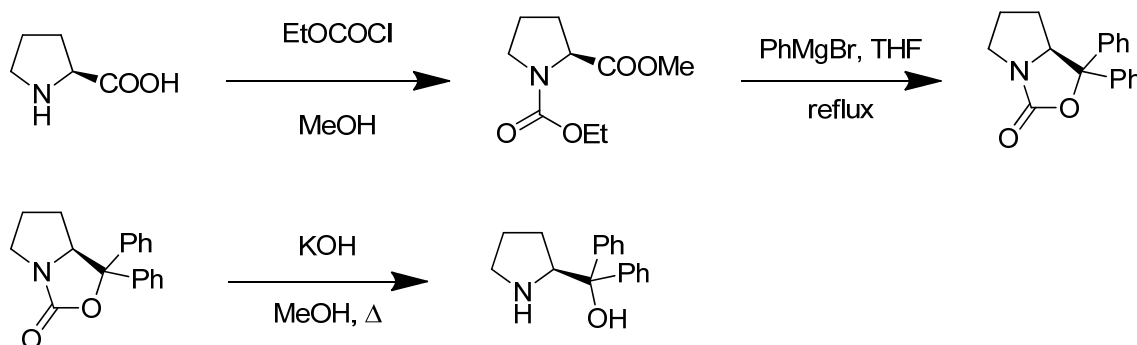


Fig. 7: Synthesis of diphenylprolinol from (*S*)-proline.

Moreover the installation of an ion-tagged chain can be easily achieved by a simple nitrogen alkylation step. We prepared a few ion-tagged tertiary aminoalcohols **8a-c**, by reacting **5** with the alkyl bromides **7a-c** (fig.8). A simple trialkylammonium tag was selected instead of the widely used imidazolium ion, to avoid the possible *N*-heterocyclic carbene formation during reaction with diethylzinc. The choice of NTf_2^- as counter ion was dictated by solubility (very low in water) and stability reasons.

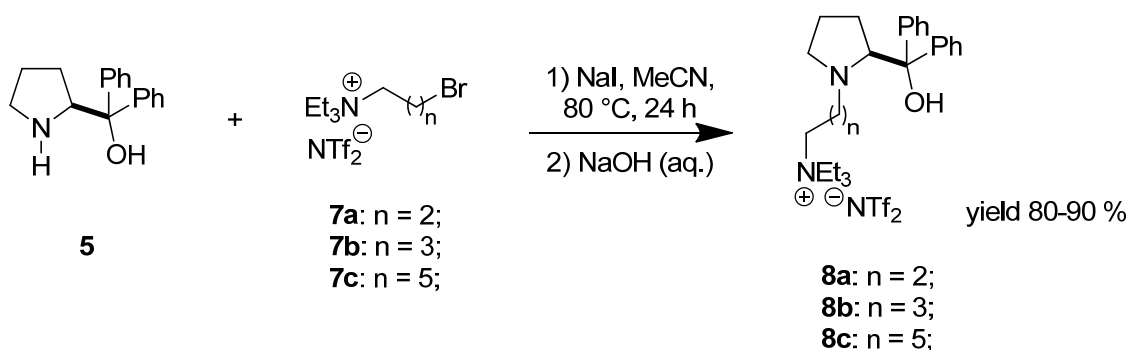


Fig. 8: Synthesis of ion-tagged DFP **8a-c**.

The alkyl bromides **7a-c** were synthesized by alkylation of TEA with an excess amount of the suitable dibromo alkyl, followed by anion metathesis with LiNTf_2 in water (fig.9).

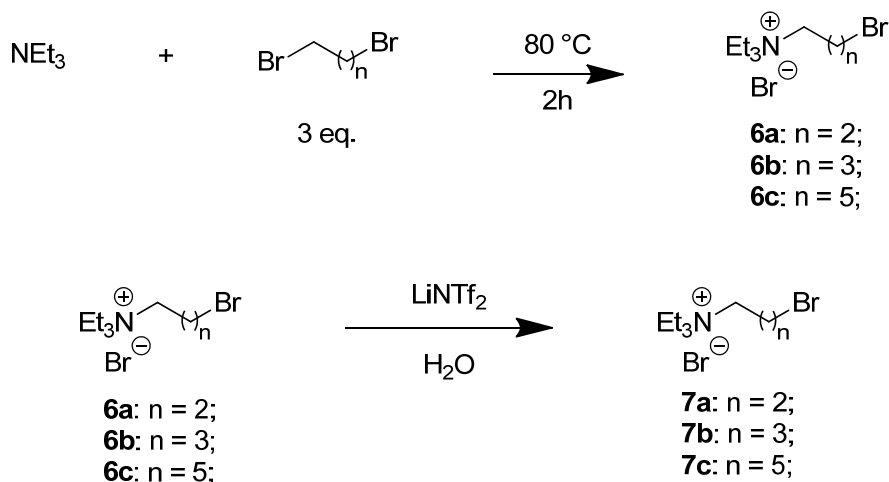
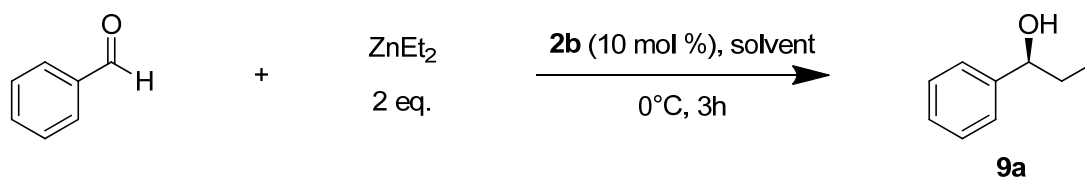


Fig. 9: Synthesis of ionic alkyl bromides **7a-c**.

With ligands **8a-c** in our hands, we started testing the simple addition of ZnEt_2 to benzaldehyde as the benchmark reaction in different ILs using the ligand **8b** (Tab.1).



Entry	Solvent	Yield (%) ^a	ee (%) ^b
1	hexane	90	23
2	[bpy][BF ₄]	92	30
3	[bpy][NTf ₂]	88	69
4	[bmpy][NTf ₂]	92	89
5	[bmpy][OTf]	90	87

(a) Yield of isolated product.

(b) The absolute configuration was assigned by comparison of the optical rotation with that of the known product. The ee was determined by HPLC analysis (chiralcel OD column).

Tab. 1: Effect of the IL on the addition of ZnEt_2 to benzaldehyde catalyzed by ligand **8b**.

We first compared the effect of the IL structure on reactivity and selectivity using 10 mol % of ligand **8b** at 0 °C. Yields were independent of the IL used (88–92 %), while the *ees* were strongly affected by its structure. As a matter of fact, the electrostatic environment associated to the RTIL seems essential for selectivity, since the reaction in *n*-hexane delivered only a 23 %*ee* (Entry1). Using 1-butylpyridinium ILs, the effect of the counter anion on selectivity was apparent, since tetrafluoroborate gave a 30 %*ee* (Entry2), while NTf_2^- ensured a 40 % gain (Entry 3). The best enantioselectivity was achieved by combining the pyrrolidinium cation and NTf_2^- anion (entry 4) or

triflate (entry 5). Since [bmpy][NTf₂] is much more easily synthesized and handled with respect to the corresponding triflate, due to its insolubility in water, it was elected as the solvent of choice in the next study. The effect of the catalyst loading and temperature was then evaluated (Tab.2). When the catalyst loading was decreased to 5 mol %, 80 % isolated yield after 4.5 h at 0 °C was obtained, with identical *ee* with respect to the use of 10 mol % ligand (Entry 1-2). When the reaction was carried out at 20 °C, we recorded a 10 % loss in *ee* (Entry 3), but using the ligand in 20 mol %, a 95 % *ee* and 91 % isolated yield was obtained within 2 h at 20 °C (Entry 4).



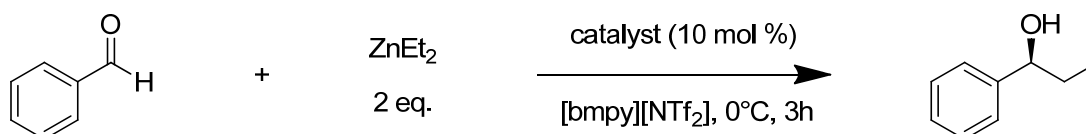
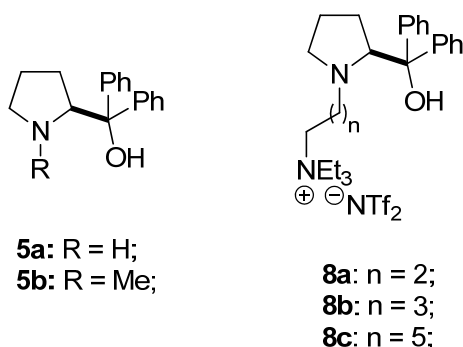
Entry	2b (mol %)	Temperature (°C)	Time (h)	Yield (%) ^a	<i>ee</i> (%) ^b
1	5	0	4.5	80	89
2	10	0	3	92	89
3	10	20	2	85	75
4	20	20	2	91	95

(a) Yield of isolated product.

(b) The absolute configuration was assigned by comparison of the optical rotation with that of the known product. The *ee* was determined by HPLC analysis (chiralcel OD column).

Tab.2: Effect of catalyst loading and temperature on the addition of ZnEt₂ to benzaldehyde catalyzed by ligand **8b**.

Finally the effect of spacer length and of the ion-tag was assessed performing the reaction with ligands of different structures (Tab.3). The length of the alkyl spacer (**8a-c**) did not affect the high yields, but reflected in lower enantioselectivities with respect to the use of **8b** (Entry 1-3). The efficiency of ion-tagged ligands was then compared to that of simple diphenylprolinol (**5a**) and *N*-methyl-diphenylprolinol (**5b**). The former required longer reaction times to ensure a good conversion but with only a 38 % *ee* (Entry 3). The latter was less efficient both in terms of yield and selectivity (Entry 4) with respect to ligand **8b**. Therefore we elected ligand **8b** as the ligand of choice for the reaction, which was carried out in [bmpy][NTf₂] at 0 °C using a commercial solution of ZnEt₂ in *n*-hexane. Using this optimized conditions, we attempted the reaction adding only a slightly excess amount of ZnEt₂ (1.1 equiv), and we were delighted to obtain essentially the same results, both in terms of yield and selectivity (87 %, 90 % *ee*), with respect to the use of a larger excess of the organometallic reagent.



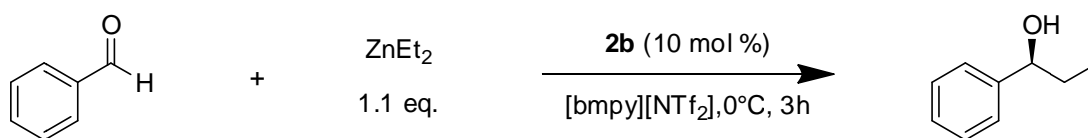
Entry	Catalyst	Time (h)	Yield (%) ^a	ee (%) ^b
1	8a	3	92	72
2	8b	3	92	89
3	8c	3	90	80
4	5a	24	91	38
5	5b	3	75	78

(a) Yield of isolated product.

(b) The absolute configuration was assigned by comparison of the optical rotation with that of the known product. The ee was determined by HPLC analysis (chiralcel OD column).

Tab.3: Effect of ligand structure on the addition of ZnEt₂ to benzaldehyde in the IL [bmpy][NTf₂].

After the protocol optimization we focused on catalyst recycling. This task was efficiently addressed when a very simple work-up was developed to easily remove the inorganic zinc salts formed during the aqueous work-up and to quantitatively recover the alkylation product. In detail, the reaction mixture was quenched with a basic aqueous solution of sodium salt of ethylenediamine tetraacetic acid (EDTA), washed with water and extracted with Et₂O. The ligand-containing IL phase was dried by heating for 2–3 h at 70 °C under reduced pressure (~0.1 mmHg), and eventually reloaded with diethylzinc and the appropriate aldehyde. Results obtained in ten consecutive cycles are reported in Tab.4. An outstanding reproducibility was displayed and no loss of activity and enantioselectivity was apparent up to the tenth cycle, as shown also by the chiral HPLC chromatograms recorded in the ten recycling runs (fig.10).



Run	Yield (%) ^a	ee (%) ^b	Run	Yield (%) ^a	ee (%) ^b
1	96	89	6	96	89
2	94	89	7	98	88
3	95	90	8	95	90
4	98	89	9	98	88
5	96	89	10	96	90

(a) Yield of isolated product.

(b) The absolute configuration was assigned by comparison of the optical rotation with that of the known product. The ee was determined by HPLC analysis (chiralcel OD column).

Tab.4: Recycling experiments.

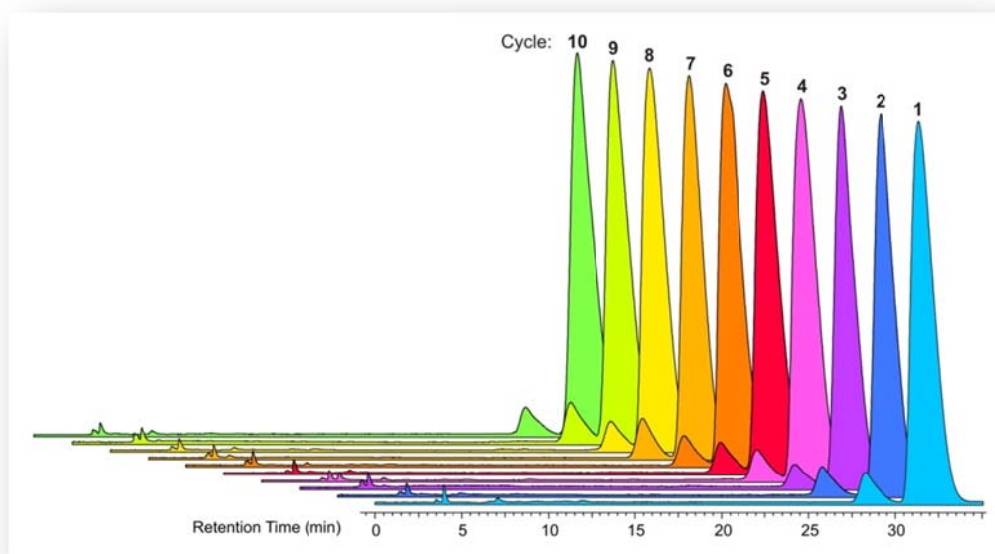
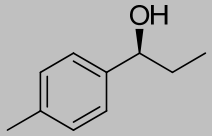
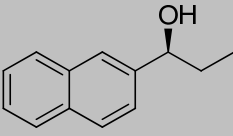
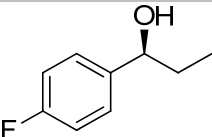
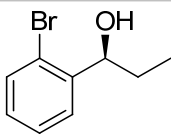
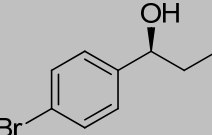
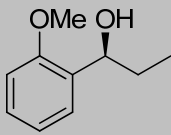
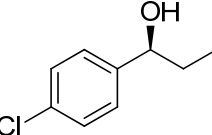
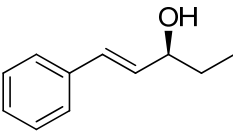
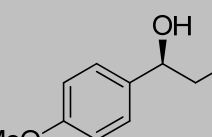
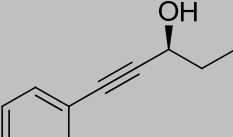
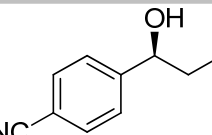
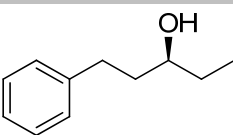


Fig.10: Chiral HPLC chromatograms recorded in the 10 recycling experiments.

Finally, we performed an aldehyde screening to explore the scope of this catalytic system, by applying the same optimized protocol reported for the recycling experiments (Tab.5). Very good yields and enantioselectivities were obtained with aromatic aldehydes substituted in the *para* position with electron-withdrawing or donating groups (Entries 1–7), while 2-substituted aromatic aldehydes (Entries 8, 9), α,β -unsaturated aldehydes (Entries 10, 11) afforded a lower ee, although the yield was still high. Aliphatic aldehydes provided the product with good ee, but with a substantial lower yield (Entry 12).

Entry	Product	Yield (%) ^a	ee (%) ^b	Entry	Product	Yield (%) ^a	ee (%) ^b
1		92	91 ^c	7		99	91 ^e
2		90	92 ^c	8		92	80 ^c
3		92	92 ^d	9		97	66 ^e
4		94	90 ^e	10		90	70 ^e
5		95	92 ^e	11		99	55 ^d
6		98	94 ^f	12		50	85 ^e

(a) Yield of isolated product.

(b) The absolute configuration was assigned by comparison of the optical rotation with that of known product.

(c) Determined by GC analysis (Megadex cyclodextrin chiral column).

(d) Determined by HPLC (chiralcel OJ column).

(e) Determined by HPLC (chiralcel OD column).

(f) Determined by HPLC (chiralpak AD column).

Tab. 5: Scope of the addition reaction.

2.1.3. Conclusion.

In conclusion, we have developed a new procedure for the asymmetric addition of diethylzinc to aryl aldehydes in ILs. Remarkable was the use of only a slight excess of diethylzinc to obtain isolated yields higher than 90 % of alkylation products. Adopting the ionic-tag concept aimed at tailoring ligands capable to provide metal complexes soluble in ILs, we envisaged diphenylprolinol-derived **8b** as a promising candidate to accelerate the asymmetric addition of diethylzinc to aromatic aldehydes. Besides to the operational simplicity and efficiency, the catalytic system was easily recyclable, making the use of 10 mol % loading of **8b** a minor problem.

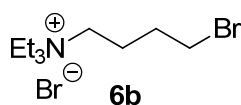
2.1.4. Experimental section.

General information

^1H and ^{13}C NMR were recorded on a Varian Inova 300 and on a Varian Gemini 200; chemical shifts (δ) are reported in ppm relative to TMS. Gas chromatographic analyses were performed with a Agilent 6850 GC-system coupled to a Agilent 5975 mass selective detector ($50 \pm \text{C}$, 2 min \nearrow ! $280 \pm \text{C}$, 10 $\pm \text{C}$ / min \nearrow ! $280 \pm \text{C}$, 10 min). Chiral GC analyses were performed on a HP 5890 II instrument using a chiral Megadex cyclodextrin column (5.25 m). Chiral HPLC studies were carried out on a Hewlett-Packard series 1090 instrument. Optical rotations were measured with a Perkin-Elmer 343 polarimeter. Reactions were monitored by TLC and GC-MS. Flash-chromatography was carried out using Merck silica gel 60 (230-400 mesh particle size). All reagents were commercially available and were used without further purification, unless otherwise stated. Diphenylprolinol was synthesized according to the reported procedure.¹¹ ILs were commercially available or synthesized according to literature procedure (see paragraph 2.2.4 for an example).¹²

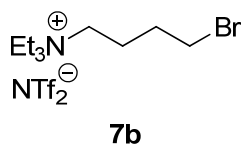
Synthesis of the catalyst 8b.

N,N,N,N-(4-Bromo-butyl)-triethyl-ammonium bromide (6b).



Triethylamine (1.39 mL, 10 mmol) is added to 1,4-dibromoethane (3.58 mL, 30 mmol) and the solution was stirred at 80 °C for 3 h. The resulting suspension was cooled to 0 °C, EtOAc was added and the title product was isolated by filtration as a white solid in 96% yield (3.05 g, 9.26 mmol). ^1H NMR (300 MHz, CDCl_3): δ = 1.40 (t, J = 7.2 Hz, 9 H), 1.86-1.99 (m, 2 H), 1.99-2.11 (m, 2 H), 3.43-3.60 (m, 10 H). ^{13}C NMR (75 MHz, CDCl_3): δ = 7.1, 19.4, 27.9, 32.0, 52.4, 55.4. $[\text{M}^+]$: 237.

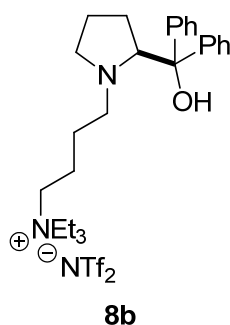
N,N,N,N-(4-Bromo-butyl)-triethyl-ammonium bis(trifluoromethylsulfonyl)imide (7b).



Lithium bis(trifluoromethylsulfonyl)imide (0.6 g, 2.1 mmol) was added at rt to a solution of *N,N,N,N*-(4-bromo-butyl)-triethyl-ammonium bromide (0.63 g, 2 mmol) in water (1 mL) and the solution was stirred at rt for 12 h. The title product was extracted with CH_2Cl_2 (2×5 mL) and the combined organic phases were washed with water until a negative AgNO_3 test was obtained. The

organic phase was dried (Na_2SO_4) and evaporated at reduced pressure to give 0.96 g (1.86 mmol, 93%) of the title compound as a clear dense oil. ^1H NMR (300 MHz, CDCl_3): δ = 1.36 (t, J = 7.3 Hz, 9 H), 1.79 - 1.93 (m, 2 H), 1.93- 2.05 (m, 2 H), 3.16 - 3.25 (m, 2 H), 3.31 (q, J = 7.5 Hz, 6 H), 3.50 (t, 2 H); ^{13}C -NMR (75 MHz, CDCl_3): δ = 6.9, 19.7, 28.4, 31.9, 52.7, 55.7, 117.4, 121.6; $[\text{M}^+]$: 237.

Ligand 8b.



N,N,N,N-(4-bromo-butyl)-triethyl-ammonium bis(trifluoromethylsulfonyl)imide (0.78 g, 1.5 mmol) was added to a solution of diphenylprolinol (0.4 g, 1.58 mmol) and NaI (0.224 g, 1.5 mmol) in CH_3CN and the solution was stirred at 80 °C for 24 h. After cooling to rt the organic solvent was evaporated at reduced pressure, CH_2Cl_2 is added (5 mL) and the organic layer was washed with NaOH water solution (1 mL, 2 M). The organic phase was dried (Na_2SO_4) and evaporated at reduced pressure to afford a dense oil that was further purified by flash-chromatography on silica eluting with $\text{CH}_2\text{Cl}_2/\text{MeOH}$ 95:5. The title product was obtained as a clear dense oil in 98% yield (1.01 g, 1.47 mmol). $[\alpha]_{20}^{\text{D}}$ (c = 4.7, CHCl_3) = +8.9; ^1H NMR (300 MHz, CDCl_3): δ 0.96 - 1.12 (m, 1 H), 1.22 (t, J = 7.1 Hz, 9 H), 1.26 - 1.46 (m, 3 H), 1.60 - 1.77 (m, 3 H), 1.93 (ddd, J = 16.8, 8.6, 4.6 Hz, 1 H), 2.23 (ddd, J = 12.2, 7.8, 4.4 Hz, 1 H), 2.36 - 2.47 (m, 2 H), 2.62 - 2.81 (m, 2 H), 3.11 (q, J = 7.2 Hz, 6 H), 3.16 - 3.29 (m, 1 H), 3.90 (dd, J = 9.0, 4.2 Hz, 1 H), 7.10 - 7.19 (m, 2 H), 7.28 (t, J = 7.7 Hz, 3 H), 7.52 (dd, J = 8.3, 1.2 Hz, 2 H), 7.64 (dd, J = 8.3, 1.2 Hz, 2 H); ^{13}C -NMR (75 MHz, CDCl_3): δ = 7.3, 19.0, 24.5, 25.3, 29.2, 52.9, 55.4, 55.5, 56.7, 71.2, 77.9, 117.7, 122.0, 125.5, 125.9, 126.2, 126.4, 128.0, 128.1, 146.0, 148.4; $[\text{M}^+]$: 409.

Typical procedure for the addition of ZnEt_2 benzaldehyde.

A solution of diethylzinc (1.0 M in hexanes, 0.6 mL, 0.6 mmol) was added to a solution of catalyst **8b** (35.9 mg, 0.05 mmol) in $[\text{bmpy}][\text{NTf}_2]$ (1.0 mL) and the mixture was stirred at room temperature for 5 min. Benzaldehyde (0.051 mL, 0.5 mmol) was then added at 0 °C and the solution

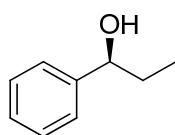
was stirred until thin-layer chromatography (TLC) showed the disappearance of the starting aldehyde (3 h). The reaction was quenched with a few drops of water and the resulting mixture was directly charged on the top of a silica gel column diluting with CH₂Cl₂. Elution with 9:1 cyclohexane/AcOEt afforded the alcohol adduct (0.067 g, 98 %) as a colorless oil. The ee value (90 %) was determined by high-performance liquid chromatography (HPLC) by using a Chiralcel OD column: *n*-hexane/*i*PrOH 99:1, 0.8 mL min⁻¹, *t*_R=28.4 min (minor), 31.2 min (major). The absolute *S* configuration was assigned by comparison of the optical rotation with that of the known product: $[\alpha]_{20}^D = -42.0$ (*c* = 1.9 in CHCl₃), 90 % ee; literature value: (*S*) isomer, : $[\alpha]_{20}^D = -45.6$ (*c* = 5.55 in CHCl₃), 95.4 % ee.¹³

Recycling procedure.

The experimental procedure for the recycling of catalyst and IL was the same as described above, except the reaction was quenched by adding a solution of EDTA disodium salt (0.57 g, 1.5 mmol) and NaOH (0,08 g, 2 mmol) in H₂O (2 mL). The aqueous phase was removed with a syringe and the IL was further washed with H₂O (2×2 mL). The alcohol adduct was then extracted with Et₂O (5×2 mL), and the combined organic phases were dried (Na₂SO₄) and evaporated under reduced pressure. The title product was purified by flash-chromatography on silica eluting with cyclohexane/EtOAc 9:1. The IL was dried by heating at 70 °C under vacuum (~0.1 mmHg) for 2–3 h and directly reloaded with the starting reagents.

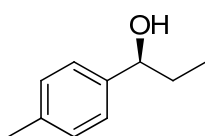
Spectroscopic data for compounds 9a-m.

1-phenylpropan-1-ol (9a).



¹H NMR (300 MHz, CDCl₃): δ 0.88 (t, *J*=7.55 Hz, 3H), 1.65-1.81 (m, 2H), 1.96 (bs, 1H), 4.53 (t, *J*=6.79 Hz, 1H), 7.21-7.30 (m, 5H). ¹³C NMR (300 MHz, CDCl₃): δ 10.1, 31.78, 75.9, 125.9, 127.4, 128.3, 144.5. HPLC: OD column: *n*-hexane/*i*PrOH 99:1, 0.8 mL min⁻¹, *t*_R = 28.4 min (*R*), 31.2 min (*S*).

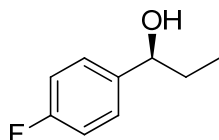
1-(p-tolyl)propanol (9b).



¹H NMR (200 MHz, CDCl₃) δ 0.91 (t, *J* = 7.5 Hz, 3H), 1.68-1.89 (m, 2H), 2.36 (s, 3H), 4.54 (t, *J* =

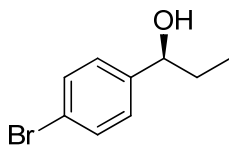
6.9 Hz, 1H), 7.16 (d, $J = 7.8$ Hz, 2H), 7.23 (d, $J = 7.8$ Hz, 2H). ^{13}C NMR (50 MHz, CDCl_3) δ 10.1, 21.0, 31.7, 75.8, 125.9, 129.0, 137.0, 141.6. $[\text{M}^+]$: 150. GC chiral column Megadex-5, 120 $^\circ\text{C}$, 3.13 min^{-1} , $t_{\text{R}} = 11.2 \text{ min}$ (*R*), 13.0 min (*S*).

1-(4-fluorophenyl)propanol (9c).



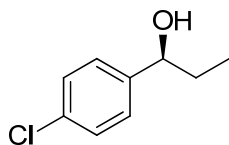
^1H NMR (200 MHz, CDCl_3) δ 0.89 (t, $J = 7.5$ Hz, 3H), 1.66-1.84 (m, 2H), 2.18 (br, 1H), 4.56 (t, $J = 6.9$ Hz, 1H), 6.99-7.06 (m, 2H), 7.27-7.31 (m, 2H). ^{13}C NMR (50 MHz, CDCl_3) δ 10.0, 31.9, 75.3, 115.1 (d, $J = 21$ Hz), 127.5 (d, $J = 8$ Hz), 140.2, 162. (d, $J = 243$ Hz). $[\text{M}^+]$ 154. GC chiral column Megadex-5, 110 $^\circ\text{C}$, 3.13 min^{-1} , $t_{\text{R}} = 15.1 \text{ min}$ (*R*), 17.8 min (*S*).

1-(4-Bromophenyl)-1-propanol (9d).



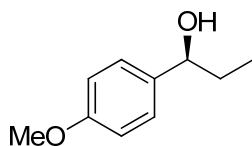
^1H NMR (300 MHz, CDCl_3): δ 0.89 (t, $J = 7.2$ Hz, 3H), 1.68–1.79 (m, 2H), 2.03 (bs, 1H), 4.55 (t, $J = 6.4$ Hz, 1H), 7.20 (d, $J = 8.4$ Hz, 2H), 7.45 (d, $J = 8.4$ Hz, 2H); ^{13}C NMR (75 MHz, CDCl_3): δ 9.9, 31.8, 75.2, 121.1, 127.6, 131.3, 143.4. $[\text{M}^+]$: 214, 216. . HPLC: OJ column: *n*-hexane/*i*PrOH 97:3, 0.8 mL min^{-1} , $t_{\text{R}} = 17.9 \text{ min}$ (*S*), 19.4 min (*R*).

1-(4-Chlorophenyl)propanol (9e).



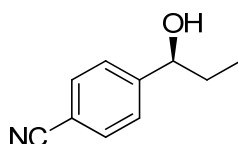
^1H NMR (300 MHz, CDCl_3) δ 0.89 (t, $J = 7.5$ Hz, 3H), 1.62-1.85 (m, 2H), 2.04 (br, 1H), 4.56 (t, $J = 6.9$ Hz, 1H), 7.25 (d, $J = 8.7$ Hz, 2H), 7.31 (d, $J = 8.7$ Hz, 2H). ^{13}C NMR (75 MHz, CDCl_3) δ 10.0, 32.0, 75.3, 127.4, 128.6, 133.1, 143.1. $[\text{M}^+]$: 170. . HPLC: OD column: *n*-hexane/*i*PrOH 99:1, 0.8 mL min^{-1} , $t_{\text{R}} = 25.2 \text{ min}$ (*S*), 27.6 min (*R*).

1-(4-methoxyphenyl)propanol (9f).



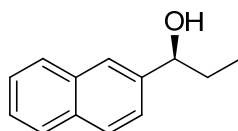
^1H NMR (300 MHz, CDCl_3) δ 0.90 (t, $J = 7.5$ Hz, 3H), 1.62-1.84 (m, 2H), 1.80 (br, 1H), 3.78 (s, 3H), 4.49 (t, $J = 6.9$ Hz, 1H), 6.86 (d, $J = 8.4$ Hz, 2H), 7.23 (d, $J = 8.4$ Hz, 2H). ^{13}C NMR (75 MHz, CDCl_3) δ 10.2, 31.7, 55.3, 75.5, 113.8, 127.3, 136.8, 158.9. $[\text{M}^+]$: 166. HPLC: OD column: *n*-hexane/*i*PrOH 99:1, 1.0 mL min^{-1} , $t_{\text{R}} = 35.5$ min (*R*), 42.4 min (*S*).

1-(4-cyanophenyl)propanol (9g).



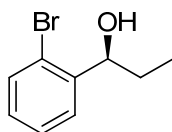
^1H NMR (200 MHz, CDCl_3) δ 0.92 (t, $J = 7.3$ Hz, 3H), 1.70-1.79 (m, 2H), 2.05 (bs, 1H), 4.82 (m, 1H), 7.44 (d, $J = 8.3$ Hz, 2H), 7.61 (d, $J = 8.3$ Hz, 2H). ^{13}C NMR (50 MHz, CDCl_3) δ 9.7, 31.9, 74.8, 110.7, 118.8, 126.5, 132.0, 150.1. $[\text{M}^+]$: 161. HPLC: AD column: *n*-hexane/*i*PrOH 97:3, 0.8 mL min^{-1} , $t_{\text{R}} = 31.6$ min (*R*), 34.2 min (*S*).

1-(2-naphthalenyl)propanol (9h).



^1H NMR (200 MHz, CDCl_3) δ 0.96 (t, $J = 7.5$ Hz, 3H), 1.80-1.96 (m, 2H), 4.71 (m, 1H), 7.45-7.55 (m, 3H), 7.75-7.88 (m, 4H). ^{13}C NMR (50 MHz, CDCl_3) δ 10.2, 31.7, 76.0, 124.2, 124.7, 124.8, 125.7, 126.0, 127.7, 128.0, 132.9, 133.2, 142.0. $[\text{M}^+]$: 186. HPLC: OD column: *n*-hexane/*i*PrOH 95:5, 1.0 mL min^{-1} , $t_{\text{R}} = 15.2$ min (*S*), 17.0 min (*R*).

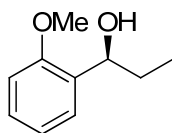
1-(2-Bromophenyl)-1-propanol (9i).



^1H NMR (200 MHz, CDCl_3): δ 0.99 (t, $J = 7.2$ Hz, 3H), 1.64-1.87 (m, 2H), 1.98 (d, $J = 4.0$ Hz, 1H), 4.99 (m, 1H), 7.09-7.13 (m, 1H), 7.30-7.34 (m, 1H), 7.49-7.53 (m, 2H). ^{13}C NMR (50 MHz,

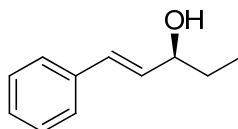
CDCl₃): δ 10.0, 30.4, 74.0, 122.0, 127.3, 127.5, 128.6, 132.5, 143. [M⁺]: 214, 216. GC chiral column Megadex-5, 130 °C, 3.13 min⁻¹, t_R = 22.5 min (*R*), 25.2 min (*S*).

1-(2-methoxyphenyl)propan-1-ol (9j).



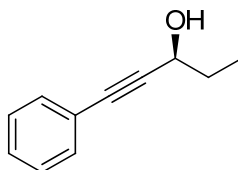
¹H NMR (200 MHz, CDCl₃): δ 0.97 (t, J = 7.4 Hz, 3H), 1.76-1.91 (m, 2H), 2.56 (d, J = 6.2 Hz, 1H), 3.86 (s, 3H), 4.75-4.85 (m, 1H), 6.87-7.00 (m, 2H), 7.22-7.32 (m, 2H). ¹³C NMR (50 MHz, CDCl₃): 10.3, 30.1, 55.1, 72.2, 110.4, 120.6, 126.9, 128.1, 132.3, 156.5. [M⁺]: 166. HPLC: OD column: *n*-hexane/*i*PrOH 98:2, 1.0 mL min⁻¹, t_R = 16.9 min (*S*), 18.8 min (*R*).

trans-1-phenylpent-1-en-3-ol (9k).



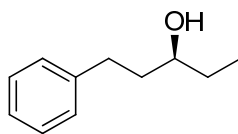
¹H NMR (300 MHz, CDCl₃) δ 0.99 (t, J = 7.5 Hz, 3H), 1.63-1.74 (m, 2H), 1.68 (bs, 1H), 4.27 (m, 1H), 6.24 (dd, J = 15.9, 6.6 Hz, 1H), 6.59 (d, J = 15.9 Hz, 1H), 7.23-7.45 (m, 5H). ¹³C NMR (75 MHz, CDCl₃) δ 9.8, 30.2, 74.4, 126.4, 127.6, 128.6, 130.4, 132.3, 136.7. [M⁺]: 162. HPLC: OD column: *n*-hexane/*i*PrOH 95:5, 1.0 mL min⁻¹, t_R = 11.9 min (*R*), 19.6 min (*S*).

1-phenyl-1-pentyn-3-ol (9l).



¹H NMR (300 MHz, CDCl₃) δ 1.08 (t, J = 7.5 Hz, 3H), 1.76-1.88 (m, 2H), 4.56 (t, J = 6.9 Hz, 1H), 7.28-7.34 (m, 3H), 7.37-7.48 (m, 2H). ¹³C NMR (75 MHz, CDCl₃) δ 9.4, 30.9, 64.1, 84.8, 90.0, 122.6, 128.2, 128.3, 131.6. [M⁺]: 160. HPLC: OJ column: *n*-hexane/*i*PrOH 90:10, 1.0 mL min⁻¹, t_R = 7.9 min (*R*), 9.2 min (*S*).

3-phenylpentanol (9m).



^1H NMR (300 MHz, CDCl_3) δ 0.95 (t, $J = 7.5$ Hz, 3H), 1.42 (bs, 1H), 1.47-1.58 (m, 2H), 1.71-1.86 (m, 2H), 2.67-2.81 (m, 2H), 3.57 (m, 1H), 7.17-7.33 (m, 5H). ^{13}C NMR (75 MHz, CDCl_3) δ 9.8, 30.3, 32.0, 38.6, 72.6, 103.9, 125.7, 128.4, 142.2. $[\text{M}^+]$: 164. HPLC: OD column: *n*-hexane/*i*PrOH 90:10, 1.0 mL min^{-1} , $t_{\text{R}} = 6.1 \text{ min (R)}$, 7.7 min (S) .

Bibliography

- (1) Lombardo, M.; Chiarucci, M.; Trombini, C. *Chem. Eur. J.* **2008**, *14*, 11288-11291.
- (2) Hursthouse, M. B.; Motewaili, M.; O'Brien, P.; Walsh, J. R.; Jones, A. C. *J. Mater. Chem.* **1991**, *1*, 139-140.
- (3) Soai, K.; Niwa, S. *Chem. Rev.* **1992**, *92*, 833-856.
- (4) Pu, L.; Yu, H. B. *Chem. Rev.* **2001**, *101*, 757-824.
- (5) Oguni, N.; Omi, T. *Tetrahedron Lett.* **1984**, *25*, 2823-2824.
- (6) Kitamura, M.; Suga, S.; Kawai, K.; Noyori, R. *J. Am. Chem. Soc.* **1986**, *108*, 6071-6072.
- (7) Kitamura, M.; Okada, S.; Suga, S.; Noyori, R. *J. Am. Chem. Soc.* **1989**, *111*, 4028-4036.
- (8) Oguni, N.; Matsuda, Y.; Kaneko, T. *J. Am. Chem. Soc.* **1988**, *110*, 7877-7878.
- (9) Law, M. C.; Wong, K.-Y.; Chan, T. H. *Green Chem.* **2004**, *6*, 241-244.
- (10) Berrisford D. J.; Bolm C.; Sharpless, K. B.; *Angew. Chem. Int. Ed.* **1995**, *34*, 1059 - 1070.
- (11) Kanth J. V. B.; Periasamy M.; *Tetrahedron* **1993**, *49*, 5127 -5132.
- (12) Earle, M. J.; Gordon, C. M.; Plechkova, N. V.; Seddon K. R.; Welton, T.; *Anal. Chem.*, **2007**, *79*, 758-764.
- (13) Kitamura M.; Oka H.; Suga S.; Noyori R; *Org. Synth.* **2002**, *79*, 139 - 142.

2.2. A recyclable triethylammonium ion-tagged diphenylphosphine palladium complex for the Suzuki–Miyaura reaction in ionic liquids.¹

2.2.1. Reaction overview.

The Pd catalyzed cross-coupling (CC) is a seminal process for the formation of new C-C bond. The extreme usefulness and widespread application of this reactions are witnessed by the recent Nobel Prize in Chemistry (2010), that was awarded jointly to Richard F. Heck, Ei-ichi Negishi and Akira Suzuki “for palladium-catalyzed cross couplings in organic synthesis”.² Perhaps the most widely used among these reactions is the Suzuki-Miyaura (SM) coupling, which is the CC of various organoboron compounds with organic electrophiles, mainly aryl and vinyl halides and triflates.³ One of the most useful application of the SM reaction is the challenging formation of new aryl-aryl bonds, exploiting the reaction of arylboronic acids and aryl halides (fig.1).

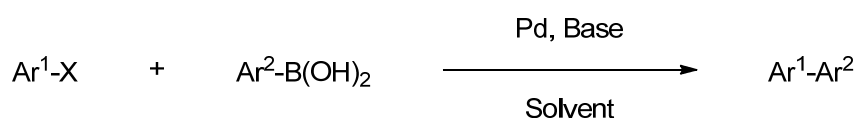


Fig.1: General scheme of SM reaction between aryl halides and arylboronic acids to form biaryl compounds.

This reaction presents many advantages over the other Pd CC protocols: boronic acids are readily available, nontoxic, air- and water-stable. They react under mild conditions and are amenable to a variety of reaction conditions, including the use of aqueous solvents. The inorganic boron byproducts can be easily removed after the reaction. Most important of all, the coupling proceeds with high regio- and stereoselectivity, it is little affected by steric hindrance and tolerates the presence of many functional groups.³ Major limitations of this methodology are the low reactivity of aryl chloride, the possibility of boronic acid homocoupling if oxygen is not carefully excluded from the reaction environment, and the mandatory use of a base, which can give rise to side reaction if base-sensitive materials are present.⁴ The mechanism for the SM reaction is analogous to the catalytic cycle for the other Pd CC reactions (fig.2). The first step is the oxidative addition of the aryl halide to the Pd(0) to form a Pd(II) complex. The boronic acid alone is not capable of transmetalation, but the nucleophilicity of the aryl group is increased by the formation of an “ate” complex, formed by reaction of the boronic acid with the base. The boronate so formed gives rise to transmetalation with the Pd(II) complex to form a biaryl-Pd complex, which regenerates the Pd(0) catalyst after reductive elimination of the biaryl product. The SM coupling can be carried out with a number of different Pd precatalysts because spontaneous reduction of Pd(II) complexes takes place in the reaction conditions to form the active Pd(0) species.

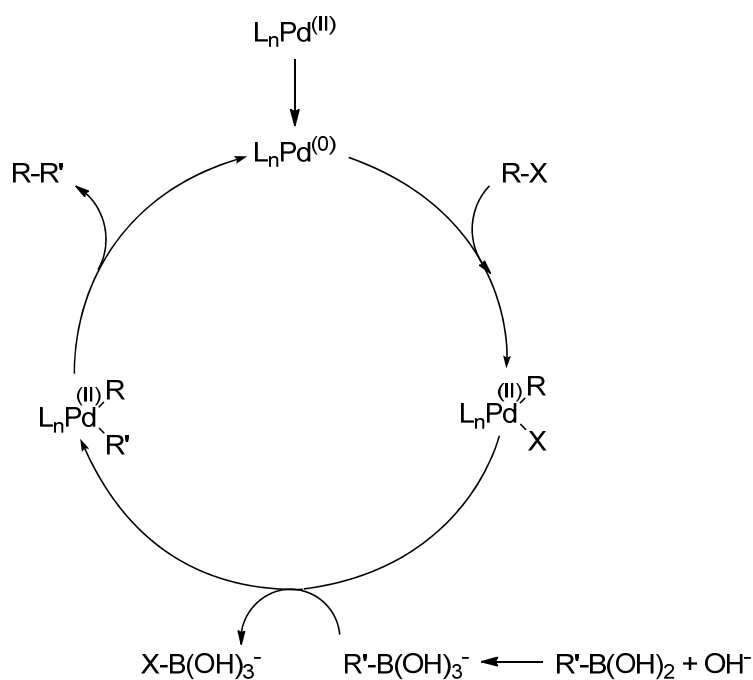


Fig. 2: Mechanism for the SM coupling.

Other than Pd source, a great variety of solvents and bases can be employed successfully in the SM coupling, so that a large number of different conditions can be exploited in order to obtain the best performance for each specific substrate. Many ligands can be chosen in order to modulate the metal reactivity and to increase the catalyst stability. Phosphines and *N*-heterocyclic carbenes (NHCs) are among the most widely employed. Sterically hindered, electron rich ligands increase the reactivity, favoring the formation of a highly nucleophilic, mono-coordinated Pd complex which smoothly undergoes oxidative addition. Despite the tolerance of a broad range of functional groups and reaction conditions, the cost of Pd and environmental regulations urge to develop procedures which minimize metal loading and leaching. Catalyst recyclability and metal leaching issues can be addressed in two ways. The first one involves metal immobilization on a solid support, a strategy that not only reduces product contamination but also allows the use of inherently less wasteful flow-through technologies.⁵ The second approach makes use of extremely low loadings of metal.⁶ The active form of Pd is considered to be a mononuclear Pd(0) entity which originates from the precatalyst. However, on heating, the mononuclear Pd(0) species tends to cluster and, eventually, to precipitate as inactive Pd black, unless highly diluted conditions are used. Pd nanoparticles (NPs) proved to be an active catalyst for Pd CC, but they must be synthesized in presence of a stabilizing agent preventing their aggregation.⁷ As we reported in paragraph 1.3.6., Dyson and co-workers demonstrated that ILs tailored with a metal coordinating group are capable of NPs stabilization *via* coordination and electrostatic effect.⁸

2.2.2. Discussion.

Intrigued by the ability of the coordinating ILs to effectively stabilize the Pd NPs we designed the ion-tagged diphenylphosphine **1** as a potential Pd ligand (Fig.3). Unlike Dyson's group, we did not use the coordinating IL **1** as a solvent for the reaction, but only as Pd ligand to prepare the complex **2** (fig.3).

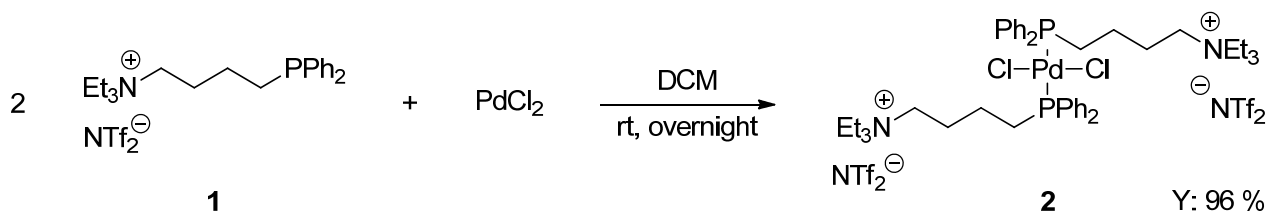


Fig. 3: Synthesis of the ion-tagged Pd pre-catalyst **2**.

Due to the ionic nature of **2** we envisaged that it might be successfully immobilized onto an IL. In order to prevent the formation of Pd-carbene complexes imidazolium based ILs were avoided. We instead focused our attention on the thermoregulated biphasic system consisting of [bmpy][NTf₂] and water. This system was heterogeneous at 25 °C but, when heated at 65 °C, it became a single phase, where the SM reaction could be carried out in a homogeneous fashion. Eventually, upon cooling the mixture to rt, the system turned heterogeneous again. This interesting behavior allowed us to perform the reaction in homogeneous condition and to recover easily the ionic phase at the end of the reaction. The product was extracted with an apolar solvent (pentane), which did not dissolve the IL, and the inorganic salts were removed by extraction with water, given that at room temperature water and [bmpy][NTf₂] formed two immiscible phases. The synthesis of the ligand **1** was carried out according to the scheme reported in fig.4.

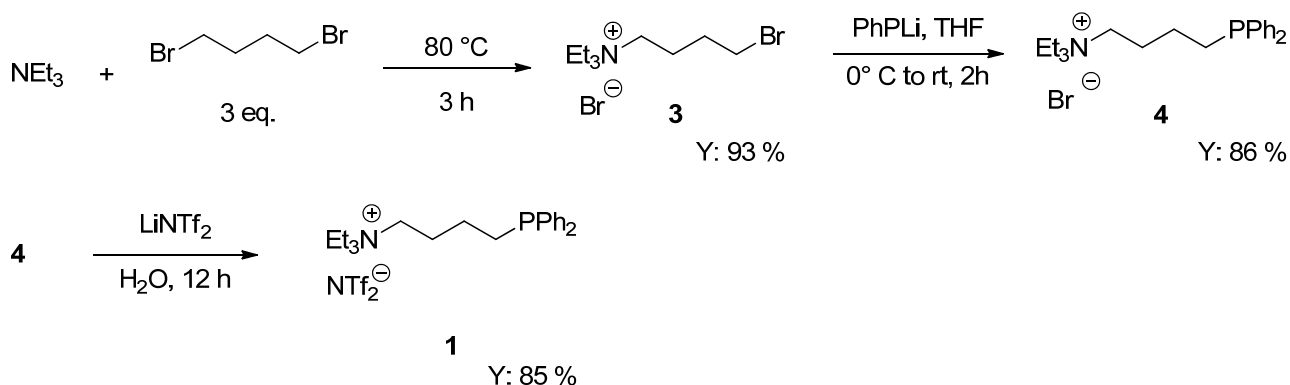
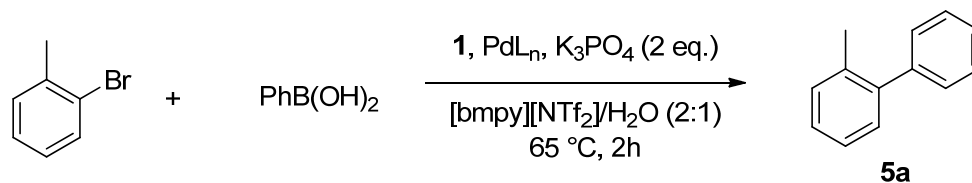


Fig. 4: Synthesis of the ion-tagged phosphine **1**.

4-Bromobutyl-triethyl-ammonium bromide (**3**) was prepared by alkylation of TEA with excess amount of 1,4-dibromobutane. **3** was then submitted to reaction with Ph₂PLi to yield the phosphine **4** which, after anion metathesis with LiNTf₂, afforded the desired ligand **1**. With ligand **1** in our

hands, and using the above described system [bmpy][NTf₂]/H₂O as solvent, we started to study the CC of *o*-bromotoluene and phenyl boronic acid as benchmark reaction. First of all the effect of the Pd source was evaluated (Tab.1).

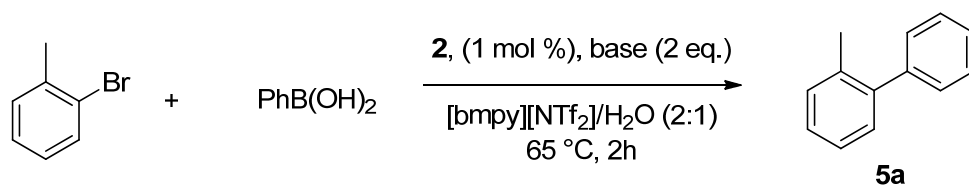


Entry	PdL _n (mol %)	1 (mol %)	Yield (%) ^a
1	Pd ₂ (dba) ₃	2	-
2	Pd(OAc) ₂	2	79
3	PdCl ₂	2	92
4	PdCl ₂	1	60
5	PdCl ₂	3	-

(a) Isolated yields after purification by flash-chromatography on silica.

Tab. 8: Effect of Pd source and metal/ligand ratio.

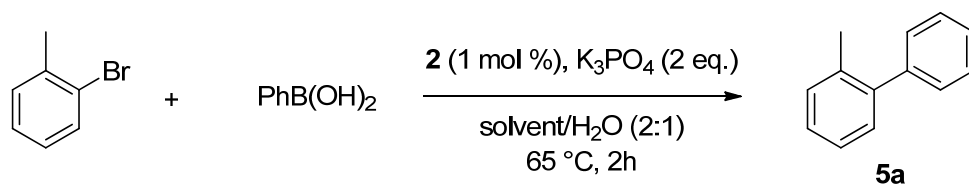
The catalytically active species was efficiently stabilized using a 1 : 2 Pd/ligand ratio, since the formation of Pd black, even after prolonged heating at 65 °C, was never observed. While Pd₂(dba)₃ failed to afford the desired product (Entry 1), PdCl₂ revealed itself as a better source of Pd than Pd(OAc)₂ (Entry 2 and 3). By changing the metal/ligand ratio to 1 : 1, the formation of Pd black was rapidly observed and the yield dropped significantly (Entry 4). Using a 1 : 3 palladium/ligand ratio did not result in formation of Pd black, but the catalytic system became totally inactive (Entry 5). These results are in good agreement with the observation that the active catalyst in many palladium mediated transformations is a monoligated species derived from the initial loss of a phosphine ligand from the precatalyst.⁹ PdCl₂ and the ligand could be directly mixed in 1 : 2 ratio in the reaction flask. However essentially the same results were obtained using the preformed L₂PdCl₂ complex **2**. Thus we continued the optimization study using the preformed complex **2**, since it was more practical to handle than the free ligand **1**. In Tab.2 the results obtained with different inorganic bases are reported. Yields strongly depended on the base used, K₃PO₄ being more effective as a base than K₂CO₃ and Na₂CO₃ (Entries 1–3). This order of reactivity could be possibly ascribed to the greater solubility of K₃PO₄ in H₂O. Using these preliminary optimized conditions, we tested several organic solvents and ILs (Tab.3).



Entry	Base	Yield (%)
1	Na ₂ CO ₃	57
2	K ₂ CO ₃	79
3	K ₃ PO ₄	94

(a) Isolated yields after purification by flash-chromatography on silica.

Tab. 2: Effect of the base.



Entry	Solvent	Yield (%) ^a
1	THF	-
2	CH ₃ CN	12
3	[mC ₁ CNpy][NTf ₂] ^b	-
4	[P(6,6,6,14)][Cl] ^c	-
5	[bmpy][OTf]	39
6	[bmpy][NTf ₂]	93
7	[bmim][NTf ₂]	87

(a) Isolated yields after purification by flash-chromatography on silica.

(b) 1-Cyanomethyl-pyridinium bis(trifluoromethylsulfonyl) imide.

(c) Trihexyl-tetradecyl-phosphonium chloride.

Tab. 3: Effect of the solvent.

At 65 °C the reaction mixture is a single-phase homogeneous system, even in the case of ILs insoluble in water (Entries 3,6,7). THF and CH₃CN afforded disappointing results (Entry 1 and 2). While the complex **2** was only sparingly soluble in THF, it dissolved completely in CH₃CN. In both cases, however, formation of Pd black was observed after heating the reaction mixture at 65 °C. The reactivity of the catalytic system was completely suppressed if a nitrile-functionalized IL (Entry 3) or an IL with a coordinating counter anion (Entry 4) were used. Using 1-butyl-1-methylpyrrolidinium ILs, the effect of the counter anion on the reactivity was apparent (Entry 5 and 6), with NTf₂ giving much better results than triflate. When the 1-butyl-3-methyl-imidazolium cation

was used (Entry 7), a slightly lower yield was obtained. From these results, [bmpy][NTf₂] was selected as the solvent of choice, also considering, as stated above, that imidazolium-based ILs could produce mixed phosphine/NHC complexes. Moreover, NTf₂, chosen as the anion of both the catalyst and the IL, confers them the lowest solubility in H₂O and in pentane, a property necessary to separate biaryls and water soluble co-products from the catalyst-containing IL phase. The effect of the temperature on the catalytic system under the optimized conditions of (Tab.3, Entry 6) was reported in Fig.5. To obtain good conversion in short reaction times a temperature above 40 °C was needed, while the product was formed very slowly at room temperature (25 °C).

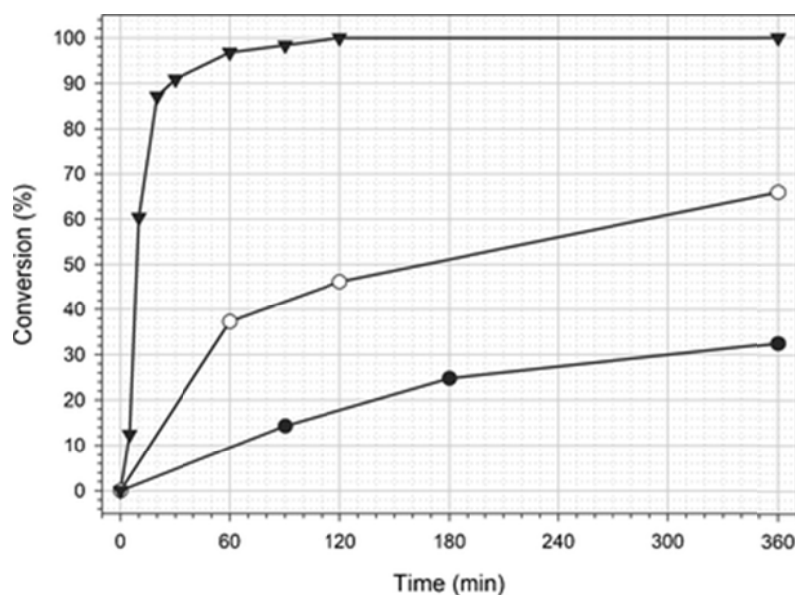


Fig. 5: Effect of the temperature conversion. ▼: 65 °C; ○: 40 °C; ●: 25 °C.

Finally, we tested different aryl electrophiles with boronic acids and, surprisingly, the order of reactivity was ArBr > ArI ≫ ArOTf, while ArCl were not reactive under the reaction conditions tested (fig.6). Initial slopes in Fig. 6 suggested the presence of an induction effect, particularly for aryl triflates and iodides. Since the aromatic electrophile was added pure as the last reagent to the reaction mixture, the induction time observed reflects, in our opinion, a slow mass transfer rate of the aryl triflate or halide in this viscous reaction medium. In order to evaluate the possible effect of anion exchange with [bmpy][NTf₂] on reaction rates, we performed a series of experiments using the same optimized conditions, but adding 1 equivalent of different potassium salts to the reaction mixtures. The results obtained are reported in Fig. 7.

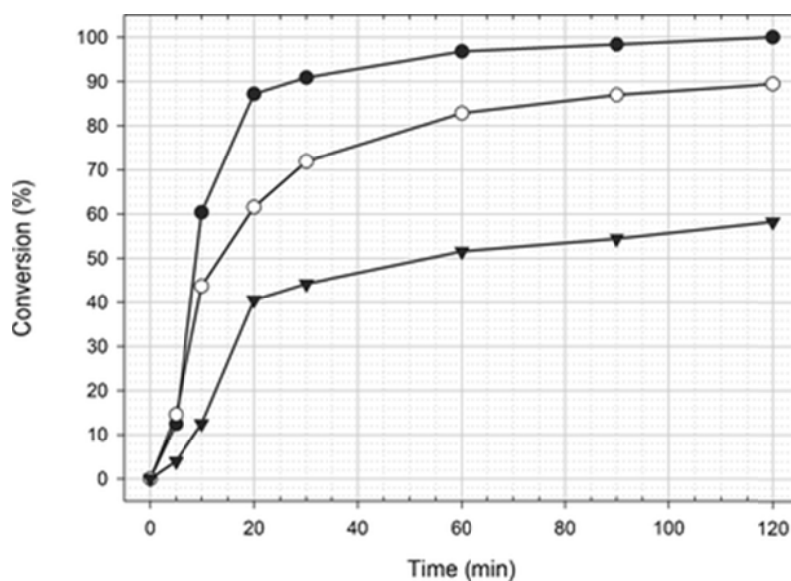


Fig. 6: Comparison of reactivity among aryl bromide (●), iodides (○) and triflates (▼).

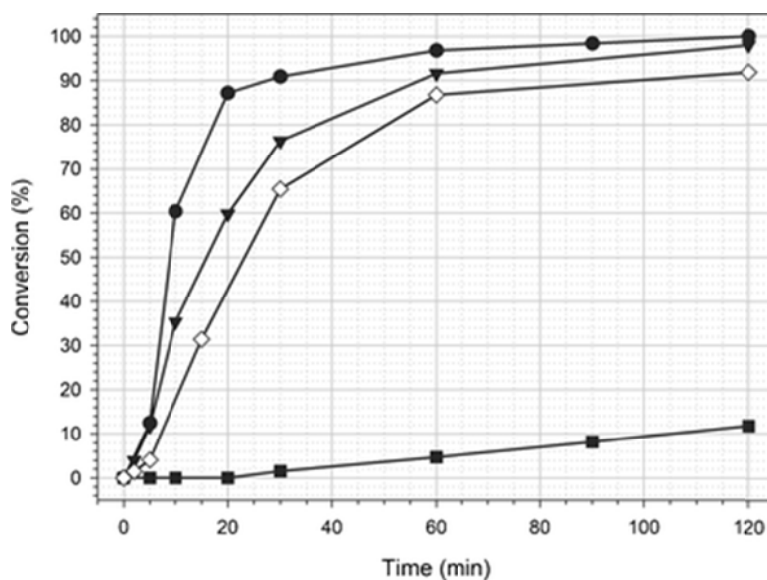
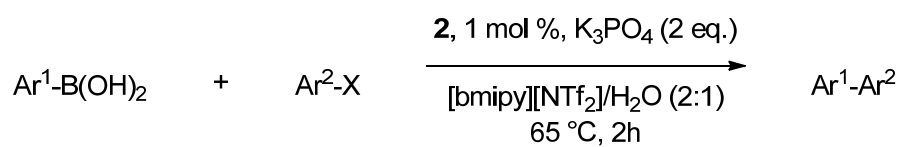
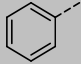
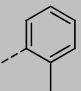
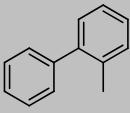
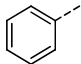
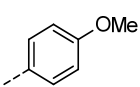
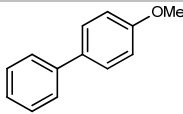
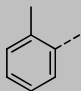
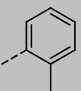
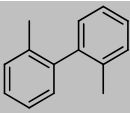
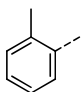
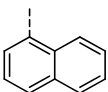
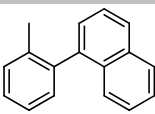
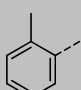
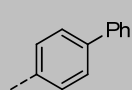
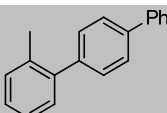
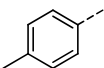
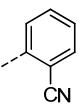
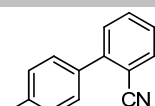
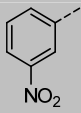
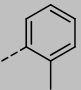
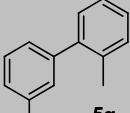
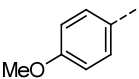
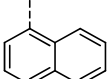
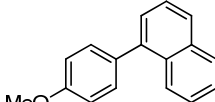
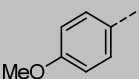
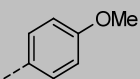
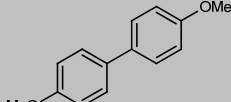
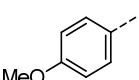
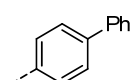
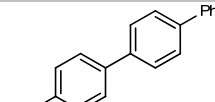


Fig. 79: Comparison of reaction rates without adding salts (●); by adding 1 eq. of KBr (▼); 1 eq. of KOTf (◇), 1 eq. of KI (■).

The addition of 1 eq. of KI considerably reduced the reaction rate, while a much smaller effect was observed in the case of KBr. Thus, the lower reactivity of aryl iodides with respect to bromides could be explained by considering that the corresponding potassium halide salts were formed during the course of the reaction. Conversely, the decrease of reaction rate due to the addition of 1 eq. of KOTf cannot alone explain the much lower reactivity of triflates. Moreover, no trace of [bmpy][OTf] deriving from anion exchange was apparent by NMR analyses of the ionic liquid after the reaction work-up. On the basis of these observations, a reference protocol was derived based on the use of 1 mol % of Pd in the form of L_2PdCl_2 complex **2**, which was applied to a number of aryl bromide/aryl boronic acid pairs in [bmpy][NTf₂] as the solvent at 65 °C for 2 h, as outlined in Tab.4.



Entry	Ar ¹	Ar ²	Product	Yield (%) ^a
1			 5a	92
2			 5b	89
3			 5c	89
4			 5d	99
5			 5e	99
6			 5f	97
7			 5g	86
8			 5h	98
9			 5i	93
10			 5j	84

Entry	Ar ¹	Ar ²	Product	Yield (%) ^a
11				89
12				92

(a) Isolated yields after purification by flash-chromatography on silica.

Tab. 9: Scope of the SM coupling using catalyst **2**.

Good to excellent results were confirmed for aryl bromides and boronic acids containing electron-withdrawing or electron-donating groups and reactivity was not depressed even if two *ortho* substituents were present (Entry 3). Particularly interesting the reaction of *o*-bromobenzonitrile and *p*-methyl phenylboronic acid (Entry 6), which afforded 97 % of a coupled product which is a known intermediate for the synthesis of angiotensin II receptor antagonists.¹⁰ The time dependence study of the reaction conversions showed that the highest rates were recorded at the beginning of the reaction, in contrast to other catalytic Pd systems in ILs, which present induction periods.¹¹ Irrespective of the true identity of the catalyst, a point of strength of this reaction protocol was the catalyst recyclability, which was ensured by the strong interaction between the ligand **1** and the IL, both being quaternary ammonium ions. Fig.8 shows the results of six consecutive cycles carried out under the optimized conditions reported in Tab.4 (Entry 1), and no significant change in the catalytic activity and the reaction rates were observed.

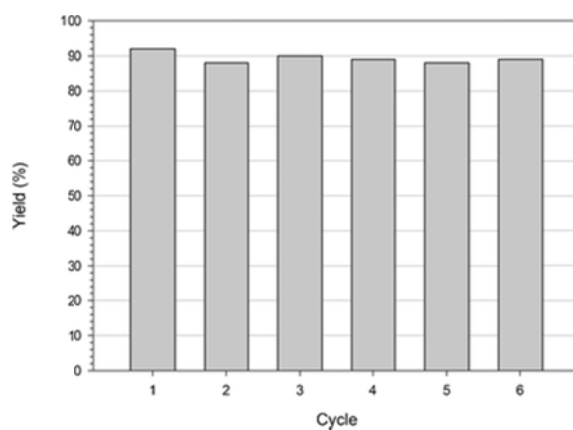
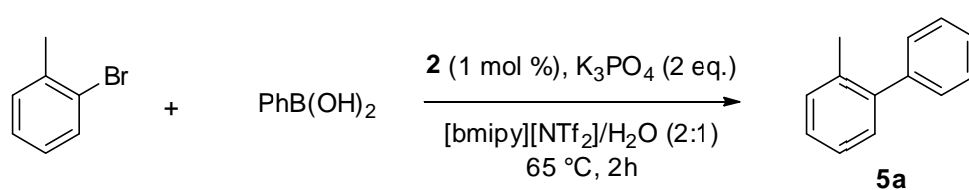


Fig.8: Results of six consecutive runs for the SM coupling adopting the optimized conditions.

The procedure for the recycle of the ionic phase containing the catalyst is reported in fig.9.

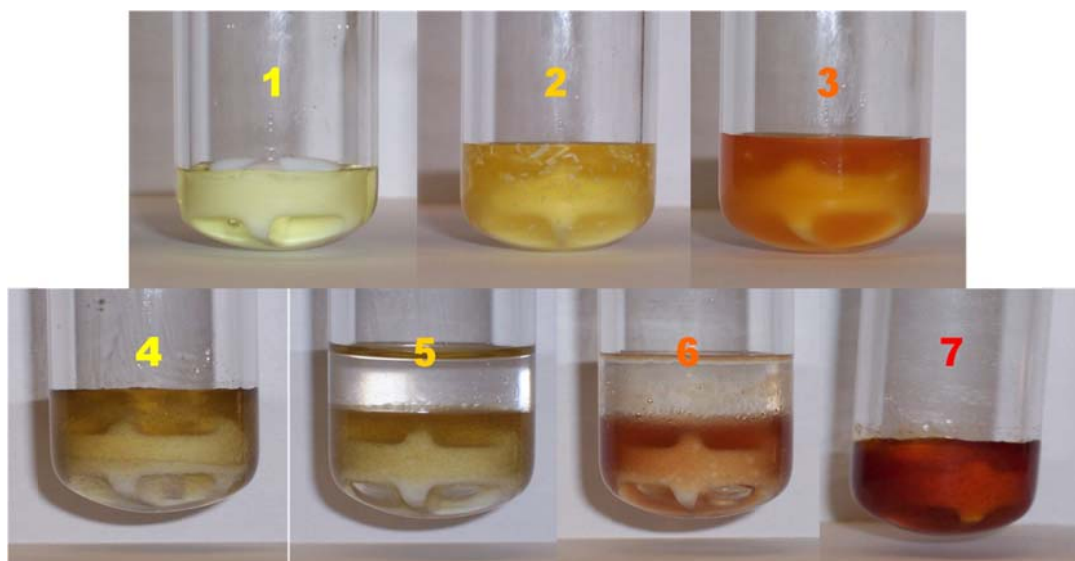
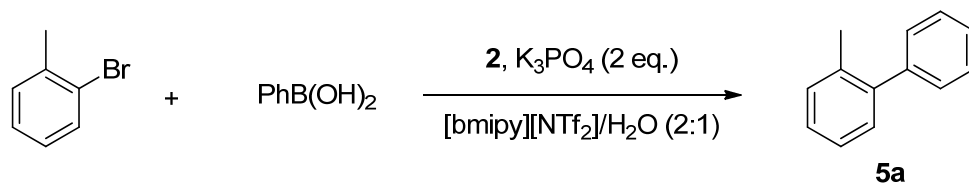


Fig. 80: Procedure for the recycle of the ionic phase containing the Pd catalyst: **1.** Dissolution of catalyst **2** in [bmpy][NTf₂]. **2.** Addition of boronic acid, base and water. **3.** Heating and addition of aryl bromide. **4.** End of reaction: aqueous phase rich in salts was at the bottom of the reaction vessel. **5.** Extraction of the product with pentane. **6.** Washing of the ionic phase with water. **7.** Ionic phase after drying.

Catalyst **2** was dissolved in [bmpy][NTf₂], then boronic acid, base and water were added (Fig.9, 1 and 2). After heating and aryl bromide addition the reaction mixture turned orange and homogeneous (Fig.9, 3). At the end of the reaction the aqueous and the ionic phases became immiscible again (Fig.9, 4). The product was extracted with pentane (Fig.9, 5) and the ionic phase was washed with water to remove the inorganic by-products (Fig.9, 6). Finally, after drying under vacuum (~ 1 mmHg), the ionic phase could be employed in the following run (Fig.9, 7) as no precipitation of Pd black occurred. To demonstrate that the ionic ligand **1** was the true stabilizer of the Pd catalyst the reaction was carried out in the optimized condition using PPh₃ instead of **1** as ligand for PdCl₂. In this condition product yield was lower than 30 % and extensive precipitation of Pd black occurred. Lowering the Pd loading is a further way to check catalyst activity. The benchmark reaction between *o*-bromotoluene and phenyl boronic acid was carried out using two different catalyst loadings, 0.1 and 0.01 mol % of Pd, respectively (Tab.5). The first reaction, run for 6 h at 65 °C, gave an 81% yield, with a TON of 810 and a TOF of 135 h⁻¹ (Entry 1). In the second reaction, after 1.5 h at 95 °C, a 78% yield was recorded, corresponding to a TON of 7800 and a TOF of 5200 h⁻¹ (Entry 2). The high affinity of the catalyst for the ionic phase was further witnessed by the low metal leaching recorded. Preliminary analyses of Pd contents in the organic phase extracts by atomic-absorption spectroscopy (AAS), showed that <10 ppb of the metal was released from the IL into the product during recycling.



Entry	2 (mol %)	Temperature (°C)	Time (h)	Yield (%) ^a	TON	TOF (h ⁻¹)
1	0.1	65	6	81	810	135
2	0.01	95	1.5	78	7800	5200

(a) Isolated yields after purification by flash-chromatography on silica.

Tab. 5: Reaction carried out with low Pd loading.

2.2.3. Synthesis of tetracene derivatives by Suzuki-Miyaura coupling in ionic liquids.¹²

With this efficient protocol for the reaction of Suzuki in our hands, we decide to further expand the scope of the reaction, facing more challenging substrates. Thus we exploited our protocol for the synthesis of tetracene (TC), derivatives. Tetracene, pentacene and their derivatives are among the most studied molecular organic semiconductors due to their high charge mobility.¹³ Some TC derivatives, like 5,6,11,12-tetraphenyltetracene (rubrene) or 5,11-dichlorotetracene, show very high charge mobilities. Indeed, rubrene represents the state of the art in this field, showing exceptional charge carrier mobility values of up to 20 cm²/V s (fig.10).¹⁴

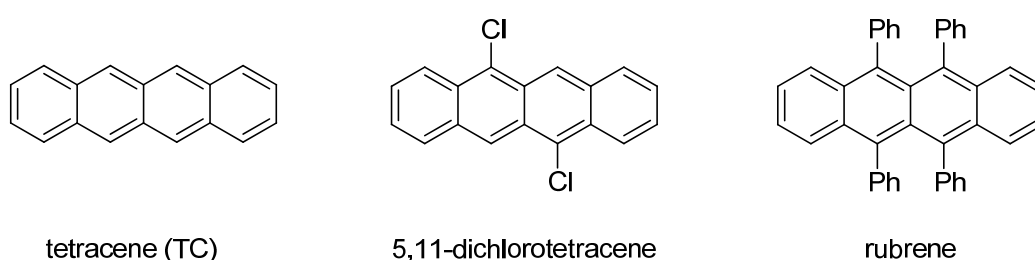


Fig. 10: Tetracene and some of its derivatives displaying interesting electronic properties.

Therefore the “decoration” of TC core in order to modulate its physical properties, is a topic of great practical interest, aimed at the synthesis of new organic materials potentially suitable for optoelectronic applications. Although CC procedures look very attractive for the derivatization of these polycyclic aromatic substrates, this strategy was only rarely employed successfully. Main problem concerns the low reactivity of TC (and similar molecules) in the CC reactions, mainly due to the high steric hindrance of these substrates (especially in the position 5 and 11). Moreover

molecules with such an extended π -system often suffer of poor solubility in many organic solvents generally employed in Pd CC reactions. On the other side, the traditional synthesis of acenes derivatives based on multistep aryl-lithium addition to naphthacendiones, followed by Diels-Alder reactions, displays often low yields and lack of generality, setting a limit to the preparation of a wide spectrum of new derivatives.¹⁵

5,11-dibromotetracene (**6**) could be selectively achieved, after recrystallization, by electrophilic bromination of TC in $\text{CHCl}_3 - \text{DMF}$ (Fig.11).¹⁶

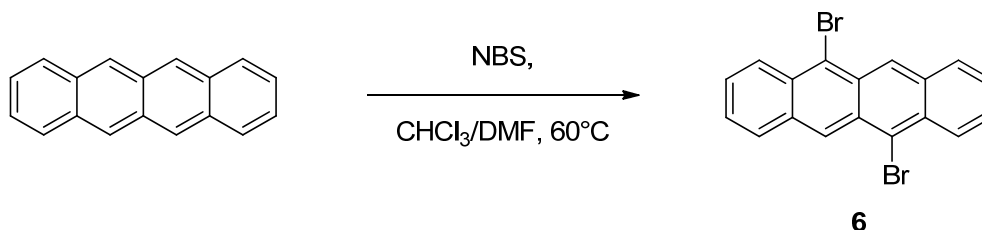


Fig. 11: Synthesis of 5,11-dibromotetracene **6**.

Due to the high reactivity displayed by aryl bromides in the condition developed for SM coupling, we attempted the coupling of **6** with phenylboronic acid, although the classic Suzuki protocol in water /toluene with $\text{Pd}(\text{PPh}_3)_4$ as catalyst had resulted ineffective. We were delighted to observe that, although compound **6** did not dissolved completely in the IL $[\text{bmpy}][\text{NTf}_2]$, the reaction took place smoothly affording the desired product in a few hours with high yield (Fig.12). Formation of the disubstituted product was accompanied by the formation of a characteristic bright-yellow fluorescent spot on the TLC, while the color of the reaction turned from deep red to yellow.

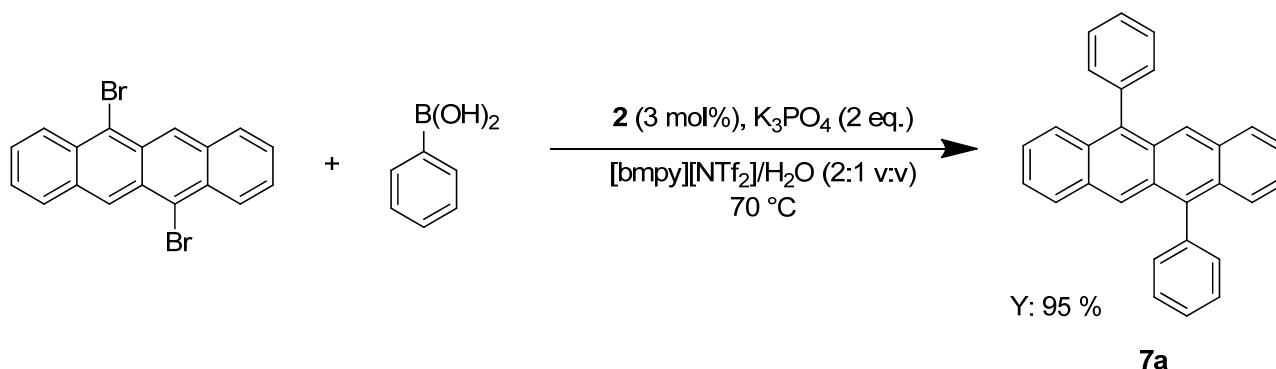
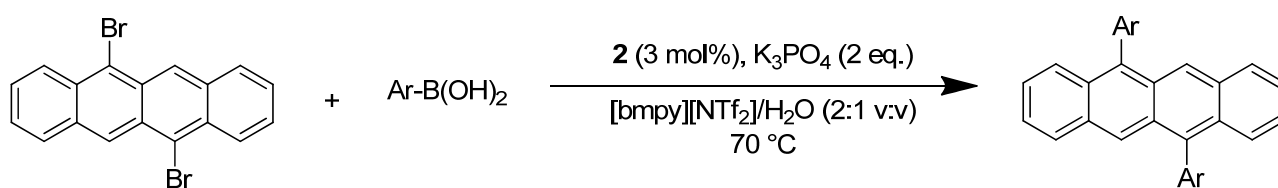


Fig.12: Synthesis of 5,11-diphenyltetracene with SM coupling in ILs.

Adopting the same procedure we prepared the TC derivatives **7b-d** bearing different aryl substituents (Tab.6). As shown in the table derivatives with phenyl (Entry 1), *p*-methoxyphenyl (Entry 2), biphenyl (Entry 3) and 2-naphthyl (Entry 3) substituents were achieved in high yield and adopting condition.



Entry ^a	Product	Time (h)	Yield (%) ^b
1	 7a	2	97
2	 7b	2	94
3	 7c	2	93
4	 7d	7	85

(a) Reaction condition: catalyst (3 mol %), [bmpy][NTf₂] (0.5 ml), arylboronic acid (3 eq.), K₃PO₄ (4 eq.), degassed water (0.25 ml), **6** (0.065 mmol, 1 eq.), 65-70 °C.

(b) Isolated product after flash-chromatography.

Tab. 6: 5,11-diaryltetracene derivatives (**7a-d**) prepared by SM coupling in ILs.

Unfortunately no product was obtained, even after prolonged heating, with heteroaromatic boronic acids, like 2-thiophenboronic acid or 4-pyridineboronic acid. Therefore, in order to expand the scope of the method we attempted the synthesis of the 5,11-pinacol boronate derivative of TC (**8**), that we speculated could be a suitable substrate for the SM coupling. The boronate **8** was prepared starting from 5,11- dibromotetracene **6** and bis(pinacolato)diboron in DMF with Pd(OAc)₂ as catalyst (Fig.13).¹⁷

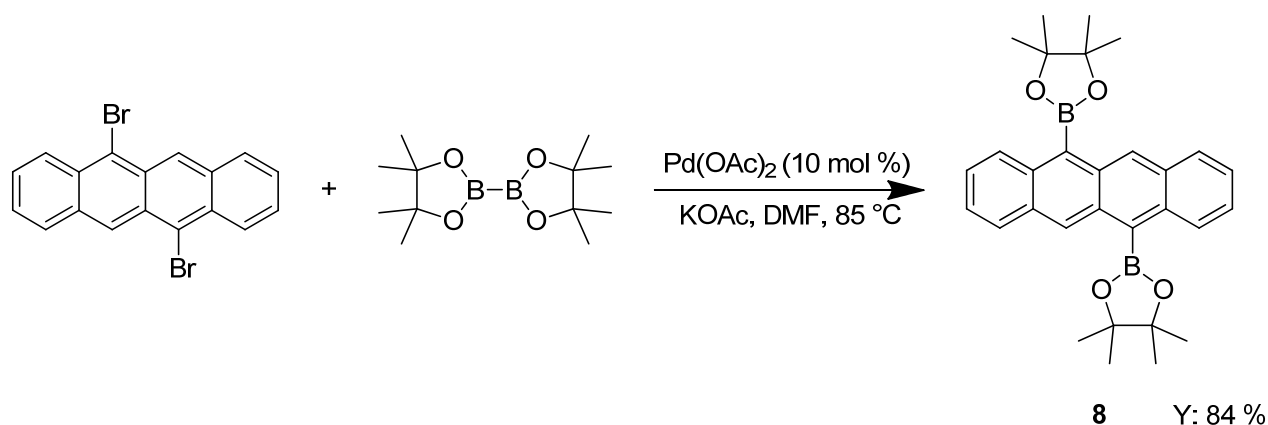
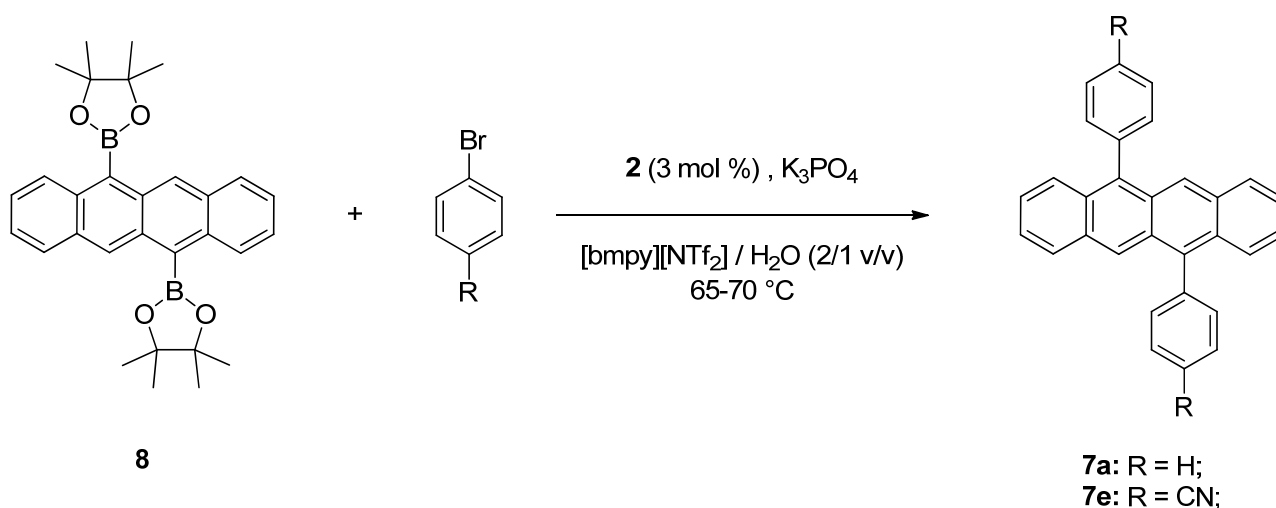


Fig.13: Synthesis of 5,11-pinacol boronate derivative of TC (**8**).

Although the desired product was obtained in high yield, the results in the CC reaction were disappointing (Tab.7).



Entry ^a	Product	Time (h)	Yield (%) ^b
1	7a	2.5	38
2	7e	4	37

(a) *Reaction condition:* catalyst **2** (3 mol %), [bmpy][NTf₂] (0.5 ml), arylboronic ester **8** (0.044 mmol, 1 eq.), K₃PO₄ (4 eq.), degassed water (0.25 ml), aryl bromide (3 eq.), 65-70 °C.

(b) Isolated product after flash-chromatography.

Tab. 7: Synthesis of diaryl TC derivatives starting from TC boronate **8**.

In both the reactions (Entry 1 and 2) the coupling product was obtained only in low yield. We thought that a possible explanation could be the higher steric demands of **8** in comparison to the simpler boronic acids used in reaction with **6**, that slowed the trans-metalation step. Moreover the longer permanence of the boronic ester in the reaction mixture could even enable some side-processes to occur which could lead to the degradation of the boronate.¹⁸

2.2.4. Conclusions.

We showed that the triethylammonium tagged complex **2** provides a highly active catalyst for the SM reaction of aryl bromides in an IL. Formation of Pd black was never observed and the catalyst-containing IL phase could be recycled six times without any substantial decrease of catalytic activity. Moreover the protocol developed was successfully applied to the synthesis of valuable and challenging substrates, such as 5,11-diaryl-tetracenes, in high yield and under mild reaction conditions.

2.2.5. Experimental section.

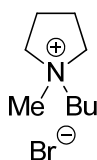
General information

^1H and ^{13}C NMR were recorded on a Varian Inova 300 and 400 and on a Varian Gemini 200; chemical shifts (δ) are reported in ppm relative to TMS. Gas chromatographic analyses were performed with a Agilent 6850 GC-system coupled to a Agilent 5975 mass selective detector ($50 \pm \text{C}$, 2 min \nearrow $!280 \pm \text{C}$, $10 \pm \text{C} / \text{min}$ \nearrow $!280 \pm \text{C}$, 10 min). Reactions were monitored by TLC and GC-MS. Flash-chromatography was carried out using Merck silica gel 60 (230-400 mesh particle size). All reagents were commercially available and were used without further purification, unless otherwise stated. HPLC were carried out with a reverse phase column (ZORBAX-Eclipse XDB-C8 Agilent Technologies) using the following conditions: *Method A*: $\text{H}_2\text{O}/\text{MeCN}$ from 90:10 to 0:100 in 20 minutes. Flow 0.5 ml/min . T: 30°C ; *Method B*: $\text{H}_2\text{O}/\text{MeCN}$ from 70:30 to 20:80 in 8 minutes. Flow 0.4 ml/min . T: 30°C . 5,11- dibromotetracene was kindly furnished by the group of Prof. Antonio Papagni and it was prepared according to the literature procedure.¹⁶

Synthesis of the [bmpy][NTf₂]

All the ILs employed were commercially available or were prepared according to literature procedure¹⁹. The synthesis of [bmpy][NTf₂] is reported as example.

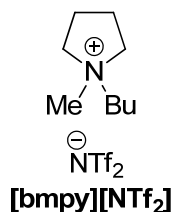
1-butyl-1-methyl-pyrrolidinium bromide [bmpy][Br].



[bmpy][Br]

Bromobutane (15 mL, 140 mmol) was slowly added to a stirred solution of *N*-methylpyrrolidine (13.5 mL, 127 mmol) in CH_3CN (38 mL). The solution was stirred at room temperature for 12 h and then at 70°C for 3 h. After cooling to room temperature, AcOEt was added to the solution and the precipitate was collected by filtration and dried under vacuum to afford 26.6 g (119 mmol, 94 %) of title compound as a white solid. $^1\text{H-NMR}$ (300 MHz, CDCl_3) δ 0.99 (t, $J = 7.4 \text{ Hz}$, 3 H), 1.46 (sxt, $J = 7.4 \text{ Hz}$, 2 H), 1.69-1.84 (m, 2 H), 2.26-2.37 (m, 4 H), 3.31 (s, 3 H), 3.64-3.73 (m, 2 H), 3.79-3.93 (m, 4 H). $^{13}\text{CNMR}$ (75 MHz, CDCl_3) δ 12.6, 18.6, 20.5, 24.8, 47.5, 62.9, 63.3. [M^+]: 142.

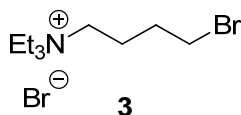
1-butyl-1-methyl-pyrrolidinium bis(trifluoromethylsulfonyl) imide [bmpy][NTf₂].



LiNTf₂ (15.8 g, 55 mmol) was added to a solution of *N*-butyl-*N*-methyl-pyrrolidinium bromide (11.1 g, 50 mmol) in water (15 mL) and the solution is vigorously stirred at room temperature for 12 h. The solution was extracted with CH₂Cl₂ and the combined organic phases were washed with water until no bromide was detected by AgNO₃ test. The combined organic phases were dried (Na₂SO₄) and CH₂Cl₂ was removed at reduced pressure to afford the title compound as a colorless liquid (20.1 g, 47.5 mmol, 95 %). The ionic liquid can be further purified by stirring for 12 h at 40 °C in the presence of decolorizing charcoal and filtering through a short pad of neutral alumina eluting with CH₂Cl₂. ¹H-NMR (300 MHz, CDCl₃) δ 1.01 (t, *J* = 7.3 Hz, 3 H), 1.44 (sxt, *J* = 7.5 Hz, 2 H), 1.68-1.84 (m, 2 H), 2.23-2.36 (m, 4 H), 3.07 (s, 3 H), 3.28-3.38 (m, 2 H), 3.48-3.61 (m, 4 H). ¹³C-NMR (300 MHz, CDCl₃) δ 12.8, 19.0, 21.0, 25.2, 47.8, 64.0, 117.3, 121.6. [M⁺]: 142.

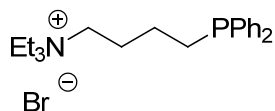
Synthesis of the catalyst 2.

4-Bromobutyl-triethyl-ammonium bromide (3).



Triethylamine (2.8 mL, 20 mmol) was added to 1,4-dibromobutane (7.1 mL, 60 mmol) and the solution was stirred for 2+3 h at 70+80 °C. The resulting suspension was cooled to 0 °C, the solid was collected by filtration and washed with AcOEt. 4-Bromobutyl-triethylammonium bromide (**3**) was obtained as an hygroscopic white solid (5.91 g, 18.7 mmol, 93%). ¹H-NMR (300 MHz, CDCl₃) δ 1.40 (t, *J* = 7.2 Hz, 9H), 1.86+1.99 (m, 2 H), 1.99+2.11 (m, 2 H), 3.43+3.60 (m, 10 H). ¹³C-NMR (75 MHz, CDCl₃) δ 7.1, 19.4, 27.9, 32.0, 52.4, 55.4. [M⁺]: 236, 238.

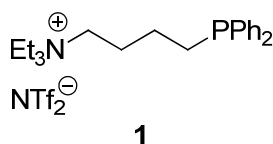
4-Diphenylphosphinobutyl-triethyl-ammonium bromide (4).



n-BuLi (1 mL, 2.5 M in cyclohexane) was slowly added at 0 °C to a solution of Ph₂PH (350 ml, 2.48 mmol) in THF (1 mL). The orange solution was allowed to reach room temperature and further

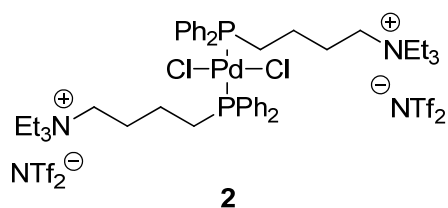
stirred for 30 min. The solution of Ph₂PLi was slowly added *via* syringe at 0 °C to a suspension of 4-bromobutyltriethyl-ammonium bromide (0.66 g, 2.07 mmol) in THF(2 mL). The colorless suspension was allowed to reach room temperature and further stirred for 2 h. The reaction was quenched by adding water (2 mL), the organic solvent was evaporated the residue was extracted with CH₂Cl₂. The combined organic phases were washed with water, dried (Na₂SO₄) and evaporated under reduced pressure. The solid obtained was washed with Et₂O to afford the title compound as a white solid (0.753 g, 1.78 mmol, 86 %). ¹H-NMR (300 MHz, CDCl₃) δ 1.36 (t, *J* = 7.2 Hz, 9H), 1.48⁺1.66 (m, 2 H), 1.78⁺1.94 (m, 2 H), 2.16 (t, *J* = 7.4 Hz, 2 H), 3.19⁺3.30 (m, 2 H), 3.49 (q, *J* = 7.2 Hz, 6 H), 7.24⁺7.57 (m, 10 H). ¹³C-NMR (75 MHz, CDCl₃) δ 7.3, 22.2, 26.3, 26.5, 52.7, 56.2, 127.5, 127.6, 127.8, 128.0, 129.8, 129.9, 130.0, 130.9, 131.0, 131.7, 131.8, 132.0, 137.1, 137.3. [M⁺]: 342.

4-Diphenylphosphinobutyl-triethyl-ammonium bis(trifluoromethylsulfonyl)imide (1).



LiNTf₂ (0.474 g, 1.65 mmol) was added to a solution of 4-diphenylphosphinobutyl-triethyl-ammonium bromide (0.633 g, 1.5 mmol) in water (1 mL) and the reaction mixture was vigorously stirred at room temperature for 12 h. The solution was extracted with CH₂Cl₂ and the combined organic phases were washed with water until no bromide was detected by the AgNO₃ test. The combined organic phases were dried (Na₂SO₄) and CH₂Cl₂ was removed at reduced pressure to afford the title compound as a viscous liquid (0.793 g, 1.28 mmol, 85%). **1** can be further purified through a short pad of neutral alumina and of decolorizing charcoal, eluting with CH₂Cl₂. ¹H-NMR (300 MHz, CDCl₃) δ 1.26 (t, *J* = 7.1 Hz, 9H), 1.36⁺1.64 (m, 2H), 1.64⁺1.92 (m, 2H), 2.12 (t, *J* = 7.5 Hz, 2H), 2.92⁺3.12 (m, 2H), 3.21 (q, *J* = 7.1 Hz, 6H), 7.28⁺7.86 (m, 10H). ¹³C-NMR (75 MHz, CDCl₃) δ 7.4, 22.7, 26.9, 27.1, 53.1, 56.8, 117.7, 122.0, 128.6, 128.6, 128.7, 128.8, 128.9, 129.0, 130.6, 130.8, 132.5, 132.6, 132.6, 132.8, 137.7, 137.9. [M⁺]: 342.

Complex 2.



PdCl₂ (0.044 g, 0.25 mmol) was added to a solution of ligand **1** (0.311 g, 0.5 mmol) in CH₂Cl₂ (1 mL) and the suspension was stirred at room temperature for 12 h, until a clear solution was obtained. The solution was filtered through a short pad of Celite® and the solvent was evaporated at reduced pressure to afford **2** as a yellow solid (0.338 g, 0.24 mmol, 95%). ¹H-NMR (300 MHz, CD₃CN) δ 1.16 (t, *J* = 6.4 Hz, 18 H), 1.46⁺1.83 (m, 8 H), 2.43⁺2.54 (m, 4H), 2.88⁺3.04 (m, 4 H), 3.04⁺3.17 (m, 12 H), 7.29 (t, *J* = 7.0 Hz, 2 H), 7.39⁺7.59 (m, 12 H), 7.67⁺7.77 (m, 6 H). ¹³C-NMR (75 MHz, CD₃CN) δ 7.8, 22.4, 23.3, 23.4, 23.4, 23.6, 23.7, 23.7, 24.9, 25.1, 25.3, 53.8, 57.2, 118.9, 123.1, 129.4, 129.5, 129.6, 129.7, 129.7, 129.9, 130.2, 130.3, 130.6, 130.9, 131.2, 131.5, 131.7, 132.0, 132.4, 132.8, 132.8, 134.2, 134.3, 134.4, 134.5, 134.6, 134.7.

General procedure for the Suzuki coupling.

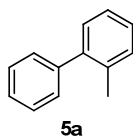
Reactions have to be conducted under argon. In the presence of air, biphenyl, the homocoupling product of boronic acid, was formed up to ~15%, while in the absence of air it was limited to less than 2 %. Complex **2** (14.5 mg, 0.01 mmol) was added to [bmpy][NTf₂] (1 mL) and the yellow solution was stirred at 65 °C for a few minutes. Phenylboronic acid (0.183 g, 1.5 mmol), K₃PO₄ (0.424 g, 2 mmol) and degassed water (0.5 mL) were added to the solution. After a few minutes, an orange homogeneous solution was formed. 2-Methyl-bromobenzene (0.12 mL, 1 mmol) was added to the reaction mixture and the solution was stirred at 65 °C for 2 h. After cooling to room temperature, the reaction mixture was directly charged onto a silica gel column and the desired product was isolated by elution with cyclohexane (0.155 g, 0.92 mmol, 92%).

Optimized procedure for catalyst recycling.

Reactions were carried out as described in the general procedure. After cooling to room temperature, the product was extracted with pentane (5 x 4 mL) and further purified by flash-chromatography on SiO₂. The ionic liquid was washed with degassed water (2 x 2 mL), dried under vacuum (~1 mmHg) for 6⁺8 h and directly reused for the next cycle.

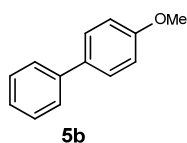
Spectroscopic data for compounds 5a-l.

2-Methylbiphenyl (5a).



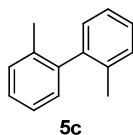
^1H NMR (300 MHz, CDCl_3) δ 2.32 (s, 3 H), 7.25⁺7.50 (m, 10 H). ^{13}C NMR (75 MHz, CDCl_3) δ 20.4, 125.7, 126.7, 127.2, 128.0, 129.10, 129.13, 129.7, 130.3, 135.2, 141.89, 141.92. $[\text{M}]^+$: 168.

4-Methoxybiphenyl (5b).



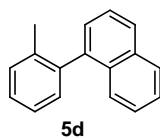
m.p. = 85⁺86 °C. ^1H NMR (300 MHz, CDCl_3) δ 3.87 (s, 3H), 7.00 (d, J = 8.5 Hz, 2H), 7.32 (t, J = 7.3Hz, 1H), 7.43 (t, J = 7.6 Hz, 2 H), 7.49⁺7.62 (m, 4 H). ^{13}C NMR (75 MHz, CDCl_3) δ 55.3, 114.2, 126.6, 126.7, 128.1, 128.7, 133.7, 140.8, 159. $[\text{M}]^+$: 184.

2,2'-Dimethylbiphenyl (5c).



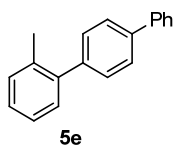
^1H NMR (300 MHz, CDCl_3) δ 2.07 (s, 6 H), 7.08⁺7.15 (m, 2 H), 7.18⁺7.33 (m, 6 H). ^{13}C NMR (50 MHz, CDCl_3) δ 19.8, 125.5, 127.1, 129.2, 129.8, 135.8, 141.6. $[\text{M}]^+$: 182.

1-o-Tolynaphthalene (5d).



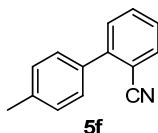
m.p. = 88⁺89 °C. ^1H NMR (300 MHz, CDCl_3) δ 2.32 (s, 3 H), 7.33⁺7.52 (m, 9 H), 7.56⁺7.71 (m, 2H). ^{13}C NMR (75 MHz, CDCl_3) δ 20.5, 125.8, 126.7, 127.0, 127.2, 127.3, 128.8, 129.6, 129.8, 130.4, 135.3, 139.6, 140.8, 140.9, 141.4. $[\text{M}^+]$: 218.

2-Methyl-4'-phenylbiphenyl (5e)



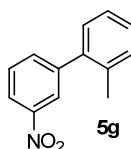
m.p. = 88+89 °C. ¹H NMR (300 MHz, CDCl₃) δ 2.32 (s, 3 H), 7.33+7.52 (m, 9 H), 7.56+7.71 (m, 4 H). ¹³C NMR (75 MHz, CDCl₃) δ 20.5, 125.8, 126.7, 127.0, 127.2, 127.3, 128.8, 129.6, 129.8, 130.4, 135.3, 139.6, 140.8, 140.9, 141.4. [M⁺]: 244.

4'-Methylbiphenyl-2-carbonitrile (5f).



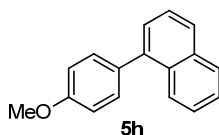
m.p. = 49+51 °C. ¹H NMR (200 MHz, CDCl₃) δ 2.41 (s, 3 H), 7.26+7.34 (m, 2 H) 7.35+7.54 (m, 4H) 7.56+7.68 (m, 1 H) 7.74 (dd, *J* = 1.5/ 7.7 Hz, 1 H). ¹³C NMR (50 MHz, CDCl₃) δ 21.1, 103.7, 111.0, 127.1, 128.4, 129.3, 129.8, 132.6, 133.5, 135.1, 138.5, 145.3. [M⁺]: 193.

2-Methyl-3'-nitrobiphenyl (5g).



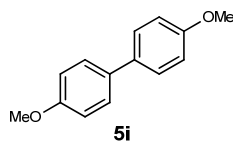
¹H NMR (300 MHz, CDCl₃) δ 2.29 (s, 3 H), 7.21+7.36 (m, 4 H), 7.55+7.70 (m, 2 H), 8.19+8.25 (m, 2 H). ¹³C NMR (75 MHz, CDCl₃) δ 20.1, 121.6, 123.8, 126.0, 128.2, 128.9, 129.4, 130.5, 135.0, 135.2, 139.1, 143.3, 147.9. [M⁺]: 213.

1-(4-Methoxyphenyl)naphthalene (5h).



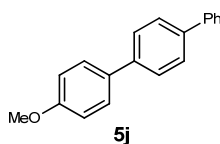
m.p. = 115+117 °C. ¹H NMR (300 MHz, CDCl₃) δ 3.91 (s, 3 H), 7.02+7.08 (m, 2 H), 7.39+7.56 (m, 6 H), 7.79+7.97 (m, 3 H). ¹³C NMR (50 MHz, CDCl₃) δ 55.3, 113.7, 125.4, 125.7, 125.9, 126.0, 126.9, 127.3, 128.2, 131.1, 131.8, 133.1, 133.8, 139.9, 158.9. [M⁺]: 234.

4,4'-Dimethoxybiphenyl (5i).



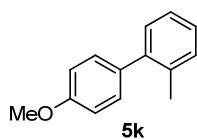
m.p. = 178+179 °C. ¹H NMR (200 MHz, CDCl₃) δ 3.86 (s, 6 H), 6.97 (d, *J* = 8.9 Hz, 4 H), 7.49 (d, *J* = 8.9 Hz, 4H). ¹³C NMR (50 MHz, CDCl₃) δ 55.3, 114.1, 127.7, 133.4,158.6. [M⁺]: 214.

4-Methoxy-4'-phenylbiphenyl (5j).



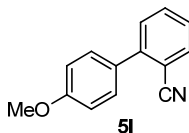
m.p. = 222+223 °C. ¹H NMR (300 MHz, CDCl₃) δ 3.88 (s, 3 H), 7.01 (d, *J* = 8.8 Hz, 2 H), 7.32-7.42 (m, 1 H) 7.43+7.52 (m, 2 H) 7.55+7.71 (m, 8 H). ¹³C NMR (75 MHz, CDCl₃) δ 55.4, 114.3, 127.0, 127.0, 127.2, 127.5, 128.0, 128.8, 133.2, 139.5, 139.7, 140.8, 159.2. [M⁺]: 260.

4'-Methoxy-2-methylbiphenyl (5k).



¹H NMR (300 MHz, CDCl₃) δ 2.31 (s, 3 H), 3.88 (s, 3 H), 6.98 (d, *J* = 8.8 Hz, 2 H), 7.22+7.33 (m, 6 H). ¹³C NMR (75 MHz, CDCl₃) δ 20.5, 55.2, 113.4, 125.7, 126.9, 129.8, 130.2, 130.2, 134.3, 135.4, 141.5, 158.5. [M⁺]: 198.

4'-Methoxybiphenyl-2-carbonitrile (5l).

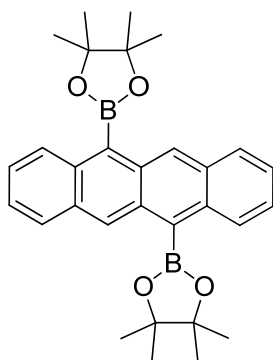


¹H NMR (300 MHz, CDCl₃) δ 3.88 (s, 3 H), 7.03 (d, *J* = 8.8 Hz, 2 H), 7.25+7.28 (m, 1 H), 7.41 (t, *J* = 7.6 Hz, 1 H), 7.47+7.56 (m, 2 H), 7.63 (t, *J* = 7.7 Hz, 1 H), 7.75 (d, *J* = 7.7 Hz, 1 H). ¹³C NMR (75 MHz, CDCl₃) δ 55.3, 111.0, 114.1, 118.9, 127.0, 129.8, 129.9, 130.5, 132.7, 133.7, 145.1, 160.0. [M⁺]: 209.

General procedure for the synthesis of 5,11-diaryltetracene 7a-d.

In an oven dried Schlenk tube, under argon atmosphere, Pd complex **2** (2.8 mg, 0.0020 mmol, 3 mol %) was dissolved in 0.5 mL of [bmpy][NTf₂] and the yellow, clear solution was stirred under vacuum for a few minutes. Arylboronic acid (0.194 mmol, 3 eq.), K₃PO₄ (0.260 mmol, 4 eq.) and 0.25 mL of degassed water were added to the solution and the reaction mixture was heated at 70 °C. After a few minutes an orange homogeneous solution was formed. 5,11-dibromotetracene **6** (25 mg, 0.065 mmol, 1 eq.) was added to the reaction mixture that was vigorously stirred at 70 °C until complete consumption of the starting material (monitored by TLC). After cooling to room temperature, the reaction mixture was taken up with dichloromethane, adsorbed on silica and directly charged onto a silica gel column. The desired product was isolated by elution with cyclohexane and dichloromethane mixtures. During the whole process products exposure to light and air should be minimized in order to avoid the possible formation of oxidized side products.

Synthesis of pinacol boronate **8**.



8

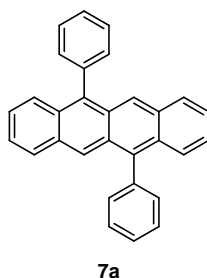
In an oven dried round bottom flask equipped with a reflux condenser, under argon atmosphere, Pd(OAc)₂ (4.4 mg, 0.019 mmol), bis(pinacolato)diboron (148 mg, 0.582 mmol), KOAc (86 mg, 0.873 mmol) and 5,11-dibromotetracene **6** (75 mg, 0.194 mmol) were dissolved in 15 mL of anhydrous DMF and heated at 80 °C for 7 hours. The red solution turned yellow-green during the reaction. The reaction mixture was then cooled to 0 °C and 30 mL of water were added. The aqueous layer was extracted two times with ethyl acetate (30 mL). The collected organic phases were washed with brine, dried over Na₂SO₄ and concentrated under vacuum. The crude product was purified by flash chromatography using cyclohexane and dichloromethane (80:20) as the eluent (yellow solid, Y: 84 %). ¹H-NMR (400 MHz, CDCl₃). δ (ppm): 9.21 (s, 2H), 8.42 (d, 2H, *J* = 9.2 Hz), 7.97 (d, 2H, *J* = 8.0 Hz), 7.45-7.36 (m, 4H), 1.66 (s, 24H). ¹³C-NMR (100 MHz, CDCl₃). δ (ppm): 135.77, 133.43, 131.02, 130.36, 129.58, 128.10, 125.67, 124.48, 84.45, 25.23. (carbon attached to boron was not observed).²⁰ [MH⁺]:481. HPLC (λ = 280 nm, method B). t_R = 21.3 min.

General procedure for the SM coupling with boronic ester **8**.

In an oven dried Schlenk tube, under argon atmosphere, Pd complex **2** (1.9 mg, 0.0013 mmol, 3 mol %) was dissolved in 0.5 mL of [bmpy][NTf₂] and the yellow, clear solution was stirred under vacuum for a few minutes. **8** (21 mg, 0.044 mmol, 1 eq.), K₃PO₄ (0.176 mmol, 4 eq.) and 0.25 mL of degassed water were added to the solution that was heated at 70 °C. The aryl bromide (0.132 mmol, 3 eq.) was added to the reaction mixture that was vigorously stirred at 70 °C until complete consumption of the diboronic ester (monitored by TLC). After cooling to room temperature, the reaction mixture was taken up with dichloromethane, adsorbed on silica and directly charged onto a silica gel column. The desired product was isolated by elution with cyclohexane and dichloromethane mixtures. During the whole process products exposure to light and air should be minimized in order to avoid the possible formation of oxidized side products.

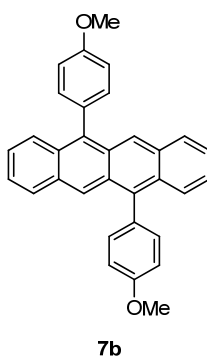
Spectroscopic data of compound **7a-e**

5,11-diphenyltetracene (7a).



¹H-NMR (400 MHz, CDCl₃). δ 8.36 (s, 2H), 7.83 (d, 2H, *J* = 8.5 Hz), 7.66-7.61 (m, 8H), 7.55 (d, *J* = 6.7 Hz, 4H), 7.33-7.23 (m, 4H). ¹³C-NMR (100 MHz, CDCl₃). δ 139.14, 136.82, 131.50, 130.99, 129.35, 129.04, 128.96, 128.50, 127.58, 126.59, 125.94, 125.27, 124.68. [M⁺]: 380. HPLC (λ = 280 nm, method A). t_R = 23.7 min.

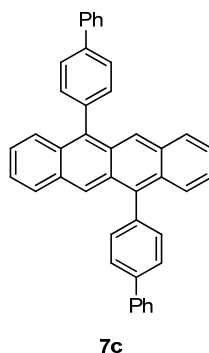
5,11-bis(4-methoxyphenyl)tetracene (5b).



¹H-NMR (400 MHz, CDCl₃). δ 8.40 (s, 2H), 7.85 (d, *J* = 8.4 Hz, 2H), 7.68 (d, *J* = 8.8 Hz, 2H), 7.47 (d, *J* = 8.4 Hz, 4H), 7.34-7.24 (m, 4H), 7.21 (d, *J* = 8.4 Hz, 4H), 4.02 (s, 6H). ¹³C-NMR (100

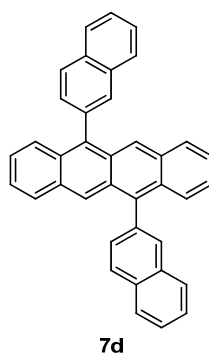
MHz, CDCl₃). δ 159.11, 136.62, 132.57, 131.23, 131.02, 129.66, 129.46, 129.00, 126.69, 125.85, 125.15, 124.62, 113.97, 55.43. [MH⁺]: 441. HPLC (λ = 280 nm, method A). t_R = 23.0 min.

5,11-di(biphenyl-4-yl)tetracene (5c).



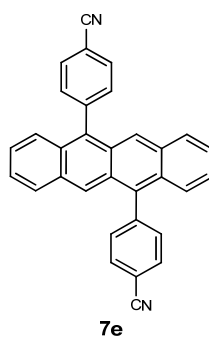
¹H-NMR (400 MHz, CDCl₃). δ 8.48 (s, 1H), 8.43 (s 1H), 7.94-7.91 (m, 4H), 7.88-7.79 (m, 7H), 7.73 (d, J = 9.1 Hz, 1H), 7.65 (dd, J = 7.7 Hz; 7.3 Hz, 4H), 7.57 (dd, J = 7.7 Hz; 7.3 Hz, 4H), 7.45 (dd J = 7.3 Hz; 7.1 Hz, 2H), 7.36-7.29 (m, 4H). [M⁺]: 532. HPLC (λ = 280 nm, method A). t_R = 26.7 min.

5,11-di(naphthalen-2-yl)tetracene (5d).



Y: 85 %. ¹H-NMR (400 MHz, CDCl₃). δ (ppm): 8.43 (s, 1.3 H), 8.14 (s, 0.7 H), 8.18-8.14 (m, 2H), 8.09 (d, J = 10.5 Hz, 4H), 7.98 (d, J = 7.1 Hz, 2H), 7.80 (d, J = 8.5 Hz, 1H), 7.73-7.62 (m, 9H), 7.32-7.21 (m, 4H). [M⁺]: 480. HPLC (λ = 280 nm, method A). t_R = 25.3 min.

4,4'-(tetracene-5,11-diyl)dibenzonitrile (5e).



$^1\text{H-NMR}$ (400 MHz, CDCl_3). δ (ppm): 8.25 (s, 2H), 7.99 (d, $J = 8.4$ Hz, 4H), 7.86 (d, $J = 8.4$ Hz, 2H), 7.68 (d, $J = 8.4$ Hz, 4H), 7.49 (d, $J = 9.2$ Hz, 2H), 7.40-7.32 (m, 4H). $[\text{M}^+]$: 430.

Bibliography

- (1) Lombardo, M.; Chiarucci, M.; Trombini, C. *Green Chem.* **2009**, *11*, 574–579.
- (2) "The Nobel Prize in Chemistry 2010", http://nobelprize.org/nobel_prizes/chemistry/laureates/2010/.
- (3) Suzuki, A. *Chem. Comm.* **2005**, 4759-4763.
- (4) Kurti, L; Czako B. *Strategic Applications of Named Reactions in Organic Synthesis*, **2005**, Elsevier Academic Press.
- (5) Yin, L.; Liebscher, J. *Chem. Rev.* **2007**, *107*, 133-173.
- (6) Alimardanov, A.; Schmieder-van de Vondervoort, L.; Vries, A. H. M. de; Vries, J. G. de *Adv. Synth. Cat.* **2004**, *346*, 1812–1817.
- (7) Astruc, D.; Lu, F.; Aranzas, J. R. *Angew. Chem. Int. ed.* **2005**, *44*, 7852–7872.
- (8) Zhao, D.; Fei, Z.; Geldbach, T. J.; Scopelliti, R.; Dyson, P. J. *J. Am. Chem. Soc.* **2004**, *126*, 15876-15882.
- (9) Biscoe, M. R.; Fors, B. P.; Buchwald, S. L. *J. Am. Chem. Soc.* **2008**, *130*, 6686-6687.
- (10) Ismail, M. a H.; Barker, S.; Abou el-Ella, D. a; Abouzid, K. a M.; Toubar, R. a; Todd, M. H. *J. Med. Chem.* **2006**, *49*, 1526-1535.
- (11) Hamill, N. a; Hardacre, C.; McMath, S. E. *J. Green Chem.* **2002**, *4*, 139-142.
- (12) Papagni, A.; Trombini, C.; Lombardo, M.; Bergantin, S.; Chiarucci, M.; Miozzo, L.; Parravicini, M.; manuscript in preparation.
- (13) Wu, W.; Liu, Y.; Zhu, D. *Chem. Soc. Rev.* **2010**, 1489-1502.
- (14) Moon, H.; Zeis, R.; Borkent, E.-J.; Besnard, C.; Lovinger, A. J.; Siegrist, T.; Kloc, C.; Bao, Z. *J. Am. Chem. Soc.* **2004**, *126*, 15322-15323.
- (15) Paraskar, A. S.; Ravikumar Reddy, A. R.; Patra A.; Wijsboom Y. H.; Gidron O.; Shimon L. J; Leitus W.G.; Bendikov M.; *Chem. Eur. J.* **2008**, *14*, 10639-10647.
- (16) Avlasevich, Y.; Müllen, K. *Chem. Comm.* **2006**, *9*, 4440-4442.
- (17) Zhu, L.; Duquette, J.; Zhang, M. *J. Org. Chem.* **2003**, *68*, 3729-3732.
- (18) Butters, M.; Harvey, J. N.; Jover, J.; Lennox, A. J. J.; Lloyd-Jones, G. C.; Murray, P. M. *Angew. Chem. Int. ed.* **2010**, *49*, 51-56.
- (19) Earle, M. J.; Gordon, C. M.; Plechkova, N. V.; Seddon K. R.; Welton, T.; *Anal. Chem.*, **2007**, *79*, 758-764.
- (20) Kimoto, T.; Tanaka, K.; Sakai, Y.; Ohno, A.; Yoza, K.; Kobayashi, K. *Org. Lett.* **2009**, *11*, 3658–3661.

2.3. Ion-Tagged Imidazolidinone for the Enantioselective Organocatalytic Diels-Alder Reaction .¹

2.3.1. Reaction overview.

The asymmetric Diels–Alder (DA) reaction is one of the most important organic transformations and has proven to be a versatile means of synthesis of complex molecules with elevated level of stereocontrol. It is well known that Lewis acid (LAs) are capable to catalyze the DA reaction and if chiral metal complexes are employed enantiocontrol on the formation of the new stereocenters can be achieved.² In his seminal work in 2000, McMillan’s group reported that the reversible formation of iminium ions, from α,β -unsaturated aldehydes and amines, could emulate the equilibrium dynamics and π -orbital electronics (LUMO lowering) that are inherent to Lewis acid catalysis (Fig.1).³

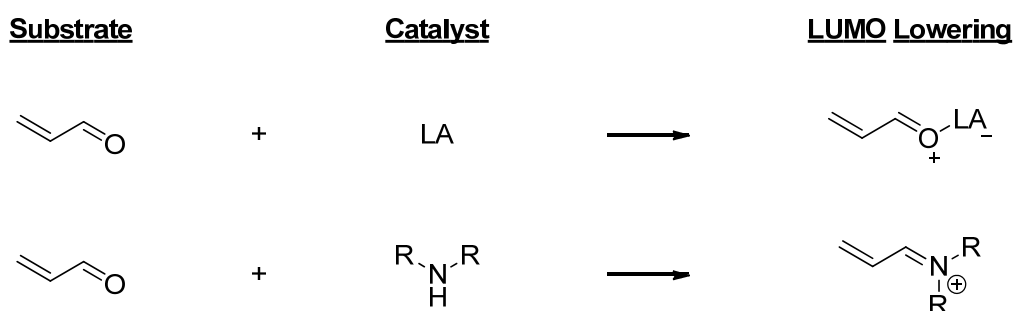


Fig. 1: Comparison of LA and iminium catalysis.

Importantly, this approach revealed the attractive prospect that chiral amines might function as enantioselective catalysts for a large range of transformations that traditionally employ metal salts. The first application of iminium organocatalysis was in the activation of α,β -unsaturated aldehydes as dienophiles in the asymmetric DA reaction. Among various primary and secondary amines tested for this transformation, imidazolidinone **1** turned out to afford the highest yields and enantioselectivities (fig.2). When *trans*-cinnamaldehyde reacted with cyclopentadiene in presence of 5 mol % of organocatalyst **1**HCl, in methanol/water as solvent, the cyclohexane adduct was obtained in quantitative yield with low diastereomeric ratio, but good enantiocontrol for both the diastereoisomers.³ The elevated level of enantiocontrol observed in the reaction could be ascribed to the capability of organocatalyst **1** to effectively control the geometry of the iminium ion, and to shield efficiently one of the two faces of the dienophile.

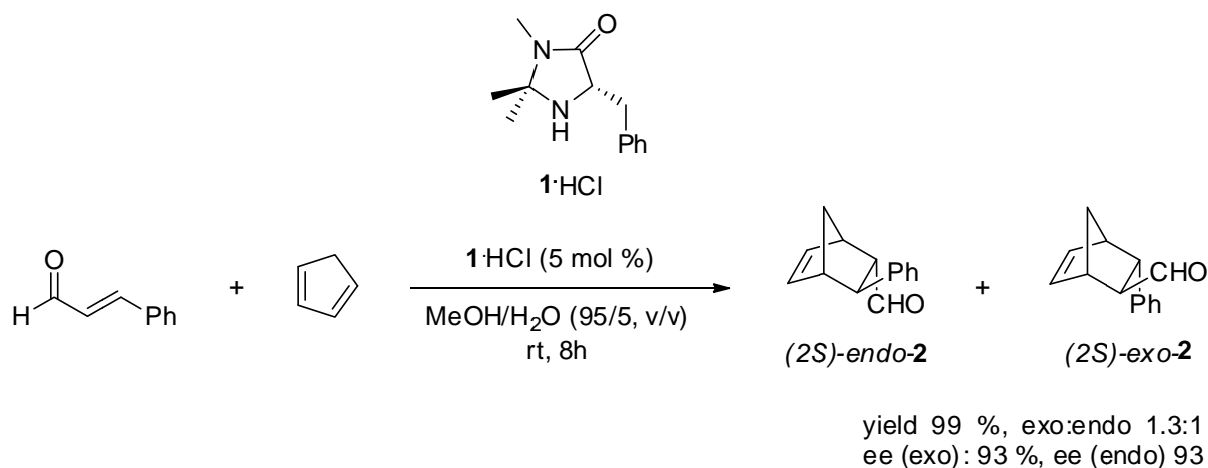


Fig. 2: Asymmetric DA reaction catalyzed by imidazolidinone **1**.

As indicated from computational studies, the catalyst-activated iminium ion was expected to form with only the (*E*)-conformation, to avoid non-bonding interactions between the substrate double bond and the *gem*-dimethyl substituents on the catalyst framework. In addition, the benzyl group of the imidazolidinone moiety should effectively shield the iminium-ion *Si*-face, leaving the *Re*-face exposed for enantioselective bond formation (fig.3).⁴

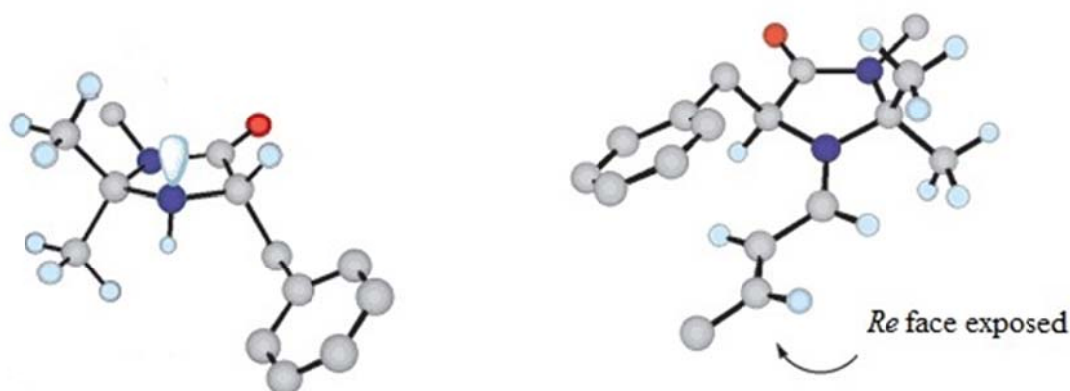


Fig. 3: Structure of the iminium ion formed by catalyst **1** with crotonaldehyde.

In the course of the reaction, the formation of the iminium ion is followed by diene attack and hydrolysis of the iminium ion with release of the catalyst, as shown in fig.4. Computational studies suggest an asynchronous mechanism for the cycloaddition, where the attack of the diene to the β -carbon atom of the iminium ion is the rate-limiting step.⁴ Since this first report iminium organocatalysis has witnessed an impressive growth and McMillan catalyst **1**, and its derivatives, proved to be very versatile catalysts, amenable to afford high enantioselectivity in a number of organocatalytic transformations, proceeding either *via* enamine or iminium ion, and even to be suitable for cascade reaction where both the mechanism are into play. Some of this transformation,

like 1,3-dipolar cycloaddition, Fiedel-Crafts alkylation of electron rich aromatics, α -halogenation of aldehydes and Michael addition are summarized in Fig.5.⁵

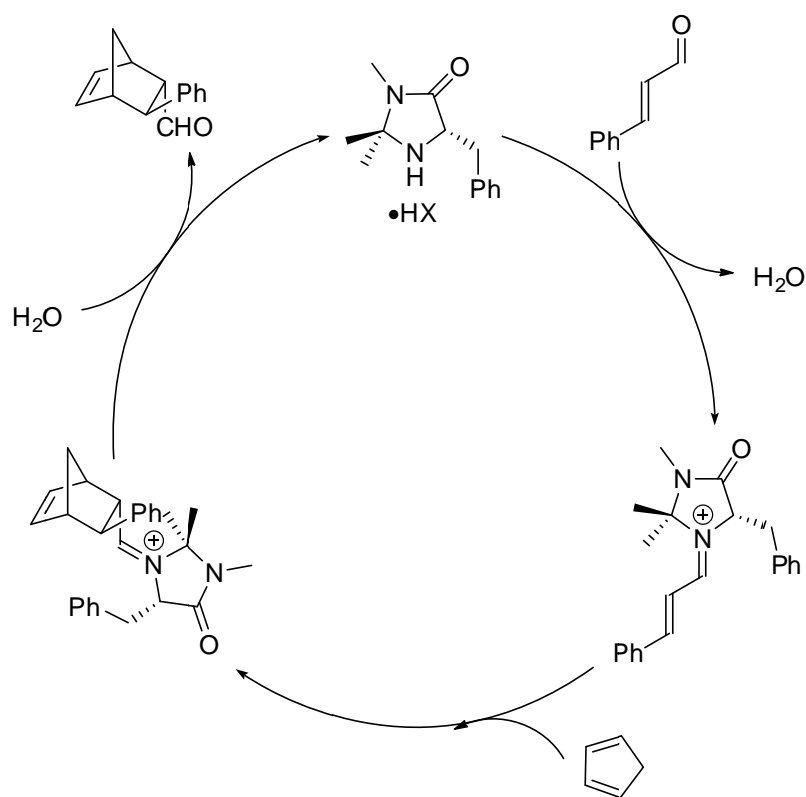


Fig. 4: Mechanism for the DA reaction catalyzed by 1.

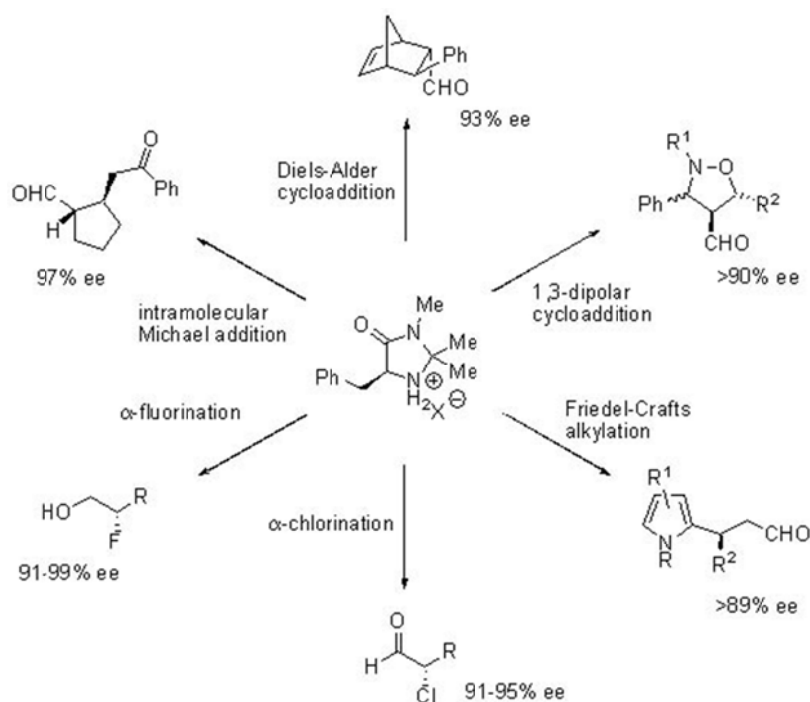


Fig. 5: Asymmetric reactions catalyzed by 1.

2.3.2. Discussion.

The impressive versatility and efficiency of catalyst **1** and the fact that it still suffer from typical drawbacks of many organocatalysts, like high catalyst loading, scarce recyclability and difficult product isolation, prompted us to design an ion-tagged derivative of the imidazolidinone **1**. We speculated that the ion tag might be a suitable means for catalyst recovery and that the ionic group might play a non-innocent role in a reaction, such as the amino catalyzed DA, where many ionic intermediates are present. The amide moiety in catalyst **1** was addressed as a suitable point for imidazolidinone functionalization, so the ion-tagged catalyst **8** was synthesized according to the procedure reported in Fig.6.

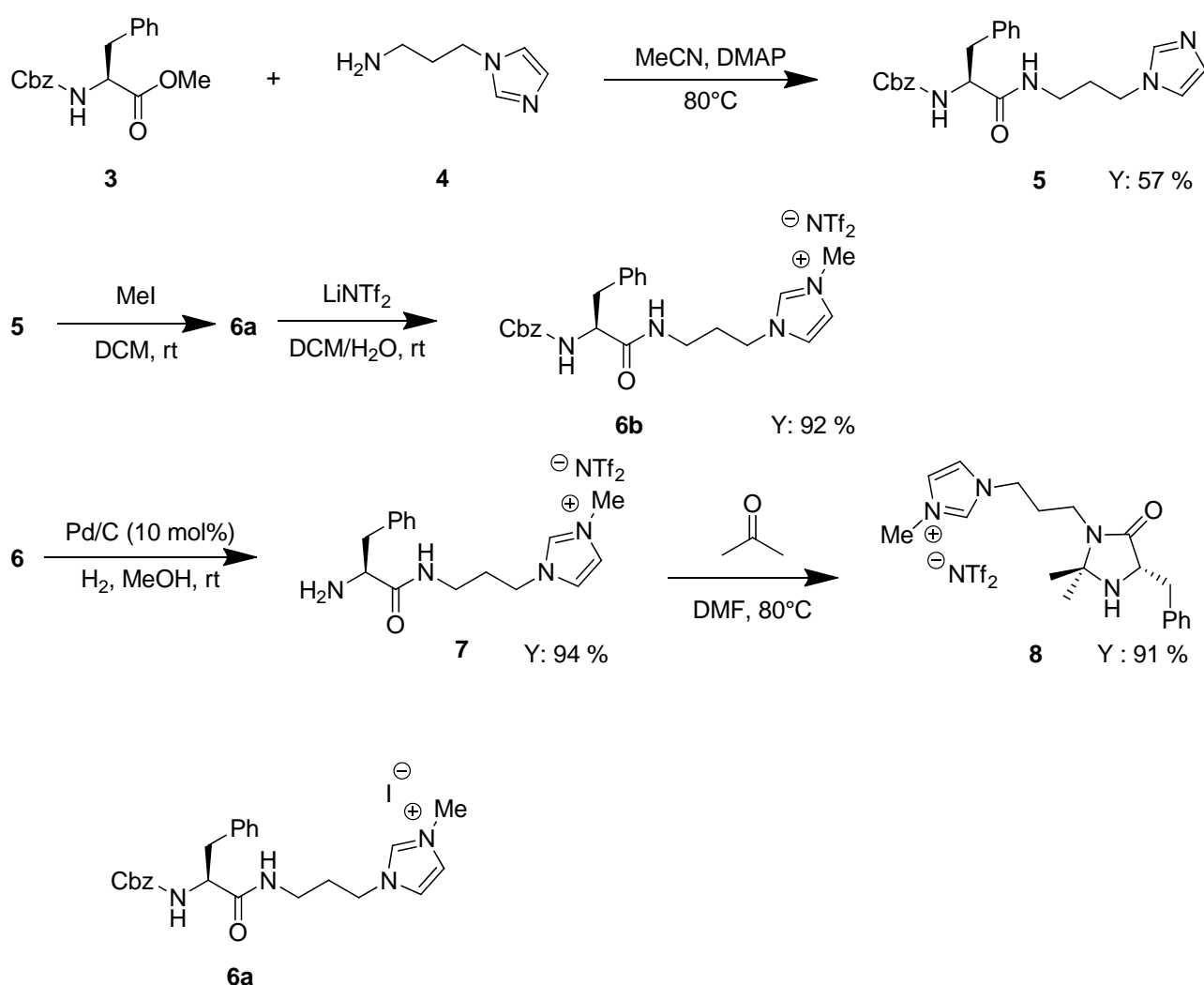
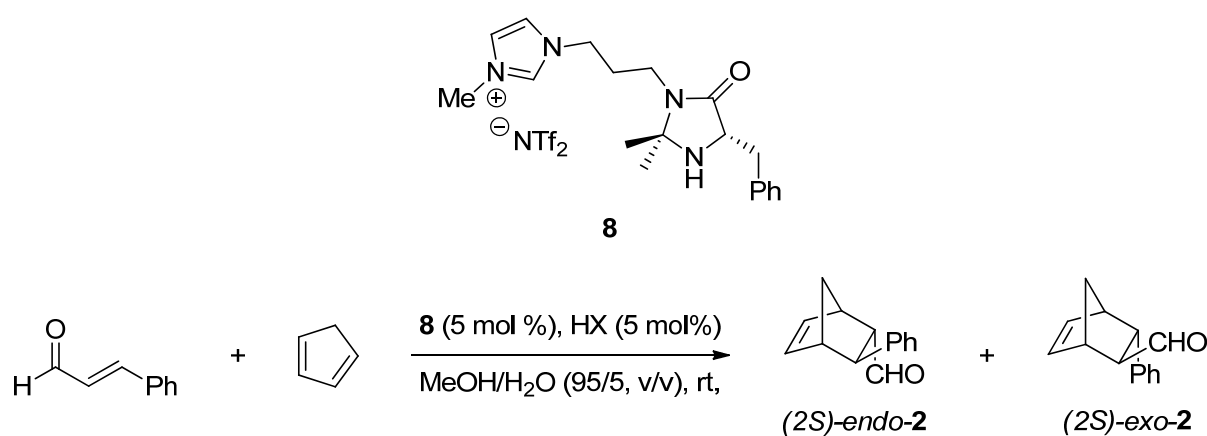


Fig. 6: Synthesis of ion-tagged imidazolidinone **6**.

The procedure adopted was analogous to the synthesis reported by McMillan for 1.3 *N*-Cbz-L-phenylalanine methyl ester (**3**) and *N*-(3-aminopropyl)-imidazole (**4**) were heated in CH₃CN at 80 °C with a catalytic amount of DMAP to yield the amide **5** in moderate yield (57 %). Alkylation of the imidazole moiety with MeI followed by anion metathesis afforded **6** in 92 % overall yield.

Cleavage of the Cbz protecting group by Pd catalyzed hydrogenolysis gave **7** in 94 % yield. Finally cyclization of **5** with acetone formed **8** in 91 % of yield (during the course of this work a manuscript reporting the use of **8**, in the form of iodide salt, for the catalyst immobilization on silica was published, but the synthetic procedure for its preparation was not reported).⁶ Thanks to the presence of the NTf₂ counter ion **8** displayed a solubility profile which made it amenable for catalyst recycling. Indeed **8** was soluble in many polar organic solvents, like alcohols, CH₃CN, CH₂Cl₂, but was insoluble in non-polar solvents, like pentane and Et₂O. With **8** in our hands we choose the DA reaction between *trans*-cinnamaldehyde and cyclopentadiene as benchmark reaction to investigate its catalytic properties. First of all the effect of the acid co-catalyst was addressed (Tab.1).



Entry	Acid	Time (h)	Conversion ^a	exo:endo ^a	ee(<i>exo</i>) (%) ^b	ee(<i>endo</i>) (%) ^b
1	-	24	-	-	-	-
2	PhCOOH	24	-	-	-	-
3	CF ₃ COOH	23	>99%	59:41	92	91
4	HCl	18	81%	58:42	91	92
5	HClO ₄	18	68%	56:44	92	92
6	TfOH	18	73%	52:48	88	75

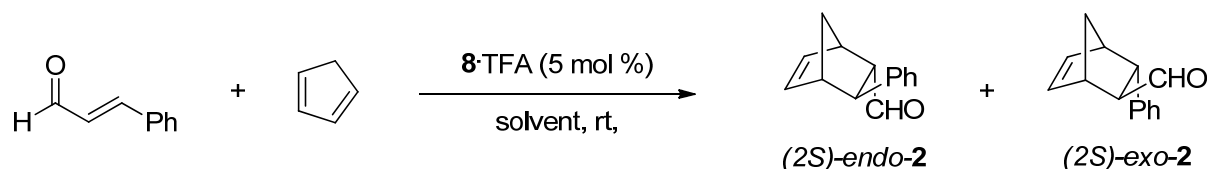
(a) Determined by NMR.

(b) Determined by HPLC analysis (Chiralpak IC column) after reduction of the product with NaBH₄.

Tab. 1: Effect of the acid co-catalyst.

The table shows that the presence and the nature of the acid co-catalyst were critical for the outcome of the reaction. In the absence of acid (Entry 1) or in the presence of a weak acid, like benzoic acid (Entry 2), no reaction took place. Among the strong acids tested (Entries 3-6), TFA and HCl displayed the better results in terms of yield and reactivity (Entry 3 and 4). The use of HClO₄ preserved the stereoselection but displayed a lower reactivity (Entry 5), whereas TfOH

showed lower reactivity and enantioselectivity (Entry 6). With all the acids the diastereoselectivity was low, but this behavior is typical of cyclopentadiene and was observed in the original work as well. With TFA chosen as acid co-catalyst we explored the effect of the solvent (Tab.2).



Entry	Solvent	Time (h)	Conversion (%) ^a	exo:endo ^a	ee(exo) (%) ^b	ee(endo) (%) ^b
1	MeOH/H ₂ O (95:5)	23	>99	59:41	92	91
2	MeNO ₂ /H ₂ O (95:5)	20	>99	58:42	85	89
3	H ₂ O (95:5)	20	>99	57:43	82	87
4	DCM/H ₂ O (95:5)	23	46	71:29	88	89
5	MeCN/H ₂ O (95:5)	23	32	56:44	86	90
6	i-PrOH/H ₂ O (95:5)	20	55	55:45	89	91
7	THF/H ₂ O (95:5)	20	6%	54:46	87	86
8	[bmpy][NTf ₂]	18	94	66:34	86	79
9	[bmpy][NTf ₂]/H ₂ O (95:5)	8	69	57:43	84	87
10	[bmim][NTf ₂]/H ₂ O (95:5)	5	85	65:35	88	91

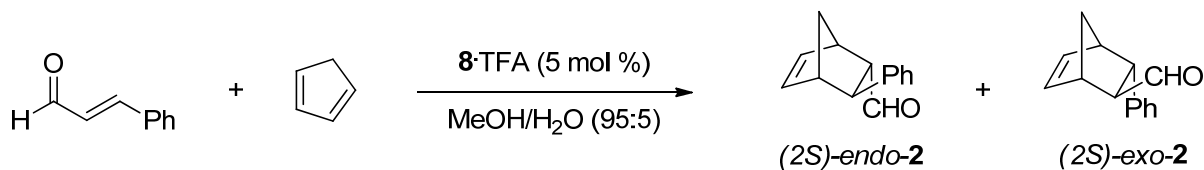
(a) Determined by NMR.

(b) Determined by HPLC analysis (Chiralpak IC column) after reduction of the product with NaBH₄.

Tab. 2: Effect of the solvent.

The best results were obtained in methanol/water, as in the original protocol (Entry 1), but complete conversion with good enantioselectivities were achieved also in MeNO₂ and water (Entry 2 and 3). Good enantioselectivities were obtained even in DCM (Entry 4), MeCN (Entry 5), and i-PrOH (Entry 6), although in these solvents the yields were modest. In THF only traces amount of the product were formed, whereas ILs turned out to be suitable solvent for the reaction, displaying good reactivity and selectivity (Entry 8-10), especially when [bmim][NTf₂]/H₂O was employed as solvent (Entry 10). Using MeOH/H₂O some reactions at lower temperature were carried out (Tab.3). Decreasing the temperature from 25 to 0 °C had a negligible effect on the enantioselectivity and the diastereoselectivity was even lower (Entry 1 and 2). At – 20 °C the reaction was so slow that only

traces amount of product were detected after 3 days (Entry 3). Finally we attempted the recycle of the catalyst both in organic solvent and in the IL (Tab.4).

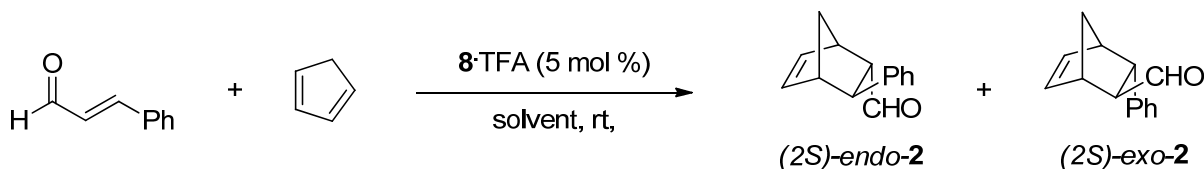


Entry	Temperature (°C)	Time (h)	Conversion (%) ^a	exo:endo ^a	ee(exo) (%) ^b	ee(endo) (%) ^b
1	25	23	>99	59:41	92	91
2	0	72	91	55:45	94	94
3	-20	72	4	54:46	94	94

(a) Determined by NMR.

(b) Determined by HPLC analysis (Chiralpak IC column) after reduction of the product with NaBH₄.

Tab. 3: Effect of the temperature.



Entry	Solvent	Time (h)	Yield (%) ^a	exo:endo ^b	ee(exo) (%) ^c	ee(endo) (%) ^c
1 (Run 1)	[bmpy][NTf ₂]/H ₂ O	8	64	57:43	84	87
2 (Run 2)	[bmpy][NTf ₂]/H ₂ O	12	86	56:44	83	84
3 (Run 1)	MeOH/H ₂ O	16	81	58:42	90	91
4 (Run 2)	MeOH/H ₂ O	16	70	57:43	81	80
5 (Run 3)	MeOH/H ₂ O	16	46	57:43	70	67

(a) Product isolated after flash-chromatography

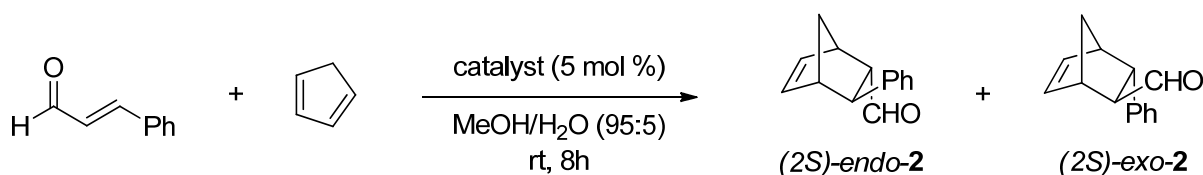
(b) Determined by NMR

(c) Determined by HPLC analysis (Chiralpak IC column) after reduction of the product with NaBH₄.

Tab. 4: Recycling experiments.

When the reaction was carried out in the IL [bmpy][NTf₂] (Entry 1 and 2), at the end of the reaction the product was extracted with ether, the ionic phase was dried and then charged with fresh water, acid, aldehyde and cyclopentadiene. In this way the catalyst could be recycled with no significant loss of activity or selectivity (Entry 1 and 2). However this was no surprising, since untagged McMillan catalyst **1** was already supported onto ILs and recycled successfully.⁷ Thanks to presence

of the ion-tag recycle of catalyst **8** was possible also using an organic solvent like methanol (Entries 3-5). In this case, after the reaction completion, the solvent was removed under reduced pressure and the DA adduct extracted with diethyl ether. The ether-insoluble catalyst was then dried and used in the following run, after addition of fresh solvent, acid and starting materials. In this way catalyst **8** was recycled three times, but a progressive erosion of catalyst activity and selectivity was observed, likely due to mechanical loss of catalyst during the extraction procedure and to the intrinsic hydrolytic lability of McMillan-type catalysts. Although the ion-tag made catalyst **8** at least partially recyclable we did not observe any influence on the reaction outcome respect to the use of **1**, as summarized in Tab.5, where the behavior of the two catalyst in the same condition are compared.



Entry	Catalyst	Conversion (%)	exo:endo	ee(exo) (%)	ee(endo) (%)
1	1 -HCl	99	1.3:1	93	93
2	8 -TFA	88	1.4:1	92	91

Tab. 5: Comparison of the catalytic performance of catalyst **8** and its parent, untagged catalyst **1**.

Probably the ion-tag was too far away from the reactive centre to establish any fruitful interaction, therefore the two catalyst exhibited an almost identical catalytic performance. To prove our hypothesis we synthesized a new ion tagged catalyst (**14**), where the phenyl ring of catalyst **1** was replaced by a triphenylphosphonium ion, bringing the ionic group much nearer to the reactive centre of the catalyst (Fig.7).

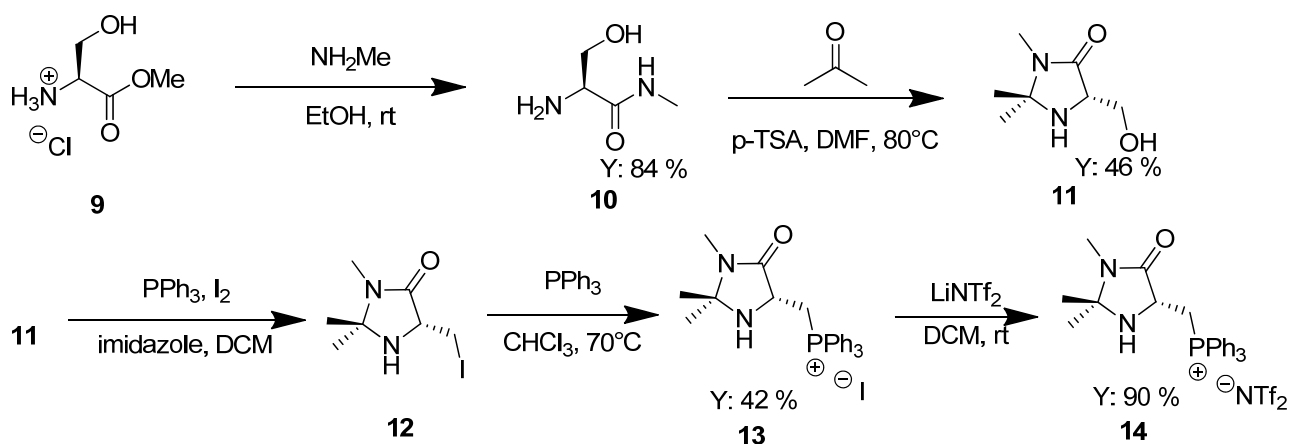
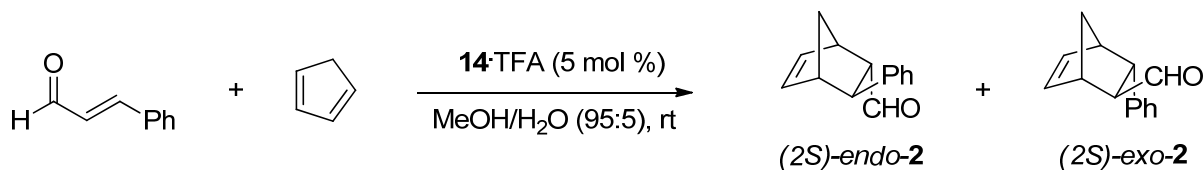


Fig. 7: Synthesis of ion-tagged organocatalyst **14**.

The title compound was synthesized starting from L-serine methyl ester (**9**), which was transformed in the corresponding methyl amide **10** (yield 84 %), which was subjected to cyclization with acetone to afford **11** in 46 % yield. Alcohol **11** was then transformed into iodide **12** by reaction with iodine and PPh₃. Product **12** was not isolated, but immediately reacted with PPh₃ at 70°C to form the phosphonium salt **13** in 42 % overall yield. Finally anion metathesis with LiNTf₂ afforded the desired product **14**, with 90 % of yield. However when we utilized **14** as organocatalyst for the benchmark DA reaction the results were disappointing (Tab.6).



Entry	Solvent	Time (h)	Conversion (%) ^a	exo:endo ^a	ee(exo) (%) ^b	ee(endo) (%) ^b
1	MeOH/H ₂ O	24	-	-	-	-
2	H ₂ O	24	21%	62:38	33%	58%
3	[bmim]NTf ₂ /H ₂ O	24	91%	64:36	47%	72%

(a) Determined by NMR.

(b) Determined by HPLC analysis (Chiralpak IC column) after reduction of the product with NaBH₄.

Tab. 6: Asymmetric DA reaction catalyzed by **14**.

When the reaction was carried out in the previously optimized conditions, no reaction occurred (Entry 1). This result was ascribed to the low solubility of the catalyst in methanol; when water was used as solvent the product was formed in low yield and with low enantioselectivity (Entry 2). **14** turned out to be soluble in the IL [bmim][NTf₂] and when the reaction was conducted in homogeneous conditions, product **2** was obtained in good yield after 24 hours, although with a remarkably lower ee compared to catalyst **8** (Entry 3). Although, as expected, the ionic group closer to the active catalytic centre affected the catalyst performance, the effect on both reactivity and selectivity was detrimental. We explained this behavior speculating that, due to the proximity of the two charged group and to the great steric hindrance of the triphenylphosphonium ion, the two moieties tend to move apart, leading to a less effective shielding of one face of the dienophile and then to a lower enantiomeric excess for the reaction (Fig.8)

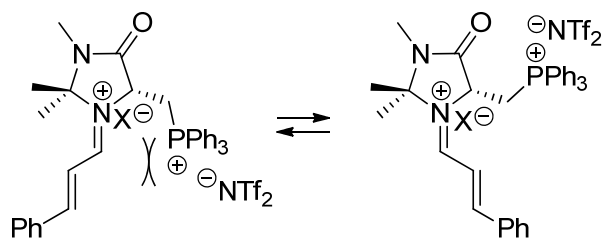


Fig. 8: Supposed effect of the close ionic groups on catalyst **14**.

2.5.3. Conclusions.

Ion-tagged imidazolidinones **8** and **14** were synthesized and their catalytic behavior studied in the asymmetric DA reaction between *trans*-cinnamaldehyde and cyclopentadiene. The different results observed highlighted the importance of the strategy adopted to install the ion-tag and of the carefully choice of the linker for the outcome of the reaction. In catalyst **8** the ionic group was too far away from the active catalytic centre and no difference, from the parent untagged catalyst, were recorded in the catalytic activity. However, in that case, the ion-tag still enabled catalyst recycling using ILs as solvents and, partially, using organic solvents as well. On the other hand catalyst **14**, bearing an ionic group very close to the reactive centre, exhibited a disappointing catalytic performance, probably due to the repulsion between the two near charged group.

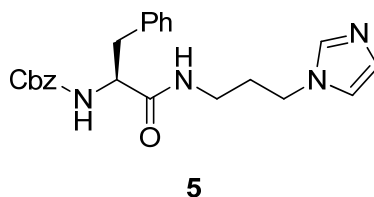
2.3.4. Experimental section.

General information.

^1H and ^{13}C NMR were recorded on a Varian Gemini 200 or Varian Inova 400; chemical shifts (δ) are reported in ppm relative to TMS. Chiral HPLC studies were carried out on a Hewlett-Packard series 1090 instrument and on a Agilent Technologies 1200 Series instrument. Optical rotations were measured with a Perkin-Elmer 343 polarimeter. Gas chromatographic analyses were performed with a Agilent 6850 GC-system coupled to a Agilent 5975 mass selective detector. Reactions were monitored by TLC and GC-MS. Flash-chromatography was carried out using Merck silica gel 60 (230-400 mesh particle size) and Fluka aluminum oxide, Brockmann Activity I (0.05-0.15 mm particle size, pH = 7.0 \pm 0.5). *trans*-cinnamaldehyde and cyclopentadiene were distilled previous to use. All other reagents were commercially available and were used without further purification. All reactions are conducted under Ar atmosphere, unless otherwise stated

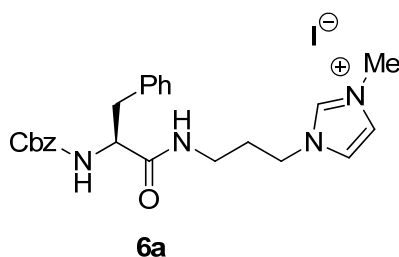
Synthesis of organocatalyst 8.

Synthesis of 3.



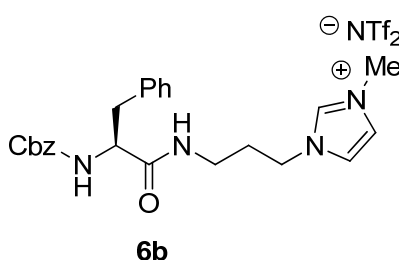
N-Cbz-*L*-phenylalanine methyl ester **3** (3.40 g, 10.85 mmol) was dissolved in 10 ml of anhydrous MeCN. *N*-(3-aminopropyl)-imidazole **4** (2.59 mL, 21.70 mmol) and DMAP (132 mg, 1.085 mmol) were added. The reaction mixture was heated under reflux for 5 days. Then the solution was concentrated under reduced pressure and the residue was taken up with 20 ml of DCM. The organic phase was washed with HCl 0.5 M (2 x 5 mL), water (10 ml) and saturated NaHCO₃ (10 ml). The organic layer was dried (Na₂SO₄), filtered and concentrated. The crude product was purified by silica gel flash chromatography (DCM/MeOH 95:5). The product (yield 57 %) was collected as a sticky solid. ^1H NMR (400 MHz, CDCl₃) δ 7.43 – 7.13 (m, 11H), 7.03 (s, 1H), 6.84 (s, 1H), 6.13 (bs, 1H), 5.42 (bs, 1H), 5.09 (s, 2H), 4.36 (dd, J = 14.5, 7.6 Hz, 1H), 3.86 – 3.64 (m, 2H), 3.25 – 2.90 (m, 4H), 1.88 – 1.74 (m, 2H). ^{13}C NMR (100 MHz, CDCl₃) δ 171.13, 155.95, 137.07, 136.39, 135.99, 129.56, 129.52, 129.26, 128.74, 128.54, 128.27, 128.03, 127.13, 118.71, 67.12, 56.44, 44.12, 38.42, 36.45, 30.69. $[\text{M}+\text{H}]^+ = 407$.

Synthesis of 6a.



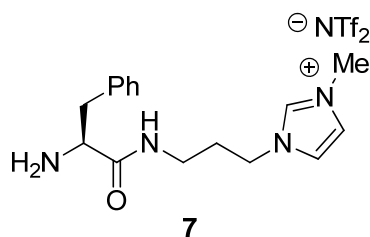
5 (2.40 g, 5.90 mmol) was dissolved in 10 mL of anhydrous DCM and MeI (735 μ L, 11.81 mmol) was added dropwise at 0°C. After stirring the solution overnight at room temperature, the volatiles were removed under reduced pressure to afford the analytically pure product (white solid) in quantitative yield. ^1H NMR (400 MHz, CDCl_3) δ 9.47 (s, 1H), 7.75 (s, 1H), 7.54 (s, 1H), 7.31 – 7.11 (m, 11H), 5.78 (OCONH, d, $J = 7.2$ Hz, 1H), 4.98 (s, 2H), 4.51 (dd, $J = 13.6, 7.8$ Hz, 1H), 4.18 (t, $J = 6.1$ Hz, 2H), 3.87 (s, 3H), 3.33 – 2.95 (m, 4H), 2.11 (m, 2H). ^{13}C NMR (50 MHz, CDCl_3) δ 172.43, 156.07, 137.18, 136.61, 136.48, 129.46, 128.52, 128.43, 127.97, 127.72, 126.83, 123.11, 122.51, 66.67, 56.54, 47.12, 38.31, 36.84, 35.30, 29.31. HPLC-MS: MW = 548; $[\text{M}^+]$: 421.

Synthesis of 6b.



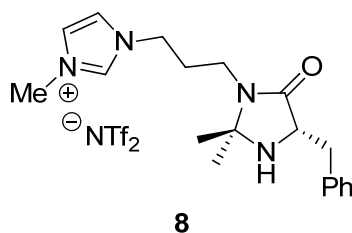
6a (557 mg, 1.02 mmol) was dissolved in 2 ml DCM and LiNTf_2 was added (350 mg, 1.22 mmol). The reaction mixture was stirred at rt overnight. 1 mL of water was then added the reaction was further stirred for 1 hour. Aqueous phase was extracted with DCM (2 x 5 ml) and the collected organic phases were washed until no precipitation of AgI occurred in the AgNO_3 test. The organic layer was dried (Na_2SO_4), filtered and the solvent removed under reduced pressure, to afford the product as a clear, viscous oil in 92 % yield. ^1H NMR (200 MHz, CDCl_3) δ 8.69 (s, 1H), 7.56 – 7.09 (m, 12H), 6.75 (t, $J = 5.8$ Hz, 1H), 5.58 (d, $J = 7.0$ Hz, 1H), 5.05 (s, 2H), 4.35 (dd, $J = 14.2, 6.9$ Hz, 1H), 4.01 (t, $J = 6.1$ Hz, 2H), 3.86 (s, 3H), 3.33 – 2.85 (m, 4H), 2.00 (m, 2H). ^{13}C NMR (50 MHz, CDCl_3) δ 172.36, 156.16, 136.35, 136.29, 129.14, 128.64, 128.44, 128.06, 127.64, 127.02, 123.35, 122.91, 122.62, 116.52, 110.13, 66.81, 56.76, 46.80, 37.98, 36.16, 35.16, 29.71. $[\text{M}^+]$: 421.

Synthesis of 7.



6b (569 mg, 0.81 mmol) was dissolved in anhydrous methanol and Pd/C (86.3 mg, 0.081 mmol) was added and the reaction was stirred under hydrogen atmosphere for 24 hours. The solution was filtered through a pad of Celite® and the solvent was removed under reduced pressure, to give **7** as a viscous oil in 94 % yield. ¹H NMR (200 MHz, CDCl₃) δ 8.97 (s, 1H), 8.43 (bs, 1H), 7.66 (bs, 1H), 7.58 (s, 1H), 7.45 – 7.20 (m, 6H), 7.17 (bs, 1H), 4.19 (t, *J* = 6.6 Hz, 2H), 3.99 (s, 3H), 3.68 (dd, *J* = 9.4, 4.4 Hz, 2H), 3.22 (m, 1H), 2.75 (dd, *J* = 13.6, 9.3 Hz, 2H), 2.17 – 2.00 (m, 2H). ¹³C NMR (100 MHz, CDCl₃) δ 175.74, 137.63, 136.80, 129.57, 129.28, 128.73, 126.83, 123.26, 122.88, 118.25, 109.95, 56.36, 47.22, 40.95, 36.43, 34.96, 30.52. [*M*⁺]: 287.

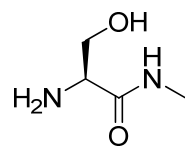
Synthesis of 8.



7 (354.0 mg, 0.624 mmol) was dissolved in 3 mL of anhydrous DMF and 1 mL of anhydrous acetone was added. The reaction was stirred at 80 °C for 48 hours, then the volatiles were removed under reduced pressure and the crude product was purified by flash chromatography on neutral alumina (DCM/MeOH 98:2). **8** was collected as a viscous oil in 91 % yield. ¹H NMR (200 MHz, CDCl₃) δ 9.03 (s, 1H), 7.65 (s, 1H), 7.37 – 7.18 (m, 6H), 4.29 – 4.01 (m, 2H), 3.98 (s, 3H), 3.82 (t, *J* = 5.5 Hz, 1H), 3.52 – 3.13 (m, 2H), 3.08 (m, 2H), 2.16 – 1.84 (m, 2H), 1.76 (bs, 1H), 1.29 (s, 3H), 1.23 (s, 3H). ¹³C NMR (100 MHz, CDCl₃) δ 175.51, 136.78, 136.71, 129.57, 128.62, 127.10, 123.26, 123.02, 119.15, 109.42, 72.20, 58.83, 47.36, 36.86, 36.47, 36.22, 30.29, 27.90, 25.98. [*M*⁺]: 327.

Synthesis of organocatalyst 14.

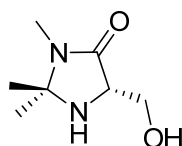
(S)-2-amino-3-hydroxy-*N*-methylpropanamide (**10**).



10

5 mL of MeNH₂ (8 M solution in EtOH) were added to L-serine methyl ester hydrochloride **9** (1.55 g, 10 mmol) and the solution was stirred at rt for 20 hours. The volatiles were removed under reduced pressure to give the solid hydrochloride salt, which was dissolved in saturated NaHCO₃ solution and extracted with chloroform (3 x 8 mL). The combined organic phases were dried (Na₂SO₄), filtered and the solvent was removed under reduced pressure, to afford **10** in 83 % yield. ¹H NMR (200 MHz, CD₃OD) δ 3.81 – 3.65 (CH₂, m, 2H), 3.62 – 3.51 (CH, m, 1H), 2.77 (CH₃, s, 3H).

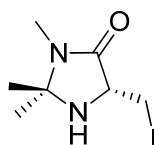
Synthesis of **11**.



11

10 (1.04 g, 8.8 mmol), was dissolved in 4 mL of anhydrous DMF. Anhydrous acetone (4 mL) and *p*-TSA (151.6 mg, 0.88 mmol) were added and the reaction was stirred at 80 °C for 5 days. Volatiles were removed under vacuum and the crude product was purified by silica gel flash chromatography (DCM/MeOH 95:5) to give **11** in 46 % yield. ¹H NMR (400 MHz, CD₃OD) δ 3.91 (CHH, dd, *J* = 11.4, 3.4 Hz, 1H), 3.69 (CHH, dd, *J* = 11.4, 3.4 Hz, 1H), 3.54 (CH, t, *J* = 3.2 Hz, 1H), 2.80 (NCH₃, d, *J* = 0.7 Hz, 3H), 1.46 (CH₃, s, 3H), 1.35 (CH₃, s, 3H).

Synthesis of **12**.

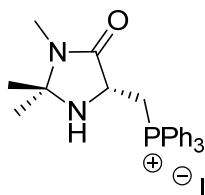


12

PPh₃ (207.2 mg, 0.79 mmol) and imidazole (53.8 mg, 0.79 mmol) were dissolved in 4 mL of anhydrous DCM and cooled at 0°C. Iodine (200.6 mg, 0.79 mmol) was added and the solution was

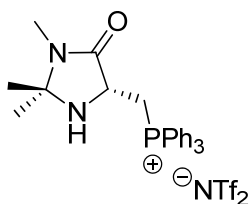
warmed to rt and stirred for 10 minutes. **12** (100 mg, 0.63 mmol) was added at 0°C and the reaction mixture was stirred at rt for 28 hours. The reaction was quenched with aqueous Na₂S₂O₃ and diluted with DCM. The organic phase was washed with brine, dried (Na₂SO₄), filtered and the solvent was removed under reduced pressure without heating. The crude product was immediately used for the following step without further purification. ¹H NMR (400 MHz, CDCl₃) δ 3.54 (dd, *J* = 11.2, 5.9 Hz, 1H), 3.42 (m, 2H), 2.73 (s, 3H), 1.59 (bs, 1H), 1.43 (s, 3H), 1.28 (s, 3H).

Synthesis of 13.



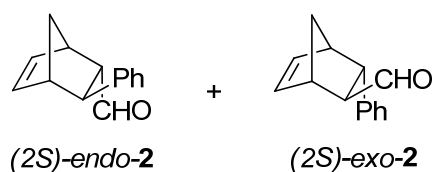
12 (169 mg, 0.63 mmol) and PPh₃ (331.6 mg, 1.26 mmol) were dissolved in 4 mL of anhydrous chloroform and stirred under reflux for 48 hours. The solvent was removed under reduced pressure and the crude product was washed with ether and purified by silica gel flash chromatography (DCM/MeOH 95:5). to give the product as a pale yellow solid in 42 % yield. ¹H NMR (200 MHz, CDCl₃) δ 7.90 – 7.53 (m, 15H), 4.25 – 3.99 (m, 1H), 3.99 – 3.73 (m, 1H), 3.73 – 3.47 (m, 1H), 2.59 (s, 1H), 1.25 (s, 1H), 1.10 (s, 1H).

Synthesis of 14.



13 (70.0 mg, 0.13 mmol) was dissolved in 2 mL of DCM and LiNTf₂ was added (45.5 mg, 0.16 mmol). The reaction mixture was stirred at rt for the week-end and then 1 mL of water was added and the solution was further stirred for 45 minutes. The aqueous phase was extracted with DCM (3 x 5 mL) and the combined organic layers were washed with water until no precipitation of AgI occurred in the AgNO₃ test. The organic phase was dried (Na₂SO₄), filtered and the solvent removed under reduced pressure to give **13** as a viscous oil in 90 % yield. ¹H NMR (200 MHz, CDCl₃) δ 7.90 – 7.53 (m, 15H), 4.25 – 3.99 (m, 1H), 3.99 – 3.73 (m, 1H), 3.73 – 3.47 (m, 1H), 2.59 (s, 1H), 1.25 (s, 1H), 1.10 (s, 1H).

General procedure for the organocatalyzed Diels-Alder reaction.



In a screw-cap vial, the catalyst (0.015 mmol) was dissolved in 300 μL of solvent and 15 μL of water. Then the acid (0.015 mmol), the *trans*-cinnamaldehyde (0.3 mmol) and the freshly distilled cyclopentadiene (0.9 mmol) were added. Upon consumption of the limiting reagent, the reaction mixture was diluted with Et_2O and washed with water and brine. The organic layer was dried (Na_2SO_4), filtered and concentrated. When the reaction was carried out in methanol hydrolysis of the dimethyl acetal was performed stirring the crude product with $\text{TFA}:\text{H}_2\text{O}:\text{CHCl}_3$ (1:1:2) for 2 hours, followed by neutralization with saturated NaHCO_3 solution and extraction with Et_2O . The crude product was purified with silica gel flash chromatography (cyclohexane/ AcOEt 96:4) affording the product **2** as a mixture of diastereoisomers: ^1H NMR (400 MHz, CDCl_3), *exo*: δ 9.93 (d, $J = 2.0$ Hz, 1H), 7.35 – 7.13 (m, 5H), 6.35 (dd, $J = 5.7, 3.6$ Hz, 1H), 6.08 (dd, $J = 5.7, 3.3$ Hz, 1H), 3.74 (m, 1H), 3.23 (m, 1H), 2.99 (m, 1H), 2.60 (m, 1H), 1.58 (dd, $J = 3.5, 1.7$ Hz, 1H), 1.56 (dd, $J = 3.5, 1.7$ Hz, 1H). ^1H NMR (400 MHz, CDCl_3) *endo*: δ 9.61 (d, $J = 2.2$ Hz, 1H), 7.35 – 7.13 (m, 5H), 6.43 (dd, $J = 5.7, 3.2$ Hz, 1H), 6.18 (dd, $J = 5.7, 2.8$ Hz, 1H), 3.34 (m, 1H), 3.14 (m, 1H), 3.10 (m, 1H), 2.99 (m, 1H), 1.82 (dt, $J = 8.7, 1.5$ Hz, 1H), 1.63 (ddd, $J = 8.7, 3.4, 1.7$ Hz, 1H).

The enantiomeric excess of the product was determined by HPLC analysis after reduction of product with NaBH_4 : aldehyde (**2**) was dissolved in 1 mL of methanol and 2 equivalents of NaBH_4 were added at 0°C . The reaction was stirred at rt until no starting material was detected by TLC (30 minutes). Then the reaction was quenched at 0°C with 1 mL of 1 M KHSO_4 solution. The aqueous phase was extracted with DCM (2 x 5 ml). The organic phase was dried (Na_2SO_4), filtered and the organic solvent was removed under reduced pressure. The crude product was filtered through a short pad of silica and analyzed by HPLC (Chiralpak IC, *n*-hexane/*i*-PrOH 98:2, 1 mL/min): t_{R} *endo* = 17.7 min, 22.1 min. t_{R} *exo*: 14.8 min, 19.8 min. The absolute configuration was assigned by comparison with known product.

General procedure for recycle with organic solvent.

The DA reaction was carried as reported above. At the end of the reaction the solvent was removed under reduced pressure and the residue was washed with ether (6 x 2 ml) to extract the product. The catalyst was then dried under vacuum for 3-4 hours and, after addition of fresh water, acid and starting materials, it was employed in the following run. The ether layer was dried (Na_2SO_4), filtered and the solvent was evaporated to afford the crude product **2** as dimethyl acetal.

General procedure for recycle with IL.

The DA reaction was carried as reported above. At the end of the reaction the ionic phase was extracted with ether (6 x 2 ml) to collect the product. The IL was then dried under vacuum for 3-4 hours and, after addition of fresh water, acid and starting materials, it was employed in the following run. The ether layer was dried (Na_2SO_4), filtered and the solvent was evaporated to afford the crude product **2**.

Bibliography.

- (1) Montroni, E. *Sintesi e Applicazione di Nuovi Organocatalizzatori Chirali con Tag-Ionico*, **2010**, unpublished dissertation.
- (2) Corey, E. *Angew. Chem. Int. ed.* **2002**, *41*, 1650–1667.
- (3) Ahrendt, K. A.; Borths, C. J.; Macmillan, D. W. C.; *J. Am. Chem. Soc.* **2000**, 4243–4244.
- (4) Berkessel, A.; Gröger, H.; *Asymmetric Organocatalysis – From Biomimetic Concepts to Applications in Asymmetric Synthesis*, **2005**, WILEY-VCH, Weinheim.
- (5) Lelais, G.; Macmillan, D. W. C.; *Aldrichimica Acta* **2006**, *39*, 79–87.
- (6) Hagiwara, H.; Kuroda, T.; Hoshi, T.; Suzuki, T. *Adv. Synth. Cat.* **2010**, *352*, 909–916.
- (7) Park, J. K.; Sreekanth, P.; Kim, B. M. *Adv. Synth. Cat.* **2004**, *346*, 49–52.

2.4. Highly Efficient Ion-Tagged Catalyst for the Enantioselective Michael Addition of Aldehydes to Nitroalkenes ¹

2.4.1. Reaction overview.

The addition of nucleophiles to activate olefins is an important process for the formation of new C-C bond. Aminocatalysis provides a means to activate the Michael addition either *via* iminium or enamine formation (fig.1). When iminium activation occurs, the electrophilic partner is activated (LUMO lowering), whereas enamine formation leads to activation of nucleophilic species (HOMO rising).

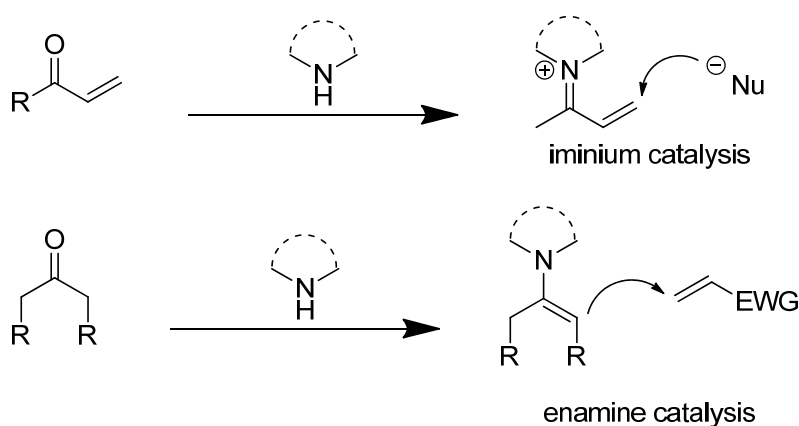


Fig. 1: Iminium and enamine catalysis in the Michael addition.

When chiral amine, mainly pyrrolidines, are employed, the addition can take place in an enantioselective manner. If enamine catalysis is into play the geometry of the enamine is determinant for the stereoselectivity of the reaction (fig.2).

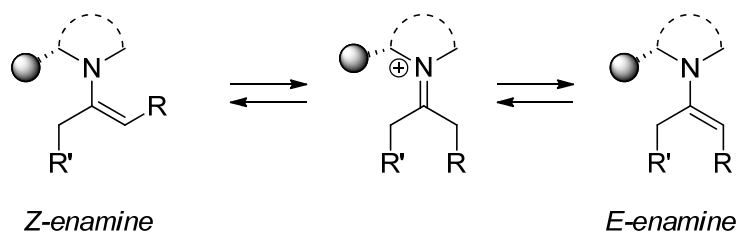


Fig.2: Geometry of the enamine.

Supposing that the *E* enamine is formed predominantly, the formation of two rotamers is still possible. Since one of the enamine face is shielded by the bulky group in the catalyst backbone, the two rotamers expose the two opposite face of the enamine to the attack of the electrophile determining the facial selectivity of the process (fig.3).²

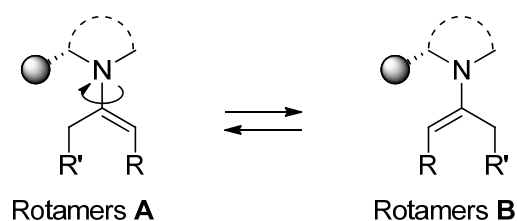


Fig. 3: Enamine rotamers affecting the stereocontrol.

In 2005 Hayashi reported the use of O-TMS-diphenylprolinol (TMS = trimethylsilyl) as an efficient catalyst for the addition of aldehydes to nitroolefins in hexane (fig.4).³ The reaction proceeded with good yield and almost complete selectivity towards one of the four possible stereoisomers.

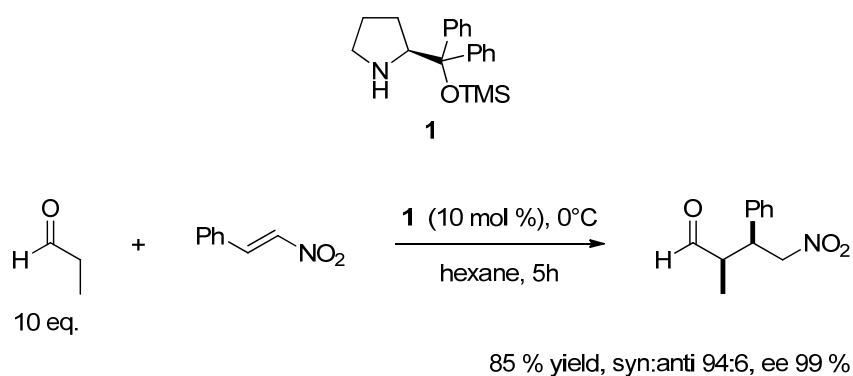


Fig. 4: Addition of aldehydes to nitroolefins catalyzed by 1.

The mechanism of the reaction involves the formation of an enamine between the organocatalyst and the aldehyde, followed by attack to the nitroalkene to give the product, after hydrolysis of the iminium ion intermediate (fig.5).⁴

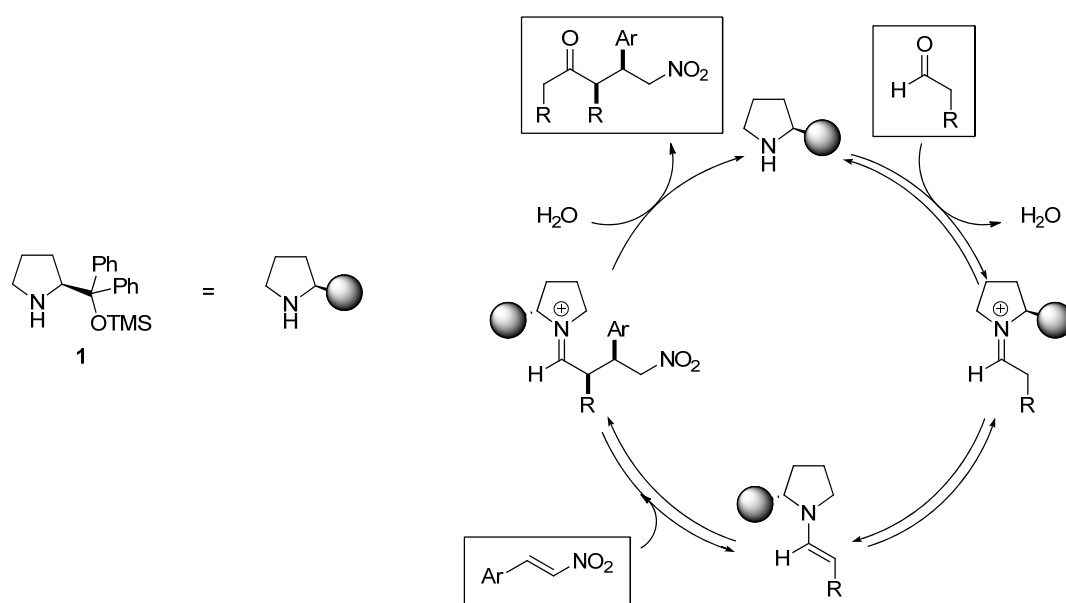


Fig.5: Mechanism of the enamine-catalyzed Michael addition of aldehydes to nitroolefins.

The high diastereoselectivity and the excellent enantioselectivity could be explained by the selective formation of the *anti* enamine, with its double bond oriented away from the diphenylsiloxymethyl group (rotamer A, fig.3). Thus the enamine would react with the nitrostyrene approaching the less hindered face *via* an acyclic synclinal transition state (fig.6).⁵

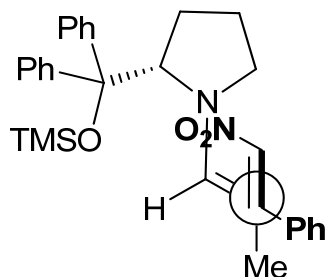


Fig. 6: Transition state for the Michael addition of propanal to nitrostyrene catalyzed by **1**.

Protection of the hydroxyl group as trimethylsilyl ether turned out to be fundamental to obtain high yield. Indeed, when the reaction was carried out with unprotected DPP, the ee remained high, but the reaction was sluggish and only low product yield was achieved. This behavior probably arose from the interaction of the hydroxyl moiety with the iminium ion, formed in the early stage of the reaction. The cyclic hemiaminal formed subtracts the active species from the catalytic cycle, diminishing the amount of catalyst really available for the process (fig.7).

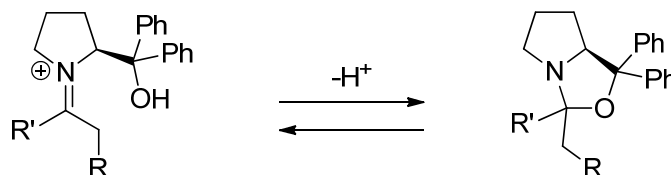
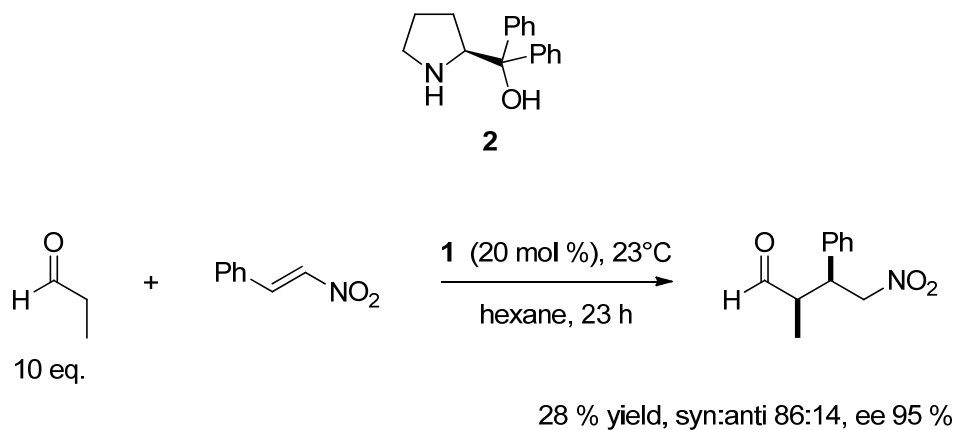


Fig. 7: Addition of propanal to nitrostyrene catalyzed by DPP **2**.

Further improvement for this reaction was successively reported by Ma and co-workers for long-chain, water insoluble aldehydes. When the reaction was carried out in water, with benzoic acid as additive, a wide range of aliphatic aldehydes reacted efficiently with nitroacrylates and nitroalkenes

using catalyst loading as low as 0.5 - 2 mol % (fig.8). The improvement probably resulted from a combination of the excellent asymmetric induction ability of the catalyst **1**, the quick formation of enamine species in the presence of benzoic acid, and the highly concentrated organic phase directed by the aqueous medium.⁶

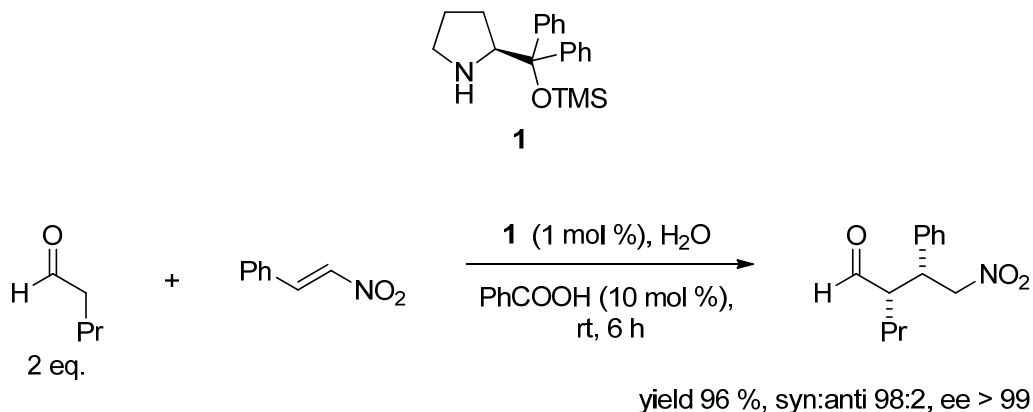


Fig. 8: Addition of aldehydes to nitroalkenes in water catalyzed by **1**.

2.4.2. Discussion.

Although the reaction developed by Hayashi displayed outstanding selectivity, in order to obtain satisfactory reactivity, catalyst loading of 5-20 mol % and excess of donor aldehyde were required. The aqueous conditions developed by Ma addressed these problem successfully, but the use of water as solvent was mandatory. The worthwhile reaction and the remarkable effect of water on the process outcome prompted us to investigate the use of an ion-tagged catalyst in this reaction. We speculated that the tunable solubility conferred by the ion tag, along with its capability to stabilize charged transition state (see paragraph 1.2. for electrosteric activation) might lead to further process improvement. Therefore we designed the ion-tagged DPP **3** (fig.9) as a possible organocatalyst for the Michael addition of aldehydes to nitroalkenes.

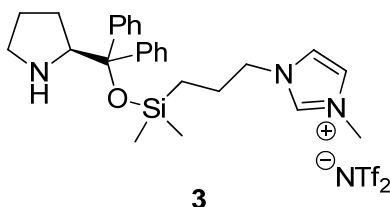


Fig. 9: Ion-tagged organocatalyst for Michael addition of aldehydes to nitroalkenes.

The ion tag was installed exploiting the silyl ether linkage; a spacer constituted of a three carbon alkyl chain was chosen to ensure sufficient flexibility, in order to allow the approach of the ionic group towards the reactive center. The choice of Tf_2N as counter ion was dictated by its stability towards hydrolysis, a property not shared by the commonly used BF_4 or PF_6 anions. The latter

produce traces amounts of fluoride anions in the presence of water, that catalyze the desilylation of **3**. The synthesis of **3** was accomplished in high yield using operational simple procedure, according to the scheme reported in fig.10.

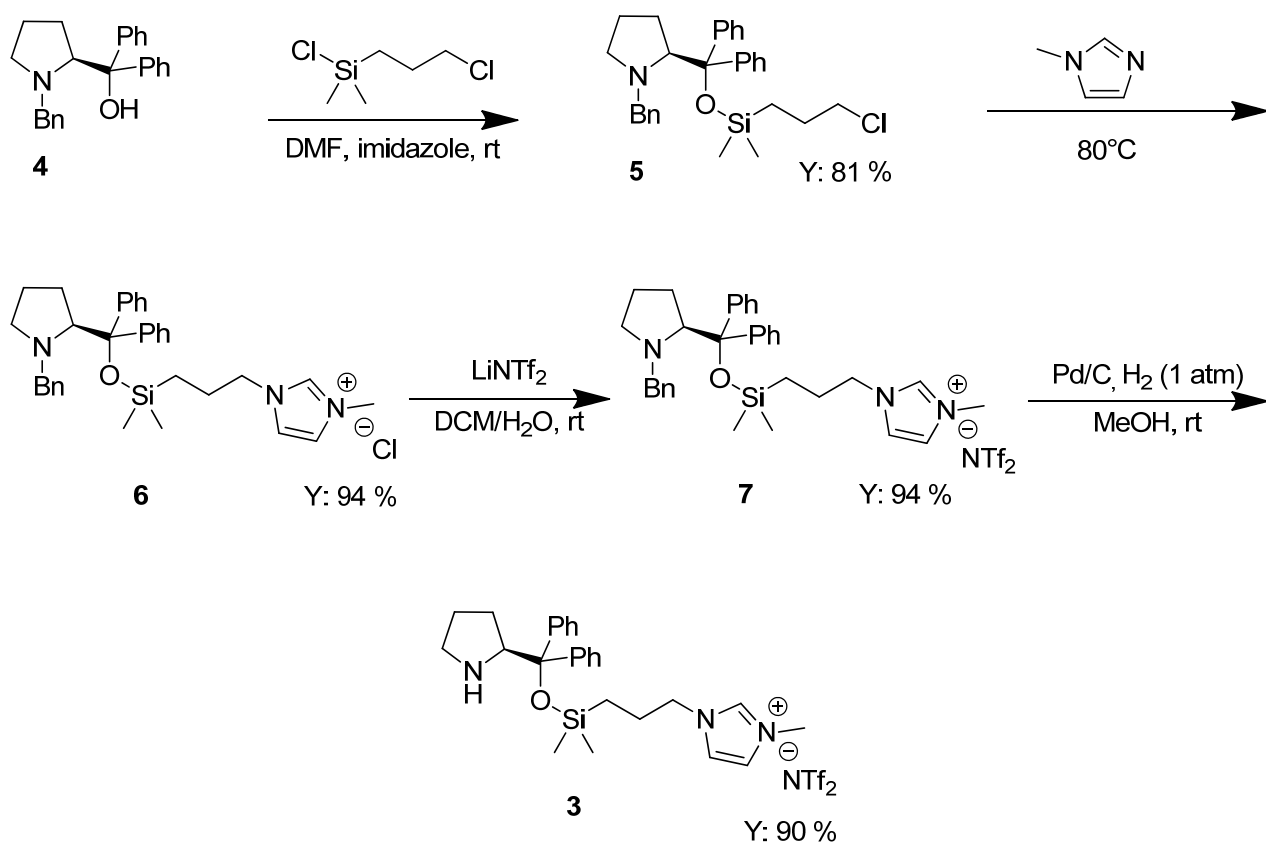


Fig. 10: Synthesis of the ion-tagged organocatalyst **3**.

N-benzyl-diphenylprolinol (**4**) hydroxyl group was silylated with chloro(3-chloropropyl)dimethylsilane (**8**), which was prepared by iridium catalyzed hydrosilylation of allyl chloride (fig.11).⁷

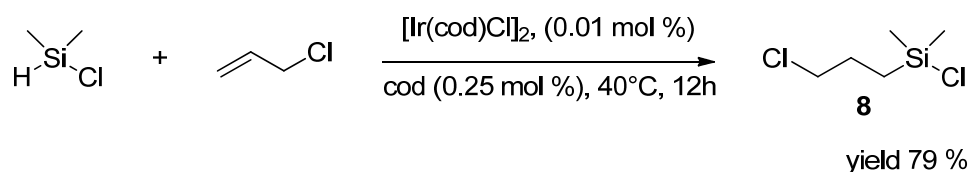
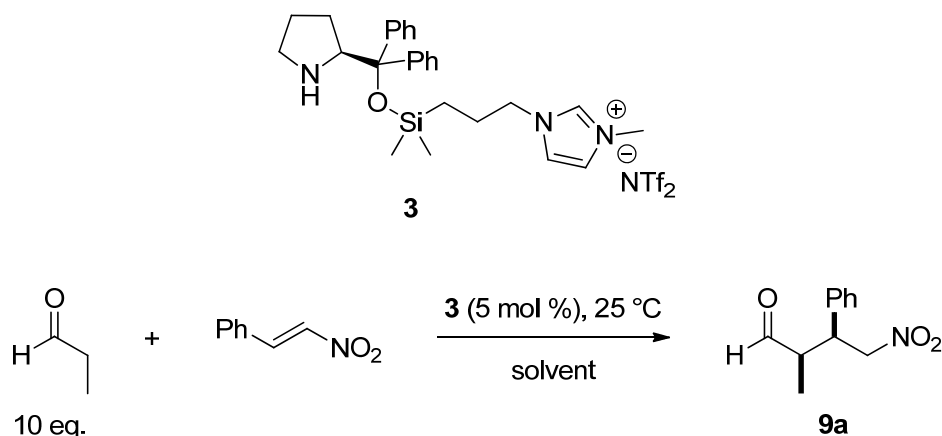


Fig. 11: Synthesis of chloro(3-chloropropyl)dimethylsilane **8**.

Reaction in neat *N*-methyl-imidazole afforded the chloride salt **6**, which was subjected to anion metathesis with LiNTf₂, affording **7** in 94 % yield. Finally deprotection of the *N*-benzyl amine by Pd catalyzed hydrogenation led to the formation of desired product **3** in 90 % yield. With organocatalyst **3** in our hands, we started testing the simple addition of propanal to nitrostyrene as the model reaction in different solvents, using 5 mol% catalyst loading in the presence of 10 equiv. of aldehyde (Tab.1).



Entry	Solvent	Time (min)	Yield (%) ^a	ee (%) ^b	syn:anti ^c
1	[bmim] [NTf ₂] ^[e]	15	95	99	85:15
2	[bmpy] [NTf ₂] ^[f]	15	95	99	85:15
3	CH ₂ Cl ₂	15	96	99	84:16
4	CHCl ₃	15	96	99	72:28
5	H ₂ O	15	94	99	88:12
6	neat	30	97	99	86:14
7	CH ₃ CN	30	98	99	80:20
8	<i>n</i> -hexane	45	99	99	77:23
9	<i>o</i> -hexane	45	98	99	84:16
10	Et ₂ O	45	97	99	85:15
11	THF	45	96	99	82:18
12	<i>t</i> -BuOMe	45	99	99	85:15
13	EtOAc	90	99	99	84:16
14	MeOH	90	98	99	92:8
15	EtOH	90	97	99	84:16

(a) Yield of isolated product.

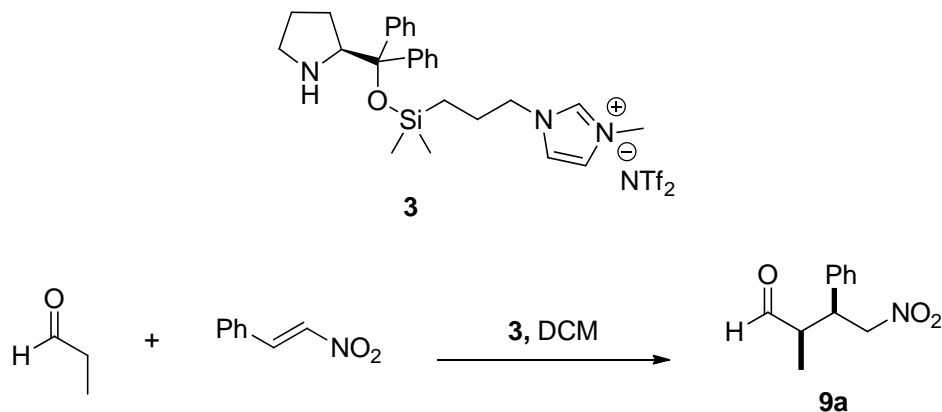
(b) The ee was determined by HPLC analysis (Chiralpak IC column). The absolute configuration was assigned by comparison of the optical rotation with that of the known products.

(c) Determined by HPLC on crude reaction mixture.

Tab.1: Solvent screening in the addition of propanal to (*E*)-β-nitrostyrene catalyzed by **3** (5 mol %).

The catalytic system displayed an outstanding activity in all the solvents examined, but especially in ILs (Entries 1 and 2), in halogenated solvents (Entries 3 and 4) and in water (Entry 5), where reactions were complete after 15 min. The reaction outcome turned out to be only marginally affected from the nature of the solvent and complete conversion, with good diastereoselectivity and excellent enantioselectivity, was achieved even in neat condition (Entry 6), in MeCN (Entry 7), in hydrocarbons (Entry 8 and 9), in ethers (Entry 10-12), in AcOEt (Entry 13) and in alcohols (Entry

14 and 15). In all the cases enantioselectivities were invariably high (99% ee) and good diastereoselectivities in favor of *syn* isomers were obtained. On the basis of the results obtained in Tab.1, we chose CH₂Cl₂ and water as benchmark solvents. Using CH₂Cl₂ we optimized the reaction conditions in terms of catalyst loading and excess of aldehyde (Tab.2).



Entry	Propanal (eq.)	3 (mol %)	T (°C)	t (h)	Yield (%) ^a	ee (%) ^b	syn:anti ^c
1	10	5	0	1.5	97	99	92:8
2	2	5	25	0.5	98	99	88:12
3	2	5	0	3	97	99	90:10
4	10	1	25	1.5	98	99	86:14
5	10	1	0	8	96	99	90:10
6	2	1	25	1	98	99	86:14
7	2	1	0	4	94	99	90:10
8	1.2	1	25	1.5	98	99	86:14
9	1.2	1	0	6	99	>99	93:7

(a) Yield of isolated product.

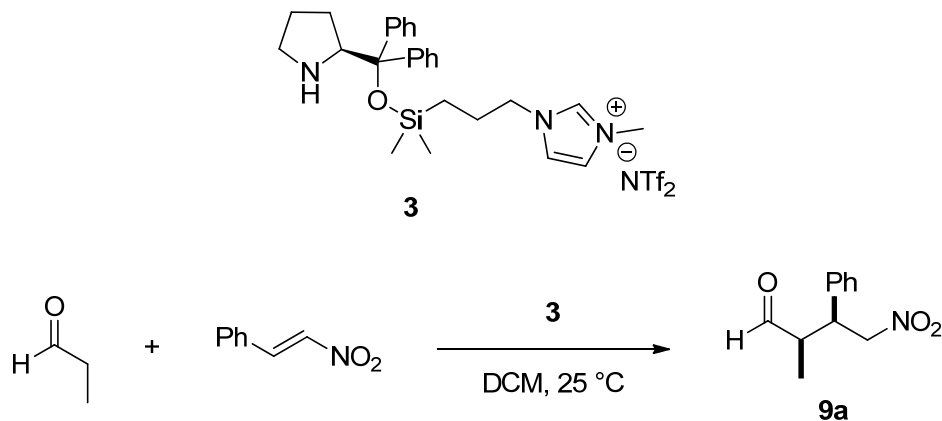
(b) The ee was determined by HPLC analysis (Chiralpak IC column).

(c) Determined by HPLC on crude reaction mixture.

Tab. 2: Optimization of reaction conditions.

Excellent levels of reaction efficiency and enantioselectivity were obtained in all conditions tested. In almost every case, decreasing the reaction temperature from 25 °C to 0 °C had a negligible impact on enantioselectivity and only a small effect on the diastereomeric ratio, but the reaction times, needed to achieve complete conversion, became notably longer (Entries 1, 3, 5, 7 and 9). Catalyst loading was decreased from 5 to 1 mol % (Entry 4) and the donor aldehyde excess was progressively lowered from 10 up to 1.2 equivalents (Entry 4-9). Eventually we were delighted to

observe that using catalyst loading of 1 mol % in the presence of only 1.2 equivalents of aldehyde a quantitative conversion to the desired product was achieved in only 1.5 h at room temperature (entry 8). To demonstrate the synthetic usefulness of the protocol developed reactions on a larger scale (1-5 mmol) were carried out (Tab.3).



Entry	Propanal (eq.)	Nitrostyrene (mmol)	PhCOOH (mol %)	3 (mol %)	t (h)	Yield (%) ^a	ee (%) ^b	syn:anti ^c
1	1.2	5	-	1	1.5	97	99	89:11
2	2	1	5	0.5	1.5	99	>99	95:5
3	2	2.5	2.5	0.25	4	88	>99.5	96:4
4	2	2.5	1	0.1	6	35	>99.5	96:4

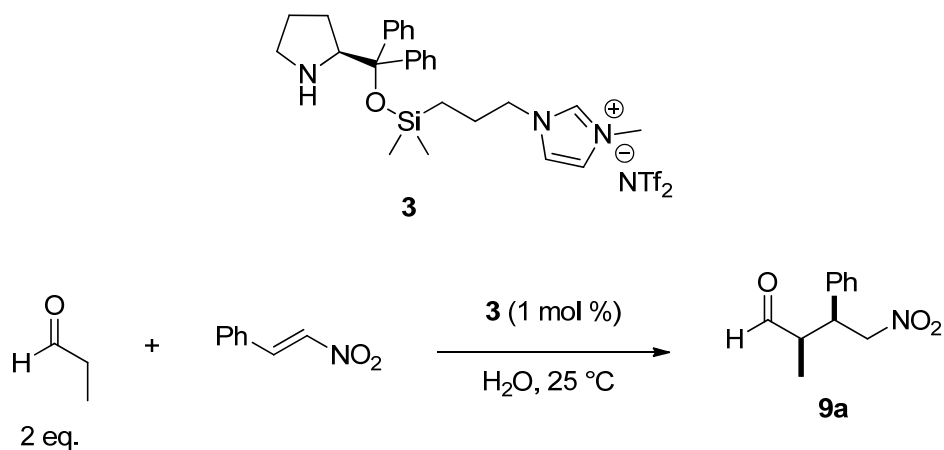
(a) Yield of isolated product.

(b) The ee was determined by HPLC analysis (Chiralpak IC column).

(c) Determined by HPLC on crude reaction mixture.

Tab. 3: Reactions carried out on a larger scale.

The reaction maintained its high efficiency even when carried out on 5 mmol scale (Entry 1) yielding the product in 97 % yield, with a diastereomeric ratio syn:anti 89:11 and with 99 % ee. To confirm the efficiency of **3**, we performed some more reactions lowering further the catalyst loading (Entries 2–4). In these cases, the presence of 10 equiv. of benzoic acid with respect to **3** allowed us to achieve good conversions in reasonable reaction times. Astonishing results were obtained when the catalyst was used at 0.5 and 0.25 mol %, with excellent conversions and enhanced selectivities after a few hours (Entry 2 and 4). When the catalyst was used at 0.1 mol % a 35 % yield was obtained after 6 h, with improved values of enantio- and diastereoselectivity. Finally the model reaction was also examined using water as the solvent (Tab.4). With 1 mol % of **3** and 2 equivalents of aldehyde, a slower reaction occurred with respect to CH₂Cl₂ (Entry 1), but the use of water slightly improved the diastereomeric ratio. The reaction became much faster in the presence of benzoic acid, while maintaining a high level of stereoselectivity (Entry 2).



Entry	PhCOOH (mol %)	t (h)	Yield (%) ^a	ee (%) ^b	syn:anti ^c
1	-	2	98	99	93:7
2	10	1	97	99	90:10

(a) Yield of isolated product.

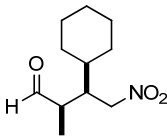
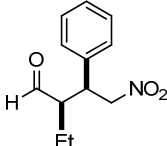
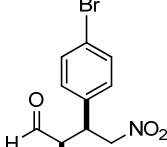
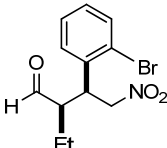
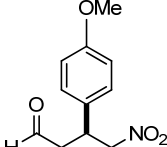
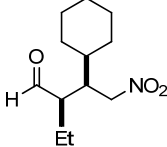
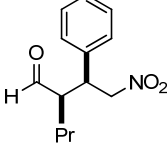
(b) The ee was determined by HPLC analysis (Chiralpak IC column).

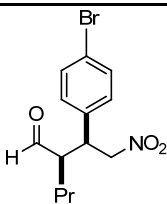
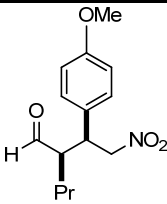
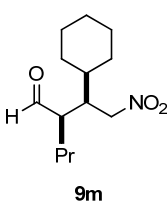
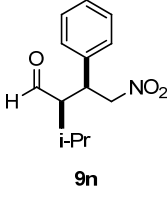
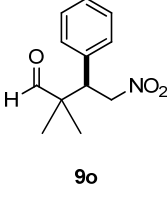
(c) Determined by HPLC on crude reaction mixture.

Tab. 4: Michael addition in water.

Therefore CH₂Cl₂ and H₂O as solvents were selected for expanding the scope of the reaction. Four different protocols were established: in protocol **A** the reaction was carried out in DCM without any additive; in protocol **B** 10 mol % of benzoic acid were added to the reaction in DCM; in protocol **C** the reaction was carried out in water and, finally, in protocol **D** 10 mol % of benzoic acid were added to the reaction in water. For each substrate, when the result in condition **A** were unsatisfactory, the following protocols were tested in order to maximize yield and selectivity. The results obtained with a wide range of aliphatic aldehydes and nitroalkenes are reported in Tab.5.

Entry ^a	Product	Reaction Conditions	t (h)	Yield (%) ^b	ee (%) ^c	syn:anti ^d
1	<p style="text-align: center;">9b</p>	A	1	97	99	86:14
		C	4	98	99	92:8
2	<p style="text-align: center;">9c</p>	A	1	96	99	87:13
		C	4	96	99	91:9

Entry ^a	Product	Reaction Conditions	t (h)	Yield (%) ^b	ee (%) ^c	syn:anti ^d
3 ^e	 9d	A	24	28	98	78:22
		B	22	66	99	89:11
		C	24	89	99	78:22
4	 9e	A	5	94	>99	87:13
		C	4	90	>99	92:8
		D	2	94	>99.5	94:6
		D ^f	3.5	84	>99.5	93:7
5	 9f	A	8	92	99	90:10
		C	4	86	>99	95:5
6	 9g	A	8	96	>99	88:12
		C	4	94	>99	96:4
7	 9h	A	12	87	99	80:20
		C	4	92	99	92:8
8 ^e	 9i	A	22	48	97	90:10
		B	22	65	95	85:15
		C	22	50	95	89:11
		D	22	81	97	79:21
9	 9j	A	6	94	>99	85:15
		C	4	99	>99.5	95:5
		D	2	98	>99.5	96:4

Entry ^a	Product	Reaction Conditions	t (h)	Yield (%) ^b	ee (%) ^c	syn:anti ^d
10	 9k	A	6	95	>99	81:19
		C	4	99	>99.5	95:5
11	 9l	A	10	92	>99.5	83:17
		C	4	98	>99.5	93:7
12 ^e	 9m	A	24	43	>99	91:9
		B	24	98	>99.5	95:5
		C	24	54	>99	91:9
		D	9	99	>99.5	92:8
13	 9n	B	24	42	>99	92:8
		D	7	65	>99	98:2
14	 9o	A	53	49	58	-
		C	22	99	76	-

(a) Reaction conditions: nitroalkene (0.25 mmol), aldehyde (0.5 mmol), 1 mol % **3** at rt for the specified time. **A**: 0.25 mL of CH₂Cl₂; **B**: benzoic acid (0.025 mmol), 0.25 mL of CH₂Cl₂; **C**: 0.5 mL of H₂O; **D**: benzoic acid (0.025 mmol), 0.5 mL of H₂O.

(b) Yield of isolated product.

(c) Determined by chiral HPLC analysis (Chiralpak IC column). The absolute configuration was assigned by comparison of the optical rotation with that of the known products.

(d) Determined by HPLC on crude reaction mixture.

(e) 2 mol% of **3**.

(f) The reaction was carried out on a 4-mmol scale using 1.2 equiv. of butanal.

(g) 5 mol% of **3**.

Tab. 5: Scope of the Michael addition of aliphatic aldehydes to nitroalkenes catalyzed by **3**.

By inspection of the table, some general trends could be derived. First of all, CH₂Cl₂ was a much better solvent compared to water for reactions of propanal with aromatic nitroalkenes (Entries 1 and 2). On the other hand, water is a better reaction medium when less reactive aliphatic nitroalkenes or longer chain aldehydes are used (entries 3–14). This behavior can be ascribed to the rapid solubility

decrease of aldehydes in water when the molecular weight increases. Indeed, at 20 °C the solubility of propanal in water is much higher (22.9 mass %) compared to butanal (7.44), 2-methylpropanal (5.62), 4-methylpentanal (2.02) and pentanal (1.43) (fig.12).⁸

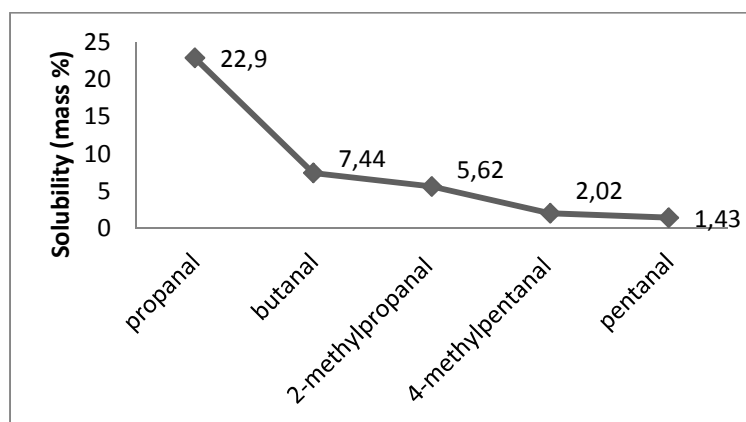


Fig. 812: Solubility in water of some aliphatic aldehydes.

These values possibly represent the ability of aldehydes to generate with water liquid-liquid biphasic systems, where faster reactions occur in a highly concentrated organic phase. Second, when sterically hindered nitroalkenes or aldehydes were used (entries 3, 8, 12–14), the presence of an acid additive was necessary to ensure high conversions. Moreover, the use of water and addition of benzoic acid generally afforded better enantio- and diastereomeric ratios. Finally, an increased catalyst loading was necessary for the less reactive aliphatic nitroalkene (entries 3, 8 and 12) and 2-methylpropanal (entry 14). This last reaction proved once more the great efficiency of **3**, since a quantitative yield of product was recovered after 22 h using 5 mol % of catalyst and without the addition of benzoic acid. Although the *ee* was moderate the condition adopted were exceptionally mild for such a challenging substrate.

2.4.3. Conclusion.

In summary, we developed a new efficient ion-tagged organocatalyst for the asymmetric Michael addition of aldehydes to nitroalkenes, which displayed remarkable features. Not only it gave excellent enantioselectivities and very good diastereoselectivities in a wide range of reaction media, ranging from water to organic solvents, but it showed enhanced reactivity compared to the known organocatalysts reported for this Michael reaction, also when used at 0.25–1 mol% and in the presence of only a slight excess of donor aldehyde (1.2–2 equiv.). The improved reactivity of **3** compared to the parent non-ionic catalyst can be addressed as an example of electrosteric activation.⁹ Unfortunately the hydrolysable nature of the silyl ether linker didn't allow us to recycle efficiently the ion-tagged catalyst.

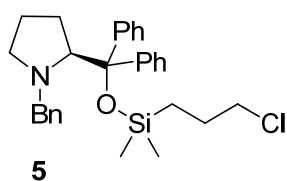
2.4.4. Experimental section.

General information.

^1H and ^{13}C NMR were recorded on a Varian Gemini 200; chemical shifts (δ) are reported in ppm relative to TMS. Chiral HPLC studies were carried out on a Hewlett-Packard series 1090 instrument and on a Agilent Technologies 1200 Series instrument. Optical rotations were measured with a Perkin-Elmer 343 polarimeter. Gas chromatographic analyses were performed with a Agilent 6850 GC-system coupled to a Agilent 5975 mass selective detector. Reactions were monitored by TLC and GC-MS. Flash-chromatography was carried out using Merck silica gel 60 (230-400 mesh particle size) and Fluka aluminum oxide, Brockmann Activity I (0.05-0.15 mm particle size, pH = 7.0 ± 0.5). All reagents were commercially available and were used without further purification, unless otherwise stated. Nitroalkenes were synthesized using reported literature procedures.

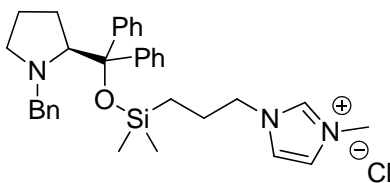
Synthesis of the catalyst (3).

(S)-1-benzyl-2-(((3-chloropropyl)dimethylsilyloxy)diphenylmethyl)pyrrolidine (5)



Chloro(3-chloropropyl)dimethylsilane (0.99 mL, 6 mmol) was slowly added at 0 °C to a solution of *N*-benzyl-diphenylprolinol (**4**, 1.37 g, 4 mmol) and imidazole (0.48 g, 7 mmol) in DMF (4 mL). The reaction mixture was allowed to reach room temperature and stirred for 12 h. The solution was quenched with phosphate buffer (pH = 7.00, 4 mL) and extracted with ethyl acetate (3 x 10 mL). The combined organic layers were washed with brine (2 x 10 mL) and dried on Na_2SO_4 . Solvent evaporation afforded a white solid that was washed with cold *n*-pentane to afford **5** as white crystals (1.54 g, 3.24 mmol, 81 %). m.p. = 80-82 °C. $[\alpha]_{20}^{\text{D}} = +62$ (c = 1.0, CH_2Cl_2). ^1H NMR (200 MHz, CDCl_3): δ 7.72 + 7.47 (m, 4H), 7.44 + 7.06 (m, 11H), 4.31 (d, $J=13.2$, 1H), 3.90 (dd, $J = 9.0, 2.9$ Hz, 1H), 3.52 + 3.22 (m, 3H), 2.61 + 2.37 (m, 1H), 2.22 + 1.87 (m, 2H), 1.86 + 1.53 (m, 3H), 1.45 + 1.20 (m, 1H), 0.80 + 0.48 (m, 1H), 0.35 (ddd, $J=6.2, 5.7, 2.7$ Hz, 2H), -0.18 (s, 6H). ^{13}C -NMR (50 MHz, CDCl_3): δ 144.04, 143.63, 140.97, 129.62, 129.58, 128.24, 127.90, 127.04, 126.93, 126.23, 84.90, 71.55, 62.16, 54.80, 47.76, 29.15, 27.18, 23.50, 15.92, 0.23. $[\text{M}]^+$: 478.

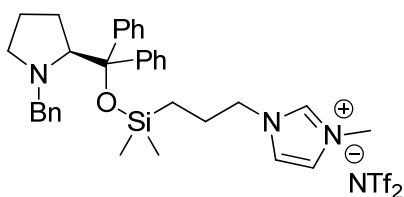
(S)-1-(3-(((1-benzylpyrrolidin-2-yl)diphenylmethoxy)dimethylsilyl)propyl)-3-methyl-1H-imidazol-3-ium chloride (6)



6

5 (1.43 g, 3 mmol) was dissolved in freshly distilled *N*-methyl-imidazole (2.4 mL, 30 mmol) and the reaction mixture is stirred under argon at 80 °C for 12 h. The reaction mixture was allowed to reach rt and excess *N*-methyl-imidazole was removed under reduced pressure. The residue was washed with anhydrous diethyl ether (3 x 5 mL) and dried under vacuum to afford **6** as a white very hygroscopic solid (1.58 g, 2.82 mmol, 94 %). m.p. = 50-51 °C. $[\alpha]_{20}^D = \pm 44$ (c = 1.2, CH₂Cl₂). ¹H NMR (200 MHz, CDCl₃): δ 10.81 (s, 1H), 7.59 + 7.46 (m, 4H), 7.41 + 7.13 (m, 13H), 4.33 (d, *J* = 13.3 Hz, 1H), 4.14 + 4.00 (m, 5H), 3.89 (d, *J* = 8.6 Hz, 1H), 3.46 (d, *J* = 13.4 Hz, 1H), 2.50 (t, *J* = 7.3 Hz, 1H), 2.17 + 1.87 (m, 2H), 1.86 + 1.63 (m, 3H), 1.46 + 1.23 (m, 1H), 0.79 + 0.50 (m, 1H), 0.35 + 0.16 (m, 2H), -0.21 (s, 3H), -0.25 (s, 3H). ¹³C-NMR (50 MHz, CDCl₃): δ 143.24, 143.04, 140.58, 136.93, 129.09, 129.02, 127.73, 127.52, 126.78, 126.58, 126.40, 125.83, 123.41, 120.88, 84.62, 70.88, 61.75, 54.29, 51.86, 35.91, 28.67, 24.18, 23.03, 14.32, -0.25. $[M]^+$:524.

(S)-1-(3-(((1-benzylpyrrolidin-2-yl)diphenylmethoxy)dimethylsilyl)propyl)-3-methyl-1H-imidazol-3-ium bis(trifluoromethylsulfonyl)amide (7)

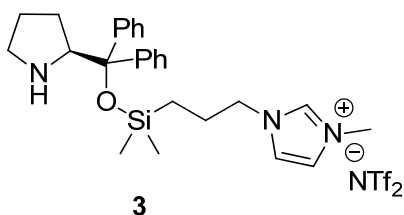


7

6 (0.84 g, 1.5 mmol) was dissolved in water (5 mL) and LiNTf₂ (0.65 g, 2.25 mmol) was slowly added at rt under stirring. A white insoluble gummy solid immediately formed. CH₂Cl₂ (5 mL) was added and the heterogeneous reaction mixture was stirred for 2 h at rt. The solution was extracted with CH₂Cl₂ (2 x 2 mL) and the combined organic layers were washed with distilled water (5 x 5 mL) until no chloride was detected by AgNO₃ test. The combined organic layers were dried (Na₂SO₄) and evaporated at reduced pressure. The residue was purified by flash-chromatography on neutral alumina eluting with CH₂Cl₂/MeOH 99/1 to give **7** as light yellow viscous oil (1.14 g, 1.42 mmol, 94 %). $[\alpha]_{20}^D = \pm 32$ (c = 1.4, CH₂Cl₂). ¹H NMR (200 MHz, CDCl₃): δ 8.76 (s, 1H), 7.68 +

7.46 (m, 5H), 7.41 + 7.24 (m, 10H), 7.10 (s, 1H), 6.79 (s, 1H), 4.33 (d, $J = 13.4$ Hz, 1H), 4.05 + 3.78 (m, 6H), 3.46 (d, $J = 13.4$ Hz, 2H), 2.58 + 2.34 (m, 1H), 2.21 + 1.87 (m, 2H), 1.85 + 1.64 (m, 3H), 1.41 + 1.13 (m, 1H), 0.79 + 0.45 (m, 1H), 0.36 + 0.12 (m, 2H), -0.20 (s, 3H), -0.25 (s, 3H). ^{13}C NMR (50 MHz, CDCl_3): δ 143.60, 143.47, 141.02, 135.27, 129.44, 129.37, 128.08, 127.86, 127.12, 126.86, 126.68, 126.16, 123.50, 122.84, 121.80, 116.45, 85.01, 71.20, 62.11, 54.63, 52.35, 35.83, 28.96, 24.27, 23.36, 14.43, -0.19. $[\text{M}^+]$: 524.

(S)-1-(3-((diphenyl(pyrrolidin-2-yl)methoxy)dimethylsilyl)propyl)-3-methyl-1H-imidazol-3-ium bis(trifluoromethylsulfonyl)amide (3)



To a solution of the imidazolium bis(trifluoromethylsulfonyl)imide salt **7** (0.805 g, 1 mmol) in anhydrous MeOH (5 mL) was added 10 % palladium on charcoal (0.212 mg, 0.2 mmol). The mixture was stirred under atmospheric pressure of hydrogen at room temperature overnight. It was then filtered on Celite® and washed with CH_2Cl_2 . The combined organic layers were evaporated under vacuum and the residue was purified by flash-chromatography on neutral alumina eluting with $\text{CH}_2\text{Cl}_2/\text{MeOH}$ 98/2 to give **3** as viscous oil (0.645 g, 0.9 mmol, 90 %). $[\alpha]_{20}^{\text{D}} = +36$ ($c = 1.4$, CH_2Cl_2). ^1H NMR (200 MHz, CDCl_3): δ 9.11 (s, 1H), 7.48 + 7.17 (m, 12H), 4.33 + 4.20 (m, 1H), 4.12 (td, $J = 7.2, 4.0$ Hz, 2H), 3.98 (s, 3H), 3.05 + 2.89 (m, 1H), 2.73 + 2.55 (m, 1H), 1.90 (dq, $J = 10.1, 7.0$ Hz, 2H), 1.77 + 1.57 (m, 3H), 1.41 + 1.25 (m, 1H), 0.52 + 0.37 (m, 2H), -0.09 (s, 3H), -0.18 (s, 3H). ^{13}C -NMR (50 MHz, CDCl_3): δ 144.91, 143.03, 136.07, 128.39, 128.28, 128.10, 127.96, 127.78, 125.90, 125.29, 123.42, 122.88, 122.20, 116.49, 82.39, 65.92, 52.55, 46.84, 36.10, 26.94, 26.30, 25.10, 14.62, -0.30. $[\text{M}^+]$: 434.

Michael addition.

General procedure for the Michael addition in CH_2Cl_2 .

The aldehyde (1.2+2 equiv.) was slowly added at 25 °C or at 0 °C to a solution of nitroalkene (0.25+5 mmol) and catalyst **3** (0.25+5 mol%) in CH_2Cl_2 (0.25+5 mL) in a screw-capped vial and the reaction mixture was stirred at the desired temperature until thin-layer chromatography (TLC) showed the disappearance of the starting nitroalkene. The solvent was evaporated at reduced pressure and the residue was purified by flash chromatography on silica eluting with cyclohexane/

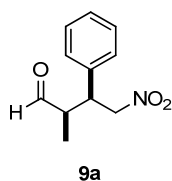
ethyl acetate, 9:1. The enantiomeric excess was determined on the crude reaction mixture by (HPLC) using a Chiralpak IC column.

General procedure for the Michael addition in CH₂Cl₂.

The aldehyde (1.2⁺2 equiv.) was slowly added at room temperature to a suspension of nitroalkene (0.25⁺4 mmol) and catalyst **3** (1⁺5 mol%) in H₂O (0.5⁺8 mL) in a screw-capped vial and the reaction mixture was vigorously stirred at room temperature until thin-layer chromatography (TLC) showed the disappearance of the starting nitroalkene. The aqueous phase was extracted with CH₂Cl₂, the combined organic layers were dried (Na₂SO₄) and evaporated at reduced pressure. The residue was further purified by flash chromatography on silica eluting with cyclohexane/ethyl acetate 9:1. The enantiomeric excess was determined on the crude reaction mixture by HPLC using a Chiralpak IC column.

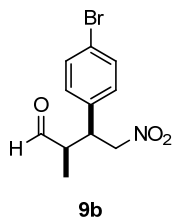
Spectroscopic data for compounds 9a-o.^{3,6,10,11}

(2R,3S)-2-methyl-4-nitro-3-phenylbutanal (9a).



¹H NMR (200 MHz, CDCl₃): δ = 9.73 (s, 1H), 7.43 + 7.13 (m, 5H), 4.90 + 4.62 (m, 2H), 3.94 + 3.73 (m, 1H), 2.90 + 2.69 (m, 1H), 1.02 (d, *J* = 7.3, Hz 3H). ¹³C NMR (50 MHz, CDCl₃): δ = 202.27, 136.49, 128.84, 127.92, 77.96, 48.21, 43.83, 11.87. [M-HNO₂]⁺: 160. [α]_D²⁰ = +36.1 (c = 1.23, CHCl₃). HPLC: Column IC, *n*-hexane/*i*-PrOH 90:10, 1.0 ml/min, *t*_R = *anti*: 15.4 min, 28.7 min; *syn*: 22.8 min, 26.5 min.

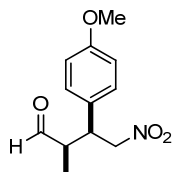
(2R, 3S)-(4-Bromophenyl)-2-methyl-4-nitrobutanal (9b).



¹H NMR (200 MHz, CDCl₃) δ = 9.67 (s, 1H); 7.45 (d, *J* = 8.4 Hz, 2H), 7.03 (d, *J* = 8.4 Hz, 2H), 4.57-4.80 (m, 2H), 3.71-3.81 (m, 1H), 2.67-2.81 (m, 1H) 0.98 (d, *J* = 7.3 Hz, 3H). ¹³C NMR (50 MHz, CDCl₃) δ = 201.8, 135.6, 132.3, 129.8, 129.7, 122.2, 77.8, 48.2, 43.5, 12.2. [M-HNO₂]⁺: 240,

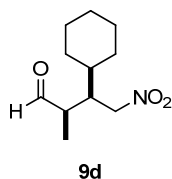
238. HPLC: Column IC, *n*-hexane/*i*-PrOH 90:10, 1.0 ml/min, $t_R = anti$: 15.6 min, 27.6 min; *syn*: 22.5 min, 24.5 min.

(2*R*, 3*S*)-2-methyl-4-nitro-3-(4-methoxyphenyl)-butanal (9c).



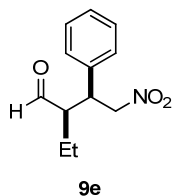
^1H NMR (200 MHz, CDCl_3): δ 9.73 (s, 1H), 7.11 (d, $J = 8.9$ Hz, 2H), 6.89 (d, $J = 8.7$ Hz, 2H), 4.80 - 4.66 (m, 2H), 3.81 (s, 3H), 3.80 (m, 1H), 2.81 + 2.71 (m, 1H), 1.03 (d, $J = 7.2$ Hz, 3H). ^{13}C NMR (50 MHz, CDCl_3) δ 202.49, 159.30, 129.15, 128.36, 114.4, 78.37, 55.27, 48.61, 43.38, 12.07. $[\text{M}-\text{HNO}_2]^+$: 190. HPLC: Column IC, *n*-hexane/*i*-PrOH 80:20, 0.5 ml/min, $t_R = anti$: 26.3 min, 41.2 min; *syn*: 35.9 min, 40.2 min.

(2*R*, 3*R*)-3-Cyclohexyl-2-methyl-4-nitro-butanal (9d).



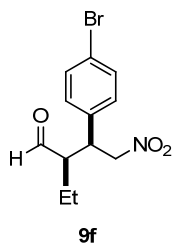
^1H NMR (200 MHz, CDCl_3): δ 9.68 (s, 1H), 4.59 - 4.38 (m, 2H), 2.61 + 2.54 (m, 2H), 1.81 + 1.56 (m, 5H), 1.50 + 1.41 (m, 1H), 1.27 + 0.90 (m, 5H), 1.20 (d, 3H, $J = 7.0$ Hz);). ^{13}C NMR (50 MHz, CDCl_3) δ 203.2, 75.8, 46.6, 43.6, 38.0, 31.6, 30.0, 26.4, 26.3, 26.1, 10.8. $[\text{M}-\text{HNO}_2]^+$: 166. HPLC: Column IC, *n*-hexane/*i*-PrOH 90:10, 1 ml/min, $t_R = anti$: 15.6 min, 27.6 min; *syn*: 22.5 min, 24.5 min.

(2*R*, 3*S*)-2-ethyl-4-nitro-3-phenylbutanal (9e).



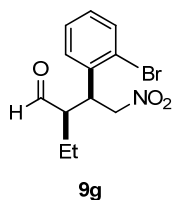
^1H -NMR (200 MHz, CDCl_3) δ 9.72 (s, 1H), 7.36-7.28 (m, 3H), 7.19-7.17 (m, 2H), 4.72 - 4.63 (m, 2H), 3.79 (m, 1H), 2.71-2.66 (m, 1H), 1.53-1.49 (m, 2H), 0.83 (t, $J = 7.5$ Hz, 3H). ^{13}C -NMR (50 MHz, CDCl_3) δ 203.2, 136.7, 129.1, 128.1, 128.0, 78.5, 55.0, 42.7, 20.4, 10.7. $[\text{M}-\text{HNO}_2]^+$: 174. HPLC: Column IC, *n*-hexane/*i*-PrOH 90:10, 1.0 ml/min, $t_R = anti$: 13.1 min, 16.4 min; *syn*: 19.6 min, 22.1 min.

(2R, 3S)-3-(4-Bromophenyl)-2-ethyl-4-nitrobutanal (9f).



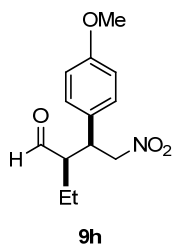
^1H NMR (200 MHz, CDCl_3) δ 9.72 (s, 1H), 7.52-7.40 (m, 2H), 7.20-7.01 (m, 2H), 4.80-4.55 (m, 2H), 3.85-3.70 (m, 1H), 2.70-2.50 (m, 1H), 1.60-1.45 (m, 2H), 0.84 (t, $J = 7.5$ Hz, 3H); ^{13}C -NMR (50 MHz, CDCl_3) δ 202.6, 135.9, 132.3, 129.7, 122.1, 78.2, 54.7, 42.1, 20.3, 10.5. $[\text{M}-\text{HNO}_2]^+$: 255, 253. HPLC: Column IC, *n*-hexane/*i*-PrOH 90:10, 1.0 ml/min, $t_{\text{R}} = \text{anti}$: 13.3 min, 16.3 min; *syn*: 19.4 min, 20.8 min.

(2R,3S)-3-(2-bromophenyl)-2-ethyl-4-nitrobutanal (9g).



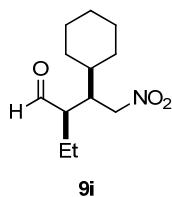
$[\text{M}-\text{HNO}_2]$: 268, 266. HPLC: Column IC, *n*-hexane/*i*-PrOH 95:5, 1.0 ml/min, $t_{\text{R}} = \text{anti}$: 16.1 min, 33.8 min; *syn*: 25.7 min, 27.1 min.

(2R,3S)-2-ethyl-3-(4-methoxyphenyl)-4-nitrobutanal (9h).



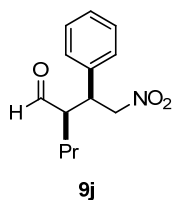
^1H NMR (200 MHz, CDCl_3) δ 9.71 (m, 1H), 7.09 (d, $J = 8.4$ Hz, 2H), 6.86 (d, $J = 8.4$ Hz, 2H), 4.58 - 4.68 (m, 2H), 3.79 (s, 3H), 3.70-3.79 (m, 1H), 2.59-2.66 (m, 1H), 1.47-1.55 (m, 2H), 0.82 (t, $J = 8.0$ Hz, 3H); ^{13}C -NMR (50 MHz, CDCl_3) δ 203.3, 159.3, 129.3, 129.0, 114.5, 78.7, 55.2, 42.1, 20.3, 10.7. $[\text{M}-\text{HNO}_2]^+$: 204. HPLC: Column IC, *n*-hexane/*i*-PrOH 80:20, 1.0 ml/min, $t_{\text{R}} = \text{anti}$: 11.5 min, 13.2 min; *syn*: 15.9 min, 17.3 min.

(2*R*,3*R*)-3-cyclohexyl-2-ethyl-4-nitrobutanal (9i).



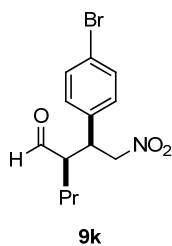
¹H NMR (200 MHz, CDCl₃) δ 9.70 (s, 1H), 4.57 - 4.39 (m, 2H), 2.55-2.47 (m, 2H), 1.91-1.72 (m, 3H), 1.72-1.63 (m, 3H), 1.63-1.40 (m, 2H), 1.31-1.07 (m, 3H), 1.07-0.89(m, 5H); ¹³C-NMR (50 MHz, CDCl₃) δ 203.5, 75.6, 53.3, 42.9, 38.9, 31.2, 30.0, 26.4, 26.3, 26.1, 20.3, 12.3. [M-HNO₂]: 180. HPLC: Column IC, *n*-hexane/*i*-PrOH 90:10, 0.7 ml/min, *t_R* = *anti*: 17.5 min, 23.7 min; *syn*: 14.9 min, 16.4 min.

(*R*)-2-((*S*)-2-nitro-1-phenylethyl)pentanal (9j)



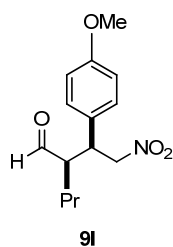
¹H NMR (200 MHz, CDCl₃) δ 9.70 (s, 1H), 7.38-7.26 (m, 3H), 7.19-7.16 (m, 2H), 4.71- 4.64 (m, 2H), 3.78 (m, 1H), 2.70 (m, 1H), 1.50-1.16 (m, 4H), 0.80 (t, *J* = 7.2 Hz, 3H); ¹³C-NMR (50 MHz, CDCl₃) δ 203.2, 136.8, 128.9, 127.9, 78.3, 53.6, 43.0, 29.3, 19.6, 13.7. [M-HNO₂]: 188. HPLC: Column IC, *n*-hexane/*i*-PrOH 90:10, 1.0 ml/min, *t_R* = *anti*: 11.8 min, 15.4 min; *syn*: 17.5 min, 19.8 min.

(*R*)-2-((*S*)-1-(4-bromophenyl)-2-nitroethyl)pentanal (9k).



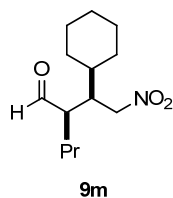
¹H NMR (200 MHz, CDCl₃) δ 9.70 (s, 1H), 7.48 (d, *J* = 8.1 Hz, 2H), 7.07 (d, *J* = 8.4 Hz, 2H), 4.70 - 4.61 (m, 2H), 3.75 (m, 1H), 2.69 (m, 1H), 1.53-1.12 (m, 4H), 0.82 (t, *J* = 7.2 Hz, 3H); ¹³C-NMR (50 MHz, CDCl₃) δ 202.7, 136.0, 132.2, 129.6, 122.0, 78.0, 53.4, 42.5, 29.4, 19.6, 13.8. [M-HNO₂]: 268, 266. HPLC: Column IC, *n*-hexane/*i*-PrOH 90:10, 1.0 ml/min, *t_R* = *anti*: 12.3 min, 15.8 min; *syn*: 17.8 min, 19.4 min.

(R)-2-((S)-1-(4-methoxyphenyl)-2-nitroethyl)pentanal (9l).



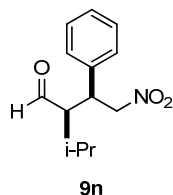
^1H NMR (200 MHz, CDCl_3) δ 9.69 (s, 1H), 7.08 (d, $J = 8.7$ Hz, 2H), 6.86 (d, $J = 9.0$, 2H), 4.67 - 4.58 (m, 2H), 3.77 (s, 3H), 3.71 (m, 1H), 2.65 (m, 1H), 1.49-1.10 (m, 4H), 0.80 (t, $J = 6.9$ Hz, 3H); ^{13}C -NMR (50 MHz, CDCl_3) δ 203.4, 159.2, 129.0, 128.5, 114.4, 78.6, 55.1, 53.9, 42.4, 29.3, 19.7, 13.9. [M-HNO₂]: 218. HPLC: Column IC, *n*-hexane/*i*-PrOH 80:20, 1.0 ml/min, $t_R = \text{anti}$: 10.8 min, 12.4 min; *syn*: 14.2 min, 15.7 min.

(R)-2-((R)-1-cyclohexyl-2-nitroethyl)pentanal (9m).



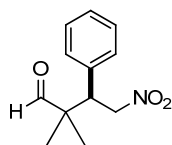
^1H NMR (200 MHz, CDCl_3) δ 9.68 (s, 1H), 4.58 - 4.38 (m, 2H), 2.62-2.54 (m, 1H), 2.48 (m, 1H), 1.77-1.60 (m, 6H), 1.47-1.35 (m, 4H), 1.27-1.08 (m, 3H), 1.04-0.93 (m, 5H); ^{13}C -NMR (50 MHz, CDCl_3) δ 203.5, 75.6, 51.3, 43.1, 38.8, 31.1, 29.0, 26.3, 26.2, 26.0, 20.9, 13.9; [M-HNO₂]: 194. HPLC: Column IC, *n*-hexane/*i*-PrOH 90:10, 0.7 ml/min, $t_R = \text{anti}$: 13.2 min, 13.8 min; *syn*: 15.8 min, 22.5 min.

(2R,3S)-2-isopropyl-4-nitro-3-phenylbutanal (9n).



^1H NMR (200 MHz, CDCl_3) δ 9.93 (s, 1H), 7.38-7.28 (m, 3H), 7.21-7.18 (m, 2H), 4.67 - 4.57 (m, 2H), 3.90 (m, 1H), 2.77 (m, 1H), 1.77-1.66 (m, 1H), 1.10 (d, $J = 7.2$ Hz, 3H), 0.89 (d, $J = 6.9$ Hz, 3H); ^{13}C -NMR (50 MHz, CDCl_3) δ 204.3, 137.1, 129.0, 127.9, 78.9, 58.6, 41.8, 27.7, 21.4, 16.8. [M-HNO₂]⁺: 188. HPLC: Column IC, *n*-hexane/*i*-PrOH 90:10, 1.0 ml/min, $t_R = \text{anti}$: 8.3 min, 9.9 min; *syn*: 12.9 min, 14.3 min.

(R)-2,2-dimethyl-4-nitro-3-phenylbutanal (9o).



9o

^1H NMR (200 MHz, CDCl_3) δ 9.53 (s, 1H), 7.36-7.28 (m, 3H), 7.21-7.18 (m, 2H), 4.86 - 4.69 (m, 2H), 3.78 (m, 1H), 1.14 (s, 3H), 1.01 (s, 3H); ^{13}C -NMR (50 MHz, CDCl_3) δ 204.2, 135.4, 129.0, 128.6, 128.0, 76.2, 48.4, 48.1, 21.5, 18.7. $[\text{M}-\text{HNO}_2]^+$: 174. HPLC: Column IC, *n*-hexane/*i*-PrOH 80:20, 1.0 ml/min, $t_{\text{R}} = R$: 12.2 min; *S*: 17.1 min.

Bibliography.

- (1) Lombardo, M.; Chiarucci, M.; Quintavalla, A.; Trombini, C. *Adv. Synth. Cat.* **2009**, *351*, 2801-2806.
- (2) Dalko, P.I.; *Enantioselective Organocatalysis: Reaction and Experimental Procedures*, Wiley-VCH, Weinheim, **2007**.
- (3) Hayashi, Y.; Gotoh, H.; Hayashi, T.; Shoji, M. *Angew. Chem. Int. ed.* **2005**, *44*, 4212-4215.
- (4) Zhao, J.-Q.; Gan, L.-H. *Eur. J. Org. Chem.* **2009**, *2009*, 2661-2665.
- (5) Seebach D.; Golinski J.; *Helv. Chim. Acta* **1981**, *64*, 1413-1423.
- (6) Zhu, S.; Yu, S.; Ma, D. *Angew. Chem. Int. ed.* **2008**, *47*, 545-548.
- (7) Shimada, T.; Aoki, K.; Shinoda, Y.; Nakamura, T.; Tokunaga, N.; Inagaki, S.; Hayashi, T. *J. Am. Chem. Soc.* **2003**, *125*, 4688-4689.
- (8) R. M. Stephenson, *J. Chem. Eng. Data* **1993**, *38*, 630.
- (9) Lombardo, M.; Trombini, C. *ChemCatChem.* **2010**, *2*, 135-145.
- (10) Andrey, O.; Alexakis, A.; Tomassini, A.; Bernardinelli, G. *Adv. Synth. Cat.* **2004**, *346*, 1147-1168.
- (11) Lu, D.; Gong, Y.; Wang, W. *Adv. Synth. Cat.* **2010**, *352*, 644-650.

FINAL REMARKS

The many environmental, safety and economical issues arisen in recent years have inspired the search of more sustainable processes. Catalysis play a key role in this field, allowing either the development of new transformations or the efficiency improvement of known chemistry. Many strategies are undertaken to address these goals. In this work we focused our attention on the use of ion-tagged catalysts, since this simple functionalization of known catalysts may lead to significant improvement in terms of recyclability and reactivity. Little attention has been paid in literature to this latter effect. The hypothesis which drove our work was that, if the ionic group can approach the developing charge in the transition state, interaction lowering the activation energy can be established, thus a rate enhancement for the reaction can be observed. However the many factors involved, like the nature of the ionic group, the length and flexibility of the spacer, the process considered and the reaction media, make problematic working out a rational strategy for the installation of the ionic group. Our work on the ion-tagged imidazolidinones is an example of how hard it can be to make effective prediction on the reactivity of the catalyst after the ion-tagged installation. On the other hand, the ion-tagged *O*-TMS-diphenylprolinol, employed for the organocatalyzed Michael addition of aldehydes to nitroalkenes, was a clear example of electrosteric activation, leading to a significant increase in the reaction rate.

The affinity of ion-tagged catalyst for ILs is another interesting properties of these molecules, which enables the developing of highly recyclable catalytic systems. Exploiting again the diphenylprolinol core we, designed an ion-tagged ligand for Zinc, which demonstrated outstanding recyclability when grafted on the IL [bmpy][NTf₂], allowing us to report the first example of asymmetric ZnEt₂ addition carried out in an ionic liquid. Finally, using an ion tagged phosphine and exploiting the thermoregulated biphasic system consisting of [bmpy][NTf₂] and water, we developed a recyclable and efficient system for the Pd catalyzed Suzuki cross coupling. The usefulness of this protocol was further demonstrated facing the functionalization of substrates, as challenging and valuable, as 5,11-dibromotetracene.

Many efforts are made to develop catalytic systems combining high activity, easy product isolation and catalyst recyclability and, in this view, ion-tagged catalysts represents an attractive and straightforward solution, although the difficulties in predicting the behavior of modified catalysts is still a major drawback in the development of this methodology.

ABBREVIATIONS

AAS	Atomic-Absorption Spectroscopy
acac	acetylacetonate
BINOL	1,1'-Bi-2-naphthol
bmim	1-butyl-3-methylimidazolium
BOX	bis(oxazolines)
bpy	1-butylpyridinium
C ₂ pic	N-ethyl-3-methylpicolinium
C ₅ mpy	1-methyl-1-pentylpyrrolidinium
CC	cross coupling
cod	1,5- cyclooctadiene
DA	Diels-Alder
dba	dibenzylideneacetone
DMAP	<i>N</i> -dimethylamino pyridine
DPP	diphenylprolinol
ee	enantiomeric excess
etmim	1-ethyl-3-methylimidazolium
EWG	electron withdrawing groups
GC	Gas Chromatography
HPLC	High Performance Liquid Chromatography
IL	ionic liquid
LA	Lewis Acid
MBH	Morita – Baylis – Hillman
mC ₁ CNpy	1-Cyanomethyl-pyridinium
MCPBA	<i>meta</i> -chloroperbenzoic acid
Mes	mesityl = 1,3,5-trimethylphenyl
MTBE	methyl tert-butyl ether
MW	microwaves
NBD	bicyclo(2.2.1)hepta-2,5-diene (norbornadiene)
NHC	N-heterocyclic carbene
NMO	N-methylmorpholine oxide
NP	Nano Particles
NTf ₂	bis(trifluoromethane)sulfonimide or bistriflimide

P(6,6,6,14)	Trihexyl-tetradecyl-phosphonium
PEG	polyethylene glycol
pmim	1-propyl-1-methylimidazolium
RCM	ring closing metathesis
rt	room temperature
<i>sc</i> CO ₂	super critical CO ₂
silc	supported ionic liquid catalyst
SM	Suzuki Miyaura
TEA	triethylamine
TEMPO	2,2,6,6-tetramethylpiperidine-1-oxyl
TFA	trifluoroacetic acid
TOF	turnover frequency
TON	Turn Over Number
tppts	3,3',3''-Phosphinidynetris(benzenesulfonic acid) trisodium salt